

**University of Alberta**

**Properties of Cemented Rockfill at Diavik Mine**

by



Basanta Kumar Shrestha

A thesis submitted to the Faculty of Graduate Studies and Research in partial fulfillment  
of the requirements for the degree of Master of Science

in

Mining Engineering

Department of Civil and Environmental Engineering

Edmonton, Alberta

Fall 2008



Library and  
Archives Canada

Bibliothèque et  
Archives Canada

Published Heritage  
Branch

Direction du  
Patrimoine de l'édition

395 Wellington Street  
Ottawa ON K1A 0N4  
Canada

395, rue Wellington  
Ottawa ON K1A 0N4  
Canada

*Your file* *Votre référence*

*ISBN: 978-0-494-47411-2*

*Our file* *Notre référence*

*ISBN: 978-0-494-47411-2*

**NOTICE:**

The author has granted a non-exclusive license allowing Library and Archives Canada to reproduce, publish, archive, preserve, conserve, communicate to the public by telecommunication or on the Internet, loan, distribute and sell theses worldwide, for commercial or non-commercial purposes, in microform, paper, electronic and/or any other formats.

The author retains copyright ownership and moral rights in this thesis. Neither the thesis nor substantial extracts from it may be printed or otherwise reproduced without the author's permission.

**AVIS:**

L'auteur a accordé une licence non exclusive permettant à la Bibliothèque et Archives Canada de reproduire, publier, archiver, sauvegarder, conserver, transmettre au public par télécommunication ou par l'Internet, prêter, distribuer et vendre des thèses partout dans le monde, à des fins commerciales ou autres, sur support microforme, papier, électronique et/ou autres formats.

L'auteur conserve la propriété du droit d'auteur et des droits moraux qui protègent cette thèse. Ni la thèse ni des extraits substantiels de celle-ci ne doivent être imprimés ou autrement reproduits sans son autorisation.

---

In compliance with the Canadian Privacy Act some supporting forms may have been removed from this thesis.

Conformément à la loi canadienne sur la protection de la vie privée, quelques formulaires secondaires ont été enlevés de cette thèse.

While these forms may be included in the document page count, their removal does not represent any loss of content from the thesis.

Bien que ces formulaires aient inclus dans la pagination, il n'y aura aucun contenu manquant.

  
**Canada**

## **Abstract**

This thesis examines the properties of cemented rockfill used in a unique application as a cap or crown pillar above the A154N kimberlite pipe being mined at the Diavik Diamond Mine. The techniques used to prepare and place the cemented rockfill as well as the field and laboratory tests conducted to measure cemented rockfill physical properties for quality control and quality assurance purposes are described. The moisture content of the aggregate was 1 to 2%. The moisture content of the cemented rockfill was approximately 7%, which was optimal for achieving a maximum compacted dry density of approximately  $2117 \text{ kg/m}^3$  at cement contents of 5.5% to 6% by weight. The measured 28-day unconfined compressive strength using 100 mm test specimens was typically 6 to 12 MPa. This strength is higher than values reported elsewhere for a similar cemented rockfill and easily exceeded the targeted design strength of 2.5 MPa.

## **Acknowledgments**

I would like to express my profound and sincerest gratitude to my thesis supervisor Dr. Dwayne D. Tannant for his invaluable time, precious suggestions, and continuous guidance, inspiration and encouragement through out this thesis work without which this thesis would not have been completed. I would also like to express my gratitude to Dr. Adam Lubell and Dr. Qi Liu for serving as thesis committee members.

I am extremely grateful to my supervisor for providing me a financial support without which it was impossible for me to pursue a higher study at University of Alberta.

I would like to extend my deepest and sincere gratitude to EBA Engineering Consultants Ltd. for providing me an opportunity to work at the Diavik Diamond Mine. Therefore, a heartfelt appreciation and a deepest acknowledgment go to the EBA staff related to this study for their support and help. Without this support, this thesis would not have been possible. I specifically thank Mr. Mark D. Watson, Dr. Sam Proskin, Mr. Scott Dimitroff, Mr. Jason Smith, Mr. Les May, and the summer students especially Mr. Jonathan Marsh, Mr. Jeremy Hoy and Mr. Haider Ahmed. An appreciation also goes to other staff and summer students from EBA who directly or indirectly involved and helped me during this study. I would also like to acknowledge the Diavik Diamond Mine for giving me permission to use their data to carry out this study.

I am also grateful to my family members especially my parents, my wife Manju Khadka and son Prafull Shrestha, relatives and friends who provided encouragement, help and suggestions directly or indirectly in various ways to complete this study. An appreciation also goes to Mr. Peter Klovan who supported for editing some parts of the thesis.

## Table of Contents

<b>1</b>	<b>Introduction</b> .....	<b>1</b>
1.1	Research Objectives.....	1
1.2	Research Scope.....	2
1.3	Outline of Thesis .....	3
<b>2</b>	<b>Backfill and Roller Compacted Concrete</b> .....	<b>4</b>
2.1	Introduction .....	4
2.2	Roller Compacted Concrete .....	4
2.2.1	Introduction.....	4
2.2.2	Properties of RCC .....	5
2.3	Backfill Types .....	11
2.3.1	Hydraulic or Slurry Fill .....	12
2.3.2	Paste Fill .....	12
2.3.3	Rockfill .....	13
2.3.4	Summary.....	14
<b>3</b>	<b>Cemented Rockfill (CRF)</b> .....	<b>16</b>
3.1	Introduction .....	16
3.2	Factors Influencing CRF Strength.....	17
3.2.1	Aggregate Properties .....	18
3.2.2	Water and Binder Properties.....	24
3.2.3	Quality of the Slurry and its Mixing with the Aggregate.....	27
3.2.4	Segregation .....	27
3.2.5	Curing Conditions .....	28
3.2.6	Sample Size.....	28
3.3	Strength Requirement and Properties .....	29
3.3.1	Empirical Relationships.....	31
3.3.2	Reported Laboratory Properties .....	36
3.3.3	Reported In Situ Properties.....	39
3.4	Preparation and Placement Practices .....	45
3.4.1	Kidd Creek Mine, Ontario .....	45
3.4.2	Golden Giant Mine, Ontario .....	46
3.4.3	Williams Mine, Ontario .....	46
3.4.4	Mines under Barrick Gold Corporation, Ontario .....	46
3.4.5	Quebec Mines .....	47
3.4.6	Myra Falls Mine, British Columbia .....	47
3.4.7	Polaris Mine, Northwest Territories.....	48
3.4.8	Mount Isa, Australia .....	49
3.4.9	Buick and Fletcher Mines, USA .....	49

3.4.10	Lamefoot Mine, Washington, USA.....	50
3.4.11	Meikle Mine, Nevada, USA.....	51
3.4.12	Leeville Mine, Nevada, USA.....	51
3.4.13	Summary.....	53
<b>4</b>	<b>Cemented Rockfill at Diavik Mine.....</b>	<b>54</b>
4.1	Cemented Rockfill Design Specifications .....	56
4.1.1	Material Specifications .....	57
4.1.2	Mix Design Specifications.....	57
4.1.3	Preparation of Kimberlite Surface.....	57
4.1.4	Mixing and Placement Specifications .....	58
4.1.5	Quality Control and Quality Assurance.....	59
4.2	Preparation of Cemented Rockfill .....	60
4.2.1	Observations during CRF Preparation.....	64
4.3	Placement of Cemented Rockfill in the A154 Pit .....	65
4.3.1	Trial Mixes.....	65
4.3.2	Observations during Trial Mixes .....	66
4.3.3	Site Preparation .....	67
4.3.4	Observations during Site Preparation.....	70
4.3.5	CRF Placement.....	73
4.3.6	Observations during Placement .....	77
4.4	Quality Control and Testing in the Field .....	78
4.4.1	Literature Review .....	78
4.4.2	Field Density and Moisture-Content Measurements.....	81
4.4.3	Water to Cement Ratio .....	85
4.4.4	Discussion about In Situ Tests and Water to Cement Ratio .....	85
4.5	Quality Control and Testing in the Laboratory .....	86
4.5.1	Quality of Cement Slurry.....	86
4.5.2	Gradation and Moisture Content of Aggregate.....	87
4.5.3	Laboratory Moisture Content of CRF .....	91
4.5.4	Test Cylinder Preparation and UCS Test.....	91
4.5.5	Observations during Quality Control and Testing .....	95
<b>5</b>	<b>Results and Discussion .....</b>	<b>97</b>
5.1	Aggregate .....	97
5.2	Trial Mix Results .....	100
5.3	Summary of Findings during Trial Mixes.....	104
5.4	Cement Slurry and Mixing with Aggregate.....	104
5.5	Nuclear Gauge and Laboratory Densities and Moisture Contents .....	107
5.6	Unconfined Compressive Strength.....	112
5.6.1	Relationship between Strength and Modulus .....	117

5.7	Prediction of In Situ CRF Properties .....	122
5.7.1	Strength.....	122
5.7.2	Elastic Properties.....	123
5.7.3	Density and Void Ratio .....	124
<b>6</b>	<b>Conclusions and Recommendations.....</b>	<b>126</b>
6.1	CRF Preparation .....	126
6.2	CRF Placement .....	127
6.3	CRF Testing and Quality Control.....	127
6.4	Future Research .....	128
	<b>References.....</b>	<b>129</b>
	<b>Appendix.....</b>	<b>138</b>

## List of Tables

Table 1.1	Tests carried out at Diavik Diamond Mine .....	2
Table 2.1	Recommended RCC aggregate gradation (Choi and Groom, 2001) .....	6
Table 2.2	Recommended RCC aggregate gradations for pavement (PCA, 2004).....	6
Table 2.3	RCC core strength for British Columbia projects, PCA (1987).....	10
Table 2.4	Comparison of properties of the principal backfilling methods (modified after Landriault et al., 1996 and Henderson et al., 1997, in Hassani and Archibald, 1998) .....	15
Table 3.1	Effect of water to cement ratio on CRF in Nevada Mines (Stone, 2007).....	25
Table 3.2	CRF laboratory properties (Kockler, 2007) .....	36
Table 3.3	Backfill aggregate description (Brechtel et al., 1989).....	37
Table 3.4	Properties of CRF with variation of sample size and cement content (Annor, 1999).....	38
Table 3.5	CRF mix and UCS values for Nevada Mines (Stone, 2007).....	39
Table 3.6	In situ and laboratory properties of CRF (Hedley, 1995 and Annor, 1999) ....	42
Table 3.7	In situ strength parameters of CRF for Kidd Creek (Farsangi, 1996) .....	43
Table 3.8	CRF mixes for the Cannon, Buick and Turquoise Ridge Mines, and its in situ modulus (Tesarik et al., 2003).....	43
Table 3.9	Design parameters of CRF at Turquoise Ridge Mine (Tesarik et al., 2003) ...	45
Table 3.10	Mix design per m <sup>3</sup> of CRF at Leeville Mine (Reschke, 2007).....	51
Table 4.1	Gradation limits for aggregate.....	57
Table 4.2	Measurement precision of TMD nuclear gauge Model 3430 .....	85
Table 4.3	Calibration of TMD nuclear gauge Model 3430 .....	85
Table 5.1	In situ and laboratory densities and moisture content from trial mixes.....	100
Table 5.2	Cement slurry recipes (water, cement contents and their ratio).....	105
Table 5.3	Measured specific gravity of cement slurry with its water to cement ratio ...	106
Table 5.4	TMD nuclear gauge and laboratory data of densities and moisture contents	107
Table 5.5	Laboratory test results of densities and moisture content with curing time...	110
Table 5.6	UCS (MPa) of CRF cylinders at different curing times .....	112
Table 5.7	UCS and tangential Young's modulus (100 mm diameter specimens).....	118
Table 5.8	Predicted in situ parameters of the CRF at the Diavik Mine .....	125

Table A.1	In situ and laboratory densities, moisture contents and UCS values of three trial mixes in 2007.....	138
Table A.2	Grain-size analysis and moisture content results of aggregate and CRF during trial mixes in 2007 .....	139
Table A.3	Grain size analysis and moisture content during production of CRF aggregate in 2006.....	140
Table A.4	Grain size analysis and moisture content of CRF aggregate during preparation of CRF in 2007.....	141
Table A.5	Batch plant records of preparing cement slurry.....	142
Table A.6	Test results of specific gravity of cement slurry.....	152
Table A.7	In situ and laboratory results of CRF with aggregate sieve sample number during placement of CRF .....	153

## List of Figures

Figure 2.1	Desirable gradation for RCC aggregates (Choi and Groom, 2001).....	6
Figure 2.2	Influence of the coarse-fine aggregate ratio on 28 days UCS (Nanni, 1988)...	7
Figure 2.3	Moisture density relationship of RCC mix (Reeves and Yates, 1985, in Choi and Groom, 2001).....	8
Figure 2.4	Density and strength correlation of RCC (Reeves and Yates, 1985, in Choi and Groom, 2001).....	9
Figure 3.1	Ideal grading for CRF (O'Toole, 2004).....	20
Figure 3.2	Impact of clays on CRF water to cement (w:c) ratio (Stone, 2007).....	23
Figure 3.3	UCS as a function of binder/porosity ratio for CRF (Annor, 1999).....	33
Figure 3.4	Relationship between deformation modulus and UCS of cemented backfill mostly CRF and concrete (Swan, 1985).....	33
Figure 3.5	Relationship of deformation modulus and UCS of CRF (Annor, 1999).....	34
Figure 3.6	Relationship between UCS and elastic modulus (Ganano and Kirkby, 1977).....	35
Figure 3.7	Relationship between UCS and Young's modulus (Kockler, 2007).....	35
Figure 3.8	Effect of coarse aggregate content on CRF strength (Brechtel et al., 1989).....	37
Figure 3.9	UCS test on 500 mm diameter cylinders of for various CRF mixes worldwide (Stone, 1993) and 457 mm cylinders (Annor, 1999).....	41
Figure 3.10	Deformation modulus for RCC, CRF and cemented tailings (Tesarik et al., 2003).....	44
Figure 3.11	Components of a high shear colloidal mixer (Reschke, 1989 and 2007).....	48
Figure 3.12	Typical gradation curve for the CRF aggregate (Reschke, 2007).....	52
Figure 4.1	Location of Diavik Diamond Mine (modified from DDMI, 2006).....	54
Figure 4.2	Location of A148 pit and both pipes in the A154 pit (modified from DDMI, 2005a).....	55
Figure 4.3	Section of ore bodies of Diavik Mine (modified from DDMI, 2005b).....	56
Figure 4.4	Storage of GU type 10 cement near batch plant.....	60
Figure 4.5	Mixing bay used for mixing aggregate with cement slurry.....	61
Figure 4.6	Aggregate from stockpile being carried by a Caterpillar 988 G loader.....	62
Figure 4.7	All equipment used to mix the CRF.....	62
Figure 4.8	Pouring of cement slurry, and mixing it with aggregate by excavator.....	63
Figure 4.9	Cement slurry and aggregate being mixed with excavator.....	63
Figure 4.10	Mixed CRF ready to be loaded into haul truck.....	64

Figure 4.11 Plan view of A 154 N pipe at initial stage (modified from DDMI, 2007b)...	68
Figure 4.12 Proposed final stage excavation of A154 N pipe along A-A' for CRF placement (modified from DDMI, 2007b).....	69
Figure 4.13 Proposed final CRF and ROM placement after final excavation of A154 N pipe along A-A' for (modified from DDMI, 2007b) .....	69
Figure 4.14 A154 N pipe before start of box cut from 9280 to 9270 m bench levels (modified from EBA, 2007a) .....	71
Figure 4.15 Pumping arrangement to prevent flow of water at CRF placement area.....	72
Figure 4.16 Kimberlite in box cut floor covered with compacted clean gravel .....	72
Figure 4.17 CRF is being dumped at placement area by Cat 777 haul truck .....	74
Figure 4.18 Spreading of CRF by a dozer.....	74
Figure 4.19 Dumping of subsequent load after compaction of previous CRF .....	75
Figure 4.20 Spreading and compaction of CRF in first lift in progress.....	75
Figure 4.21 Spreading by excavator and roller compaction near corner areas.....	76
Figure 4.22 Placement of CRF at the remaining half of the 9270 m bench level.....	76
Figure 4.23 CRF placement up to 9290 m level in 2007 (modified from DDMI, 2007c).....	77
Figure 4.24 UCS versus cylinder weights of CRF samples at Nevada Mines (Stone et al., 2007).....	80
Figure 4.25 Close view of TMD nuclear gauge during its in situ measurement .....	81
Figure 4.26 Mud balance used for measurement of specific gravity of cement slurry .....	87
Figure 4.27 Sampling pad of CRF aggregate for its gradation.....	88
Figure 4.28 Gibson vibratory screen used for gradation of CRF aggregate.....	89
Figure 4.29 Splitter used to split the <5 mm sample.....	90
Figure 4.30 Arrow shaker for gradation of <5 mm fraction from CRF aggregate .....	90
Figure 4.31 Steel and plastic moulds used to cast 100mm diameter cylinders .....	92
Figure 4.32 Some of the cylinders after completion of their capping.....	93
Figure 4.33 Matest compression test machine with dial gauge set up .....	94
Figure 5.1 Specified grain-size distribution with Talbot and Richard (1923) curves .....	97
Figure 5.2 Grain-size analysis of CRF aggregate during production in 2006 .....	98
Figure 5.3 Grain-size analysis of CRF aggregate in 2007.....	98
Figure 5.4 Mean gradation of CRF aggregate in 2006 and 2007 compared to its specification.....	99
Figure 5.5 In situ versus laboratory moisture content for trial mixes .....	101

Figure 5.6 In situ versus laboratory moisture corrected in situ dry density .....	101
Figure 5.7 In situ dry density versus in situ moisture content for trial mixes .....	103
Figure 5.8 UCS versus age for trial mixes.....	103
Figure 5.9 Water to cement ratio versus specific gravity of cement slurry.....	106
Figure 5.10 In situ dry density versus in situ moisture content .....	108
Figure 5.11 Laboratory versus in situ moisture content of CRF .....	108
Figure 5.12 Laboratory-moisture corrected versus in situ dry density of CRF .....	109
Figure 5.13 CRF-cylinder moisture content versus in situ moisture content .....	111
Figure 5.14 CRF-cylinder wet-density versus in situ wet density .....	111
Figure 5.15 CRF-cylinder dry density versus in situ density .....	112
Figure 5.16 Unconfined compressive strength versus curing time.....	113
Figure 5.17 UCS versus moisture content of CRF cylinders.....	113
Figure 5.18 UCS versus wet density of CRF cylinders.....	114
Figure 5.19 UCS versus dry density of cylinders .....	114
Figure 5.20 UCS at different cement contents versus curing time .....	115
Figure 5.21 UCS of different CRF-cylinder sizes versus curing time .....	115
Figure 5.22 Laboratory UCS of CRF from this study compared with reported values ..	116
Figure 5.23 Stress-strain curves for 100 mm cylinders after 7 days of curing .....	117
Figure 5.24 Linear relationship between UCS and $E$ for CRF cylinders .....	119
Figure 5.25 UCS versus Young's modulus of CRF cylinders.....	120
Figure 5.26 UCS versus Young's modulus of CRF from this study compared to Swan (1985), Annor (1999) and Kockler (2007).....	121
Figure 5.27 Dry density or moisture content versus Young's modulus for the CRF cylinders .....	122
Figure 5.28 Predicted in situ UCS from this study compared with reported large-scale laboratory, in situ cored sample and estimated in situ values .....	123
Figure 5.29 Predicted in situ modulus value compared with reported large-scale laboratory and in situ cored samples.....	124
Figure A.1 Stress-strain curves for 100 mm cylinders after 3 days of curing .....	158
Figure A.2 Stress-strain curves for 100 mm cylinders after 7 days of curing .....	159
Figure A.3 Stress-strain curves for 100 mm cylinders after 7 days of curing .....	160
Figure A.4 Stress-strain curves for 100 mm cylinders after 7 days of curing .....	161
Figure A.5 Stress-strain curves for 100 mm cylinders after 28 days of curing .....	161

## Lists of Symbols and Abbreviations

CRF	Cemented rockfill
DDM	Diavik Diamond Mine
DDMI	Diavik Diamond Mines Inc.
MC	Moisture content (%)
QA	Quality assurance
QC	Quality control
RCC	Roller compacted concrete
ROM	Run-of-mine
TMD	Toxler moisture-density
UCS, $\sigma_c$	Unconfined compressive strength (MPa)
w:c	Water-to-cement ratio
$b$	Binder or cement content by weight (%)
$c$	Cohesion (MPa)
$C_c$	Uniformity coefficient
$C_u$	Coefficient of curvature
$C_v$	Cement content by volume (%)
$D_{10}$	Grain size at 10% passing (mm)
$D_{30}$	Grain size at 30% passing (mm)
$D_{60}$	Grain size at 60% passing (mm)
$e$	Void ratio
$E$	Young's modulus (GPa)
$G_s$	Specific gravity
$N$	Distribution constant
$P$	Mass passing finer than opening size, u (%)
$u$	Opening size of screen (mm)
$u_{max}$	Maximum particle size (mm)
$\phi$	Frictional angle ( $^{\circ}$ )
$\nu$	Poisson's ratio
$\eta$	Porosity (%)
$\tau$	Shear strength (MPa)
$\gamma_d / \gamma_w$	Dry density/wet density ( $\text{kg/m}^3$ )
$\gamma_t$	Bulk density ( $\text{kg/m}^3$ )
$\sigma_t$	Tensile strength (MPa)
$\gamma_{wat}$	Density of water ( $\text{kg/m}^3$ )

# 1 Introduction

This thesis examines the properties of cemented rockfill (CRF) for use as a cap or crown pillar above a kimberlite pipe being mined at the Diavik Diamond Mine (DDM). Typically, CRF is used in underground mining to fill empty stopes to provide ground stability for the subsequent mining. Work conducted at the DDM site is the first documented application of CRF being used to construct a cap or crown pillar at the bottom of a small open pit. The thesis covers the techniques used to prepare and place the CRF as well as the field and laboratory tests conducted to measure the physical properties of the CRF. Most of the field and laboratory tests were conducted for quality control (QC) and quality assurance (QA) purposes.

Diavik Diamond Mine is located 300 km northeast of Yellowknife, Northwest Territories. The A154 N kimberlite pipe is one of three kimberlite pipes being mined. This pipe is exposed on the northeast wall of the A154 pit. A portion of the A154 N kimberlite pipe has been mined from surface, and the surface exposure was decided to cover with a CRF cap to allow for continued underground mining of this pipe to depth. The CRF placed over the exposed kimberlite pipe will eventually form a crown pillar between future underground mining and the existing open-pit. The CRF along with a buttress of waste rock placed on top of the CRF also serves to stabilize a steep highwall. This is a unique application of CRF in mining and contrasts a typical use of CRF in underground mines to fill the mined-out stopes.

This study examines the preparation procedures and placement specifications for the CRF, and the QC measures adopted at this mine. The in situ CRF density and the compressive strength of CRF cylinders are the key QC parameters included in this study.

## 1.1 Research Objectives

The research objectives were to:

- conduct a literature review on CRF to better understand the preparation and placement techniques used elsewhere,
- conduct a literature review on the field and laboratory tests used for the QC and QA purposes with respect to CRF,
- observe and document the CRF preparation and placement techniques used at DDM,
- conduct field and laboratory tests to measure the physical properties of CRF,
- evaluate variations in the CRF density and strength and to establish empirical relationships between the CRF density, moisture content, strength and stiffness,
- compare the measured CRF properties with other published values,
- provide recommendations for appropriate preparation and placement of CRF,
- provide recommendations for the appropriate QC and QA testing in the field and in the laboratory, and
- predict the in situ properties of the CRF placed above the A154 N kimberlite pipe and assess whether the CRF meets the specified design requirements.

## 1.2 Research Scope

This thesis is the result of a one-year period of field and laboratory testing, observation, data gathering and interpretation before and during the CRF placement. The author worked at DDM for seven weeks, between July 19 and September 10, 2007. The work was conducted in 12-hours shifts during either the day or the night. The author and other summer students from EBA were employed at the DDM for assessing the QC and properties of the CRF as it was being prepared and placed. The measurements and test data presented in this thesis were not carried out by the author alone because a team of people from the EBA were required to complete the QC testing on the CRF.

The author was involved during his stay at the DDM site with the following activities related to the CRF:

- Observing the CRF preparation, site preparation and placement processes during a trial mix and CRF placement.
- Analysing the aggregate grain size and determining the moisture content (MC).
- Measuring specific gravity ( $G_s$ ) of the cement slurry.
- Measuring the in situ density and moisture content by using a Troxler moisture-density (TMD) nuclear gauge, and collecting CRF samples from the placement area.
- Determining the moisture content of the CRF samples.
- Estimating the cement content in the CRF by washing and sieving the samples.
- Screening samples and preparing 100 and 150 mm CRF cylinders for UCS testing.
- Conducting all strain measurements for determining Young's modulus ( $E$ ).

The tests performed at DDM under the scope of this study are summarized in Table 1.1.

Table 1.1 Tests carried out at Diavik Diamond Mine

Particulars	Measured Parameters	Measured Test Data During		Grand Total	Remarks
		Trial Mixes	Production/ Placement		
Cement Slurry	w:c Ratio	2	550	552	Obtained from a batch-plant operator or cement-truck driver
	Specific Gravity, $G_s$		54	54	Collected during the pouring from a cement truck at the mixing bay
CRF Aggregate	Grain Size Analysis	3	*101	104	*71 tests during the production in 2006 and 30 tests during the preparation of the CRF for the placement in 2007
In Situ Measurement	Wet Density, $\gamma_w$	14	95	109	Measured by using a TDM nuclear gage
	Dry Density, $\gamma_d$	14	95	109	
	Moisture Content, MC	14	95	109	
	Void Ratio, $e$		95	95	Calculated based on the in situ dry density and a assumed specific gravity of the CRF
	Porosity, $\eta$		95	95	
In Situ CRF Sample	Dry Density, $\gamma_d$	8	86	94	Corrected in situ wet density based on Laboratory MC of the CRF sample
	Moisture Content, MC	19	86	105	
	Grain Size Analysis	6		6	To estimate the cement content of the CRF sample
Laboratory CRF Cylinders	Wet Density, $\gamma_w$	3	178	181	Based on the weight and volume of a cylinder-mould, 123 with in situ test
	Dry Density, $\gamma_d$	3	178	181	Based on the wet density and MC of the CRF cylinder, 123 with in situ test
	Moisture Content, MC	3	178	181	Oven-drying of the screened CRF with <25 mm sample, 123 with in situ test
	Unconfined Compressive Strength, UCS	5	178	183	Based on the UCS tests of the CRF cylinder after curing 3, 4, 7 and 28 days
	Young's Modulus, $E$		26	26	Measured by using a dial gauge during UCS test of the CRF cylinder

The scope of the research does not cover a numerical modelling or stability analysis of the CRF crown pillar despite the author's keen interest to do so. This limitation arises because DDM did not provide encouragement or the required geometric data to do so. This may be due to the unique application of CRF with the sensitive nature and constraints placed by other consulting engineering firms.

### **1.3 Outline of Thesis**

Chapter 2 is a brief literature review on back fill's major types with their merits, demerits and limitation. The unique application of CRF in an open pit mine in this study is somewhat similar to the RCC, and hence a very brief literature review on RCC has also been covered in this chapter.

Chapter 3 presents a literature review on the CRF, covering mainly the strength properties and controlling factors, already established empirical relationships, laboratory and in situ properties, and placement practices in Canada and around the world. The presented literature review in this chapter focuses on a general use of the CRF, especially while using the CRF as the filling a mined out stope or the filling an empty space created by a pillar extraction.

Chapter 4 describes briefly about the DDM and the purpose for using CRF at this study site. This chapter describes the CRF design specifications, preparation, and placement, including the trial mixes, site preparation, and CRF actual placement. This chapter also presents a literature review on the QC and testing practices of CRF along with a description of the QC and testing practices adopted at the DDM site. Field observations, during the preparation to placement, the QC and testing are also included in this chapter.

Chapter 5 presents the in situ and laboratory test results obtained at the DDM site and includes the discussion about these test results. The test results include aggregate grain-size distribution and MC of the aggregate, specific gravity of the cement slurry, in situ densities and MC measurement by using a TMD nuclear gauge. The test results also include MC of the CRF sample, densities, MC, UCS test results and deformation measurement of the CRF cylinders. The empirical relationship obtained between stiffness and UCS from the DDM site is compared with the existing reported relationships. The field and laboratory test results obtained from this study are compared with the values reported in the literature, and the predicted in situ parameters for the DDM are presented in this chapter.

Finally, the conclusions and recommendations, as the most significant findings from this study, derived at different stages of the CRF, are presented in Chapter 6. Some suggestions for the future research are also included in this chapter.

## **2 Backfill and Roller Compacted Concrete**

### **2.1 Introduction**

A brief literature review on major backfill types covers mainly the general application in underground stope, the associated merits and demerits, and their relative comparisons among them. The literature review is carried out aiming to enhance the knowledge and better understanding of the CRF as one of the main major backfill types, its role and the governing factors in its properties. An unique application of the CRF, in an open-pit mine at the DDM site, is somewhat similar to the roller compacted concrete (RCC), and hence, a brief literature review on the RCC has also been done to assess the RCC properties.

Backfilling in Canadian mines have been practiced for close to 100 years and evidence anticipated that the application of mine fill technology would be at an increasing rate in the 21<sup>st</sup> century (Udd and Annor, 1993; Nantel, 1998).

The mine backfill refers to any material that is used to fill mine openings for the stability, environmental and other economic reasons. It is used as an engineered structural product in the mining cycle to improve safety and productivity, control subsidence, provide a pillar support, and improve the ground conditions in the deep mines or in stressed zones. It is also used to improve the ventilation (Annor, 1999).

Backfilling provides an adequate working floor for workers, mine equipment, and increases the productivity by controlling ore dilution (Dickhout, 1973). Much of the success of modern underground mining arises from our ability to fill the cavities created by the mining, and to establish and retain the safe working conditions economically (Thomas et al., 1979).

The main purposes of the backfill is to either provide a support to the surrounding rock mass or to act as a construction material used to create a floor to the mine on top of, a wall to the mine next to, and a roof or head-cover to the mine under (Nanthanathan, 2006).

### **2.2 Roller Compacted Concrete**

#### **2.2.1 Introduction**

Roller compacted concrete (RCC), used in the construction of dams and pavements, is a dry and a zero slump concrete. It is defined as a mixture of a controlled gradation aggregate, Portland cement, possibly pozzolans such as flyash and water. The RCC mixture is placed and compacted with earth moving or paving equipment, usually a vibratory roller. The construction methods used to produce the RCC involves proportioning, mixing, transporting, spreading, compacting, and curing the cement-stabilized material (Choi and Hansen, 2005).

According to Choi and Hansen (2005), the mix recipe of the RCC is designed usually based on the following:

- The consistency or workability of a mix varying its constituents to obtain the desired strength (a concrete approach where density is not a key design parameter), or
- A maximum dry density of the modified proctor or a trial placement value of the mix-proportion to achieve the required strength (a soil approach where dry density ( $\gamma_d$ ) is the key design parameter).

The field compaction is carried out by using the heavy vibratory rollers, which can reduce the porosity ( $\eta$ ) of the RCC to a relatively low value. A low  $\eta$  concrete leads to a high strength and a long-term durability and, thus, it is important to optimise the compaction procedures so that the compacted material is adequately packed usually up to 98% of the modified proctor value.

### 2.2.2 Properties of RCC

The main strength parameter for the RCC design is its UCS value (or  $\gamma_d$  in a soil approach). Sometimes, the permeability in case of hydraulic structures, the tensile strength ( $\sigma_t$ ) depending upon the loading nature of structure, the shear strength ( $\tau$ ), and the durability tests are also the important parameters. However, the durability tests for the wet-dry, freeze-thaw, and abrasion, can be expensive and time consuming, are typically not required for the RCC with the minimum UCS, usually about 5.17 MPa at 7 days. The cohesion ( $c$ ) value reported for the RCC mass ranged from the 0.83 to 4.14 MPa with a reported friction angle ( $\phi$ ) ranging from 35 to 70° (Choi and Hansen, 2005).

The  $\sigma_t$  could be measured as a part of the mix design for the RCC, but rarely does the  $\sigma_t$  control the design mix in the hydraulic applications, except in the earthquake-prone areas. Hansen and Reinhardt (1991) reported that the split- $\sigma_t$  of the RCC ranged from 7 to 13%, with a typical average of 10% of the UCS cured at the same age. The reported direct  $\sigma_t$  of the RCC had a typical average of about 5 to 10% of the UCS.

The major influencing variables for the compatibility of the RCC are the mix composition, mineral aggregate size-distribution, shape of the sand and the coarse aggregate particles, and water content (Kokubu et al., 1996).

The RCC uses a controlled-graded aggregate, which is the processed bank-run sand and gravel material or a crushed rock from a quarry with a maximum size of the aggregate averaging of about 38 mm to minimize the segregation for most of the applications for the hydraulic structures. A range of 35 to 60% passing a number 4 sieve (4.75 mm); and the range of the 5 to 10% passing a number 200 sieve (75  $\mu$ m) are used in the RCC, as shown in Figure 2.1 and Table 2.1.

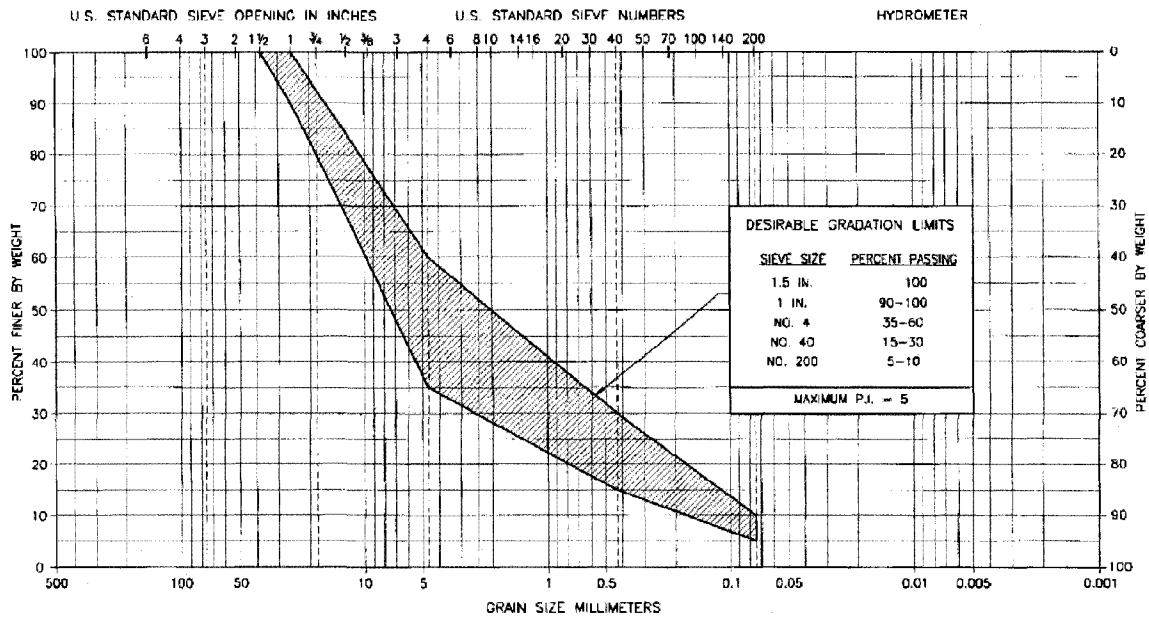


Figure 2.1 Desirable gradation for RCC aggregates (Choi and Groom, 2001)

Table 2.1 Recommended RCC aggregate gradation (Choi and Groom, 2001)

Sieve Size	Percent Passing by Weight
38 mm (1.5")	100
25 mm (1")	90 - 100
No. 4	35 - 60
No. 40	15 - 30
No. 200	5 - 10

In addition, the plasticity index of the RCC aggregate should not exceed five (Choi and Groom, 2001; Choi and Hansen, 2005; PCA, 2004), and the recommended RCC-pavement aggregate is shown in Table 2.2.

Table 2.2 Recommended RCC aggregate gradations for pavement (PCA, 2004)

Sieve Size	Percent Passing by Weight
1" (25 mm)	100
3/4" (19 mm)	90 - 100
1/2" (12.5 mm)	70 - 90
3/8" (9.5 mm)	60 - 85
No. 4 (4.75 mm)	40 - 60
No. 16 (1.18 mm)	20 - 40
No. 100 (150 $\mu$ m)	6 - 18
No. 200 (75 $\mu$ m)	2 - 8

Fine aggregate (5 mm to 80  $\mu$ m) and coarse aggregate (20 mm to 5 mm) generally accounted for 75% to 80% of the total volume of the RCC mix, and their ratios affect the strength of the RCC, as shown in Figure 2.2. The coarse aggregate may be either crushed

or rounded. Using the crushed aggregate reduced a risk of the segregation and increased the quality of the paste-aggregate bond, thereby enhancing the concrete's mechanical properties. The 28-day UCS value of the RCC mixes, by using the same Type 10 cement with the same w:c ratio of 0.35 for both crushed and rounded aggregates, was 54.8 and 49.7 MPa, respectively. The UCS value similarly obtained, by using a blended cement type 10-E/FS instead, was 61.4 and 53.6 MPa, respectively. However, their modulus of elasticity was almost identical, and around 30 GPa in 28 days (Quebec Pavement, 2005).

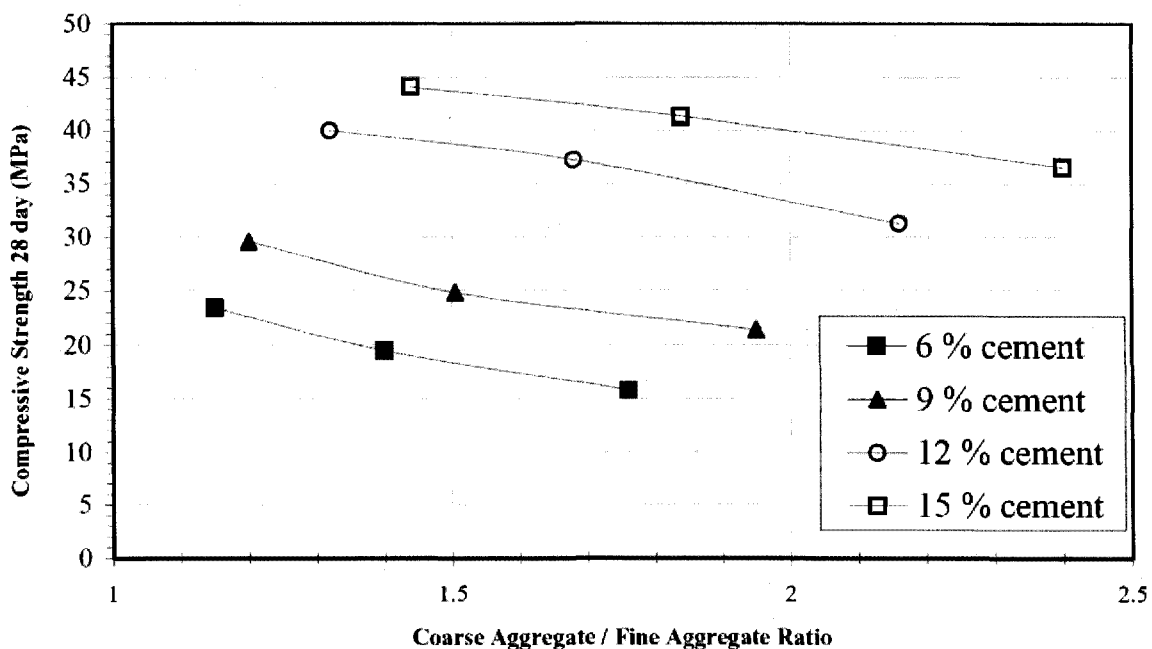


Figure 2.2 Influence of the coarse-fine aggregate ratio on 28 days UCS (Nanni, 1988)

The blended hydraulic cements, and cements containing the pozzolans or the granulated blast furnace slag, could also be used in the RCC (Hisham et al., 2005). The most RCC pavement made to the date had been constructed by using a Type I or Type II Portland cement, and a Class F or Class C flyash. A cement content of about 10 to 16% was usually expected in the mixes (ACI, 2000). However, a usual ratio of weight of the binder material to a total weight of the aggregate should be in the range of 12 to 14% (Pittman and Ragan, 1986). A typical range of cement content in the RCC pavement should be between 10% and 16% (PCA, 1987). The ranges of the binder contents, expressed as a percent of dry weight of the aggregate, reported for the RCC projects could be either as low as 4 to 5% or as high as 15 to 16% (Choi and Hansen, 2005).

For the RCC, the Type II cement is normally used because of its moderate heat generation. Most of the time, a part of the cement up to about 50% could be replaced with a Class F flyash to reduce the rate of heat generation, which controls the cracking and provide a long-term strength gain. The Class C flyash had been used in some cases. Air-entraining admixtures had been used in the RCC with a mixed success, depending on the mix design approach (Hansen and Reinhardt, 1991, in Choi and Hansen, 2005). In general, the RCC does not require a special cement, however, when the RCC is used in

mass concrete, a low-heat cement is recommended. Alternatively, the combination of the cement and a pozzolan had also been used effectively for reducing a heat generation in the concrete (ACI, 1988).

The effectiveness of the flyash on 28-day UCS was proposed to be function of a calcium oxide and a fineness of the flyash. The flyash with a spherical shape and the finer particles provided the better UCS than that with an irregular shape and/or the coarser particles (Tangtermsirikul et al., 2004). The flyash could decrease the shrinkage strain thereby decreasing the cracks, and improve a deformation resistance of the RCC dam. Flyash might fill the interface between the aggregate and the mortar, and improve the pore structure and the density of the RCC dam (Gao et al., 2006).

Lift thickness should not be less than 100 mm and not more than 250 mm. In case of the adjacent paving lanes and the multiple lifts pavement construction, it must be placed within the 60 minutes of placement of the previous lane or lift (PCA, 2004). Particularly, the RCC is subjected to the segregation due to its low paste volume. The RCC properties are particularly affected by the degree of compaction. A typical lift thickness of the RCC pavement should be 150 to 200 mm, however, the thickness for the RCC application had been up to 300 mm (Choi and Hansen, 2005). RCC lifts thicknesses might range from 150 to 600 mm depending on the placement size, a production capacity of the concrete batch plant, the mixture proportions, and the compacting equipment (ETL, 1993).

The compaction effort in the RCC increases the  $\gamma_d$  reducing the optimum MC requirement, as shown in Figure 2.3, and thereby increasing the UCS, as shown in Figure 2.4.

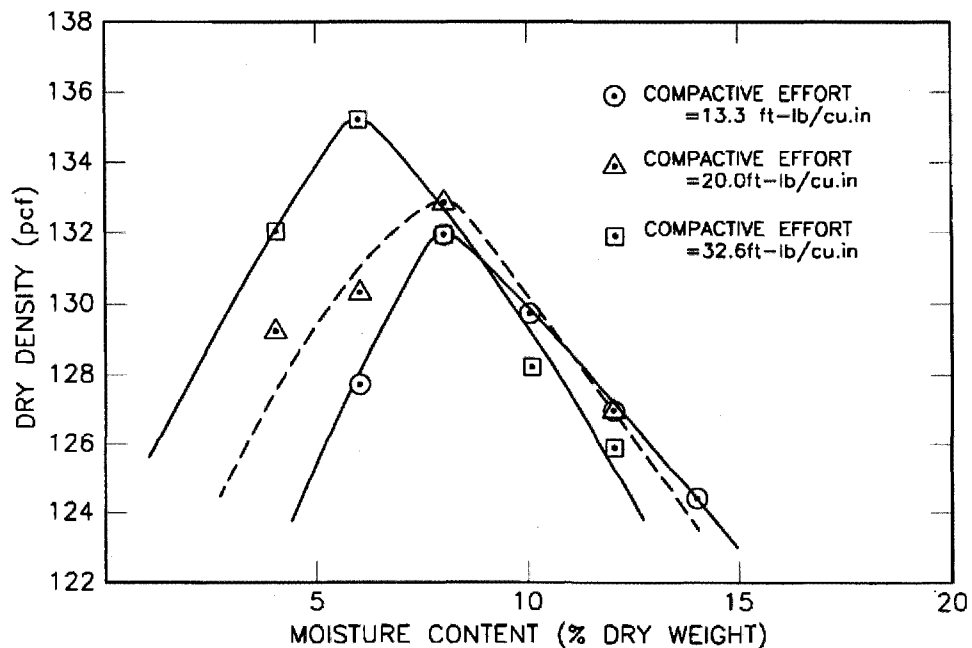


Figure 2.3 Moisture density relationship of RCC mix (Reeves and Yates, 1985, in Choi and Groom, 2001)

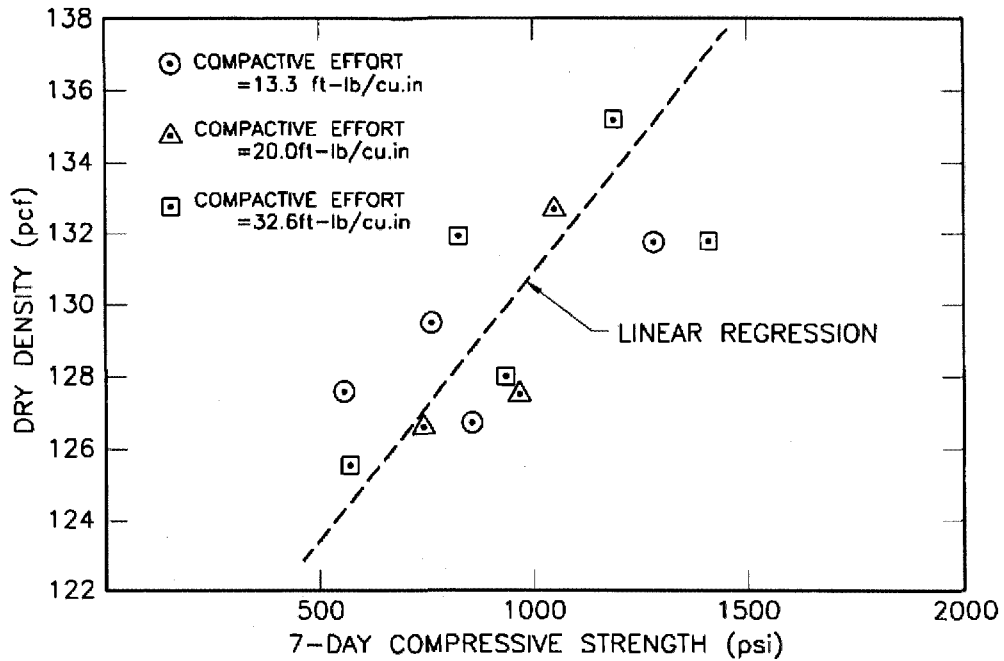


Figure 2.4 Density and strength correlation of RCC (Reeves and Yates, 1985, in Choi and Groom, 2001)

A typical range of evaluating the UCS of the RCC is proportioned for 28 days or later strength up to a year. The cement content in the RCC is determined by a minimum requirement of the UCS, usually 5.17 MPa at 7 days. The typical ranges of the RCC density was from 2,320 to 2,430 kg/m<sup>3</sup> (145 to 152 pcf) (Choi and Hansen, 2005). ACI (1999) reported that the one-year UCS of the RCC ranged from 6.89 MPa to more than 27.58 MPa.

Depending upon the cement used, 28-day UCS value could range from about 24.13 MPa to over 34.47 MPa, and the flexural strength from about 3.45 MPa to over 4.83 MPa (PCA, 1987). Table 2.3 shows the UCS of the cored samples obtained from the projects after several years of the service. Test results on the cores and beams taken from a full-scale test section showed the following relation exists between the UCS and the flexural strength at 28 days (PCA, 1987):

$$\sigma_{ft} = C\sqrt{\sigma_c} \quad 2.1$$

where

$\sigma_{ft}$  = flexural tensile strength (psi)

$\sigma_c$  = compressive strength (psi)

$C$  = constant between 9.4 and 10.8 depending on RCC mix designs.

From the same series of the test results, an average relationship between modulus of elasticity ( $E$ ) and the UCS from the several RCC mixes was determined as:

$$E = C\sqrt{\sigma_c}$$

2.2

where

$C$  = constant between 57,000 to 67,000 depending on RCC mix designs.

Table 2.3 RCC core strength for British Columbia projects, PCA (1987)

Project	Year Built	Sample Date	UCS (MPa)
Caycuse Long Sort Yard	1976	1980	29.03
Caycuse Long Sort Yard	1976	1984	40.54
Lynterm Container Port	1977	1980	32.34
Fraser Mills Long Sort Yard	1982	1983	32.41
Bullmoose Coal Mine	1983	1983	15.17
Fraser Surrey Dock	1984	1984	31.51

Botman et al., (2007) reported the properties of the RCC placed at the Norfolk International Terminals (NIT) by the Virginia Port Authority (VPA) during 2002 to the summer 2006. The 7-day UCS from 1051 numbers of the 150 mm diameter field samples ranged from 19.7 MPa to 20.1 MPa with a cement content of 11 to 12%, and the dry densities varied from 2200 to 2230 kg/m<sup>3</sup> by using the aggregate as per PCA (2004) gradation specifications. The RCC was placed with a maximum lift thickness of 230 mm with an optimum MC of 6.2 to 6.7%. Field density tests were performed by using a nuclear density gage to verify the minimum required 98% of the laboratory density was being obtained. Typically, six to eight passes with a roller (combination of static and vibratory), immediately following the pavers was required to get the required density. It was found that an increment of 1% on the  $\eta$  of concrete reduced the UCS by 3 to 5 MPa, and it was recommended that the  $\eta$  of the RCC should not be more than 3%. It was also reported that the full-depth cores were split and tested as a top and a bottom samples. Consistently, the bottom core had a 20 to 25% higher UCS, which was likely due to the improved curing and additional compaction efforts.

The 28- and 90-day UCS values of a high performance RCC obtained from a 150 mm diameter cylinder sample were higher than 132 MPa and 142 MPa, and from the 150 mm cube were higher than 156 MPa and 171 MPa, respectively, with modulus of elasticity value higher than 48 GPa. The tested samples were prepared by using a type I Portland cement, a densified silica fume, the basalt coarse aggregate with a maximum size of 38.1 mm, siliceous river sand with the maximum size of 2.38 mm, as well as a super-plasticizer (Ribeiro et al., 2000).

The strength to density ratio was the highest for a w:c ratio of 0.45, and their ratio of 0.40 to 0.50 seemed to be more suitable in a hot weather than the common 0.30 to 0.40 in a normal and cold weather (Hisham et al., 2005).

The RCC differs from the rockfill as the paste volume fills or nearly fills the aggregate voids to produce a dense mixture (Tesarik et al., 2003). A RCC dam generally had a maximum aggregate size of 76 mm and the UCS value in the same range as the rockfill. A reported average UCS and a deformation values obtained from the laboratory

specimens were 11.5% higher than that of the values obtained from tests on cored samples retrieved from a placed material. Laboratory UCS values for 28 to 365 days ranged from 4.34 to 21.37 MPa, and the deformation modulus values varied from 10 to 23 GPa, respectively (ACI, 1999, in Tesarik et al., 2003).

### **2.3 Backfill Types**

The use of a hydraulic mine backfill in the North America was first recorded by the Philadelphia and Reading Coal and Iron Company at Shenandoah, Pennsylvania in 1864. That mine backfill was used to prevent a church from being destroyed due to surface subsidence (Hassani and Archibald, 1998). The evolution of the backfill technology was closely related to the establishment of the new mining methods. Around the turn of 21<sup>st</sup> century, it was used as a means of disposing a large quantity of waste without a full knowledge of the backfill properties and other consequences (Nantel, 1998).

The Noranda's Horne Mine introduced the slag and tailings as the mining backfill as early as in 1930. The hydraulic backfill, by using the tailings and alluvial fills, to provide working floor were common in the 1940s and 1950s, thus permitting an adoption of the cut-and-fill mining. In the cut and fill stopes, an addition of a Portland cement to the portions of the backfill material was initiated in the late 1950s. In the early 1960s, the rockfill and the CRF were introduced, followed by the adoption of an undercut and fill, a blasthole, and a vertical-retreat mining method. The 1970s saw different mining methods as result of a significant development in the backfill system with a better understanding of its properties. The 1990 had been considered by many as the decade of a high-density tailings fill and a pastefill (Nantel, 1998).

The fill materials commonly used can be classified into following three groups (Hassani and Archibald, 1998):

- An inert material (commonly mill tailings, sand or gravel, waste rock and coarse slag).
- A binding agent (mostly Portland cement, ground slag, flyash) to improve the fill strength.
- The chemical additives (flocculants, accelerators, and retarders) to improve the fill permeability, flowability of a slurry and consolidation properties of a fill.

Similar to a concrete (Neville, 1987), mine backfill can be considered as a composite product that contains aggregate, cement or binder and water. In most cases, the primary components in the mine backfill are comprised of a singular aggregate such as mill tailings, rock or sand. Some of the familiar names associated with the single aggregate fills include a cemented rockfill, a hydraulic fill (mill tailings or sand), and a pastefill (Annor et al., 2003). Unlike singular aggregate fill, the composite backfill may be prepared from a mixture of the waste rock, tailings, sand and the metallurgical by-products to ensure a broad particle gradation and an optimal strength (Annor, 1999).

The three major types of the backfill are slurry fill, paste fill and rockfill (Hassani and Archibald, 1998), although the composite fill type (combination of these main fill types),

according to Annor (1999), exists as one of the kind in the modern mine backfill. These main fill types can also be classified into cemented or uncemented backfill types based on the presence of a binder in that fill or not. The three major backfill types, their advantages and disadvantages are briefly described below based on the information obtained in Hassani and Archibald (1998).

### **2.3.1 Hydraulic or Slurry Fill**

A conventional slurry fill, prepared either on the surface or underground, includes classified mill tailings (generally with 10  $\mu\text{m}$  fraction less than 20% of its total mass), sand (generally with less than 2 mm), and/or rock materials (generally less than 60 mm). It is normally mixed with a binding agent and water with its placement pulp density of less than 70% by weight (Hassani and Archibald, 1998), and a percolation rate less than 100 mm/hr (Hassani and Archibald, 1998; Nantel, 1998).

Advantages of slurry fill are the followings:

- Relatively simple to install the infrastructure and operate them, thereby requiring a minimum technical supervision.
- A better control of all the constituents at the fill stations securing the fill quality and the mixture density.
- A simple desliming technology to increase the percolation rate to a 100 mm/hr, and usually achieved by using the hydrocarbons.
- Normally, possible to avoid a pumping by optimizing the pipeline lay out.
- Tailings, as a mill waste, readily available in the most mines and reduction in the surface waste disposal by the mill waste's utilization.

The following are the disadvantages of slurry fill:

- Excess water needs to be recovered from the stopes, and pumped to the surface; the permeability of a placed backfill is a critical design criterion.
- A strength reduction of the filled body in a stope by a cement marbling because of the segregation of the cement from the inert fill due to the presence of excess water.
- The slime produced during stope drainage, which requires a time consuming and a costly clean up.
- A possibility of an interruption in the mining operations, especially in cut-and-fill mining due to the bulkhead dewatering facilities, a construction and a fill curing process.
- A possibility of a binder-washout depending on the fill property.

### **2.3.2 Paste Fill**

Paste fill, produced by utilizing the total tailings, mostly sand and waste rock, has an appearance like toothpaste with a higher pulp density between 75% to 85% by weight depending on a gradation and the  $G_s$  of the solids. The fill material generally transported from the surface, and a binder is added at preparation sites or immediately prior to the placement. There is no need of in situ dewatering as in the case of slurry fill.

The main advantages of paste fill are:

- Requires a less cementing agent than the slurry fill to achieve the same strength.
- Tailings can be almost fully utilized as backfill, thereby remarkably reducing the surface disposal and its environmental cost.
- A necessity of less bulkhead facilities as a little or no excess water to drain off from the stope, therefore, speed up the production reducing the cyclical nature of the mining.

The disadvantages of the paste fill are the followings:

- Development of a high pressure in the lateral transportation pipes at the long horizontal runs requiring a suitable positive displacement pump.
- A necessity of superior dewatering facilities to enable the concentrations required a paste-flow to be obtained without a loss of the fines.
- A possibility of a liquefaction problem.
- Requires a higher level of technology, more supervision and an accurate QC.

### **2.3.3 Rockfill**

Waste rock from an underground development or a surface quarry is often dumped into the raises, and then distributed by the trucks or conveyors to the stopes. During the CRF preparation, the cement slurry can be introduced by a pipeline and mixed with the waste rock prior to the placement or can be used to post consolidate the placed rockfill.

The advantages of rockfill are listed below:

- A simple preparation system.
- Utilizes the cost free waste rock, thereby reducing the waste disposal on the surface.
- Provides a relatively high strength when the waste rock consolidated with cement.
- Avoids the stope dewatering.

The main disadvantages of rockfill are:

- Requires crushing of the quarried rock, thus the significant transportation, surface production and the haulage costs.
- A necessity of placing the fine material and a cementing agent through the slurry fill into the voids of the rockfill to ensure its competence.
- Segregation of a coarser material to the stope sides during a placement.
- Not suitable for a tight filling of a stope.
- Only partial utilization of the tailings, so requiring a considerable surface disposal.

### 2.3.4 Summary

This summary of findings is prepared based on the literature review of the backfill's purposes, backfill types and their selection. This summary does not cover a literature review of the RCC and its properties. The followings are the main purposes of the backfilling:

- Mine wall and regional mine stability, and their support, and protect mine workings or increase safety.
- A pillar recovery, reduce mining cost, increased ore extraction and dilution control.
- A working floor or over-head roof.
- Reduce rock burst damage.
- Substitute a rock support.
- Subsidence and fire controls.
- Improve ventilation.
- Environmental protection.

Each backfill type has merits, demerits and some limitations associated with it. The fill type's selection, truly a site-specific to suite the local condition, depends upon a particular requirement of each mining system. Its selection is also usually governed by the purpose of backfilling, availability of the fill material, the mining methods, its economic viability, the environmental related issues, past experiences and its use on a similar condition. The selection of a particular fill type depends on the following aspects:

- The mining method, a production capacity and an operational schedule.
- Backfilling purpose and its strength requirements.
- Availability of the fill material, its preparation, placement system and facilities.
- Environmental requirements.
- Experience and expertise gained on a particular fill type.
- Use of a particular fill type nearly on the similar conditions, elsewhere.
- Placement location relative to the surface.
- Geology of ore, its dimensions, orientation and grade.
- Physical and mechanical properties of the ore and a surrounding host rock mass.
- An overall economic analysis.

The comparison between the properties of slurry fill, paste fill and rockfill is presented in Table 2.4.

Table 2.4 Comparison of properties of the principal backfilling methods (modified after Landriault et al., 1996 and Henderson et al., 1997, in Hassani and Archibald, 1998)

Properties	Slurry fill	Paste fill	Rockfill
Placement state	60% to 75% solids by weight	75% to 85% solids by weight	Dry
Underground transport system	Borehole/pipeline via gravity	Borehole/pipeline via gravity or pumped	Raise, mobile equipment, separate cement system
w:c ratio	High	Low to high	Low
Binder strength	Low	Low to high	High
Placement rate	100 to 200 tonne/hr	50 to 200 tonne/hr	100 to 400 tonne/hr
Segregation	Slurry settlement and segregation, low strength development	No segregation	Stockpile and placement segregation, reduced strength and stiffness
Stiffness	Low	Low to high	High stiffness if placed correctly
Tight filling	less tight fill due to settlement and segregation	Easy to tight fill	Difficult to tight fill
Binder quantity	Requires large quantity	Usually lower quantity required	Moderate quantity
Barricades	Expensive	Inexpensive	Not necessary
Water run-off	Excessive	Negligible	No
Capitol cost	Low	Higher than slurry fill	Moderate
Operating cost	Low distribution cost, lowest cost among uncemented fill	Lowest cost among cemented fill	High

While a slurry fill and paste fill can be used to fill the voids, and achieve a tight filling within a stope, the rockfill continues to provide the best strength support, and for this reason, it is unlikely to be totally replaced by other types of the fill (Hassani and Archibald, 1998). The strength and stiffness achieved by using the CRF have encouraged its increasing use as a backfill, and it has a capacity to stand over exposures not possible economically with any other fill types (Farsangi, 1996).

## 3 Cemented Rockfill (CRF)

This chapter presents a literature review on CRF, covering mainly its strength properties and controlling factors, empirical relationships, laboratory and in situ properties, and placement practices in Canada and around the world. A literature review on the QC and testing practices of CRF is presented separately in Chapter 4, along with a description of the QC and testing practices adopted at DDM site.

### 3.1 Introduction

CRF, a familiar and widely used backfill system (Stone, 1993 and Helms, 1998), is often assumed to have properties similar to those of a weak concrete (Barrett, 1973; Berry, 1980; Arioglu, 1983; McKay and Duke, 1983; Yu and Counter, 1983, 1988; Kosmatka and Panarese, 1988; Yu, 1989; Quesnel et al., 1989, Reschke, 1993; Hedley, 1995; Farsangi, 1996; Farsangi et al., 1996).

Rockfill has been described as any backfill material transported and placed in an underground workplace in a non-saturated state (Landriault, 1992). This definition suggests that the fill systems used for underground civil construction, such as sand and blended alluvial materials, can be considered as forms of rockfill. Mill tailings backfill can also be transported and placed in an underground workplace in a non-saturated state, depending on the mining method and the mode of final delivery or transportation. For the purposes of this study, CRF system refers to the use of coarse waste rock or crushed aggregate mixed or consolidated with binder for backfilling rather than a tailings or sand hydraulic fill system.

CRF is the combination of Portland cement and run-of-mine (ROM) waste rock or graded waste rock. Cement content of CRF ranges from 4% to 7% by weight, and the UCS ranges from 1.38 MPa to over 6.89 MPa (Hassani and Archibald, 1998).

The dominant forms of CRF worldwide consist of rockfill and cement slurry and typically contain cement ranging from between 3 and 5% by weight (Bloss and Greenwood, 1998). CRF in its simplest form is comprised of three basic ingredients: a graded rock aggregate, a cement binder, and water. These components are mixed together and are either conveyed or trucked to the placement area (Reschke, 1998).

A CRF may consist of sized or unsized cemented aggregates containing various types and amounts of binder (Annor, 1999; Nokken et al., 2007). In some Canadian mining operations, the CRF product consists of sized rockfill aggregates generally mixed with cement slurry, usually 5% to 6% by weight of the aggregate at a pulp density of 50 to 60% (Yu, 1990).

The main disadvantages associated with the use of CRF include problems with control of the segregation of the fill product and the need for an extensive preparation plant and transportation system. Additionally, CRF is usually porous and exhibits an average void

ratio ( $e$ ) of approximately 0.51 (Yu, 1990) and, therefore, may not be conducive to tight filling (Yu, 1990; Hassani and Archibald, 1998; Nokken et al., 2007).

Compared to conventional cemented hydraulic backfill, the CRF mixture generally produces a stiffer and higher strength fill with lower amounts of cementing agents (Reschke, 1993; Farsangi et al., 1996) and it develops a higher modulus of elasticity, and angle of friction (Thomas et al., 1979). One reported advantage of CRF is that no drainage problems have been associated with its use (Berry, 1980; Stone, 1993; Reschke, 1993; Bloss and Greenwood, 1998; Hassani and Archibald, 1998).

### **3.2 Factors Influencing CRF Strength**

The factors affecting CRF strength are the cement content, w:c ratio,  $\eta$ , aggregate gradation, and cure time. The general relationships between these factors and CRF strength are listed below (Dickhout, 1973; Thomas et al., 1979; Knissel and Helms, 1983; Lamos and Clark, 1989):

- An increase in cement content will increase the CRF strength.
- The strengths decrease with an increase in the w:c ratio.
- CRF strength increases over time.
- The aggregate gradation affects CRF porosity.
- Low porosities result in higher strengths for a given cement content.

Besides the quality of the cement slurry, a number of other factors contribute to the in situ CRF performance (Yu and Counter, 1983; Yu, 1989; Reschke, 1993; Farsangi et al., 1996):

- Cement content.
- Water to cement ratio.
- Nature and quality of admixtures.
- Degree of mixing between the cement slurry and fill aggregate.
- Aggregate size distribution and percentage of fines.
- Segregation of aggregate during placement.
- Attrition of aggregate during transport and placement.
- Aggregate temperature (i.e., freezing conditions).

Lamos and Clark (1989) tested total 16 different cemented backfill materials to determine the influence of their composition on the UCS and concluded that

- The material composition strongly influences the strength of the cemented backfill.
- Materials with low porosities produce stronger backfills with a given amount and type of cement.
- A reduced water content significantly increases the backfill strength.

Wang and Villaescusa (2001) studied the factors affecting the properties of cemented aggregate fill in terms of strength development and concluded that various factors besides cement dosage contributed significantly to the development of cemented aggregate fill strength: the aggregate particle size distribution, aggregate quality, additional fine

materials, water salinity, admixture dosage and sample scaling with respect to sample size.

Stone (2007) suggested that the aggregate particle size distribution; its strength, durability, MC and clay content; the rock fabric; the w:c ratio and admixture are the factors contributing to CRF strength.

### *Summary*

This summary is based on a literature review of the CRF and factors affecting its strength properties. The various factors affecting the properties of CRF are listed below. Some of them will be described later in section 3.3 dealing with the strength properties of CRF, and others are briefly described here separately.

- Aggregate properties, their gradation and porosity.
- Water and binder quantity and quality.
- Quality of binder slurry and its mixing with aggregate.
- Segregation during transport and placement.
- Curing age and temperature.
- Additional admixtures.
- Sample size.

### **3.2.1 Aggregate Properties**

#### *3.2.1.1 Aggregate Index and Strength Properties*

The backfill is the function of the material type and its strength property (Annor et al., 2003). According to Rodrigues (1990), the intrinsic and index properties of the aggregate such as strength, deformability,  $e$ ,  $\eta$ , rock type and its mineralogy, texture and structure, weathering grade, permeability, density,  $G_s$ , MC; and other properties like its durability, shape, roundness, and size play an important role in rockfill strength. Sometimes, it is important to know the rock type or the source of the aggregate. The durability test is designed primarily for low-strength rock types. Granites, marbles and other crystalline rocks are fissure-prone. Roundness is not a relevant parameter in quarried materials except in sedimentary gravel deposits. Quarried anisotropic rock bodies (gneiss, greywackes, schist) may tend to supply flaky and elongated particles, but not from massive and isotropic rock bodies (granites and other plutonic rocks, some limestone).

It was reported that most mines generally use crushed and screened calc-silicate sedimentary rock, limestone, dolomites, or granodioritic rocks produced as a waste rock during the mine development for the backfill aggregate. The aggregate's mechanical strength influences the backfill's ultimate strength, especially if the aggregate has been weakened by oxidation or weathering. Most sedimentary rocks have a weak bedding plane and tend to break into flat tabular pieces of rock, which can pass sideways through screen decks. Downstream, these particles can cause problems with segregation. Rocks containing high percentages of micas, clay, shales, or friable minerals will adversely affect the CRF performance. The mechanical strength will also affect the aggregate's performance in the crushing and screening plant. A weak or friable rock will tend to

crush much finer and generate more fines than a sound rock particle. The rock's strength is typically assessed in the laboratory by using a compression test or a point-load-test apparatus. While no general specification exists for the strength of an aggregate, a material several times stronger than the backfill specification is generally desired. As a guideline, a rock with a UCS value of 70 MPa or higher is usually recommended for the aggregate of CRF (Stone, 2007).

The rock fabric can have an impact on the backfill strength because the ideal aggregate grading assumes rounded or angular particles with an aspect ratio near unity. Flat or elongated particles affect the packing of the particles and thus affect the  $e$  in the fill. Rock with a strong fabric such as a foliation or bedding will tend to come off the crusher as elongated flat particles. Stone (2007) suggested that an upper limit of 25% is acceptable in the coarse fraction before the strength is impacted.

### *3.2.1.2 Aggregate Gradation and CRF Porosity*

In terms of physical characteristics, the singular aggregate backfills contain high void ratios and, during transportation and placement, are often prone to segregation, which can affect their strength and deformation behaviour as well as their suitability for tight filling (Annor, 1999). Singular aggregate fill materials are therefore required for their optimum strength development to have broad particle-size distributions in order to prevent segregation and a high  $e$ . Unlike uniformly graded aggregates, backfill materials with a well-distributed wide range of particle sizes usually develop low void ratios and porosities (Annor et al., 2003).

Aggregate grading, which controls the density of the mix, generally has the largest impact on backfill strength. A grading deficient in fines will contain voids that reduce the strength, whereas an excess of fines will cause the larger particles to float in a sea of fines. This property, in turn, requires more cement to bind the mix together. However, beyond the grading of the aggregate, the aggregate top size can have a dramatic impact on the coarse and fines segregation effects in the fill. Segregation is an issue if the fill is used to backfill large blasthole stopes, but it can also become severe when the aggregate is re-handled several times when the top size of the fill is over 75 mm (Stone, 2007).

In concrete technology, a well-established relationship exists between the UCS and the sizes of the aggregate materials used for concrete mixes (Neville, 1987). The correct choice of the particle-size distribution provides an optimum design of concrete mixes by reducing  $\eta$  and thus minimizing cement requirements. This approach is widely used as a means of optimizing all types of backfill mix designs. Swan (1985) proposed that the performance of a backfill binder might also be optimized by the correct choice of the particle-size distribution of the fill material.

The aggregate gradation is the measure of the grain sizes within the CRF aggregate, which contains a mixture of coarse and fine aggregate. Grain sizes larger than 4.75 mm define coarse aggregates, while grain sizes below this size define fine aggregates (Lamos, 1993). However, in this study at the DDM site, the grain sizes with  $\geq 10$  mm and  $< 10$  mm are considered to be the coarse and fine aggregate, respectively.

The optimal aggregate gradation minimizes the void space or  $\eta$  and enhances CRF strength. The ideal grading for a CRF aggregate has been shown to follow that of the Talbot and Richard (1923) grading formula used in concrete design (Stone, 1993) as follows:

$$P(u) = 100 \left( \frac{u}{u_{max}} \right)^N \quad 3.1$$

where

$P$  = percent passing by mass finer than opening size  $u$

$u$  = opening size (mm)

$u_{max}$  = maximum particle size (mm)

$N$  = distribution constant.

The optimal grading is that which yields the lowest inter-granular  $e$  or the least voids. For concrete, an  $N$  value of 0.5 is considered ideal since each particle is sized to fit in the voids of a coarser particle, thus minimizing the void space (Stone, 2007). The curve has been shown to work for CRF, but complete application of the Talbot curve is not practical due to placement difficulties (Swan, 1985), and it was developed for concrete containing 10% cement (Bloss and Greenwood, 1998). However, the Talbot  $N$  value can be used to manipulate the mix design based on the placement method (Stone, 2007) (Figure 3.1).

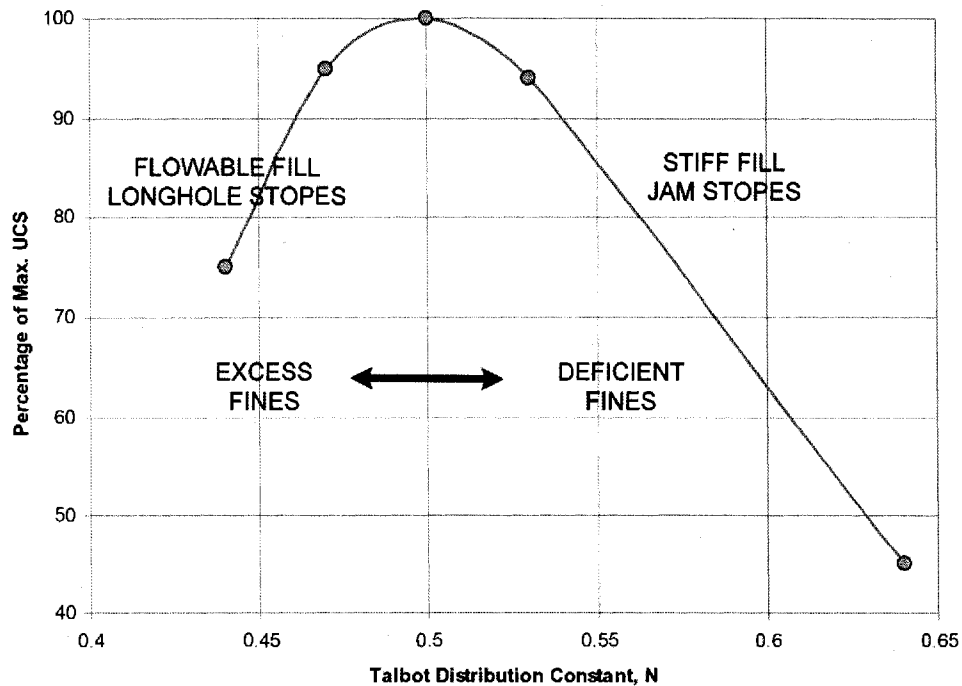


Figure 3.1 Ideal grading for CRF (O'Toole, 2004)

When  $u_{max}$  is fixed as 50 mm in case of at DDM site, then, the Talbot N value controls the ratio of coarse to fines in a CRF aggregate (fines being particles less than 10 mm diameter). A higher N value produces a fill with deficient fines and hence a larger e. A lower N value produces a fill with excess fines and a lower e. Experience has shown that CRF backfills for longhole stopes perform better on the excess fines side of the curve (i.e. on the side with lower N values). In this case, a N of 0.35 to 0.45 is considered ideal, with a minimum fines content of 25%. On the other hand, in drift and fill stopes where the fill is placed by jamming; a very stiff backfill is required. In this case, it is desirable to be on the right side of the ideal, with the N value of 0.55 to 0.65 (Stone, 2007).

Brechtel et al. (1989) reported that the strength of the CRF is optimized at Cannon Mine by using a 55% coarse and 40% fine aggregate, which will be discussed later in section 3.3.2.

The test results at Kidd Creek indicated that addition of sand at 5% of the aggregate by weight increased the UCS by 40% because of the thickening of the layer of the cement slurry coating on the aggregate. However, the UCS reduced 66% after adding sand up to 30% of the aggregate (Yu, 1989; Farsansi and Hara, 1993; Farsangi, 1996) because little cement slurry was left to coat the aggregate. A proper proportion of sand in CRF was found to enhance its strength characteristics (Yu, 1989; Farsangi, 1996).

Arioglu (1983) suggested that the UCS of aggregate fill (composite marble aggregates and tailings) was independent of its particle-size distribution. On the other hand, Annor (1999) showed that two particle-size distribution parameters, the Uniformity Coefficient ( $C_u$ ) and the Coefficient of Curvature ( $C_c$ ), could be used to indicate the effectiveness of the strength development in composite backfill materials. Well-distributed materials are generally represented by ( $C_u$ ) values greater than 4.0, and ( $C_c$ ) values of more than 1.0. They normally produce higher UCS, and their values range between 1.44 to 6.54 and 9.15 to 59.7, respectively, for the rockfill aggregate.

The coefficients of curvature and uniformity are determined as follows:

$$C_c = \frac{(D_{30})^2}{(D_{60}) \cdot (D_{10})} \quad 3.2$$

$$C_u = \frac{D_{60}}{D_{10}} \quad 3.3$$

where

$D_{10}$  = grain size at 10% passing

$D_{30}$  = grain size at 30% passing

$D_{60}$  = grain size at 60% passing.

High  $\eta$  results in a large amount of void space within the CRF mass, and this void space reduces the binding of the aggregate. Common CRF porosities range from 33% to 45% (Hassani and Archibald, 1998). Porosity is affected by the water content, aggregate gradation, and fill placement (Stone, 1993). Porosity is the measure of the void space within CRF, which directly affects CRF density or its weight. As the porosity increases, the density decreases, resulting in a decrease in CRF strength.

### 3.2.1.3 Aggregate Clay Content

Stone (2007) reported that clays have a number of deleterious impacts on CRF including the following:

- Clay coatings on aggregate fragments can prevent proper cement bonding with the aggregate, thereby significantly reducing the strength of the backfill.
- Increasing the plasticity of the cement slurry tends to increase its viscosity, reducing the workability of the slurry mix. In extreme cases, the cement slurry can become stiff enough to cause the aggregate to ball together in the mixer or in the backs of trucks.
- The clay fines can rob the aggregate of binder.
- Some clays will adsorb water into their crystalline matrix, thereby effectively reducing the w:c ratio and causing the mix appear too dry.

In general, there are three main types of problem clays (Stone (2007):

- Montmorillonitic clays derived primarily from the weathering of volcanic rocks. These clays are highly reactive and can easily absorb 4 times their weight in water, rob the backfill of free water, and make the mix become too dry.
- Illite clays primarily derived from the weathering of micas. These clays have medium reactivity and can absorb 2 times their weight in water.
- Kaolinitic clays primarily derived from weathering of feldspars in crystalline rocks such as metamorphics. These clays are low in reactivity and can absorb their weight in water, affecting the plasticity of the cement slurry and thereby increasing its viscosity or stiffness.

The impact of the clay content on the CRF quality is illustrated in Figure 3.2, which shows a hypothetical CRF mix with a total w:c ratio of 0.7. When increasing quantities of water-absorbent clays are added, the resultant or effective w:c ratio decreases. This exercise illustrates that clay contents above 3% by weight can have noticeable impacts on the resultant w:c ratio in the CRF.

The Figure 3.2 illustrates that when the targeted w:c ratio of 0.7 with its assumed maximum acceptable range of up to 0.66, highly and moderately reactive clay contents greater than 2.5% and 5%, respectively, can produce CRF mix too dry, thereby providing the resultant w:c ratio clearly at an unacceptable range.

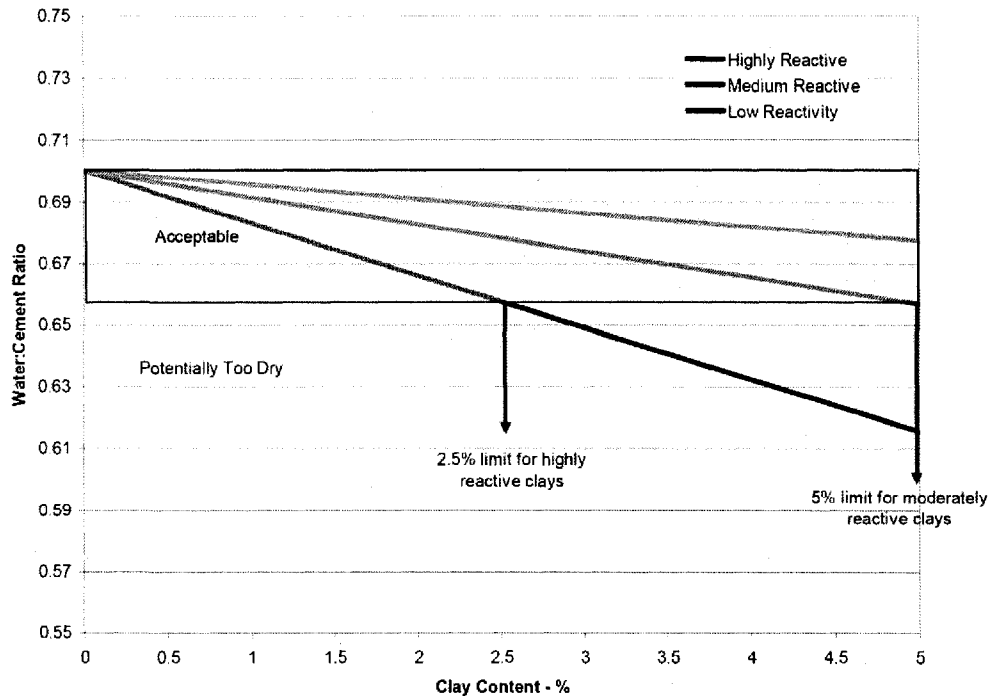


Figure 3.2 Impact of clays on CRF water to cement (w:c) ratio (Stone, 2007)

Generally, when the clay content is greater than 5%, the aggregate should be rejected. For an aggregate with excessive clay, Stone (2007) suggested the following:

- Use additives such as clay dispersants to prevent the clay from absorbing water.
- Wash the stockpiled aggregate in the wash plant.
- Use a vibrating screen deck or tumbling chute to remove the dried clay from the aggregate's surfaces.
- Reject the material if the clay is too wet.

#### 3.2.1.4 Aggregate Degradation

Aggregate degradation (Barrett, 1973) or attrition (Yu, 1989) results from the breaking down of the aggregate during its transportation to the stope. Yu (1989) and Farsangi (1996) suggested that the attrition of the aggregate, proportional to the depth to where it is transported, changes the grading sizes by generating additional finer materials and, therefore, should be taken into account in CRF mix design. Barrett (1973) reported that the introduction of excess fines often results in a higher demand for additional binder to coat the extra-fine material.

The aggregate's durability can lead to excess attrition during handling and re-handling of the aggregate, especially if it is dropped down a fill raise. Some mines have experienced severe attrition rates of more than 25% based on the size reduction of the aggregate from its initial state, and such attrition effect can lead to the presence of excess fines in the backfill. The aggregate's durability is generally assessed in the laboratory by using the Los Angeles Abrasion Index Test (LAA). Acceptable backfill aggregate products have

an LAA of less than 20, marginal materials have an LAA of less than 30, and problems with attrition become severe in materials with a LAA greater than 30 (Stone, 2007).

The aggregate should also be able to withstand extreme weather conditions like freezing and thawing if CRF is used in such conditions.

### *3.2.1.5 Aggregate Moisture Content and Temperature*

A slight change in the MC in the stockpiled aggregate may affect the fill quality significantly (Yu, 1989; Farsansi and Hara, 1993; Farsangi, 1996).

Excessive water in the slurry or aggregate will wash off the cement paste and the cement coating on the aggregate and flush it towards the lowest zone, causing dilution of the cement content in other areas except the lowest zone, resulting in a more heterogeneous fill (Yu, 1989; Farsangi, 1996).

Most mines store their aggregate outside near the portal or near an aggregate drop raise. The MC in the aggregate's stockpile can vary significantly over the year due to rainfall and snow events. This variation, in turn, can cause dramatic changes in the w:c ratio in the CRF mix because the pre-programmed recipes at the batch plant add fixed volumes of water to a batch of CRF.

Variations in the w:c ratio can have a major impact on backfill strengths. At one Newmont operation in Nevada, for example, strength reductions of up to 2.4 MPa were noted after a period of wet weather. This amount is equivalent to half of the fill's target strength. Under normal dry conditions, an aggregate will contain approximately 2 to 3% water by weight. In wet weather, the aggregate can attain MC of 12 to 15%. CRF batched with flyash binders are generally more sensitive to variations in the w:c ratio compared to straight Portland cement (Stone, 2007).

The aggregate temperature affects the CRF strength in a frozen condition. During the winter season, poor coating and delayed initial curing are caused by frozen aggregate. The reported remedial measures taken in such a condition are presented later in this chapter in section 3.2.2.4 while dealing with admixtures.

## **3.2.2 Water and Binder Properties**

### *3.2.2.1 Water Quality*

Yu (1989) and Farsangi (1996) pointed out that the UCS test results from CRF samples with the same binder composition at Kidd Creek, prepared by using underground mine water, were only 50% and less cohesive compared to the samples cast by using potable water supplied from a nearby lake or treated surface pond water. These results might have been due to contaminants such as dissolved solids, oil and grease, and water-treatment chemicals found in underground-recycled water.

The same results were obtained by using potable fresh water and treated surface pond water (Henning, 1988, in Farsangi and Hara, 1993).

Stone (2007) suggested testing the water quality as the water might contain an excess diesel fuel, lubricants, nitrates from explosives, and other contaminants that can severely degrade the strength of CRF.

### 3.2.2.2 Water to Cement Ratio

The w:c ratio is defined as the ratio of the mass of water, exclusive only of that absorbed by the aggregate, to the mass of Portland cement (ASTM C125-00). Theoretically, a w:c ratio of 0.4 is more than sufficient for the complete hydration of Portland cement, but in order to keep the CRF workable, higher w:c ratios are required (Knissel and Helms, 1983). Generally, the optimum w:c ratio of CRF ranges from 1 to 1.2 (Sacrisson & Roberts, 2001; Stone, 1993; Brechtel et al., 1989).

High w:c ratios can cause the cement slurry to percolate through the fill aggregate and rob the fill mass of binder (Stone, 1993). In addition, excessive water increases the  $\eta$ , therefore reducing the CRF strength. If w:c ratios are too low, then incomplete cement hydration is possible. Low w:c ratios also increase the chance of fill segregation. Water-reducing agents can be added to CRF to increase its workability and the dispersion of the cement while also maintaining lower w:c ratios (Farzam et al., 1998).

Stone (2007) also suggested that the w:c ratio has an impact not only on backfill strengths, but also on the fill's workability. Traditional concrete has a w:c ratio of about 0.4 to 0.5, whereas CRF has a ratio mostly from 0.7 to 1.2. Generally, the lower the w:c ratio, the higher the fill's strength; however, at the lower water contents, the resultant backfill can appear to be very dry and tends to segregate easily. The jam fills are prepared on the dry end of the w:c ratios, whereas the fills used for longhole stopes need to be flowable, so they are prepared very wet. A w:c ratio of 0.8 to 1 is generally recommended for jam fills, whereas a ratio of 1 to 1.2 is used for a longhole stope.

The test results from the same mix design in Nevada, presented in Table 3.1, show that increasing w:c ratios produce decreasing strengths.

Table 3.1 Effect of water to cement ratio on CRF in Nevada Mines (Stone, 2007)

Source	w:c ratio	UCS (MPa)
Aggregate 1	0.8	2.28
	1.0	1.70
	1.2	1.46
Aggregate 2	0.8	1.31
	1.0	1.65
	1.2	1.41

### 3.2.2.3 Quantity and Quality of Binder

The quality of the binder and its increasing proportion obviously increases CRF strength. Generally, ordinary Portland cement is used as a binder in preparing CRF mix. However, in some cases, flayash, ground blast furnace slag and other pozzolans are also used to

replace cement. In a Quebec mine using flyash as Portland cement replacement, its replacement varied between 10 to 50% (Farsangi, 1996).

In 1982, Kidd Creek Mine began to use ground blast furnace slag as a substitute for a portion of the Portland cement (Yu and Counter, 1983). In 1984, the blast furnace slag was replaced by type C flyash (Yu and Counter, 1988).

The cement content, the total weight of the binders such as Portland cement, flyash, and smelter slag, is expressed as a percentage of the total binder by weight and described by (Kockler, 2007):

$$\text{Cement (\%)} = \frac{\text{Total binder weight}}{\text{Total binder weight} + \text{Dry aggregate weight}} \times 100 \quad 3.4$$

The cement or binder content is usually considered based on the total weight of the aggregate instead of aggregate's dry weight due to the small variability in aggregate's MC. However, the aggregate's MC should be taken into account if it varies significantly while determining the w:c ratio. In this study at DDM site, the cement content is considered based on the mass of the aggregate.

#### 3.2.2.4 Admixtures

Admixtures play an important role in CRF. Their important functions are to act as retardants that increase the hydration time of the fill, and as water-reducing agents that allow the w:c ratio to be reduced, thereby increasing the fill's ultimate strength while maintaining its workability or flowability.

Retardants such as Delvo and water-reducing agents or plasticizers such as Gelnum are used in Nevada as admixtures (Stone, 2007).

The appropriate selection of an admixture provides benefits such as reduced water content, improved workability, and delayed setting time. An economic analysis can be conducted to determine the net benefit of using a relatively expensive admixture versus the benefits of the higher strength and easier fill transportation and placement that can be obtained with the addition of an admixture (Wang et al., 2002).

A reported remedial measure for dealing with a freezing aggregate during the winter is to add calcium chloride at 2% by weight of the cement to lower the aggregate's freezing point by 12°C and also to provide additional heat for curing (Yu, 1989).

Calcium chloride in solution at 0.4% of the binder by weight (Farsangi and Hara, 1993) and 0.8% of the binder by weight (Farsangi, 1996) can also be used to lower the aggregate's freezing point.

The use of calcium chloride as an accelerator in most civil engineering projects is limited to 2% by weight of the cement. Higher dosages have the potential to decrease the

concrete strengths at later ages due to the calcium chloride's breakdown over time. However, this process occurs at a slower rate at colder temperatures, and 5% calcium chloride by weight of the cement is used in Polaris Mine (Dismuke and Diment, 1996).

### **3.2.3 Quality of the Slurry and its Mixing with the Aggregate**

To obtain an acceptable CRF, the quality and quantity of the binders and aggregate used has to be maintained along with the proper mixing arrangement to coat all of the aggregate with the supplied amount of slurry within a short time duration (Yu, 1989).

A high-quality grout or slurry is regarded as having the following properties (Houlsby, 1990):

- Every particle of cement in the mix is thoroughly wetted. Individual grains are separate from each other without clumps. It is also mixed thoroughly with any other constituents of the mix or admixtures.
- Each cement grain is surrounded by a film of water, which chemically activates the particle, giving the full hydration necessary for strength and durability.
- It is uniform throughout and exhibits some colloidal characteristics because of the maximum gel formation of the cement.

The key to producing a competent CRF is to coat all of the aggregate with binder slurry (Yu, 1989; Farsangi, 1996). A high-quality binder slurry must be used, and it must be thoroughly mixed with the aggregate as quickly as possible to enhance the CRF strength.

### **3.2.4 Segregation**

The segregation of CRF when filling a stope is unavoidable. However, this process can be minimized if fill operations are well planned and closely monitored (Yu, 1989; Farsangi, 1996).

Control of the segregation mechanisms is the key to producing quality CRF as the fill's final strength is significantly influenced by the degree of segregation during placement (Bloss and Greenwood, 1998).

Product segregation often occurs when placing CRF. Differential settling of the fill material causes CRF aggregate to separate during its placement. The segregation is a function of the fill raise orientation, aggregate size, filling methods, and stope geometry (Farsangi, 1996; Annor, 1999). A zone of fine aggregate tends to occur near the impact area, consuming most of cement paste and leaving a low cement content rockfill at the perimeter of the fill cone (Barrett, 1973; Berry, 1980; Yu and Counter, 1983, 1988; Yu, 1989; Farsangi, 1996). The measured fill strength in the impact zone has been reported to be higher than that in other parts of the stope (Yu and Counter, 1983; Yu, 1989; Farsangi, 1996).

Segregation is an issue if the CRF is used to backfill large blasthole stopes, but can also become severe when the aggregate is rehandled several times. This latter impact has

been noted at several operations when the aggregate's top size was over 75 mm (Stone, 2007).

Severe segregation can occur when stopes are filled by using conveyors (Berry, 1980; Yu and Counter, 1983; Yu, 1989), because of the impact velocity caused by the belt's speed and aggregate's subsequent free fall. In contrast, when a stope is filled by using mobile vehicles, only the largest particles have the momentum to travel to the stope wall, and the rest of the material fills the stope by progressively slumping, resulting in a more uniform fill product (Yu, 1989; Farsangi, 1996).

### **3.2.5 Curing Conditions**

#### *3.2.5.1 Curing Time or Age*

Obviously, CRF strength increases with increasing curing time. For concrete, 28 days of curing is the industry standard. Concrete reaches over 90% of its maximum strength in 28 days (Camp and Lambert, 2003, in Kockler, 2007). In addition, over 70% of the 28-day strength develops in the first 7 days if the proper temperature and moisture conditions are maintained (Winter and Nilson, 1979, in Kockler, 2007). Due to the variability of CRF mixtures, curing rates will differ from one mine site to another and may not follow the curing rates for concrete. The CRF tests performed by Peterson et al. (1998) showed that the 28 day-strength was around 70% of 100-day strength. However, most of the reported laboratory strengths are 28 day-strength, which will be used in this study as well at DDM site.

#### *3.2.5.2 Curing Temperature*

The effect of curing the temperature on CRF strength was reported by Annor et al. (2003), who found a slight variation of about 5.4% in other types of composite fills, but noted a large increase in strength (443%) was noted for the CRF for 28 days at curing temperatures of 23°C and 44°C, respectively. It can be concluded that the higher curing temperature produces a higher CRF strength than the lower curing temperature.

### **3.2.6 Sample Size**

The properties of CRF samples have been found to be scale-dependent. Yu and Counter (1983) and Reschke (1993) found that the UCS value decreases with increased sample diameter and aggregate size, and suggested that the in situ CRF strength varies at approximately 66% of the laboratory value based on 150 mm diameter cylinders, and at about 90% for a sample with a 300 mm diameter. This difference has been attributed to the decrease in the weight percentage of the fine materials (Annor, 1999). Hedley (1995) has indicated that the  $\eta$  of CRF samples is controlled by the binder content and the composition of the fine material, and thereby causes the sample size effect.

Yu (1989) also reported that the UCS value obtained at a laboratory at Kidd Creek from 300 mm diameter samples was only 66% compared to that from the 150 mm diameter samples when using the same CRF mix recipe.

Farsangi (1996) suggested estimating the in situ static strength of the CRF mass by using  $(63 \pm 6)\%$  of the CRF laboratory test results obtained from using the 150 mm sample and  $(86 \pm 8)\%$  of the results obtained from using the 300 mm diameter cylinders. However, Wang and Villaescusa (2001) concluded that, for cemented aggregate fill samples with a high  $e$ , the traditional principle that the smaller the sample size, the higher the strength, was not applicable. They based this conclusion on 28-day-cured UCS test data. The test samples for the study were comprised of 100 mm diameter by 200 mm long and 150 mm diameter by 300 mm long cylinders, and their respective UCS values were found to be 7.39 MPa and 8.26 MPa. A possible explanation for this peculiar observation could be that the larger size samples were prepared at higher densities than the smaller samples (Annor et al., 2003).

Annor (1999) found that the 150 mm diameter samples achieved almost twice the UCS of 457 mm cylinders and a deformation modulus almost 10 times greater with the same cement content of 5 to 7% and curing time of 14 to 56 days. Generally for aggregate materials, the strength decreases with increasing sample size due to the presence of fractures and defects, which are often more prevalent in larger size samples than in smaller ones (Annor et al., 2003).

At the Cannon Mine, the average laboratory values of the UCS and modulus obtained from the 457 by 914 mm cylinders were 56% of values obtained from the 152 by 305 mm cylinders when using the same CRF mix (Tesarik et al., 2003).

The details about the sample effect and the justification of the need to correct the laboratory strength values are presented later in this chapter in section 3.3.3 dealing with in situ properties of CRF.

### **3.3 Strength Requirement and Properties**

The application of backfill in mining satisfies various essential functions in the mining cycle depending on the ground conditions and operational requirements. In terms of structural requirements, the following have been identified as some of the roles and purposes of backfill (Thomas et al., 1979):

- In pillar recovery operations, the fill is expected to act as a freestanding pillar, which is unsupported over a significant vertical height. The stronger the backfill, the greater the unsupported vertical height, as stabilized backfills develop higher free-standing heights.
- In conventional cut and fill operations, the backfill must serve as a bearing surface to support mining activities and assists in controlling the dilution of the mined-out ore; therefore, the fill's bearing capacity becomes an essential consideration in these operations.
- When the fill is used to apply regional support in convergence control, the fill must have sufficient stiffness to resist the movement of the surrounding rockmass into the mined void by providing passive support to improve conditions in the void adjacent to an excavation. In this regard, the tight filling to the back of stope is therefore an essential requirement for the mine's global stabilization.

The strength required of the fill to support its own span is a function of the stress that will be generated within the fill mass due to self-weight, degree of arching between solid rock walls, blast damage/abrasion, ground movements and ground support (Ley et al., 1998).

The CRF is designed to withstand gravity loading as well as the dynamic effects produced by blast vibration (Peterson, 1996; Farsangi, 1996). The CRF design requirements depend on the vertical and dynamic loadings, lateral confinement, stope geometry and its closure, strength properties, fill placement, support implications, possible failure modes, and air gaps or cold joints (Donovan et al., 2007).

The most important basic mechanical properties for the design of backfill are its UCS, and permeability in case of slurry fill. The UCS of the fill required in mining operations varies greatly depending upon its application. In cut and fill mining, the 28-day-required UCS is generally less than 1 MPa, but with delayed backfill with pillar recovery, the required UCS may be much higher at up to 5 MPa or even 7 MPa (Hassani and Archibald, 1998).

The variability of the backfill strength requirements is site-specific based on the mining methods (Annor, 1999). Yu (1989) proposed that the CRF in the range of 2.8 MPa to 7 MPa at Kidd Creek should use an average of 5% binder by weight of the aggregate to support an exposed face over 120 m high and 70 m long.

Knissel and Helms (1983) reported that the most important properties of cemented fill are

- Strength (mainly UCS).
- Deformation behaviour.
- Cohesion and angle of internal friction.
- Density and porosity.
- Consistency of the mixture.

In practice, the UCS value is quoted as the main strength, as this value is measured relatively easily in the laboratory (Yu, 1989). In a series of tests, the UCS has been identified as one of the most important parameters to be considered when dealing with a cemented backfill system (Thomas et al., 1979).

### *Summary*

When the backfill is used to provide a component and stable roof support, as in undercut and fill mining methods, the tight filling with a low  $e$  and backfill of sufficient strength are essential requirements.

CRF strength is commonly defined by the UCS, but other engineering properties such as  $\tau$ ,  $\sigma_i$ ,  $E$ ,  $c$ ,  $\phi$ , and Poisson's ratio ( $\nu$ ) all play a part in the CRF overall strength. The UCS value is usually used as an indirect measurement of the CRF modulus and  $\tau$ , and other strength properties are usually estimated based on its UCS value.

### 3.3.1 Empirical Relationships

Although mine fill types have become progressively more engineered products, the selection of fill components is usually site-specific, and the mix formulations used and cement additions made are still based on experiences and various empirical techniques.

The empirical relationships for concrete have been developed relating the UCS to  $\sigma_t$ ,  $\tau$  and  $E$  as shown below (Kosmatka and Panarese, 1988):

$$\sigma_t \approx (5 \text{ to } 7) (UCS)^{0.5} \text{ or } 0.08 \text{ to } 0.12 (UCS) \quad 3.5$$

$$\tau \approx 0.20 (UCS) \quad 3.6$$

$$E \approx 33 (\gamma_t)^{1.5} (UCS)^{0.5} \quad 3.7$$

where

$\gamma_t$  = bulk density (lb/ft<sup>3</sup>)

$UCS$  = uniaxial compressive strength (psi).

The empirical relationships for concrete may not be directly applied to CRF, but they provide a guide for developing CRF empirical relationships. As in case of concrete, the UCS value is usually used as an indirect measurement of CRF modulus and  $\tau$ .

The  $\sigma_t$  was 10% of the average UCS values obtained from 27 laboratory tests conducted at the Turquoise Ridge Mine on 152 mm by 305 mm specimens cured for 28 days (Tesarik et al., 2003).

The empirical relationship developed for UCS and  $E$  of the CRF by various researchers are summarized below.

Swan (1985) proposed that for any given backfill material, the 28-day UCS (MPa) at 20°C is proportional to the cement content by volume ( $C_v$ ), while Yu (1989) proposed that the 28-day UCS (MPa) of 150 mm diameter cylinders can be estimated by the percent weight of the Portland cement ( $b$ ) for <40 mm aggregate. The relationships for estimating the UCS by the volume or percent weight of cement reported by Swan (1985) and Yu (1989) are given below:

$$\sigma_c \propto C_v^{2.36} \quad 3.8$$

$$\sigma_c = 1.5 \cdot e^{0.25b} \text{ for } 5 \leq b \leq 25 \quad 3.9$$

Henderson and Lilley (2001) developed a relationship among  $\eta$ , percent cement or binder content by weight ( $b$ ), and the UCS at the Kanowna Belle Gold Mine, Western Australia. The relationship is shown by

$$\sigma_c \approx 63 \cdot \left( \frac{b}{\eta} \right)^{1.54} \quad 3.10$$

where

$$\text{Porosity, } \eta (\%) = \frac{\text{Void Volume}}{\text{Total CRF Volume}} \times 100 \quad 3.11$$

Berry (1980) and Hedley (1995) proposed that the strength of backfill material is directly proportional to  $b$ , and inversely proportional to  $\eta$ . Hedley (1995) determined that the following relationship exists between UCS (MPa) and cement/porosity ratio ( $b/\eta$ ) based on a selected CRF and paste backfill data:

$$\sigma_c = 27 \cdot (b/\eta)^{1.57} \quad 3.12$$

Annor (1999) developed the relationship for CRF, shown in

Figure 3.3, as given below:

$$\sigma_c = 13.2 \cdot (b/\eta)^{0.90} \quad 3.13$$

In a study of mines using mainly CRF, and using values obtained from concrete, Swan (1985) determined that the following relationship exists between the deformation modulus,  $E$  (GPa) and the UCS (MPa) of CRF, as shown in Figure 3.4:

$$E = 0.21 \cdot (\sigma_c)^{1.44} \quad 3.14$$

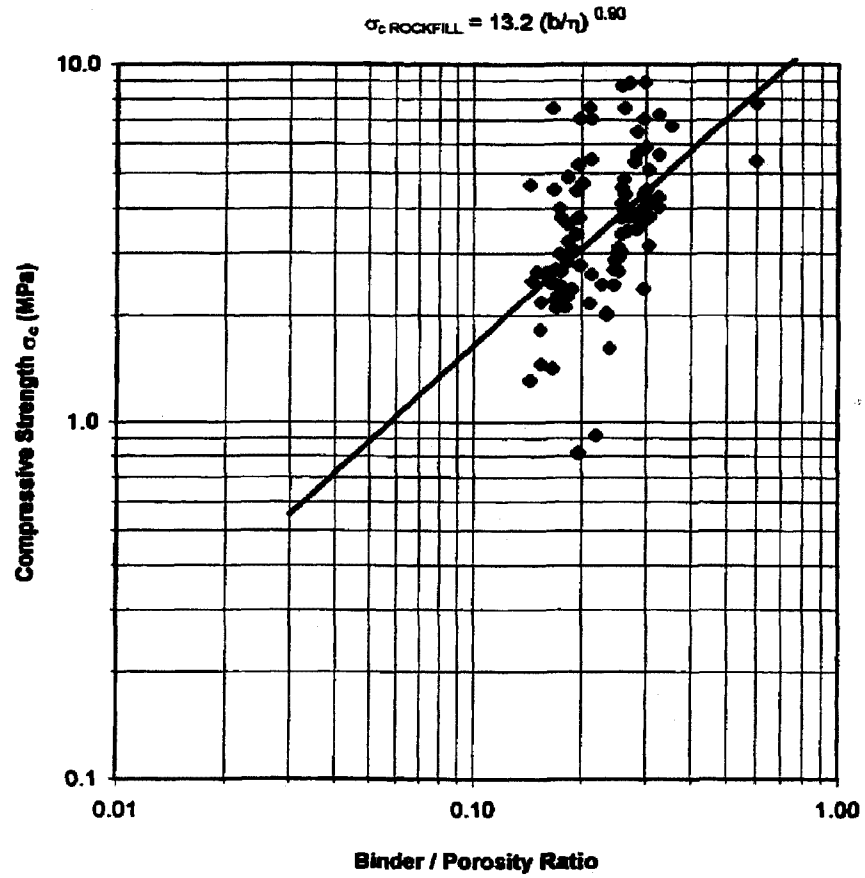


Figure 3.3 UCS as a function of binder/porosity ratio for CRF (Annor, 1999)

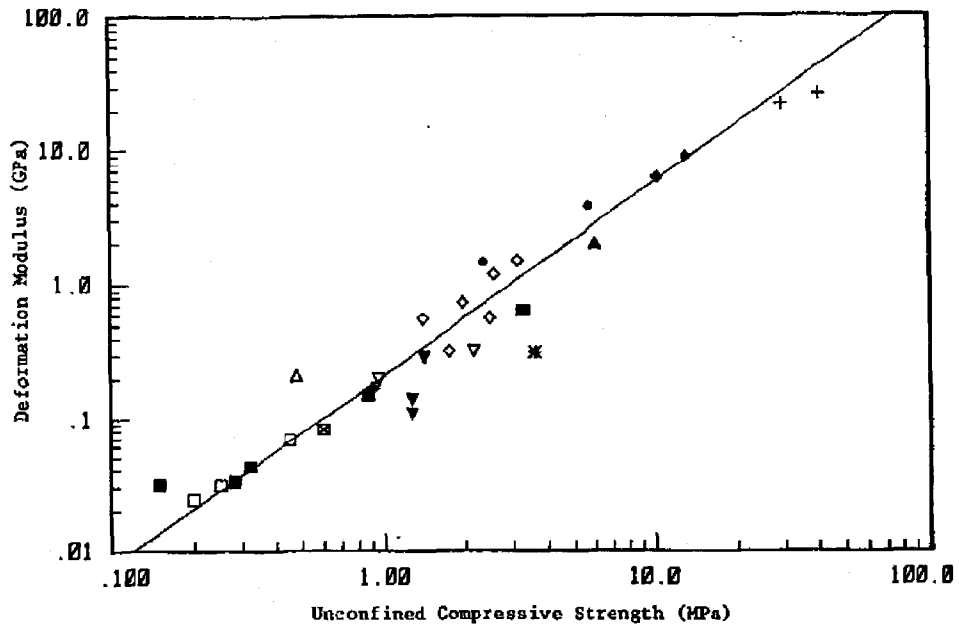


Figure 3.4 Relationship between deformation modulus and UCS of cemented backfill mostly CRF and concrete (Swan, 1985)

Annor (1999) developed a similar relationship between deformation modulus,  $E$  (GPa) and UCS (MPa) for CRF, shown in Figure 3.5 and presented below:

$$E = 0.35 \cdot (\sigma_c)^{1.16} \quad 3.15$$

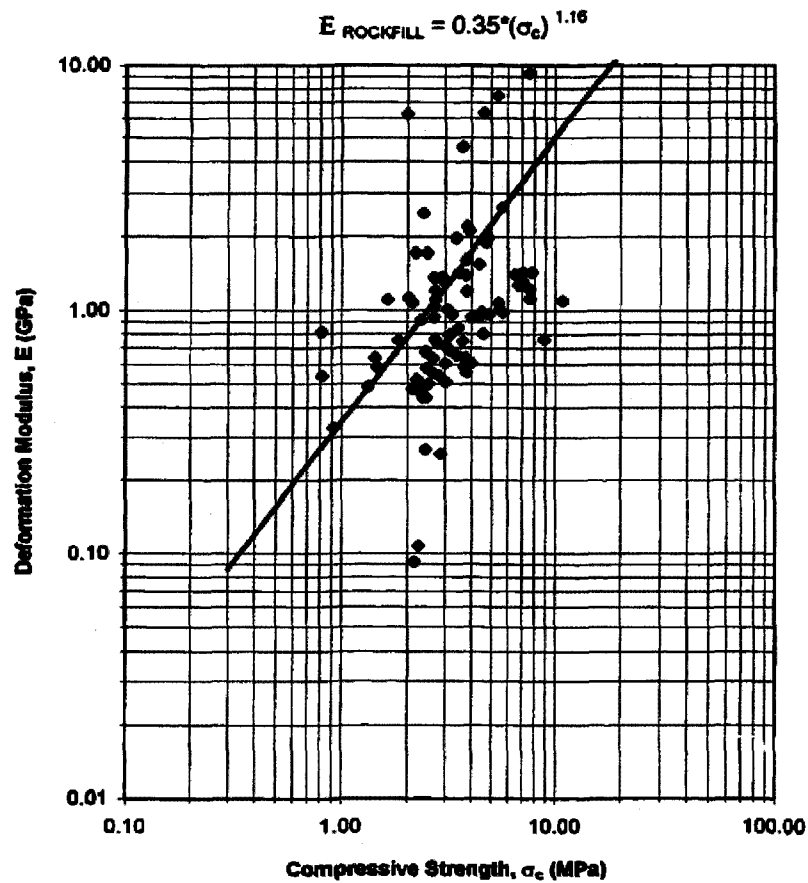


Figure 3.5 Relationship of deformation modulus and UCS of CRF (Annor, 1999)

Annor (1999) also showed that the UCS and  $E$  both are inversely related with the  $e$  and the  $\eta$  of CRF:

$$\sigma_c = 0.57 \cdot (e)^{-1.66} \quad 3.16$$

$$\sigma_c = 8086.2 \cdot (\eta)^{-2.40} \quad 3.17$$

$$E = 0.0122 \cdot (e)^{-4.88} \quad 3.18$$

$$E = 3458.5 \cdot \exp^{-0.28(\eta)} \quad 3.19$$

Zhu (2002) suggested that the value of the UCS for CRF could be determined by using the relationship proposed by Ganano and Kirkby (1977). This relationship is established by using cemented hydraulic and CRF samples (Figure 3.6). The  $\sigma_i$  is evaluated by using 10% of the UCS.

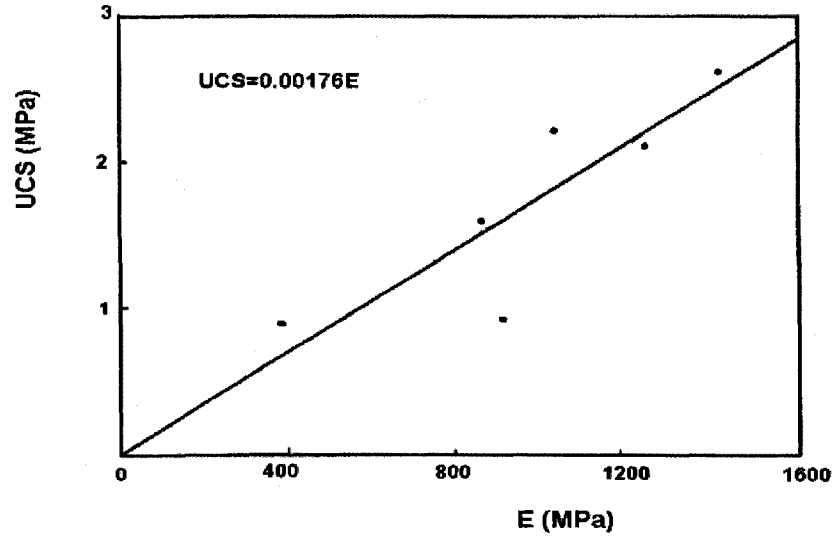


Figure 3.6 Relationship between UCS and elastic modulus (Ganano and Kirkby, 1977)

$$UCS = 0.00176 \cdot E$$

3.20

Kockler (2007) reported that the modulus value (psi) obtained between 30% and 70% of the axial stress and strain curve was related to the UCS value (psi) at 2.5% MC in 200 mm by 400 mm cylindrical specimens with curing periods from 7, 14 and 28 days. The CRF samples prepared by using <50 mm aggregate with a grain size close to Talbot and Richard curve (1923) with  $N = 0.5$  (Figure 3.7). The CRF was prepared by using 5.7% cement and a w:c ratio of 1.

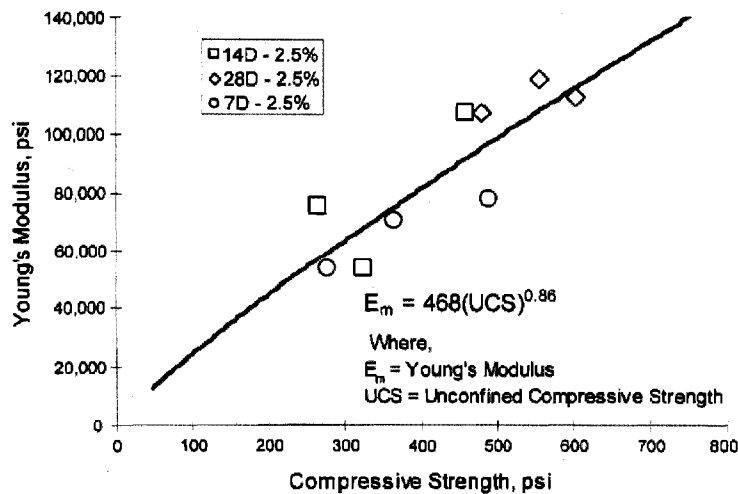


Figure 3.7 Relationship between UCS and Young's modulus (Kockler, 2007)

$$E = 468 \cdot (\sigma_c)^{0.86} \quad 3.21$$

When  $E$  (GPa) and  $\sigma_c$  (MPa), then the given relationship can be expressed as

$$E = 0.2332 \cdot (\sigma_c)^{0.86} \quad 3.22$$

### 3.3.2 Reported Laboratory Properties

Knissel and Helms (1983) pointed out that the petrographic conditions of the aggregate used in CRF are different from one mine to another and comparing the test results from different mines is difficult. Some of the reported CRF properties have already been included earlier in this chapter in section 3.2 dealing with the factors affecting CRF strength; others are described below.

In a study by Farsangi (1996), almost every mine using the CRF system was employing the blasthole stoping method with a stope size ranging from 125 m long by 3 m wide to 61 m long by 24 m wide. The UCS of the fill required in the mining operations varied over a wide range from 1.4 MPa to 7 MPa.

The UCS value of the CRF at the Williams Mine, containing 6.25 to 6.5% by weight of binder (equal portions of Portland cement and flyash), and graded rockfill maintaining 75% <150 mm and 25% <16 mm had an average 5 MPa after 28 days of curing (Ley et al., 1998).

The average UCS of 4.8 MPa was obtained from 150 mm diameter cylinders prepared from the dumped rockfill, excluding aggregate >75 mm, at Lamefoot Mine, Washington, with a w:c ratio of 0.8:1 and a maximum size of 450 mm ROM waste, as aggregate (Reschke, 1998).

The test results obtained by Kockler (2007) after 28 days of curing of CRF samples produced in the laboratory by using the <50 mm limestone aggregate containing an average of 2.5% MC by weight with an average of 5.7% cement by weight and a w:c ratio of 1:1, are summarized in Table 3.2.

Table 3.2 CRF laboratory properties (Kockler, 2007)

Property	Range
Bulk Density, $\gamma_t$ (kg/m <sup>3</sup> )	2114 - 2163
UCS, $\sigma_c$ (MPa)	3.31 - 4.17
Young's Modulus, $E$ (GPa)	0.74 - 0.82
Poisson's Ratio, $\nu$	Undetected
Tensile Strength, $\sigma_t$ (MPa)	0.74 - 0.99
Cohesion, $c$ (MPa)	0.97 - 1.31
Internal Friction Angle, $\phi$ (°)	35 - 40

Brechtel et al. (1989) reported that the strength of CRF is sensitive to both the cement and coarse aggregate contents. An optimized backfill mixture was produced at the Cannon Mine, with 55% coarse and 40% fine aggregate, 5% cement, and a w:c ratio of 1:1 (Figure 3.8). The fine aggregate was pit-run material, mostly <10 mm in size. The commercial coarse aggregate was screened to remove >70 mm and <5 mm material. The typical aggregate particle size is presented in Table 3.3.

The reported 28-day laboratory UCS value of the prepared samples from a delivery truck ranged between 2.48 MPa to 15.01 MPa with an average of 8.45 MPa.

Table 3.3 Backfill aggregate description (Brechtel et al., 1989).

Grain Size (mm)	Percent Passing (%)	
	Coarse Aggregate	Fine Aggregate
75	100	100
50	90	100
35	70	100
25	40	100
19	20	100
13	10	100
9.5	4	90
4.8	1	87
2	0	74
1	0	48
0.5	0	20
0.1	0	1
0.074	0	1

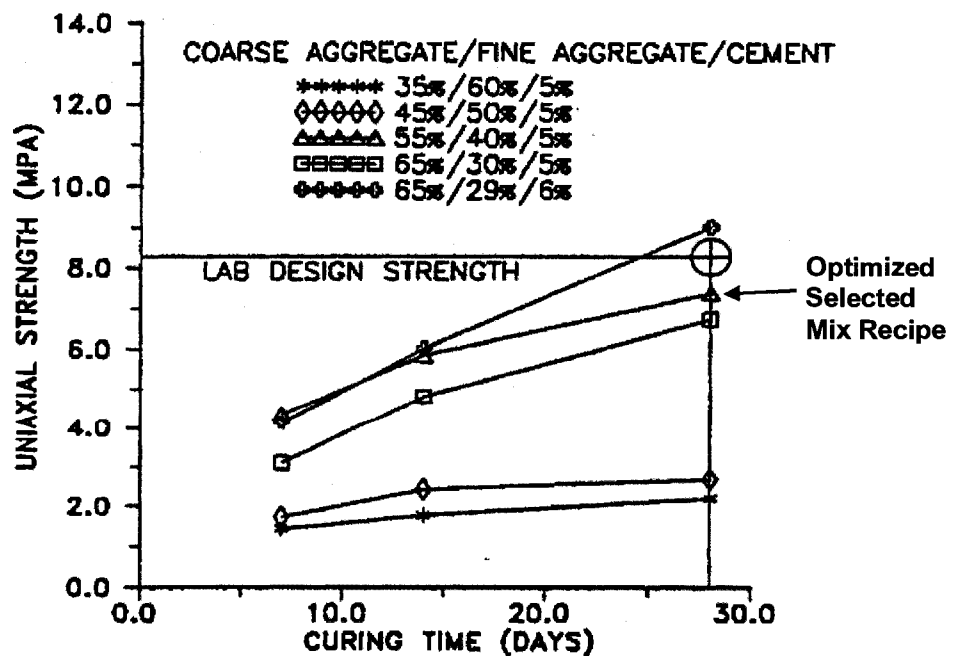


Figure 3.8 Effect of coarse aggregate content on CRF strength (Brechtel et al., 1989).

The use of a specified laboratory UCS value of 8.3 MPa obtained by using 5 to 6% cement was proposed by Brechtel et al. (1989) at the Cannon Mine to achieve a CRF in situ strength of 5.8 MPa to support a stope 7.3 m wide and up to 29 m high. The difference in the proposed strengths was to account for the impact of segregation and size effects in the field.

In a study by Nokken et al. (2007), the test result were obtained from the Northern Ontario Mine by using aggregate consisting mainly of <152 mm sized material with a binder of ordinary Portland cement (Type GU) added at 5% by weight of the dry fill material. The test result obtained from 150 mm cylinders, which were prepared without using > 50.8 mm aggregates, The  $e$  of the CRF was found to be 0.37 (27%  $\eta$ ), although other studies have suggested that the CRF possess high  $\eta$  (33%, or a 0.51  $e$ ). The 28 day- CRF strength test result showed that a UCS value of 4.37 MPa, and a deformation modulus of 12.47 GPa. According to them, the >50.8 mm rockfill aggregates were not used in the preparation of the UCS test, as the minimum cylinder diameter is required to be at least three times the largest aggregate size.

Annor (1999) concluded after comparing 152 mm by 300 mm cylinder samples that CRF achieved a UCS of more than 6 MPa and a deformation modulus more than 9 GPa, which are significantly higher than those of other backfill types.

Annor (1999) reported that 150 mm diameter samples achieved almost twice the UCS of 457 mm diameter cylinders and a deformation modulus almost 10 times greater, with the same cement content of 5 to 7% and a curing time of 14 to 56 days. The average values from the total 101 CRF samples with 150 mm and 457 mm diameter sizes with cement content 5 to 7% at a curing time of 14 to 56 days are presented in Table 3.4.

Table 3.4 Properties of CRF with variation of sample size and cement content (Annor, 1999)

Age (Days)	Diameter (mm)	Cement (%)	UCS (MPa)	$E$ (GPa)	Void Ratio, $e$	Porosity, $\eta$ (%)
14	150	5	6.33	1.17	0.30	22.9
	457	5	2.83	0.74	0.35	26.0
	150	7	6.44	7.69	0.30	22.9
	457	7	3.69	1.30	0.33	24.7
28	150	5	4.37	12.64	0.38	27.4
	457	5	2.54	0.96	0.41	29.1
	150	7	6.26	12.74	0.32	23.0
	457	7	3.66	1.48	0.35	25.7
56	150	5	5.44	7.20	0.41	28.7
	457	5	2.60	0.73	0.42	29.5
	150	7	6.63	17.91	0.35	26.0
	457	7	3.12	1.02	0.37	26.9

Based on Stone (2007), the main mix components and achieved UCS values of CRF from a range of underground mines in Nevada are presented in Table 3.5.

Table 3.5 CRF mix and UCS values for Nevada Mines (Stone, 2007)

Mine	Aggregate		Binder	
	Top size (mm)	Coarse (>10 mm)/Fine	% Binder	UCS (MPa)
Deep Post	35	70/30	6.75	5.52
Carlin East	30	70/30	6.1	4.83
Deep Star	30	75/25	6.1	4.83
Rodeo	35	87/13	8.0	4.83
Meikle	20	60/40	6.0	5.52
Bullfrog	30	70/30	7.2	4.48
Turquoise Ridge	30	70/30	7.5	5.52

The 152 by 305 mm cylindrical samples tested at the Turquoise Ridge Mine gave an average tangent modulus of 2.26 GPa with an average UCS of 9.6 MPa with 7.8% binder (5.8% cement and 2% flyash) and a water to binder ratio of 0.42, by using <51 mm crushed waste rock aggregate (Tesarik et al., 2003).

The average UCS and modulus values of 8.3 MPa and 4.03 GPa, respectively, were obtained in laboratory tests using 152 by 305 mm cylindrical specimens at the Cannon Mine. The CRF was prepared using 5.5% cement, a w:c ratio of 1:1, and <51 mm granitic alluvium 55% and alluvium sand 39.5% (Baz-Dresch, 2002, in Tesarik et al., 2003). In contrast, the average UCS and tangent modulus at 50% of peak stress were 4.1 MPa and 2.25 GPa, respectively, from 457 by 914 mm cylindrical specimens with the same CRF mix, or 56% of the values obtained from 152 mm specimens (Tesarik et al., 2003).

Yu (1989) suggested that CRF has a relatively consistent  $\phi$  of 33°. The  $c$ , however, can vary significantly with the parameters of the matrix and binder used, which was approximately 1 MPa with 5% Portland cement. From the direct shear test result of CRF at Kidd Creek Mine, Farsangi (1996) reported a  $c$  of 1.1 MPa and a  $\phi$  of 33°.

The Mohr-Coulomb criterion provides the relationship of UCS with  $c$  and  $\phi$  as shown by Brady and Brown (1985):

$$\sigma_c = \frac{2c \cdot \cos \phi}{1 - \sin \phi} \quad 3.23$$

### 3.3.3 Reported In Situ Properties

Although typical CRF plants are well monitored, very little engineering data are gathered or known once CRF is placed.

The development of mechanisms to describe the behaviour of CRF as it is placed into a stope has been fundamental in all recent CRF research. The design of CRF worldwide is based largely on laboratory testing of well-mixed average samples to assess strength and to compare them with their required functions. In reality, however, particle segregation

produces in- situ structures that can differ considerably from the average laboratory samples. Depending on the extent of particle segregation, laboratory strengths can be misleading. Therefore, in situ testing is critical for optimizing CRF design (Bloss and Greenwood, 1998).

CRF exhibits pronounced heterogeneity, and evaluation of large fill samples and in situ fill strength is necessary to supplement the measured results obtained from small samples (Yu, 1989).

The fill property parameters of rockfill materials are extremely difficult to determine in laboratory settings due to the large aggregate sizes. The standard laboratory compressive strength test for cemented specimens is performed upon cylindrical samples of limited sizes ranging between 50 to 100 mm in diameter and 120 to 200 mm in length. The range of aggregate particle sizes and the quantities of the material received or prepared for conducting tests are insufficient sample population sizes. Therefore, the data generated under laboratory test conditions often yield a maximized physical response, which would not be demonstrated in situ under bulk-sample test conditions. The laboratory test evaluation of fill properties is performed under controlled conditions, which seldom occur in situ. Therefore, the laboratory test cannot be used to provide a complete interpretation of the in situ fill properties suitable for fill design. When fill characterization is conducted on the basis of testing single batches of material, the sampled batches and the entire range of materials utilized to create the in situ mass may differ considerably. For various reasons, including technical complexity and the high cost, limited in situ measurement results are available (Archibald et al., 1993).

After estimating the fill strength and physical behaviour based on samples manufactured and tested within a laboratory environment to suit the proposed design requirements, the substantial strength variability developed within the placed fill masses in situ is very difficult to determine (Archibald et al., 1993).

Predicting the in situ strength of a CRF mass is difficult due to its heterogeneous character. In most cases, the strength requirement is over and/or under the designed value due to the segregation phenomenon of CRF, and the results could be very costly in both cases (Yu, 1989; Farsangi, 1996).

The segregation of CRF (Yu, 1989; Stone, 1993, Reschke, 1993; Bloss and Greenwood, 1998) can result in a large range of in situ densities in CRF masses. It has been reported that the typical in situ bulk densities of CRF can be 10 to 20% lower than those measured in the laboratory and can have a MC ranging from 2 to 5% with an average  $\eta$  of 34%. The MC of a placed CRF at Kidd Creek was around 5% (Farsangi, 1996) and around 4.5% at the Polaris Mine (Dismuke and Diment, 1996).

Due to the size differences between laboratory cylinders and the actual in situ product, the in situ UCS is about 50 to 67% of rockfill cylinders produced in the laboratory (Scripnick, 1991, in Peterson, 1996).

Yu and Counter (1983) and Reschke (1993) found that the UCS value decreases with increased sample diameter and aggregate size, and suggested that the in situ CRF strength varies approximately by 66% of the laboratory value when using 150 mm diameter cylinders, and by about 90% for samples of 300 mm diameter.

Farsangi (1996) suggested estimating the in situ static strength of the CRF mass by using  $(63 \pm 6)\%$  of the CRF laboratory test results obtained from using 150 mm and  $(86 \pm 8)\%$  of the results obtained from using 300 mm diameter cylinders. Farsangi (1996) recommended a safety factor of at least 2 for stage and 3 for mass blasting, whereas Yu (1989) suggested 2.5 be used to accommodate the additional dynamic loading and variability in the strength of the CRF mass due to the different zoning and segregation within it.

The reported UCS of in situ CRF varies from 1.3 to 11 MPa (Yu, 1990). In situ and the laboratory test results have showed that the elastic modulus for CRF ranges from 2 to 3.8 GPa (Yu and Counter, 1983). Cundall et al. (1978) used a value of 2.07 GPa in their modeling of backfill stability, and the in situ tests by Barrett and Cowling (1980) gave an elastic modulus of 1.6 GPa.

Stone (1993) reported the UCS values worldwide for 500 mm diameter CRF samples, and Annor (1999) included the values as shown in Figure 3.9. Table 3.6 compares the in situ properties of CRF with 5 to 7% cement content presented by Hedley (1995) and the 101 numbers of the 150 mm and large scale (457 mm by 914 mm cylinders) laboratory samples test results at the same cement content with a curing period of 14 to 56 days presented by Annor (1996).

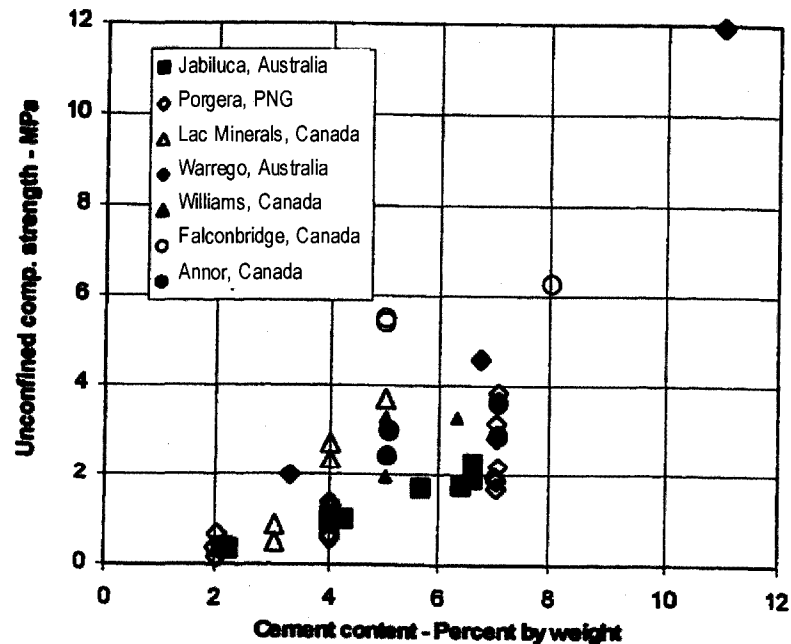


Figure 3.9 UCS test on 500 mm diameter cylinders of for various CRF mixes worldwide (Stone, 1993) and 457 mm cylinders (Annor, 1999)

Annor (1999) concluded that the laboratory UCS value based on 457 mm diameter samples could be taken as being close to the in situ value.

Table 3.6 In situ and laboratory properties of CRF (Hedley, 1995 and Annor, 1999)

CRF Properties	In situ (Hedley, 1995)		Laboratory (Annor, 1999)	
	Range	Mean	Range	Mean
Bulk Density, $\gamma_t$ (kg/m <sup>3</sup> )	1835 - 2161	2000	1790-2430	2006
UCS, $\sigma_c$ (MPa)	2.0 - 5.63	3.24	0.82-10.88	3.88
Deformation Modulus, $E$ (GPa)	0.48 - 2.63	1.00	0.09 - 24.61	3.75
Void Ratio, $e$			0.13 - 0.53	0.36
Porosity $\eta$ (%)			11.7 - 34.7	26.5

Brechtel et al. (1989) reported that the UCS value of cored samples of 150 mm diameter obtained after 30 days of placement of the CRF at the Cannon Mine ranged between 2.05 MPa to 23.44 MPa with a mean value of 5.65 MPa, and an average deformation modulus of 1.86 GPa. The placed CRF consisted of 55% coarse and 40% fine aggregate, 5% cement, and a w:c ratio of 1:1 at that site. Segregation caused zones of structural weakness within the backfill, and therefore, its mass strength was unknown as the coring through the weak zone was difficult, and the tested cores represented the backfill's strongest zones. In contrast, the reported 28-day laboratory strength value of the prepared samples from a delivery truck ranged between 2.48 MPa to 15.01 MPa with an average of 8.45 MPa with the same CRF mix.

The average calculated values of the in situ module were 29, 53, and 64% of the laboratory values from hand-constituted 152 mm, hand-constituted 457 mm, and cored 152 mm diameter specimens, respectively, at the Cannon Mine (Tesarik et al., 2003).

The reported in situ modulus of CRF ranged from 2.28 to 3.38 GPa with 5% binder, using <150 mm crushed andesite-diorite at Kidd Creek, with 28 days of curing (Yu, 1995, in Tesarik et al., 2003). The modulus value was 0.28 GPa at Mt. Isa, when using 300 mm crushed siltstone and tailings with 6 to 8% binder (Gonano and Kirkby, 1977; Thomas et al., 1976).

The in situ deformation modulus obtained from a pressuremeter test at the Kidd Creek Mine had a low range of from 0.04 GPa to 0.1 GPa close to the highwall, indicating the presence of little cement, and range of 1.5 GPa to 4 GPa in other areas. Underground observation and in situ testing have proved that such a homogeneous mass does not exist and that the effect of segregation on CRF strength is a key element that should be included in estimations of strength requirement. An ideal system would minimize the effects of segregation, and the strength requirements would be close to those expected from the homogeneous mass (Farsangi, 1996).

The UCS and deformation modulus values from 7 cored samples tested at a height to diameter ratio of 2.5:1 ranged from 10 MPa to 21.5 MPa with an average value of 17.84 MPa and 3.4 GPa to 6.7 GPa with an average of 4.92 GPa, respectively. The mean

deformation value obtained from the cored samples was roughly twice that from the pressuremeter tests carried out nearly at the corresponding same depth (Farsangi, 1996).

A plate-bearing test result conducted at the Kidd Creek Mine (Farsangi, 1996) showed that the ratio of the ultimate bearing strength to the UCS was approximately 3.2:1. The in situ strength parameters of the CRF based on the cored samples and pressuremeter test at the Kidd Creek Mine are listed in Table 3.7.

Table 3.7 In situ strength parameters of CRF for Kidd Creek (Farsangi, 1996)

Properties	Range
Bulk Density, $\gamma_t$	1880 kg/m <sup>3</sup>
UCS, $\sigma_c$	1 to 17 MPa (average 3.5 MPa) 4.9 MPa for 7% binder 3.5 MPa for 5% binder
Tensile Strength, $\sigma_t$	0.8 MPa for 7% binder 0.5 MPa for 5% binder
Elastic Modulus, $E$	0.6 to 4.5 GPa
Angle of Friction, $\phi$	37°
Cohesion, $c$	1.1 MPa
Poisson's Ratio, $\nu$	0.35
Void Ratio, $e$	0.51 (ranges from 0.20 to 0.55)

Tesarik et al. (2003) reported that the rockfill binder used at the Buick, Cannon and Turquoise Ridge Mines ranged from 4 to 7.8% of the dry components by weight, that the w:c ratio was from 0.42 to 1.0, and that the largest aggregate size in the three mixes ranged from 50 to 120 mm. The in situ deformation modulus values were calculated from the stress changes measured by using earth pressure load cells and strain changes by embedment strain gauges or vertical backfill extensometers at the Cannon and Buick Mines. The embedment strain gauges recorded negligible changes and did not work properly when the largest strain change occurred in the stope at the Cannon Mine. The data from the vertical extensometer combined with those from the load cell at Cannon, and the data from all the instruments at Buick Mines are presented in Table 3.8.

Table 3.8 CRF mixes for the Cannon, Buick and Turquoise Ridge Mines, and its in situ modulus (Tesarik et al., 2003)

Mine	Coarse Aggregate	Fine Aggregate	Cement	Fly ash	Total Binder	w:c Ratio	In situ Modulus (GPa)	
							Range	Average
Cannon	< 51 mm, granitic alluvium, 55	Alluvial sand, 39.5	5.5	NA	5.5	1.0	0.334 to 4.424	1.183
Buick	< 127 mm, crushed dolomite, 96	NA	4	NA	4	1.0	1.275 to 10.885	8.503
Turquoise Ridge	< 51 mm, crushed waste rock, 93	NA	5.8	1.95	7.8	0.42		

- 1 Buick Mine 2 Cannon Mine
- 3 Turquoise Ridge Mine
- 4 American Concrete Institute, adjusted laboratory values based on UCS of cored RRC
- 5 Williams et al, Lucky Friday Mine, slope between 20% and 50% peak stress
- 6 Lucky Friday Mine, secant modulus at peak stress
- 7 Krauland and Stille
- 8 Gurtunca et al, secant modulus at peak stress
- 9 Thomas; Gonano and Kirby 10 Hassani et al
- 11 Gonano, secant modulus at peak stress
- 12 Yu 13 Hedley, linear fit

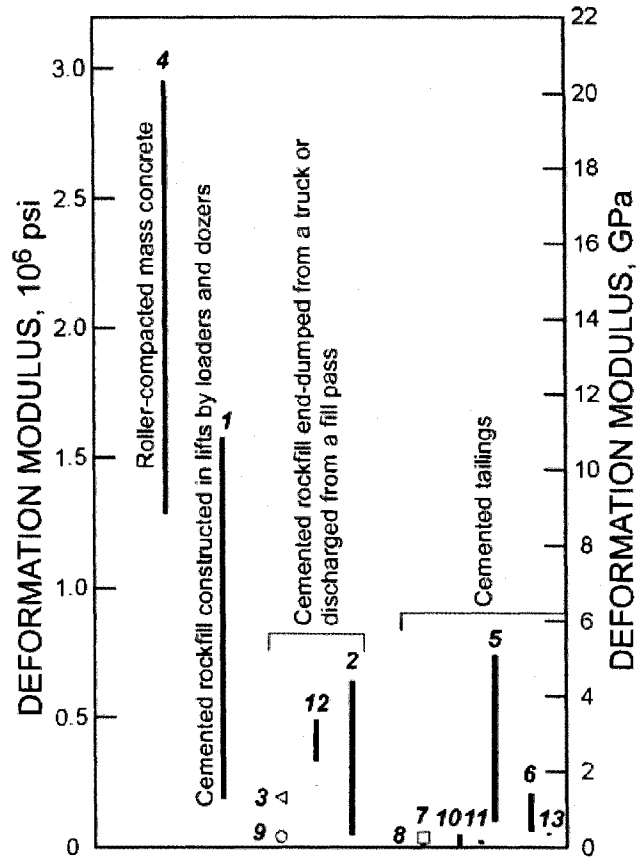


Figure 3.10 Deformation modulus for RCC, CRF and cemented tailings (Tesarik et al., 2003)

The factors affecting rockfill modulus values are water content, cementitious properties and their content, aggregate particle-size distribution, aggregate strength, water quality, age, and degree of compaction. For mixtures having similar water and cement contents, the modulus of a rockfill is likely to be less than that of RCC (Tesarik et al., 2003).

The range of the in situ deformation modulus values for the CRF at the Cannon and Buick Mines was found to be large (0.33 to 10.90 GPa), as measured by using an earth pressure cell, strain gauges, and a vertical extensometer, but was bracketed by the values of the RCC and mill tailings (Figure 3.10). These values were from 30 to 64% of the values obtained from specimens tested in the laboratory (Tesarik et al., 2003).

The 152 by 305 mm cylindrical samples tested at the Turquoise Ridge Mine had an average tangent modulus of 2.26 GPa with an average UCS of 9.6 MPa. Based on all the in situ and laboratory values, and the specific weight based on the average weight of 27 tested samples cured for 28 days, the design parameters for this mine were derived. These design parameters are summarized in Table 3.9.

Table 3.9 Design parameters of CRF at Turquoise Ridge Mine (Tesarik et al., 2003)

Properties	Values
Young's Modulus, $E$ (GPa)	1.315
Cohesion, $c$ (MPa)	0.689
Angle of Internal Friction, $\phi$	44°
Tensile Strength, $\sigma_t$ (MPa)	0.614
Bulk Density, $\gamma_t$ (kg/m <sup>3</sup> )	2146
Poisson's Ratio, $\nu$	0.2

### 3.4 Preparation and Placement Practices

Various methods (Barrett, 1973; Yu and Counter, 1983 and 1986; McKinstry and Laukkanen, 1989; Yu, 1989; Farsansi, 1996, Dismuke and Diment, 1996; Ley et al., 1998; Reschke, 1998; Evans et al., 2007; Young et al., 2007; Reschke, 2007) are used for preparing and placing CRF in stopes around the world. Helms (1998) described the various transportation systems used for different backfills including CRF.

#### 3.4.1 Kidd Creek Mine, Ontario

Yu and Counter (1983) and (1988), Yu (1989), and Farsangi (1996) reported that at the Kidd Creek Mine, the aggregate was produced by crushing and screening the waste rock (mostly rhyolite and andesite from an open pit) with a grading of coarse (<150 mm to >1 mm) and fines (<1 mm) at a proportion of 75% to 25% by weight. The aggregate was transferred underground from the surface by being dumped from a front-end loader, truck or conveyor into boreholes of around 1 to 2.4 m in diameter. Underground, the aggregate was transported by using a conveyor, truck, or scoop tram. The binder slurry was batched normally at 5% by weight of the aggregate at the surface by mixing water, cement and flyash stored in separate silos. The water quantity was controlled at the batch plant by using a flow meter, and the cement and flyash were controlled by using a weighing hopper. The binder slurry was transported to the underground by using either pipes of 100 to 150 mm diameter or boreholes.

When a conveyor system was used for transporting aggregates, a simple mixing system was fitted near to its delivery end, consisting of a baffled slide or chute, and a spray header was mounted over the top of the baffle. The spray header sprayed the binder slurry onto the aggregate as it entered the baffle, by pumping from a slurry tank.

When a truck or scoop tram was used for transporting the CRF to its placement area, an alternative method for mixing the CRF aggregate was used: cement slurry was sprayed

on top of the aggregate. This system allowed the slurry to mix sufficiently with the aggregate during transport, while the final mixing took place as the fill was dumped, spread, and levelled.

The mining method at this mine was sublevel blasthole stoping with delayed backfilling. The design UCS of the CRF was around 7 MPa.

#### **3.4.2 Golden Giant Mine, Ontario**

According to Farsangi (1996), the cement slurry at Golden Giant Mine was batched at the batch plant with a cement content of 5 to 10% by weight of the aggregate. Surface waste from a quarry was crushed to <200 mm and transferred underground through fill raises. Development waste was occasionally added to the crushed rock by removing the <1 mm fines from the crushed rock. The CRF was either directly dumped into the stope or dumped through a drop raise. The aggregate was loaded into a 17-tonne-capacity truck, and cement slurry was sprayed prior to dumping the CRF into the stope.

The mining method was sublevel blasthole stoping. The design UCS of the CRF was around 7 MPa.

#### **3.4.3 Williams Mine, Ontario**

Ley et al. (1998) and Farsangi (1996) reported that the rockfill at Williams Mine was quarried, crushed and screened to maintain a grading of 75% <150 mm and 25% <16 mm. The aggregate was fed by using a front-end loader into fill raises and transferred to underground. A fully automated surface batching plant provided cement/flyash slurry with 4 to 7% by weight of the aggregate, which was transferred underground via a borehole and pipe near the fill stations. The CRF aggregate was loaded and mixed with cement slurry on 26-tonne-capacity trucks at the underground backfill station. The mixed CRF was then transported and dumped directly into the stope to be filled. Sometimes, a portable conveyor was also utilized to transport the aggregate with baffled chutes fitted at its end to mix the binder slurry.

The mining method was sublevel blasthole stoping with delayed backfilling.

#### **3.4.4 Mines under Barrick Gold Corporation, Ontario**

According to Evans et al. (2007), the fill at the Barrick Gold Corporation's Mines consisted of minus 76 mm to 101 mm crushed limestone, binder (cement and flyash), a stabilizer admixture, and water.

In this system, cement and flyash were stored in surface silos and transferred to their respective underground surge bins via steel-cased boreholes. The aggregate was crushed on the surface and delivered into two underground aggregate storage bins through one of the three steel pipes (305 mm and 610 mm diameter) suspended in the ventilation shaft.

The batching plant was automated with a Programmable Logic Controller (PLC) and it included an aggregate feed conveyor, binder weigh hopper, water and admixture metering systems, a twin-shaft Besser batch mixer, and a truck load-out.

The operator selected the batch size and recipe, and the PLC controlled the preparation of the batch. The selected ratio of cement and flyash was fed from the two surge bins into the binder weigh hopper until the hopper load cells detected the target weight.

The selected quantity of aggregate was fed into the mixer by the weighbelt feeder from one of the two aggregate storage silos and was then mixed with the binder, admixture and water as per the selected recipe. Once the mixing was complete, the mixture was discharged into a waiting truck. The CRF was then trucked and directly dumped at the stope location or into the fill pass system and later placed into the stope by a loader.

Mining methods were either underhand cut and fill or longhole open stoping with delayed backfill. A binder of 4 to 7% was used for the design of a UCS of 0.2 to 5.5 MPa for a span of around 3 m by up to 26 m.

#### **3.4.5 Quebec Mines**

Farsangi (1996) reported that CRF was the most common fill type in Quebec and was sometimes used in conjunction with cemented hydraulic fill. Due to the smaller size of the stopes, all the filling was done by using a truck to haul the aggregate. The fill plant and fill methods were similar to those used in Ontario. The five Quebec mines utilized 10 to 50% flyash as Portland cement replacement, which were significantly different percentages than those used in Ontario mines.

#### **3.4.6 Myra Falls Mine, British Columbia**

Reschke (1998) reported that a room and pillar along with a cut and fill mining methods initially used at Myra Falls Mine, had been replaced with bulk mining by longhole stoping, and using delayed backfill to achieve higher production. Moreover, CRF with 5% cement by weight of the aggregate was being considered to replace the hydraulic fill already in use. A colloidal mixer, as shown in Figure 3.11, a hopper with a capacity of 6.5 tonnes, was constructed on top of the load cells to serve as a weighing scale for cement and water.

The PLC controlled all the plant's operations including the preparation of the batch recipes for either truck-or loader-sized quantities of slurry. The slurry was discharged through a spraybar assembly directly onto the loaded aggregate, obtained from a ROM development waste, on a truck or loader bucket. The mixed CRF was then end dumped by the truck or loader over the stope.

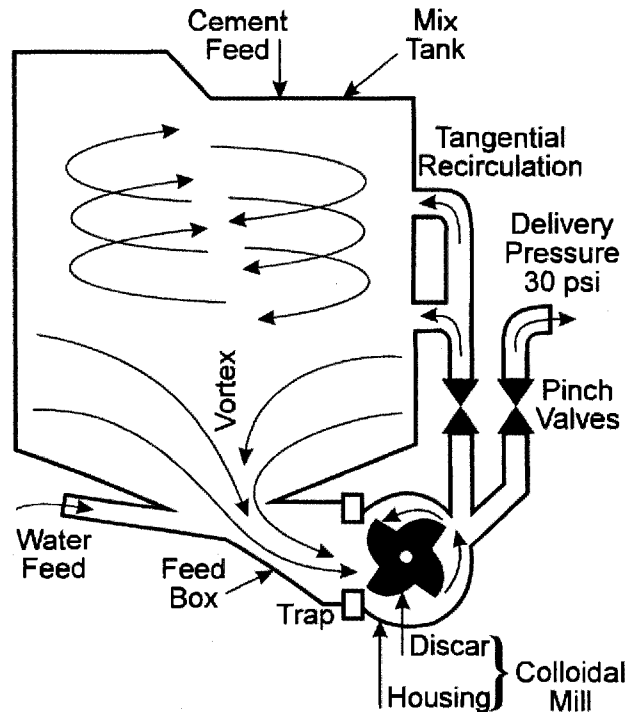


Figure 3.11 Components of a high shear colloidal mixer (Reschke, 1989 and 2007)

### 3.4.7 Polaris Mine, Northwest Territories

Dismuke and Diment (1996) and Reschke (1998) reported that in 1995, the Polaris Mine began to use CRF to replace the existing frozen rockfill system, but had difficulty using it in permafrost conditions where the surface temperatures range from  $-55^{\circ}\text{C}$  in winter to  $10^{\circ}\text{C}$  in summer.

The severe attrition associated with 250 m dump heights was shown by the test results after dumping the surface quarried limestone aggregate screened to a size range of 12.5 to 200 mm, and with approximately 45% passing 10 mm after reaching underground due to the attrition effect. Underground, the ratio of the coarse ( $>10$  mm) to the fine ( $<10$  mm) aggregate was maintained at 55% to 45%.

The entire CRF plant was located on the surface. The complete circuit was enclosed and fully heated. Three MW hot water heating circuits were designed to warm up the aggregate to  $15^{\circ}\text{C}$ . The aggregate was stored in a surge bin, conveyed to a heated load-out structure, and conveyed to the mixing chute. The binder slurry was sprayed onto the aggregate at the top of the chute to obtain optimum mixing.

The CRF haul truck had a fully enclosed dump box with a hydraulically operated hatch on top through which the CRF was loaded from the chute.

The binder slurry was prepared in colloidal mixer by using the following recipe of ingredients stored at separate silos:

- 5% type 30 high early strength cement by weight of the aggregate.
- 5% calcium chloride as an accelerator by weight of the cement.
- 3.5% water by weight of the aggregate or a w:c ratio of 0.7:1.

From the load-out, the truck proceeded to the raisebore hole and dumped the CRF directly into the stope.

The mining method was sublevel open stopping with backfill. The design UCS of CRF was around 5 MPa, and the above recipe gave a laboratory value of 4.9 MPa in 7 days.

### **3.4.8 Mount Isa, Australia**

Neindorf (1983), McKinstry and Laukkanen (1989) and Farsangi (1996) reported that at Mount Isa, the aggregate for the CRF was the local siltstone, which was crushed and screened to produce <25 to <300 mm aggregate. The aggregate was transported via conveyors at the surface feeding fill passes. The binder slurry, termed cemented hydraulic fill (CHF), was produced at the batch plant on the surface by using 3% Portland cement, 6% copper furnace slag, and 91% tailings. The CHF was fed through the fill passes to mix with the aggregate during the fall. The mix of rockfill aggregate and CHF in the ratio of 1:1 to 3:1 by weight, termed CRF, was then transported by an underground conveyor to the top of the stope being filled. This fill's characteristics varied within the stope due to the segregation of the two fill constituents during placement.

In 1994, Bloss and Greenwood (1998) suggested reducing the maximum particle size from 300 mm to 75 mm to minimize the segregation. The rejected <25 mm particles from the CRF aggregate were mixed with the CHF in the ratio of 1:3 by weight, and transported hydraulically through pipes into the stopes. This mixture was termed the aggregate fill (AF).

The mining method was sublevel open stoping. The design UCS of the CRF was around 1 MPa.

### **3.4.9 Buick and Fletcher Mines, USA**

Young et al. (2007) reported that at Buick and Fletcher Mines, the CRF was being placed into open stope areas created by pillar extraction reaching up to 49 m in width and exceeding 91 m in length. The CRF comprised a ROM rock with a maximum dimension of 1 m and containing a 2% binder by weight of the cement and flyash. CRF batch plants producing binder slurry were located on surface at the Fletcher Mine and underground at the Buick Mine. The binder slurry was made in batches at the batch plant according to the following recipe:

- 455 kg cement.
- 545 kg flyash.
- 1450 litres water.
- 3640 kg mill tailings.

The CRF areas were delineated by fill fences within which the CRF was placed from 5 m up to 24 m in height 1 m in lifts.

Two methods were used to place the CRF ROM.

1. A 45-tonne Kiruna haul truck was loaded with 36 tonnes of ROM waste rock, leaving an empty space at the front of the truck bed. The truck was driven to an underground batch plant where a 9-tonne batch of slurry (cement/flyash/sand or tailings/water) was dumped into the front of the truck bed. The loaded truck was driven to the backfill area, and the load was dumped into a mixing pit, normally located at a low spot in the area. A loader mixed the material, ensuring that the slurry was evenly distributed over all of the rock. The loader packed the mixed material into the backfill area where the material was spread in 1 m lifts. CRF placed along the outer edges of the backfill area should always be maintained 1 m higher than the CRF placed in the middle. Doing so keeps the CRF from placing excessive stress on the fill fences. The perimeter CRF should be dumped beside the fill fence and not pushed against it.
2. Batched slurry was dumped into a 6 m<sup>3</sup> or 7 m<sup>3</sup> ordinary concrete truck and driven to the backfill area to be dumped into a mixing pit, where 36 tonnes of waste rock had been previously placed. A loader mixed the slurry and waste rock, and hauled the CRF into the backfill area for placement in 1 m lifts. The CRF was sometimes loaded from the mixing pit into haul trucks, which drove into the backfill area and dumped their loads. A pusher (a loader with a pusher blade attached) spread the dumped material in 1 m lifts. Tesarik et al. (2003) also reported that a loader and dozer were used to push and level the placed CRF at the Buick Mine.

#### **3.4.10 Lamfoot Mine, Washington, USA**

Reschke (1998) reported that at Lamfoot Mine, 680 kg cement and 545 kg water with a w:c ratio of 0.8:1 were poured into 1000-litres colloidal mixer operating at 2000 rpm, constructed in 1995, located underground, and equipped with an automatic PLC system for weighing the ingredients, from different silos. The tank partially filled with water, and the colloidal mill was run to purge itself, the mixing hopper and all the delivery lines. By skipping the purge cycle, the system was capable of discharging a full batch of slurry every two minutes. The system self-cleaned and operated with minimum human intervention.

The ROM development waste with a maximum size of 450 mm was directly used as an aggregate and a haul truck of 14.5 tonnes capacity was utilized for its transportation. The batched slurry at the colloidal mixer was then dispatched through a spray bar directly onto the 11.8-tonne aggregate in the haul truck box within a minute. The mixed CRF was then end-dumped by the truck over the stope.

Mining method was longhole open stoping. The design UCS of the CRF was around 4.8 MPa.

### 3.4.11 Meikle Mine, Nevada, USA

Reschke (1998) reported that at Meikle Mine, the aggregate was produced from pit waste by crushing and screening with <50 mm size and with 40% passing 9.5 mm. The aggregate was transferred underground through three 305 mm internal diameter vertical transfer pipes located in the ventilation shaft, and 7.6 m<sup>3</sup>-Besser ribbon mixer was used to produce the cement slurry. The mixing and placing of CRF were almost the same as those used for the colloidal mixer.

In addition, the colloidal mixer used to produce the cement slurry was mounted on load cells to weigh the water and cement. The binder slurry was typically produced by using 6.3% by weight of a fill. A batch of slurry was prepared by using from 455 kg to 545 kg of water per 725 kg of cement and sprayed onto approximately 11.5 tonnes of ROM waste rock in a 14.5-tonne haul truck by using the spray bars. The final CRF was dumped into the open stope by the haul truck.

The mining method was sublevel longhole open stoping with consolidated backfill. The design UCS of the CRF was around 4.1 to 6.9 MPa.

### 3.4.12 Leeville Mine, Nevada, USA

Reschke (2007) reported the recipe used at Leeville Mine in Nevada for preparing CRF (Table 3.10).

Table 3.10 Mix design per m<sup>3</sup> of CRF at Leeville Mine (Reschke, 2007)

Particulars	8% Mix	6% Mix	5% Mix
Cement (kg)	80.7	60.5	50.4
Flyash (kg)	80.7	60.5	50.4
Total Binder, <i>b</i> (kg)	161.4	121.0	100.9
Water (litre)	193.1	143.6	118.8
w:c Ratio	1.2	1.2	1.2
Pozzolith 300-R Admixture (ml)	620	465	385
Aggregate (kg)	2017	2017	2017
Total Weight (kg)	2179	2138	2118

In 2007, cement slurry (no flyash) was delivered underground through a 100 mm pipe located in the ventilation shaft. A 5.4 m<sup>3</sup>-Normet transmixer carried the slurry to the stoping areas, where it was either added to ROM development waste to produce fill for the primary longhole stoping blocks, or added to a crushed aggregate for underhand-cut and-fill drifts. A scoop tram was generally used for mixing purposes, yet, despite the relatively poor mixing of the slurry and the aggregate, strengths in excess of 3.5 MPa were easily achieved with the ROM waste at 7% cement addition.

The CRF aggregate was <75 mm in size and was produced by crushing the limestone obtained from a nearby quarry. The typical grain size is shown in Figure 3.12, and the ideal limits were based on a consultant's recommendations.

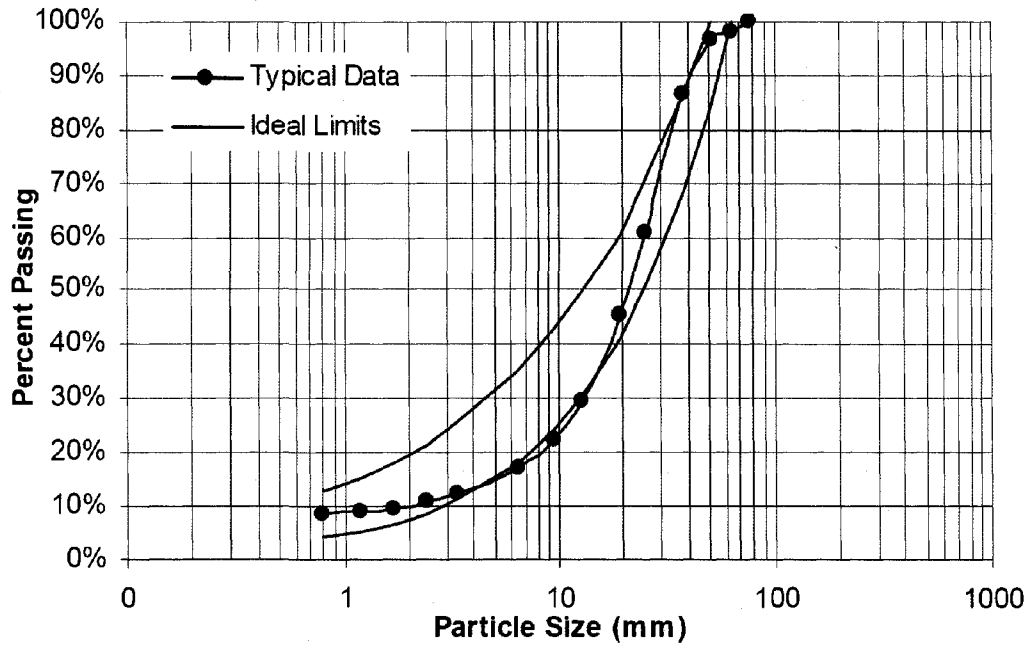


Figure 3.12 Typical gradation curve for the CRF aggregate (Reschke, 2007)

This CRF system was designed to deliver backfill automatically from underground up to the delivery trucks. Cement and flyash were blended with water in a colloidal mixing system on the surface and transferred underground via a piping system to the agitation tanks located just above the underground mixers.

The aggregate was prepared on the surface, transported underground via a skip hoist, and stored in underground silos. The aggregate from the silos was transported by a conveyor with a weigh scale. The binder slurry from the agitation tank and other additional additives from their respective silos were loaded simultaneously into the mixer, which mixed them for a set amount of time. The mixed CRF batches, varying in size and formulation, were then discharged into a Teleram-haul truck and dumped into the stope to be filled.

Mining method was underhand cut and fill and longhole open stoping. The high strength mix (8% total binder) had a target UCS of 6.9 MPa.

### 3.4.13 Summary

Open blasthole stopping with delayed backfilling is the most commonly used mining method, with the design UCS of the CRF usually ranging from 1 to 7 MPa. The CRF preparation and placement methods include the following:

- Crushing, screening and grading of the aggregate at the surface.
- Batch plants for preparing the binder slurry located mainly at the surface or sometimes even underground.
- Sometimes using a portable colloidal mixer to prepare the binder slurry underground.
- Using a truck or front wheel loader or conveyor to feed the CRF aggregate to raise borehole for transporting the aggregate to an underground mixing station.
- Raise borehole or pipe to transfer the binder slurry to an underground mixing station.
- Using a truck or scoop tram or conveyor fitted with a spray system (manual or automatic) at the mixing station to mix, transport and dump the CRF onto the stope to be filled.
- Sometimes, using a wheel loader for mixing and placing, or a grader or pusher to push and level the dumped CRF at the stope.

## 4 Cemented Rockfill at Diavik Mine

In this chapter, the purpose for using CRF at Diavik Mine site, the CRF design specifications, the trial mixes, site preparation, and CRF placement are described. A literature review of studies reporting on QC and testing practices, together with the adopted QC and testing practices used at this study site, are also covered in this chapter.

The Diavik Diamond Mine is located 300 km northeast of Yellowknife, Northwest Territories (Figure 4.1). The mine is a joint venture between Diavik Diamond Mines Inc., DDMI (60%) and Aber Diamond Mines Ltd. (40%). DDMI is a wholly owned subsidiary of Rio Tinto and is the operator of the project. Aber Diamond Mines Ltd. is wholly owned by Harry Winston Diamond Corporation.

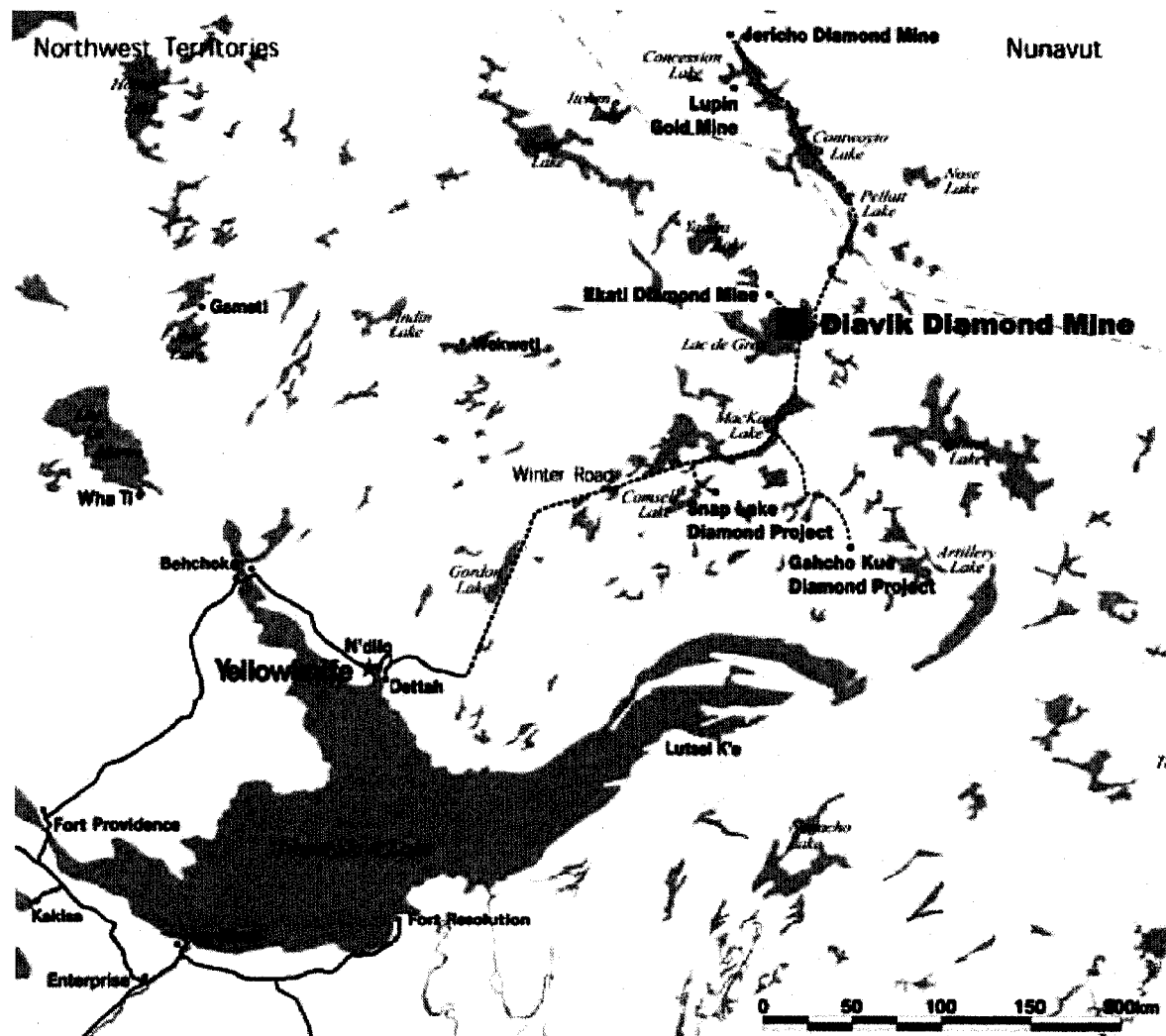


Figure 4.1 Location of Diavik Diamond Mine (modified from DDMI, 2006)

The current mine reserve consists of three kimberlite pipes: A154 South and A154 North accessed from the A154 pit, and the A418 pipe accessed from the A418 pit. All pipes are located beneath Lac De Gras, and the dikes are constructed around the pipes as shown in Figure 4.2. The A154 N pipe is exposed on the northeast wall of the A154 pit. The CRF discussed in this thesis was placed over the exposed kimberlite A154 N pipe in a series of layers not more than 1 m thick to form a crown pillar between the future underground mining and the existing open pit. A portion of the A154 N kimberlite pipe had been mined from surface, and the surface exposure was covered with a CRF cap to allow for continued underground mining of this pipe to depth. The approximate locations of the aggregate stockpile, mixing bay, batch plant, QC laboratory and CRF placed area are shown in Figure 4.2.

A cross-sectional view of the A154 and A418 pipes is shown in Figure 4.3. The A21 pipe was in exploration stage and not included in the reserves.

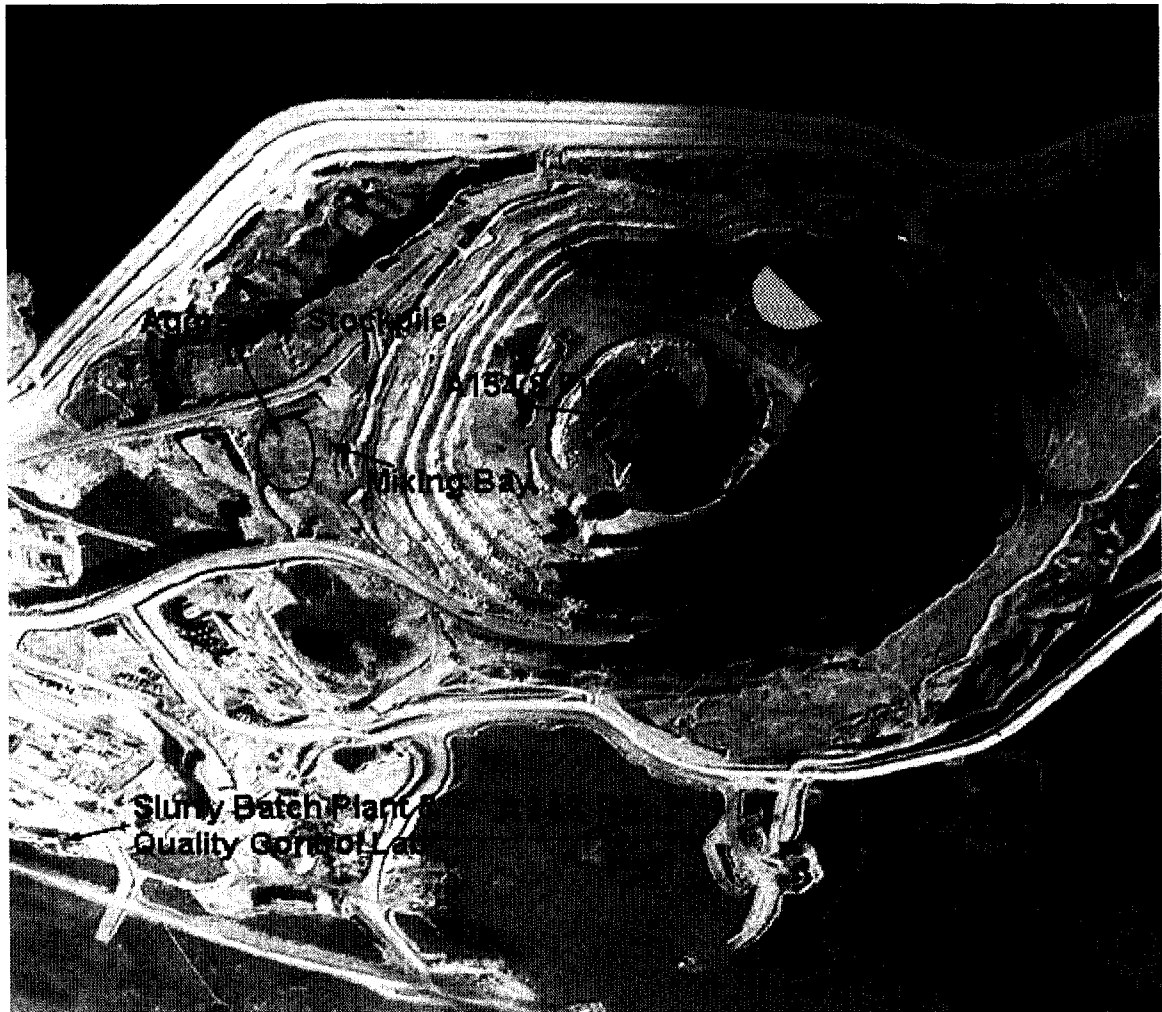


Figure 4.2 Location of A148 pit and both pipes in the A154 pit (modified from DDMI, 2005a)

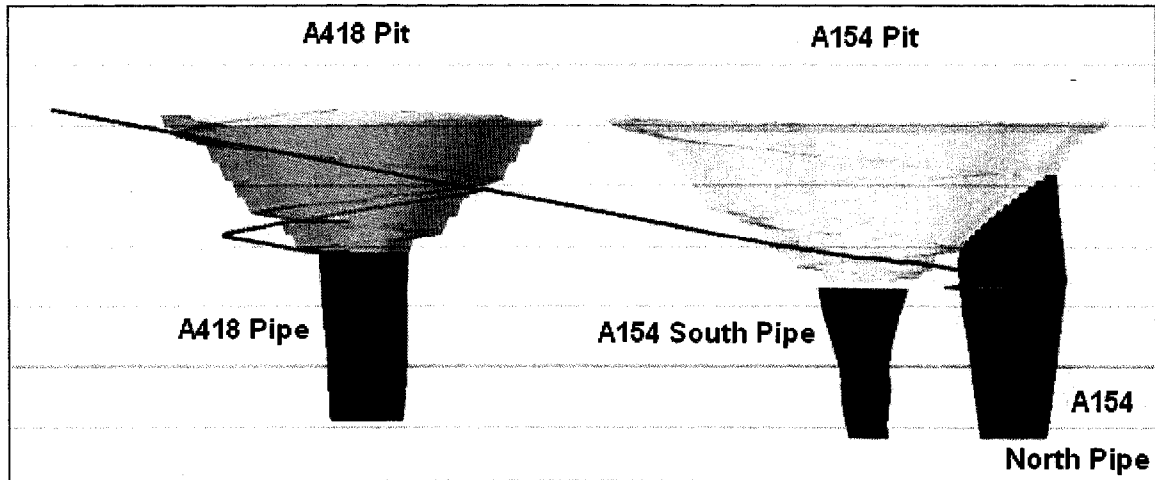


Figure 4.3 Section of ore bodies of Diavik Mine (modified from DDMI, 2005b)

Water-retention dikes were built to hold back the lake water to allow mining of the kimberlite pipes. A 3.9-km-long A154 dike was completed in July 2002 by using approximately 3.5 million tonnes of rockfill. The construction of this dike made mining of the A154 pit possible starting in December 2002. The pit had reached approximately 170 m below lake level by spring 2007. The smaller, 1.3-km-long A418 dike, built in water up to 32 m deep with approximately 1.1 million tonnes of rockfill, was completed in 2006 joining the existing A154 dike and East Island.

A 1.6 km long airstrip, capable of accepting Boeing 737 jet service, allows regular access to the mine. The mine is accessible in winter via a 353-km-long ice road from Yellowknife. This road opens early in February and closes early in April.

Diavik's kimberlite pipes are the roots of relatively young volcanoes approximately 55 million years old. The surrounding host rocks are ancient Precambrian granites and metamorphosed sedimentary rocks approximately 2.7 billion years old. The detailed geology of this site is described in SNC - Lavalin (2000), Bryan and Bonner (2003), and Roscoe Postle Associates (RPA) Inc. (2005). Granitic rocks predominantly underlie the area and have intruded into slightly older meta-sedimentary rocks originally deposited as sandstone and shale.

It is estimated that the mine will produce over 100 million carats of diamonds over its expected mine life of 16 to 22 years with an annual ore production of approximately 2 million tonnes and an annual peak diamond production of approximately 10 million carats. This mine produced 9.8 million carats of diamonds in 2006 (DDMI, 2006).

#### **4.1 Cemented Rockfill Design Specifications**

The CRF design specifications include the physical property, specifications of the materials used to prepare the CRF and the mixing and placement procedures. The CRF design specifications were based on reports by Golder Associates (2007a and 2007b).

These specifications also outline the QC measures to be adopted to ensure that the design specifications are met. These specifications are summarized here.

#### 4.1.1 Material Specifications

The aggregate shall fall within the gradation limits as shown below in Table 4.1 and shall be free of clay, organic matter, debris, cinders, ash, refuse, snow, ice and other deleterious material. The aggregate shall be surface dry. Any deviation from this MC should be compensated for by adjustments in the w:c ratio of the cement slurry.

Table 4.1 Gradation limits for aggregate

Grain Size (mm)	Percent Passing by Mass (%)
50	100
38.1	76 - 100
25.4	61 - 86
19.1	52 - 74
12.7	42 - 60
9.5	36 - 52
4.76	25 - 37
2	16 - 25
0.84	10 - 18
0.42	7 - 14
0.25	5 - 12
0.15	3 - 10
0.074	2 - 8

The cement shall be GU Type 10 Portland cement, and the cement shall have been stored in dry conditions. The cement temperature shall be at least 5°C at the time of use. Cement containing hardened lumps in excess of 5% by weight shall be screened to remove material greater than 15 mm or shall be rejected.

#### 4.1.2 Mix Design Specifications

The following specifications shall be considered for the mix recipe of the cement slurry:

- The cement content to be 5% (min 4.5%, max 6%) of the mass of the aggregate.
- The cement content to be confirmed by QC contractors based on the cement tote count records and truck load records. Contractors shall confirm the average mass of the rock in the bucket of the loader by weighing a truckload of aggregate.
- The w:c content of cement slurry to be 1:1 (min 0.95:1, max 1.2:1). The batch plant records are to be retained for review.

#### 4.1.3 Preparation of Kimberlite Surface

The following specifications shall be considered when preparing the kimberlite surface:

- After mining is complete, the kimberlite bench face shall be inspected, mapped and photographed by a qualified geotechnical engineer. A QA engineer shall confirm qualitatively that the exposed rock meets or exceeds the rock mass strength assumed for the design of the 9270 m drop cut.

- The kimberlite surface shall be bladed to an undisturbed, level surface while removing loose rock, blast-damaged rock and water-softened material. The surface preparation shall be approved by a QA engineer.
- Traffic on the 9270 m kimberlite surface should be minimized to avoid degradation (softening) of the kimberlite. Any softened, loose material should be removed prior to CRF placement and replaced with uncemented rock fill to establish a level surface.
- The kimberlite surface shall be graded and drained to ensure that water is not flowing within the CRF backfill. Drainage shall include a French drain along the toe of the slope to collect any flow down the bench face, tied to a French drain trending south to the drain formed by the 9265 m pre-shear blast through the 9280 m granite platform or to the sump on the west side of the pipe. Other significant springs in the 9270 m bench shall be collected in additional French drains. All drains shall be covered by clean crushed rock up to and level with the 9270 m kimberlite surface, and the drains shall be observed to be functional by the QA engineer.

#### **4.1.4 Mixing and Placement Specifications**

Mixing and placement include the following specifications:

- The cement slurry shall be mixed in a bentonite slurry mixer or at the concrete batch plant. If the batch plant is to be used, efforts must be made to ensure a thorough mix, which may require the use of cobbles in the paddle mixer or some other means for ensuring the cement is sheared and lumps are broken up.
- The cement slurry shall be placed into the mixing pit at the specified total cement content and w:c ratio.
- After the mixed rockfill has been dumped onto the 9270 m platform, a dozer shall be used to spread and track-pack the rockfill in lifts not exceeding 1 m to achieve an in situ density of 2150 kg/m<sup>3</sup> or greater. Lower densities may be accepted if supported by standard Proctor density tests of the stockpile material, and the achieved in situ density is greater than 95% standard Proctor density. At his discretion, a contractor may utilize other equipment in order to achieve the required density, but must ensure that cold joints are prevented.
- Care must be taken to avoid mixing loose kimberlite subgrade into the CRF during the blading of it over the 9270 m bench.

Cold joints in the CRF are to be prevented, with extreme care being required in the lower 2 m of the slab that will form the roof of the underground mines. The following procedures are to be practiced:

- Temporary ramps between the kimberlite surface and the rockfill are a potential source of underground roof falls. The wedge of the CRF at in the lower part of any ramp (the portion where the thickness of the CRF is less than 1 m thick) is to be removed when use of the ramp ceases. The lower part of any temporary ramp is to be removed as waste before fresh CRF is placed on the kimberlite surface.
- The angle of repose slope at the edge of the advancing CRF pad is to be cut back to a vertical slope and discarded if it has been in place and exposed for longer than 4 hours. The angle of the repose slope should not be greater than 1 m in vertical

- height at any time unless it is to be cut back to vertical before placing additional fill against it.
- Packed surfaces are to be scarified with the dozer blade as fresh CRF is spread over a compacted surface.
  - A packed surface should not be exposed for longer than 4 hours before additional lifts of CRF are placed. In the event of longer exposure, the surface is to be scarified and wetted with slurry with a w:c ratio equal to 2:1 prior to adding additional CRF.

#### **4.1.5 Quality Control and Quality Assurance**

The following specifications for QC and QA must be met:

The contractor shall perform all necessary inspection, sampling and testing of the aggregate to ensure that only materials of the specified composition, gradation and MC are supplied to the work site. The contractor's work shall include the following:

- Inspecting the MC of the aggregate by oven drying once per shift.
- Measuring the aggregate gradation by using sieve analysis once per day.
- Keeping records of the cement tote usage and loaded truck count twice per shift or every 500 m<sup>3</sup> of CRF batched, whichever is less.
- Measuring the  $G_s$  of the cement slurry twice per shift or every 30 m<sup>3</sup>, whichever is less.
- The QA Manager shall carry out QA inspection and testing to confirm the contractors' QC. This work will include verifying that the following limits are being attained:
  - Aggregate gradation and MC.
  - Cement content.
  - w:c ratio.

The contractor shall provide facilities and labour as required to assist in taking samples, and conducting tests.

- One sample of mixed fill shall be taken from the mixing pit five times per shift, and either tamped into 150 mm moulds or sieved to remove rock over 25 mm, and tamped into 100 mm concrete cylinder moulds, in either case to a  $\gamma_d$  of 2150 kg/m<sup>3</sup>. Samples shall be stored in a moist atmosphere (not submerged in water) at a controlled temperature of 20 to 25°C. Two samples shall be tested after 72 hours and two samples after 7 days and one after 28 days.
- The density and MC of the compacted CRF shall be confirmed by one nuclear densitometer test per 100 m<sup>3</sup> of material placed. The relationships between the number of track (or roller) passes, the lift thickness, and the density are established from a test pad. If any test results in a density more than 25 kg/m<sup>3</sup> below specification, the number of track passes shall be increased, or the lift thickness shall be reduced until the specification is exceeded on three successive tests.
- The QA engineer will review the QC test results and will approve the preparation of compacted surfaces prior to the placement of additional CRF. The QA engineer may, at his discretion, request additional test cylinders or compaction tests.

## 4.2 Preparation of Cemented Rockfill

The CRF was prepared at DDM site by mixing crushed granite comprised of <50 mm aggregate with cement slurry and it was zero slump concrete similar to RCC. The cement slurry was made from GU Type 10 cement and water. The cement slurry was made in batches and transported from the batch plant for mixing with the aggregate in a mixing bay.

A stockpile of aggregate was produced in 2006 by crushing the waste rock originating from the A154 open pit. The rock is non-sulphide bearing granite. A grain-size analysis and MC measurements were obtained at least once per shift during the production of the aggregate in 2006.

The binder used to make the cement slurry was GU Type 10 cement from the Lehigh Cement Company (Heidelberg Cement Group). Cement bags weighing 1760 kg each were stored near the batch plant, as shown in Figure 4.4.



Figure 4.4 Storage of GU type 10 cement near batch plant

Untreated pumped lake water was mixed with the cement at specified ratios of cement and water by mass. The slurry was prepared in a batch plant capable of mixing 6 m<sup>3</sup>. The batching plant was automated with PLC. It included a cement weigh hopper, a water metering system, and a truck load-out facility. The cement slurry was transported from the batch plant in the cement slurry truck.

The mixing bay used to mix the cement slurry with the aggregate was constructed near the stockpile of the aggregate (Figure 4.5). This bay's features included vertical steel plates on both ends, inclined concrete faces along its length, and a flat concrete bottom.

The mixing bay had a volume of  $96 \text{ m}^3$  (12 m long, 2 m deep and width from 8 m at the top to 2 m at the bottom).

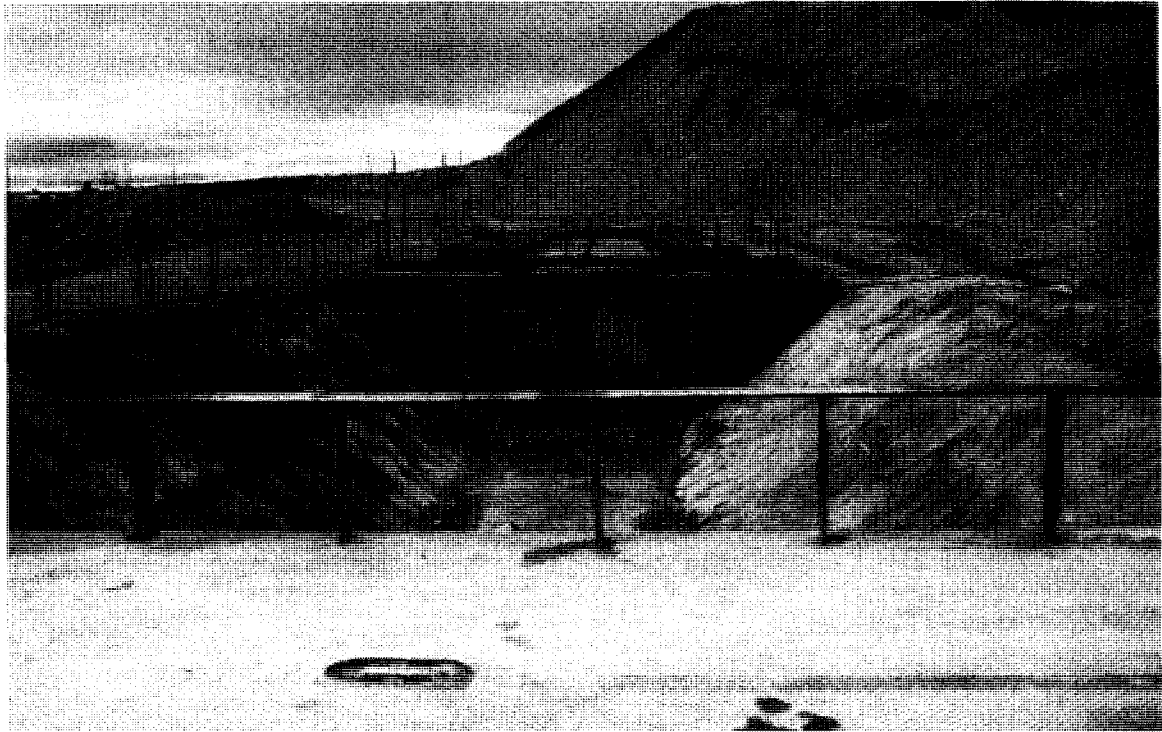


Figure 4.5 Mixing bay used for mixing aggregate with cement slurry

The aggregate from the stockpile was placed into the mixing bay by a Caterpillar 988 G loader. The quantity of the aggregate placed in the mixing bay was controlled with the loader bucket count. Seven buckets ( $42 \text{ m}^3$  at  $6 \text{ m}^3$  per bucket) of aggregate were placed into the mixing bay, as shown in Figure 4.6 and Figure 4.7. The weight of the aggregate was 71 tonnes, which was established by weighing a truck-load of the CRF aggregate with a seven buckets of the loader as per the specification. The cement slurry from the batch plant was transported by an ordinary concrete truck and poured into the mixing bay (Figure 4.7 and Figure 4.8). The aggregate and cement slurry were mixed within the mixing bay for about 10 to 15 minutes by using a Caterpillar 385 B excavator (Figure 4.8 to Figure 4.10).

The CRF was then loaded into a Caterpillar 777 truck by using the same excavator. This process of preparing the CRF was repeated to produce another truck load by the same manner.



Figure 4.6 Aggregate from stockpile being carried by a Caterpillar 988 G loader



Figure 4.7 All equipment used to mix the CRF



Figure 4.8 Pouring of cement slurry, and mixing it with aggregate by excavator

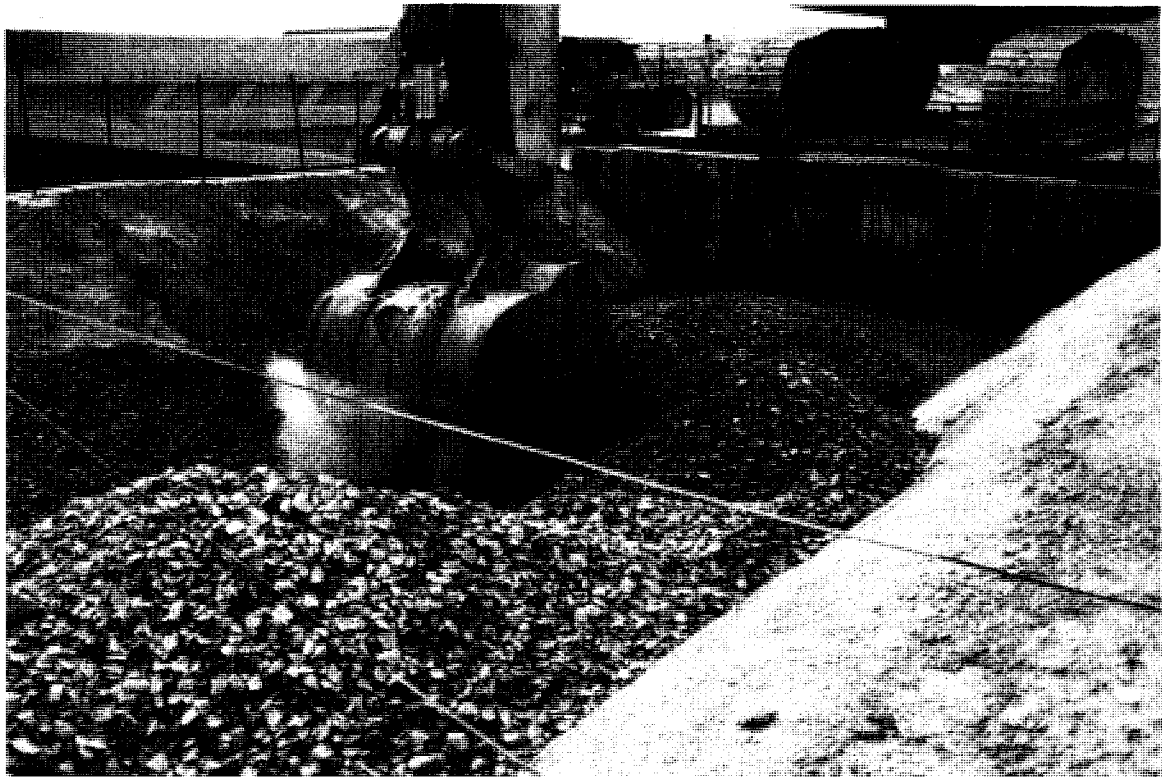


Figure 4.9 Cement slurry and aggregate being mixed with excavator



Figure 4.10 Mixed CRF ready to be loaded into haul truck

#### 4.2.1 Observations during CRF Preparation

The mixing bay's location close to the placement area might have reduced the total time required for preparing and placing the CRF. A mixing bay constructed at a certain height and the provision of a load-out opening unit at the mixing bay might have reduced the loading time and allowed the bay to be properly emptied after preparing each batch of CRF. During the preparation of this thesis, some unknown site-specific constraints might have prevented these options for locating and constructing the mixing bay from being adopted at the DDM site.

The quality of cement slurry could have potentially been maintained almost uniform as it was prepared in the batch plant by accurately weighing the cement and the metering water quantity automatically, unless some variability was present in the mixing due to the quality of the cement, especially in its lump condition, as it was stored in an open space outside the batch plant. The quality of the cement slurry has to be measured by using a proper measuring technique, and measuring its  $G_s$  is a suitable one.

Measuring the quantity of the aggregate used for preparing each batch of the CRF simply by using the bucket counts of the loader could have resulted in the known variability in the CRF properties. The ideal situation for minimizing the preparation time of the CRF is to achieve the simultaneous placing of the aggregate by the loader, the poring of the

cement slurry from concrete truck, and the mixing of the aggregate with the cement slurry by using the excavator in the mixing bay. This ideal situation during the preparation of the CRF was usually achieved at DDM site. When this ideal situation cannot be achieved, the placing of aggregate in the mixing bay has to be carried out prior to the pouring of the cement slurry to minimize the waiting time for mixing and the overall time for preparing a batch of CRF. The timing of the batched cement slurry should be accordingly adjusted based on the mixing and loading of the CRF, and the placing of the aggregate for another batch of CRF to minimize the total time required from the initial preparation of the cement slurry to its final pouring onto the aggregate.

The main objective during the preparation of CRF is to thoroughly mix and properly coat the aggregate with cement slurry as quickly as possible. Quantifying the preparation time of the CRF from the initial pouring of the cement slurry to the final loading of the prepared CRF is possible, but limiting the preparation time might prevent the ideal mixing of the aggregate with the cement slurry. From the close observation of repeated preparation cycles, one can estimate and specify the acceptable time limit and include it in a QC measure. The quantitative assessment of thorough mixing is, however, difficult to achieve and has to be based on visual inspection of the coating of the aggregate with cement slurry for each batch of CRF.

### **4.3 Placement of Cemented Rockfill in the A154 Pit**

#### **4.3.1 Trial Mixes**

Three trial mixes were prepared in the mixing bay on June 16, July 10, and August 1, 2007 in order to assess the properties of the CRF before it was placed in the A154 pit.

During the trial mix, both the procedure and the equipment types used were the same as those described for preparing the CRF. The processes of batching the cement slurry, its transportation to the mixing bay, and its mixing with the aggregate were all carried out in the same manner.

The cement slurry was batched by mixing pumped water from the lake and Type 10 GU cement at the batch plant, based on the specifications for their masses. 4562 kg and 4558 kg of cement for the second and third trial mixes, respectively, with 4504 kg of water for both mixes, were used to batch the cement slurry of 6 m<sup>3</sup>.

As described earlier in section 4.2, the CRF was prepared in a similar manner for the trial mixes. The batched cement slurry was then transported to the mixing bay by a normal concrete truck and poured into the mixing bay. Seven loader (Caterpillar 988 G) buckets of aggregate by count were placed into mixing bay. Then the cement slurry and aggregate were thoroughly mixed for about 10 to 15 minutes by the bucket of the Caterpillar 385 B excavator. The CRF mix was visually inspected to make sure that all the aggregate had been properly coated with cement slurry. The final CRF mix was then loaded into a haul Caterpillar 777 truck by the same mixing excavator.

The CRF was hauled a short distance to a flat test area and dumped on the ground. The CRF was spread and compacted by a Caterpillar D5M LGP dozer. Once compacted, in situ measurements of the wet and dry densities and the MC of the CRF were taken with a TMD nuclear gauge model 3430 by using the direct transmission mode. A smooth test surface was prepared by using a scraper plate. The extraction tool was placed first on top of the drill rod guide located on the scraper plate. The drill rod was inserted and hammered through the drill rod guide to the measurement depth up to a maximum of 300 mm. The drill rod was extracted from the hole, and the source rod of the TDM nuclear gauge was then inserted into it for the measurement. The measurement procedure is described later in this chapter in section 4.4.2.

The 1 m-thick CRF was placed by using one to three series of lifts ranging from 0.25 to 1 m. The top of the compacted CRF was 0.5, 0.75, and 1 m in the three series of lifts for the first trial mix, 0.5 and 1 m in the two series of lifts for the second mix, and a single 1 m lift for the third trial mixes. Immediately after the spreading and compaction processes were completed by the dozer, in situ density and MC tests at each lift were conducted by using a TDM nuclear gauge. The procedures for the field and laboratory tests are discussed later in this chapter in section 4.4 while dealing with the QC and testing in the field. The in situ test results for the densities and MC, and the sieve, MC, density and UCS values of the cylinders in the laboratory during the trial mixes are presented in the Appendix and discussed in Chapter 5.

#### **4.3.2 Observations during Trial Mixes**

The cement content of the CRF was estimated by using the sieving and MC methods during the trial mixes. The sieves on the aggregate and CRF mixed samples were carried out by assuming that the increment in the percent of the fines washed away by passing through the 0.08 mm sieves in both cases roughly indicated the cement content of the CRF sample. Around two kg of sugar was added during the washing of the CRF sample of around 20 kg to delay its setting due to its cement content. The increments in the MC were assumed to provide a rough indication of the cement content of the CRF. However, the MC alone could not provide useful information due to the variability of the initial MC of the CRF aggregate. However, both methods indicated that the variability of the cement content in the CRF, and some variability in CRF properties were expected. The  $G_s$  of the cement slurry would have been measured during the trial mixes.

Based on the specification, one of the purposes of the trial mix and its testing was to obtain the optimum lift thickness and the required number of passes of dozer compaction to achieve the specified  $\gamma_d$  of 2150 kg/m<sup>3</sup> of the placed CRF. However, no conclusions were made regarding the optimum lift thickness and the required number of dozer passes during the trial mix. It was decided to place CRF not exceeding 1 m lift thickness without specifying the required number of dozer passes. The compaction provided by dozer was obtained during its spreading and levelling of the CRF. With such a compaction effort, the trial mixes indicated that the average achievable in situ  $\gamma_d$  is lower than the targeted-specified density.

The trial mixes provided the values of the in situ densities and the MC of the CRF as the guidelines values. The comparison of the laboratory MC determination with the corresponding in situ MC measurement by using a TMD nuclear gauge helped to justify the nuclear measurement value. The determination of the cement content in the CRF sample by using both the sieving and MC methods indicated the variability of the cement content, (Some variability in the mixing and, hence, in the CRF properties, was expected before the CRF placement). The site- specific preparation method of the CRF cylinder with a density similar to the in situ density was identified. The CRF strength was indicated by the prepared cylinders during the trial mixes.

More conclusions from the trial mixes possibly could have been made compared to those had been achieved. It would have been preferable to optimize the lift thickness, the required number of dozer passes to achieve optimum compaction, and the  $\gamma_d$  during the trial mixes. The nuclear gauge provided a measurement for up to 0.3 m depth, so the bottom 0.7 m of the CRF was not covered during its measurement when 1 m-thick CRF was placed in a single lift. The achievable ranges of  $\gamma_d$  and MC of CRF, and their acceptable guideline values would have provided better QC measures during the CRF placement.

It would have been better to have established some comparative strength values from the 100- and 150-mm-diameter cylinder samples, and their corresponding MC, as reference values during the trial mixes. The coring and strength testing results from the trial mixes at different location would have better indicated the in situ density and strength of CRF and their possible variability. The in situ density measurement made by the TMD nuclear gauge were considered accurate, and no verification was made for the measured density. The density obtained from the cored sample close to the nuclear gauge measurement may be further utilized to justify the density measurement made by the nuclear gauge.

### **4.3.3 Site Preparation**

The A154 open pit design had been reassessed and fine-tuned several times based on operating experiences since the original design in the 2000 feasibility study carried out by SNC – Lavalin. The latest revisions were done in May 2004, when the east wall in the A514 pit was moved back to flatten the slopes to the angles recommended in a study by Golder Associates, 2003, along with additional smoothing of the walls and minor changes in the ramp width (RPA, 2005).

Prior to the placement of the CRF, the scaling and bolting of the loose wedges exposed during scaling, plus the installation of anchored mesh from 9370 to 9320 m benches (with a horizontal extent of 165 m at the 9370 m bench and tapering down to 125 m at the 9320 m bench) were recommended to reduce the hazard of rock fall from the benches above the 9320 m bench elevation. Bolted mesh along with 4.2 m long Swellex rock bolts was installed in a 3 m by 3 m pattern below the 9320 m bench during the excavation of the kimberlite pipe (EBA, 2007a and 2007b).

The task of scaling and installing mesh between the 9370 and 9320 m benches was partially completed in 2006. In late October and early November 2006, these bench

crests were lightly scaled to remove the more obvious loose rock. To the west of Dewey's fault, the slope just below the 9340 m bench elevation was trim blasted.

Based on the DDMI (2007a), the proposed mining methods and geotechnical monitoring system as preparation for placement of the CRF are briefly summarized below.

The mining of the four benches associated with the A154 N kimberlite pipe on the north-east wall between the 9320 and 9280 m levels, as shown in Figure 4.11, was initially planned from the underground workings, but was found to be uneconomical, so a plan was developed for the partial mining of these kimberlite benches from the open pit. A section of its proposed final excavation is shown in Figure 4.12. Based on the plan, the mining of the kimberlite will be followed by the placement of a CRF cap on the exposed kimberlite surfaces in order to facilitate mining from the underground development. A waste rock buttress will then be placed on top of the CRF, with the final engineered slope extending back up to the 9320 m level.

In order to facilitate the placement of the CRF cap on the lower A154 N bench, it was planned to excavate the kimberlite from the 9280 m level down to the 9270 m level, and place the 5 m CRF cap in the 'hole' created. ROM backfill would be placed on top of the CRF, and a platform would be built up to the 9290 m level. Once the bench faces above the 9320 m had been cleaned and meshed, mining would commence on the 9320 m level. The top three benches (9320, 9310 and 9300 m) would be excavated in 2.5 m lifts to 9290 m. The bench faces would be meshed and bolted concurrently to ensure slope stability. The detailed mining sequence for the placement of CRF is given in the DDMI power point presentation (2007b). A 5 m thick CRF cap would be placed on the 9290 m bench, overlain by ROM backfill to 9320 m. The section of the proposed placement of the CRF and ROM between 9270 m to 9320 m is shown in Figure 4.13.



Figure 4.11 Plan view of A 154 N pipe at initial stage (modified from DDMI, 2007b)

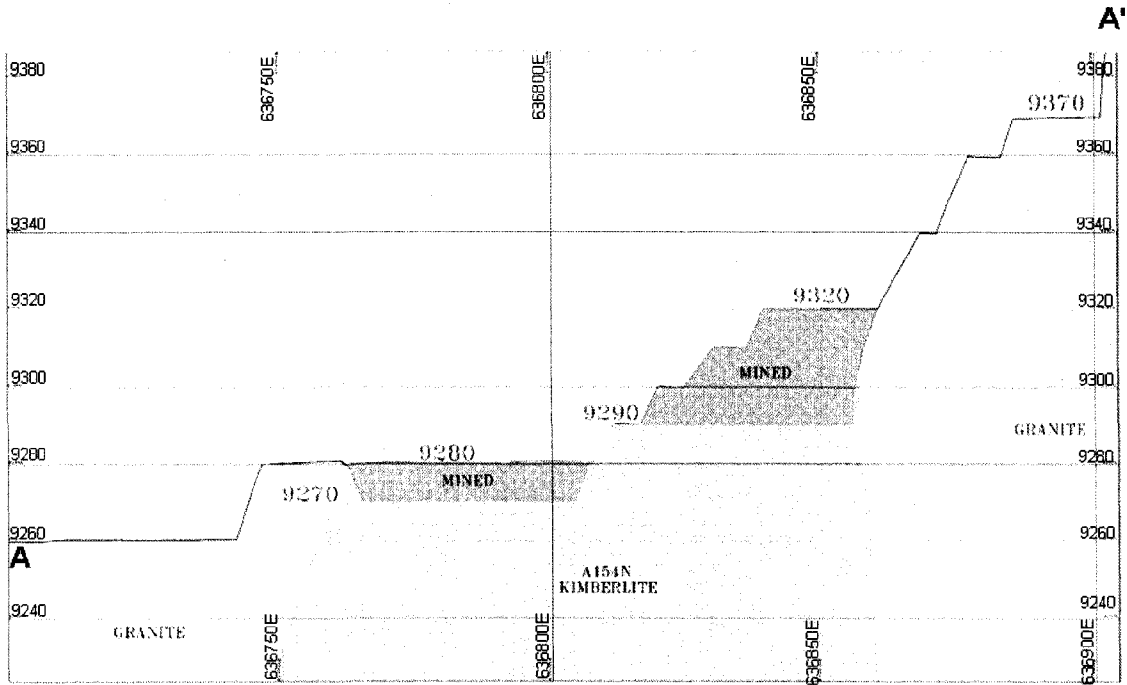


Figure 4.12 Proposed final stage excavation of A154 N pipe along A-A' for CRF placement (modified from DDMI, 2007b)

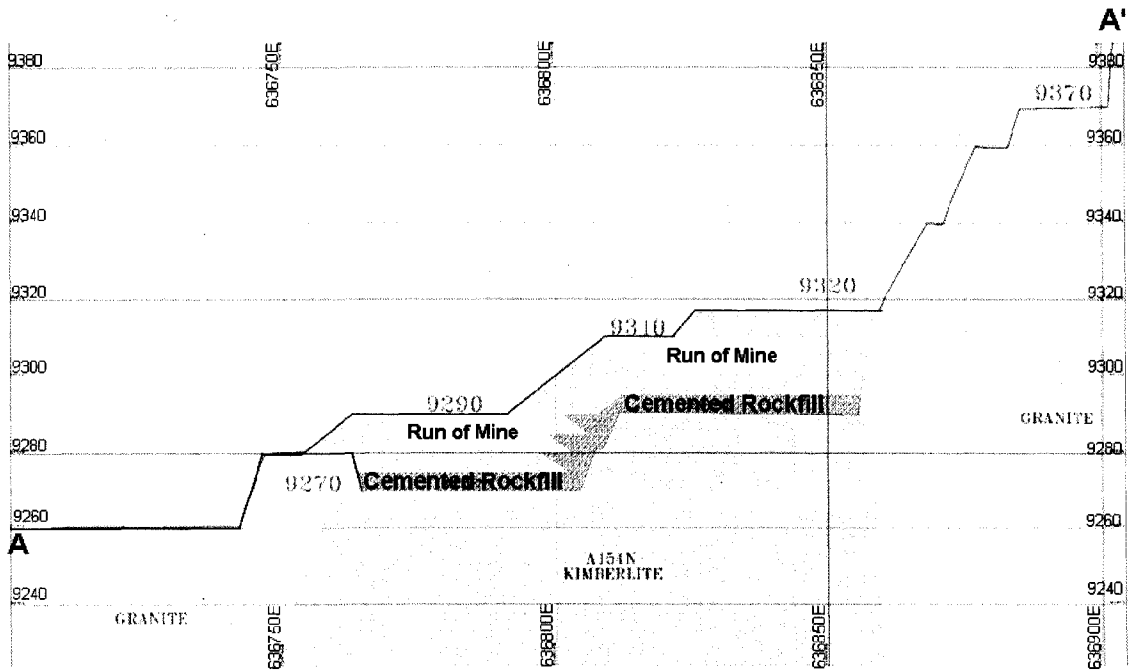


Figure 4.13 Proposed final CRF and ROM placement after final excavation of A154 N pipe along A-A' for (modified from DDMI, 2007b)

The placement of all the CRF was scheduled to occur prior to freezing conditions and September 30 was used as the final date that the CRF could be placed. It was decided that if the mining schedule fell behind, a decision would be made to stop mining prior to the final bench excavation and to cover the remaining benches with CRF.

For placement of the CRF, the proposed geotechnical monitoring during the mining includes groundwater pressure mitigation, geotechnical monitoring of the instruments, and geotechnical inspections.

- The proposed measures for groundwater pressure mitigation included the use of surface diversion ditches; a row of 30 m long vertical holes at 5 m spacing from the 9320 m bench within the kimberlite to mitigate artesian groundwater pressures close to the contact zone; sub-horizontal drain holes drilled to a depth of approximately 100 m from within the waste rock towards Dewey's fault zone; and sub-horizontal drain holes drilled to a depth of 30 m from each bench being mined, from the 9320 m bench downwards and spaced approximately at 15 m.
- The geotechnical monitoring included the surface-monitoring prisms, time domain reflectometry (TDR) cables, vibrating wire piezometers, thermistor strings, and the proposed additional instruments such as borehole extensometers, additional surface monitoring prisms, an inclinometer, and pressure transducers installed within the NE wall sector of the A154 pit. This monitoring system also included keeping the Trigger Action Response Plans (TARPS) in place for all the monitoring instruments.
- The geotechnical inspections included the full-time geotechnical supervision provided by DDM's geotechnical consultants and their rock-slope specialists. These personnel mapped the faults, shears, and joint orientations as the kimberlite-granite contact being exposed. Kinematic stability analysis of the exposed kimberlite-granite contact was completed, following the completion of the first 5 to 7 m of the excavation, to review and confirm the consistency of the modeled rock mass with the exposed rock conditions. In addition, the readings were taken from the extensometers, piezometers, and prisms, most critically shortly before and after blasting in the A154 N pipe. The data were analyzed to determine the pit wall's overall stability before proceeding with the mining of the next bench.

The view of the mining at the initial stage of the box cut from the 9280 to 9270 m bench levels is shown in Figure 4.14. The total size of the box cut was around 58 m by 120 m at its longest width and length. Based on the specifications and proposal, the mine water was drained, diverted and pumped to prevent water seepage at the CRF placement area, as shown in Figure 4.15. The prepared site prior to CRF placement at the 9270 m bench level after covering the kimberlite with a layer of about 150 mm thick clean gravel is shown in Figure 4.16.

#### **4.3.4 Observations during Site Preparation**

The entire portion of the A154 N pipe could not be covered in 2007 as planned. The covering of the flat portion created after the box cut from 9280 to 9270 m and the covering of the high wall up to 9290 m level was completed in 2007. The remaining portion above the 9290 to 9320 m levels was to be carried out in the future. All the preparatory work was carried out according to the specifications. The kimberlite surface

was covered with 150 mm thick clean gravel and levelled at the 9270 m level, preventing the kimberlite from mixing with the CRF during its placement. The water diversion and pumping arrangements were effective in preventing water flow in the CRF area.



Figure 4.14 A154 N pipe before start of box cut from 9280 to 9270 m bench levels (modified from EBA, 2007a)

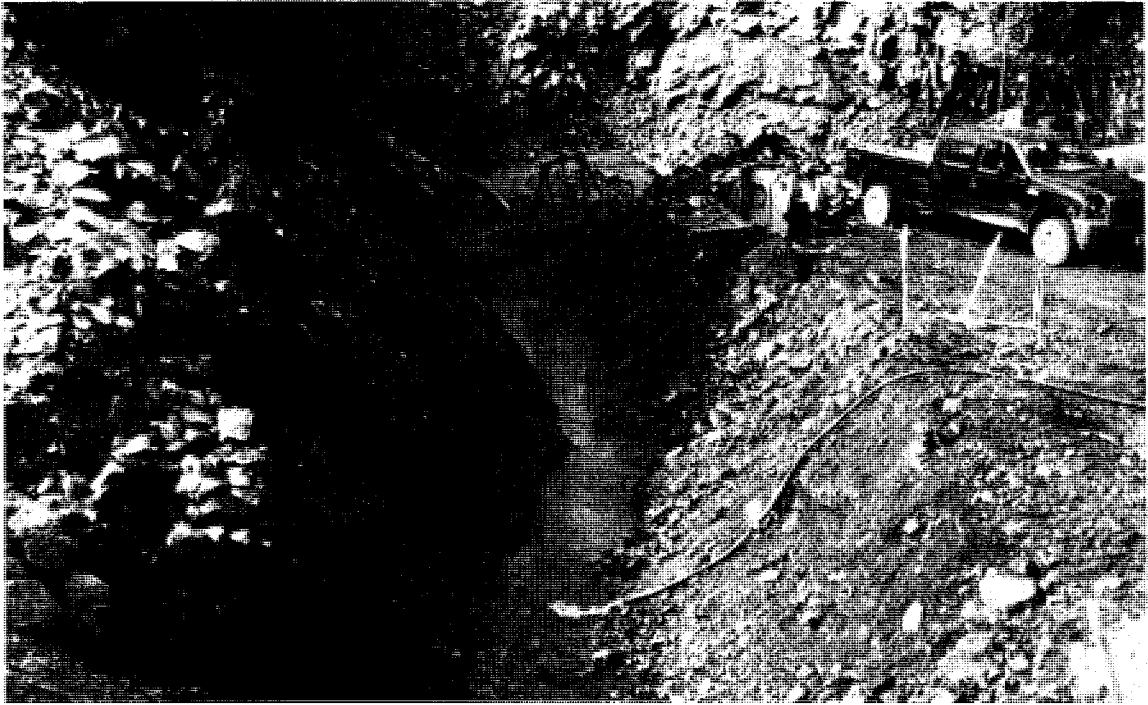


Figure 4.15 Pumping arrangement to prevent flow of water at CRF placement area

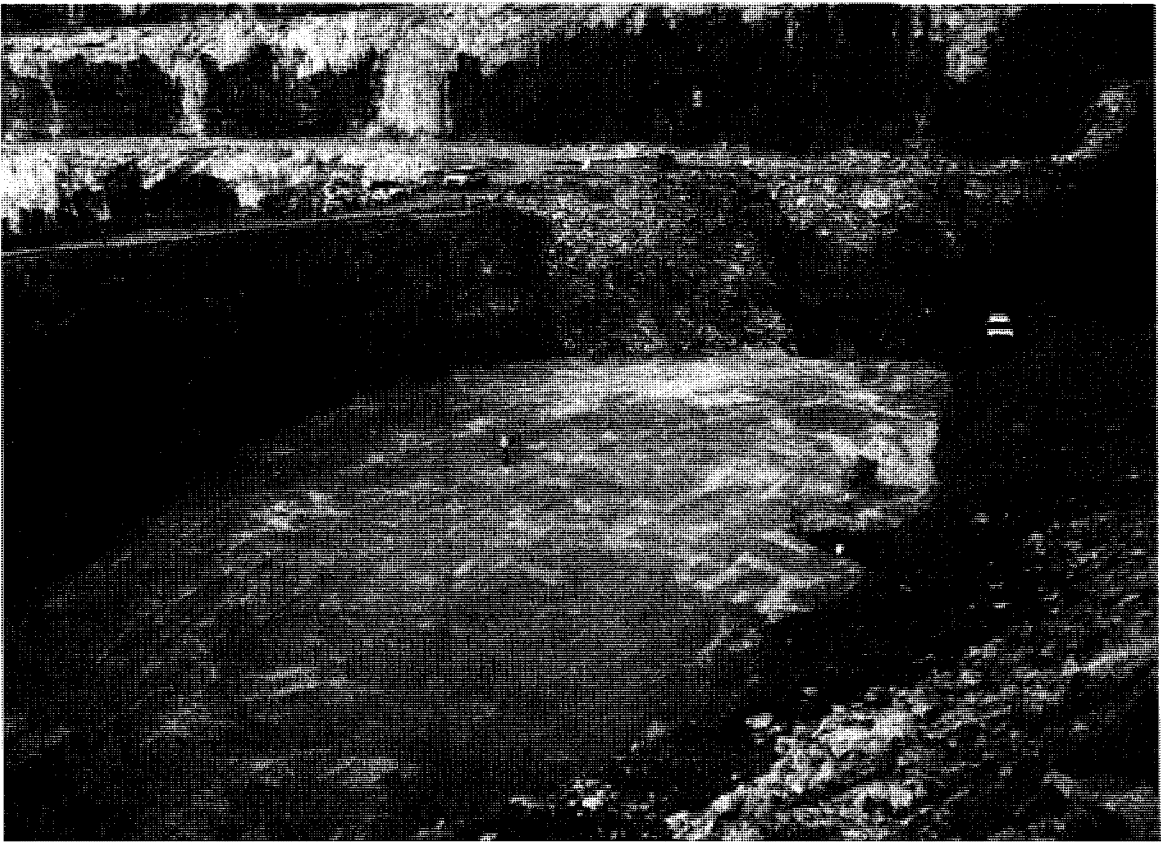


Figure 4.16 Kimberlite in box cut floor covered with compacted clean gravel

### 4.3.5 CRF Placement

The CRF placement was started at the 9270 m bench level after completing the mining of the kimberlite for the CRF placement and the installing the proposed geotechnical monitoring system in place.

Two photographs illustrating the preparation of CRF are shown in Figure 4.9 and Figure 4.10. After the CRF was prepared, it was loaded into the haul truck by the excavator, transported to the mine and dumped into the CRF placement area at the 9270 m bench level, as shown in Figure 4.17. The CRF dumped at the placement area was spread, as shown in Figure 4.18, and compacted by the dozer, to a lift thickness of not more than 1 m. The processes of placing, spreading and compacting the CRF were repeated, as shown in Figure 4.19 and Figure 4.20, until the placing of one lift thickness was completed. The initial, successive and final levels of the CRF placement levels were surveyed and verified. In the corner area, the excavator and roller compactor (Caterpillar CS 563 D) were sometimes used for spreading and compaction, as shown in Figure 4.21.

After about 8 days of site preparation and also after completing the CRF placement in nearly half of the portion from 9270 m bench level and working continuously both day and night for 6 days, the CRF placement in the other remaining half portion was carried out within another 6 days and in the same manner, as shown in Figure 4.22. CRF around 3 m thick in the layers of 3 successive lifts was placed on the top of the 9270 m bench level in two stages in 28 days, covering the exposed flat portions of the kimberlite, which was initially planned to be 5 m thick.

After allowing the CRF to set at the 9270 m level for 3 days, the CRF placement and compaction to cover the highwall slope side up to the 9290 m bench level from the top of the CRF placed at the 9270 m bench level was done by the excavator bucket even though doing so had not been specified in the specifications. As the CRF placement on the highwall slope side progressed to the higher level, an access ramp was built through the waste rock placed to cover the CRF. A total of 7 days of site preparation and 11 days of placement were required to cover highwall side in three stages.

A total of 23 days of site preparation and 23 days of placement in 5 stages, a grand total of 46 days were required to complete both site preparation and placement of CRF from 9270 m to 9290 m. A view of the A154 N pipe after placing the CRF and ROM waste in 2007 is shown in Figure 4.23.



Figure 4.17 CRF is being dumped at placement area by Cat 777 haul truck



Figure 4.18 Spreading of CRF by a dozer



Figure 4.19 Dumping of subsequent load after compaction of previous CRF



Figure 4.20 Spreading and compaction of CRF in first lift in progress



Figure 4.21 Spreading by excavator and roller compaction near corner areas

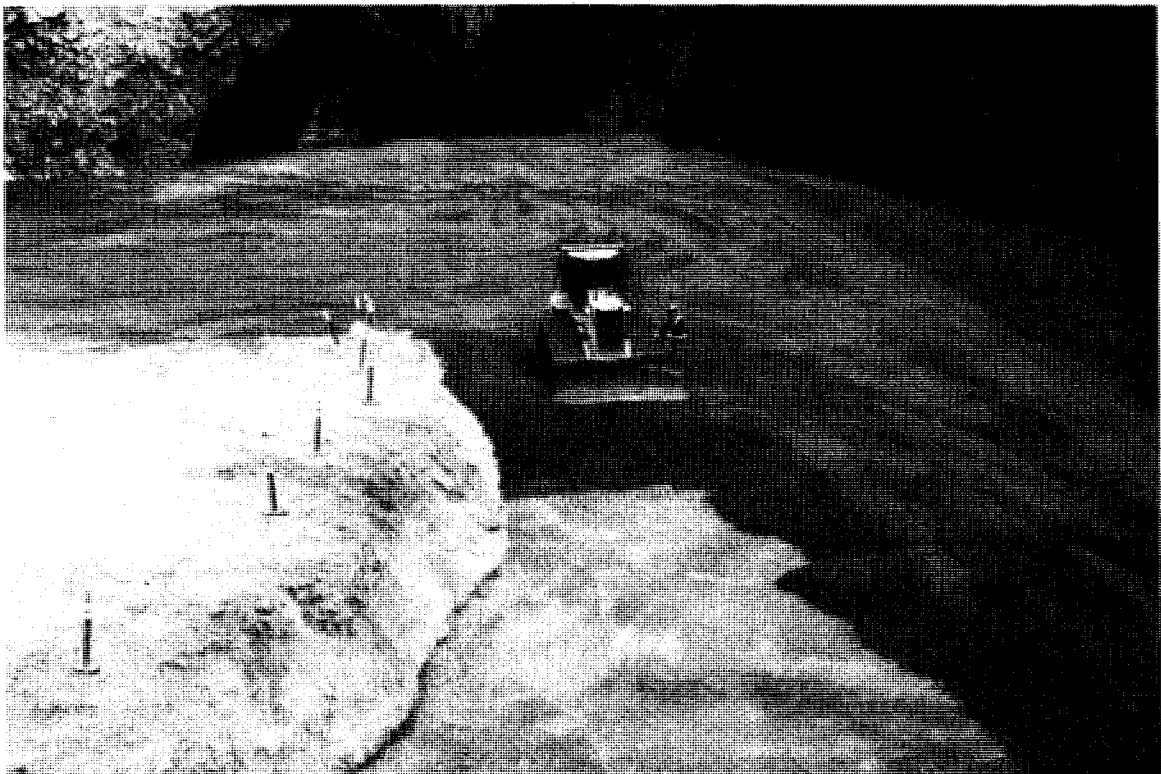


Figure 4.22 Placement of CRF at the remaining half of the 9270 m bench level

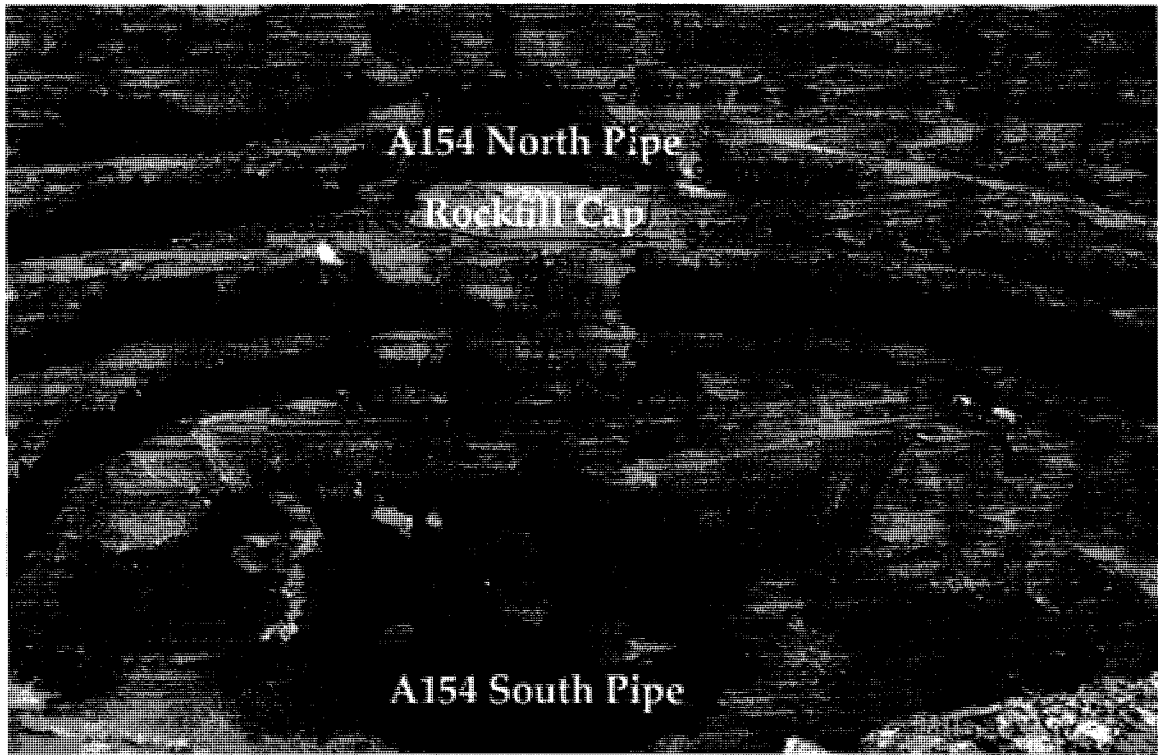


Figure 4.23 CRF placement up to 9290 m level in 2007 (modified from DDMI, 2007c)

#### 4.3.6 Observations during Placement

Cold joints between successive lifts were avoided by continuously placing the CRF while working both day and night, and placing successive lifts within 4 hours of the previous lifts. It was attempted to cut the first half of the CRF at the 9270 m level on its joining surface vertically to prevent a cold joint from forming before the remaining second half's placement as per the specifications. The CRF previously placed in the first half was too strong at its joining periphery surface where this CRF joined with the remaining second half portion, and CRF placement was carried out without cutting the joining surface vertically and also without spreading the cement slurry with a w:c ratio of 2:1, despite the specifications. However, a CRF batch was prepared by reducing one bucket of aggregate in the joining areas to allow slightly higher slurry and cement contents in the CRF placed in this contact or joining-surface zone between these two halves.

It was observed during placement that the segregation of CRF was not severe, but some segregation occurred during the loading and dumping, as the coarser size of aggregate tended to move towards the outer periphery of the loaded or dumped CRF mass. Further mixing by using the excavator bucket and further compaction of the CRF outer periphery by using the roller compactor at the DDM site may possibly minimize the effect of segregation and the forming of a weaker zone at the periphery of the CRF placement zone. The planned CRF thickness of 5 m was reduced by almost 2 m, possibly because a higher CRF strength was achieved than was expected.

## **4.4 Quality Control and Testing in the Field**

A literature review about QC and testing practices, together with the QC and testing practices adopted at the DDM site is presented in this section.

### **4.4.1 Literature Review**

The main purpose of QC is to check whether the rockfill under construction on a site meets the design parameters. In most cases, QC practices are restricted to checking the  $\gamma_d$  of the fill, as an indirect indicator of its quality (Brauns and Kast, 1990).

Metering control of the cementing agent materials and the pulp density of the mixed slurry is of the greatest importance for maintaining fill quality (Laudriault et al., 1987).

QC measures include maintaining the quality and quantity of binders and aggregates according to the design criteria (Yu, 1989; Farsangi et al., 1996) and also maintaining the aggregate attrition and MC, the water quality, and the mixing process to properly coat the aggregate with cement slurry (Yu, 1989).

Archibald et al. (1993) reported that tight controls on the quality of the backfill products produced are minimal in the mining industry relative to those that have been traditionally established by the concrete product industries. Based on their literature review and correspondence with backfill operators at 18 mines throughout the province of Ontario, these researchers concluded that the QC procedures in this province were not systematic.

The QC of in situ backfill mass is controlled by the mixing plant and the chosen methods of transport and placement (Farsangi and Hara, 1993; Archibald et al., 1993; Farsangi et al., 1996). Some of the recommended procedures include the checking for the backfill's proper mass or volume and the QC of the fill materials including routine manual sampling and checking for their verification, control of the pulp or slurry density and the MC of stockpiled aggregate, adjustment of the aggregate gradation at the surface based on attrition and daily inspection of the placement area, and routinely sampling and checking the final CRF product.

Archibald et al. (1993) and Farsangi et al. (1996) suggested carrying out strength tests in the laboratory and in situ, measuring the slurry density, and analyzing the aggregate grain size.

Brechtel et al. (1989) reported that grain-size analysis of the aggregate and compression tests of laboratory specimens, and 150 mm cored samples from a stope were used at the Cannon Mine as a QC measure.

Farsangi and Hara (1993) reported that 25 mm cylinder and 50 mm cube samples were tested weekly in a laboratory at the Kidd Creek Mine as a QC measure.

Farsangi (1996) indicated some QC factors that could affect in situ CRF properties. These factors include the use of portable water for mixing, the correct batching of the aggregates and the binder, as well as other environmental factors. He also suggested that

QC measures should be exercised during the preparation of CRF, during its transportation, and over its placement area. Once the backfill material has left the belt or been dumped from the truck into the stope, limited control or remedies are possible. During placement, the CRF mix should be closely observed to determine if any changes are needed, for example, the quality of the slurry or the amount of fines in the aggregate, or whether extra cement slurry needs to be added to lower the segregation. Some of the recommended procedures included the properly weighing, sizing, and carefully controlling the MC of the aggregate, using sufficient binder slurry to coat the aggregate adequately, and maintaining consistent bulk densities of the prepared batches.

Evans et al. (2007) suggested that the quality of the placed CRF is important in achieving the purpose of backfilling and must be effectively controlled by establishing programs, procedures, and training packages. However, each site has to develop specific programs to suit its needs. They also suggested installing a proper measuring instrument within the CRF plant to measure and monitor the various components effectively, and designing the plant control logic according to the specified recipes by using control loops, alarms and interlocks.

Evans et al. (2007) reported that the CRF plant operators at mines owned by Barrick routinely conduct QC measures by using pulp density scales to measure density, lab scale drying ovens to measure MC in the aggregate, and casting samples based on the designed CRF mix recipe in plastic moulds for UCS testing. The test data can be used for daily operating decisions and maintained in a database for further analysis. Mines owned by Barrick had operating manuals and protocols for QC and QA. These manuals were used to specify the number, type, frequency and location of samples to be collected; the type of the method to be used for testing; the approach to data analysis and reporting; and the standard operating procedures for fill preparation, delivery, placement and monitoring. Most sites had designated personnel to perform these duties.

Stone et al. (2007) described QC as the monitoring of the quality of the fill being placed. Most mines rely on sampling of the CRF from the batch plant, the backs of the truck or from stopes in order to monitor the quality of the fill being placed. Routine testing of backfill cylinders should also include recording the weight of the test cylinder along with the peak (failure) load and its supporting details. The strength of a CRF test cylinder is a function of its weight or density. This point is illustrated in Figure 4.24, which is based on test results from the Nevada Mines. This figure shows a clear statistical trend of increasing strength with weights, as was expected. The cylinder weights can be used to loosely predict the final UCS results. He also suggested testing the water and binder qualities and training the personnel involved in CRF operations, including the batch plant operator.

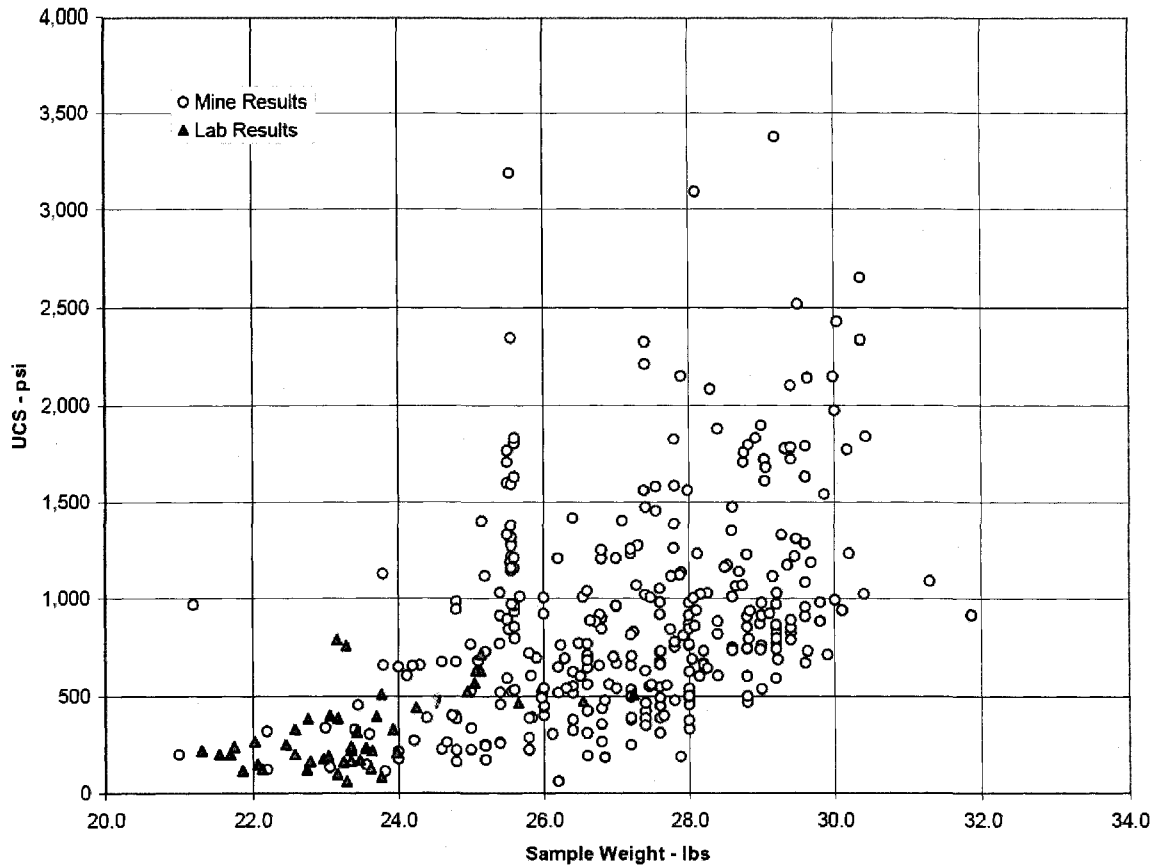


Figure 4.24 UCS versus cylinder weights of CRF samples at Nevada Mines (Stone et al., 2007)

**Summary**The literature reviewed indicated that QC and QA measures should include defined inspection, monitoring and testing procedures at certain frequencies to verify that the design mix-proportion recipe is maintained and that the placed CRF exhibits the required strength. This process should cover the following aspects:

- The aggregate's quality, gradation, and MC. The aggregate's quality and gradation have to be maintained as per the design specifications to ensure that the required targeted strength can be achieved. This form of QC is carried out routinely in every mine, as already discussed in this thesis in section 3.4 while describing the preparation and placement practices of the CRF in different mines around the world. However, the frequency of this QC procedure depends solely on the site-specific requirements.
- The type, quality and quantity of binders, and other additives, if any.
- The quality of mixed binder slurry including other additives
- The effective mixing process for coating all the aggregate with binder slurry and other additives, if any.
- Sampling and strength tests of the placed CRF.
- Close inspection or monitoring and verification of all processes on a daily basis.

#### 4.4.2 Field Density and Moisture-Content Measurements

In situ wet and dry densities and MC were measured by using the direct transmission mode of the nuclear densitometer gauge manufactured by TMD, model 3430, as shown in Figure 4.25. The details of this model are described in this section. The smooth surface was prepared by hammering a scraper plate on the top of the dozer-compacted CRF surface, a 300 mm hole was driven into this smooth CRF surface, and source rod of a nuclear gauge was inserted inside the hole. The displayed values of the wet and dry densities, MC, and, sometimes, the  $e$  were recorded. The measured  $e$ , was based on the assumed  $G_s$  and the measured  $\gamma_d$  of the CRF, and the density of water ( $\gamma_{wat}$ ), so the  $e$  is a calculable value, and the  $\eta$  is calculated based on the  $e$  by using the following formulas:

$$e = \frac{G_s \cdot \gamma_{wat} - \gamma_d}{\gamma_d} \quad 4.1$$

$$\eta = \frac{e}{1 + e} \times 100 \quad 4.2$$



Figure 4.25 Close view of TMD nuclear gauge during its in situ measurement

The in situ measurement of the densities and MC were carried out at least twice and even up to five times per shift, covering the area of each lift as it progressed. After completing

flat portion of the 9270 m bench level, the excavator bucket was used for placing and compacting of the CRF to cover the slope area of the highwall up to the 9290 m bench level, and no further measurements were taken due to some safety reason.

#### *4.4.2.1 TMD Nuclear Gauge*

Based on the manual provided by its manufacturer for the model 3430 (Troxler, 2006), its measuring procedures are summarized in this section. This model provides the basic features required for determining the density of asphalt, soil, aggregate or concrete and the MC of soil or aggregate. As well, this model complies with the ASTM Standard Test Methods D2922-91 and ASTM D3017-88, D2950-05 and C1040-93. The gauge directly displays the wet density ( $\gamma_w$ ),  $\gamma_d$ , the MC, the percent compaction, and the  $e$ .

The TMD nuclear gauge, Model 3430, can quickly and precisely determine the MC and density of soils, soil bases, aggregate, concrete, and asphalt without the use of core samples or other destructive methods. This model offers two test modes for determining the density of construction materials. The operator chooses either the backscatter or direct transmission mode to perform tests, depending on the thickness and type of material being tested. The following sections will describe this model's operation, application and features.

#### *4.4.2.2 Measurement Procedure*

This model uses the interaction of gamma radiation with matter to measure density through direct transmission or backscatter. This gauge determines the density of material by counting the number of photons emitted by a cesium-137 gamma source that are read by the detector tubes in the gauge base.

In direct transmission, the source rod extends through the base of the gauge into a predrilled hole to position the source at the desired depth, a maximum of 30 cm deep. Photons from the source travel through the material in the test area, colliding with electrons present in the material, to reach the photon detectors in the gauge. The average density between the gamma source and detectors is then determined. This gauge is used for testing lifts of soil, aggregate, asphalt and concrete up to 30 cm in depth.

Backscatter measurement is rapid and non-destructive. The gamma source remains inside the gauge, which rests on the surface of the test material. The gamma photons emitted from the source penetrate the test material, and the scattered photons through the material and, after reaching the detectors, are counted or measured by them. The backscatter method is used primarily to determine the density of layers of asphalt and concrete from the surface to a depth of approximately 10 cm. If the material thickness is over 10 cm, direct transmission is more appropriate in order to get a representative measurement.

A material with a high density increases the number of collisions between the gamma photons and the electrons present in the material. Therefore, the number of photons reaching the detector tubes is reduced. In short, the lower the number of photons

reaching the detector tubes, the higher the material density. The opposite is true for material with a lower density; fewer collisions occur between the gamma photons and electrons present in the material. More photons will reach the detector tubes, increasing the density count. A microprocessor in the gauge converts these counts into a density reading.

The MC determination occurs in much the same way as the backscatter density reading. A Americium - 241: Beryllium source is located inside of the gauge base. Fast neutrons from this source enter the test material and are slowed by collisions with the hydrogen atoms present in the material. The helium 3 detector in the gauge base counts the number of thermalized (slowed) neutrons. This number (known as the moisture count) is directly related to the amount of moisture in the tested area.

The gauge will show higher MC and the lower  $\gamma_d$  if the material contains frost (if the material is frozen). The gauge will still give the  $\gamma_w$ ,  $\gamma_d$  and MC results without the target density being entered.

The oven drying provides the true MC by removing all water from the sample. The gauge measures the hydrogen present in the material, which is usually in the form of water. If the material contains naturally occurring hydrogen or bound hydrogen, the gauge will measure the MC falsely high in many cases. Some of these materials include mica, lime, flyash, cement, organic materials, gypsum, coal, and phosphates. A false low reading can also occur but is less common (causes include high salt or iron oxide content or presence of boron, lithium or cadmium). A moisture offset will adjust for this problem.

#### 4.4.2.3 Gauge Operation

This model offers two user-specified modes of operation to determine the MC and density of construction materials: soil and asphalt. Although all gauge-moisture and-density systems are active during each test, the microcontroller processes and presents data differently for each mode.

The soil mode is designed for measurement of soils, stone or other materials where both density and MC measurements are desired. Measurements can be made in either the direct transmission or backscatter position. Direct transmission typically offers better precision and control of the depth of measurement and is the preferred method. When taking a measurement in the soil mode, the information provided by the gauge will be the  $\gamma_d$ ,  $\gamma_w$ , MC, percent proctor, percent air voids and  $e$ .

The asphalt mode is used on full depth asphalt ( $\leq 10$  cm). Typically, the source rod is in the backscatter position, on top of the asphalt; alternatively, direct transmission may be used if a hole is drilled into the asphalt. The asphalt mode displays the  $\gamma_w$ , percent marshall and percent voids.

Surface preparation for soil testing can be critical to gauge performance and test results. The scraper plate accessory provided can be used to prepare surfaces that are not smooth

by moving it back and forth across the area. Small voids, cracks, or holes can be filled with sand or native fines. Doing so is most critical when testing in the backscatter position. When performing density tests on coarse open-graded asphalt, surface voids may be filled with soft sand, cement powder or native fines. The asphalt surface should remain bare so that the gauge base makes contact with the surface, and the gauge sits flat on the asphalt surface.

The model gives the user the ability to input offsets to the gauge readings to correct for non-standard conditions. In the soil mode, a moisture offset may be needed to adjust for the presence of chemically bound hydrogen or the presence of neutron absorbers. The offsets available in both the soil and asphalt modes are a density offset to correct for material composition or for material with a density outside of the calibration range (1100 to 2700 kg/m<sup>3</sup>) and a trench offset to correct the errors due to large-above surface masses near the measurement area.

This model's keypad consists of 10 keys. Above the keypad is a 2-line by 16-character Liquid Crystal Display screen. Up-and Down-arrow keys allow scrolling through which various information displayed on the LCD screen. This gauge is equipped with a beeper to verify each key press.

The gauge runs on a rechargeable NiCad battery. Under normal conditions (an 8-hour day), a fully charged battery will remain operational for approximately 8 weeks. When the Battery Low warning appears, a few hours remain before the battery must be recharged. A full charge (16 hours) is recommended at that time, but a 30-minute recharge will provide several hours of use if necessary. Two adapters included as standard accessories with this gauge are a 115/230 VAC 50/60 Hz and a 12 VDC charger. Alkaline batteries (D size) can be used temporarily in the event that recharging is not an option. A separate battery case is supplied for this purpose.

The gauge includes several functions that ensure correct gauge operation. A daily reference standard count is performed by the operator to account for source decay and natural background factors, such as naturally occurring radiation and hydrogen. To verify gauge stability, the operator compares the daily standard to the average of the last four standard counts. The new counts must be within a stated limit of the counts to which the new counts are compared. A statistical stability test, or stat test, may be performed to validate the normal operation of the gauge. A stat test may be executed if readings are suspicious. The drift test can be performed to check the long-term drift of the gauge if the stat test has been performed (and passed).

#### 4.4.2.4 Measurement Precision and Calibration

The measurement precision based on the time allowed for taking a reading is shown in Table 4.2, and its calibration is shown in Table 4.3.

Table 4.2 Measurement precision of TMD nuclear gauge Model 3430

<i>Direct Transmission (150 mm)</i>	15 sec	1 min	4 min
Precision at 2000 kg/m <sup>3</sup>	± 6.8	± 3.4	± 1.7
Composition error at 2000 kg/m <sup>3</sup>	± 20	± 20	± 20
Surface error (1.25 mm, 100% void) kg/m <sup>3</sup>	-17	-17	-17
<i>Backscatter (98%) (100 mm)</i>			
Precision at 2000 kg/m <sup>3</sup>	± 16	± 8	± 4
Composition error at 2000 kg/m <sup>3</sup>	± 40	± 40	± 40
Surface error (1.25 mm, 100% void) kg/m <sup>3</sup>	-75	-75	-75
Moisture Precision at 250 kg/m <sup>3</sup>	± 10.3	± 5.1	± 2.5
Surface error (1.25 mm, 100% void) kg/m <sup>3</sup> Depth of measurement at 250 kg/m <sup>3</sup> = 212.5 mm	-18	-18	-18

Table 4.3 Calibration of TMD nuclear gauge Model 3430

Accuracy of density standards	± 0.2
Accuracy of moisture standards	± 2.0
Calibration range	1100 - 2700 kg/m <sup>3</sup> (density)
	0 - 640 kg/m <sup>3</sup> (moisture)
Operating temperature	-10 to 70°C
Maximum test material surface temperature	175°C
Storage temperature	-55 to 85°C

#### 4.4.3 Water to Cement Ratio

Based on the batch plant ticket provided by the cement slurry truck at the mixing bay, information about the mass of water and cement used to batch the cement slurry was generally recorded two times per shift. This information was gathered while collecting the cement slurry sample from the cement slurry truck. The w:c ratio was compared to and validated with the specification.

#### 4.4.4 Discussion about In Situ Tests and Water to Cement Ratio

The in situ test results of the CRF and w:c ratio are attached in the Appendix and described in Chapter 5 while discussing the results and discussion. The in situ densities and MC measurements of the CRF were carried out by using the nuclear gauge as per the specification. Its MC measurement was validated again with laboratory value and is discussed later in this chapter in section 4.5.3. The in situ density measurement made by the nuclear gauge was considered reasonably accurate and was not validated by using an alternative method. The in situ densities and MC were measured without any guide

values although the  $\gamma_d$  of the CRF had been specified. The placement of the CRF was continued irrespective of the measured in situ values. The in situ densities and MC measurements were usually not carried out during the CRF placement on the highwall slope sides (on top of the flat portion of the CRF placed at the 9270 m to 9290 m) due to safety reasons.

The variability of the in situ measurement values of the densities and MC indicated the possible variability in the CRF properties. The w:c ratio provided by the batch plant was not cross-checked because its weighing and metering systems are calibrated and considered to be reasonably accurate. A adjustments in the quantity of water based on the variations in the aggregate's MC were not made as per the specifications for the water quantity was fixed throughout the batching of the cement slurry, possibly because the variation in aggregate's MC was within the narrow range of 1 to 2%. The cement content was slightly reduced during the placement of the CRF on the highwall slope sides, possibly because of achieving a higher strength than expected from the CRF placed on the flat portions at the 9270 m level.

## **4.5 Quality Control and Testing in the Laboratory**

### **4.5.1 Quality of Cement Slurry**

Generally, the batched cement slurry was collected twice in a plastic container during each shift from the chute of the concrete truck during its pouring into mixing bay and brought back to the laboratory. The slurry was not collected during the initial pouring, but generally collected when more than half of the pouring from the concrete truck had been completed. At the laboratory, the transported sample of the cement slurry from the mixing bay was thoroughly mixed by using a steel rod, and quality of its mixing was checked visually to make sure that no segregation of cement had occurred at the bottom of the container and that the cement had been mixed properly.

The  $G_s$  of the cement slurry was measured by using the mud balance, Model 140, from the Fann Instrument Company, as shown in Figure 4.26. The mud balance was calibrated first with fresh water, and any deviation of its specific value from 1 was adjusted. The cement slurry was poured into the balance's cup and covered by its cap. The excess slurry outside of the cup was removed, and then the cup was placed with its beam into the base support. The rider was adjusted along the graduated scale, readable up to 0.01, until the levelling bubble was under the center-line, indicating that the beam was fully balanced. The reading of the edge of the rider towards the cup was recorded as the  $G_s$  of the slurry.

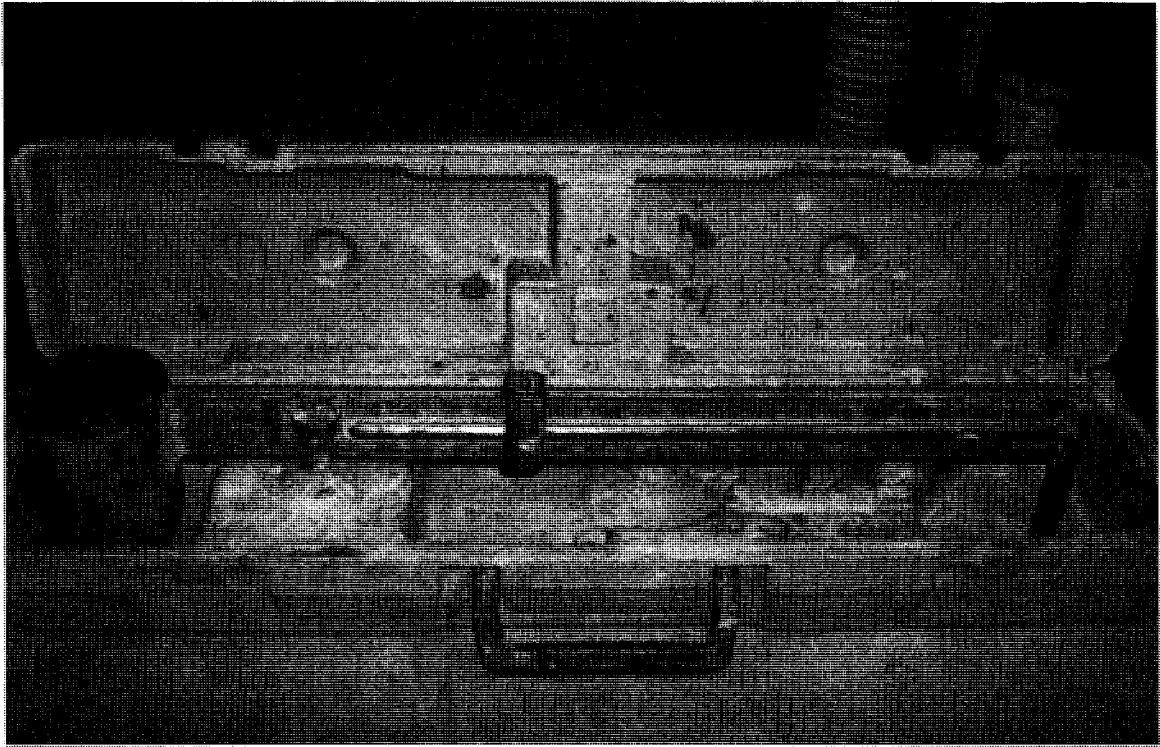


Figure 4.26 Mud balance used for measurement of specific gravity of cement slurry

#### 4.5.2 Gradation and Moisture Content of Aggregate

Generally, a sample of the aggregate was collected once during a shift for grain-size analysis and MC measurement, which were carried out according to the ASTM C136-05 and ASTM D2216-05, respectively. The MC of aggregate was calculated based on the following formula:

$$w = \frac{M_{samp} - M_{dry}}{M_{dry} - M_{cont}} \times 100 = \frac{M_{wat}}{M_{dry\ samp}} \times 100 \quad 4.3$$

where

- $w$  = moisture content (%)
- $M_{samp}$  = mass of sample and container (g)
- $M_{dry}$  = mass of oven dried sample and container (g)
- $M_{cont}$  = mass of container (g)
- $M_{wat}$  = mass of water (g)
- $M_{dry\ samp}$  = mass of oven dried sample (g).

The sample of the aggregate was collected from the stockpile from where the aggregate was being placed by the loader into the mixing bay to produce CRF. A sample of around 20 kg of aggregate was collected in a plastic bucket by using a shovel and was taken from different locations on the sampling pad, as shown in Figure 4.27. The sampling pad was prepared by placing a full loader bucket of the aggregate onto flat ground and levelled by

the loader bucket. The collection of the sample from the sampling pad was made based on visual observation to get the best possible representative sample.



Figure 4.27 Sampling pad of CRF aggregate for its gradation

#### *4.5.2.1 Aggregate Grain-Size Distribution*

The grain-size analysis was carried out based on the ASTM C 136-05. The sample was transported from stockpile site to the laboratory, and the whole sample was used for sieving by placing it into the vibratory screen of Model TS1 from the Gibson Company Inc., with its sizes of 40, 28, 20, 14, 10, 5 mm and a pan at its bottom, as shown in Figure 4.28. The sample was vibrated around 15 minutes for proper screening and gradation. The total mass of the aggregate sizes retained in each category was obtained by using the Sartorius balance with a precision of 0.1 g.

By using the splitter, as shown in Figure 4.29, the minus 5 mm sizes, retained at the pan of Gibson vibrator, were split away from the aggregate's sample.

The split sample of about 500 g to less than 1000 g was washed through the 0.08 mm sized screen, oven-dried and placed in a ATM Arrow shaker from the ATM Corporation, as shown in Figure 4.30, for about 15 minutes. This sample was sieved by using the shaker, which has screen sizes of 5, 2.5, 1.25, 0.63, 0.315, 0.16, 0.08 mm and a pan

certified by the ISO 3310-1:2000 and BS 410-1:2000. After the completion of the sieving process, the mass of the sample from the respective screen size was recorded. The gradation curve obtained by plotting the percent passing based on the mass with the respective log value of the screen size was compared with the specified gradation limit of the CRF aggregate.



Figure 4.28 Gibson vibratory screen used for gradation of CRF aggregate

#### **4.5.2.2 Moisture Content**

The MC present in a split <5 mm sample was measured according to the ASTM 2216-05, based on the ratio of the weight loss from the sample to the total weight of the dry sample obtained after oven drying by using the Equation 4.3 provided in section 4.5.2. About 750 g to 1000 g of the split sample was oven-dried at  $110 \pm 5^\circ\text{C}$  until its constant weight was reached.

The whole sample's MC was determined based on the ASTM D 4718-87 by adding the multiplied values of the corresponding fraction of the masses of >5 mm and <5 mm samples to their corresponding MC values.

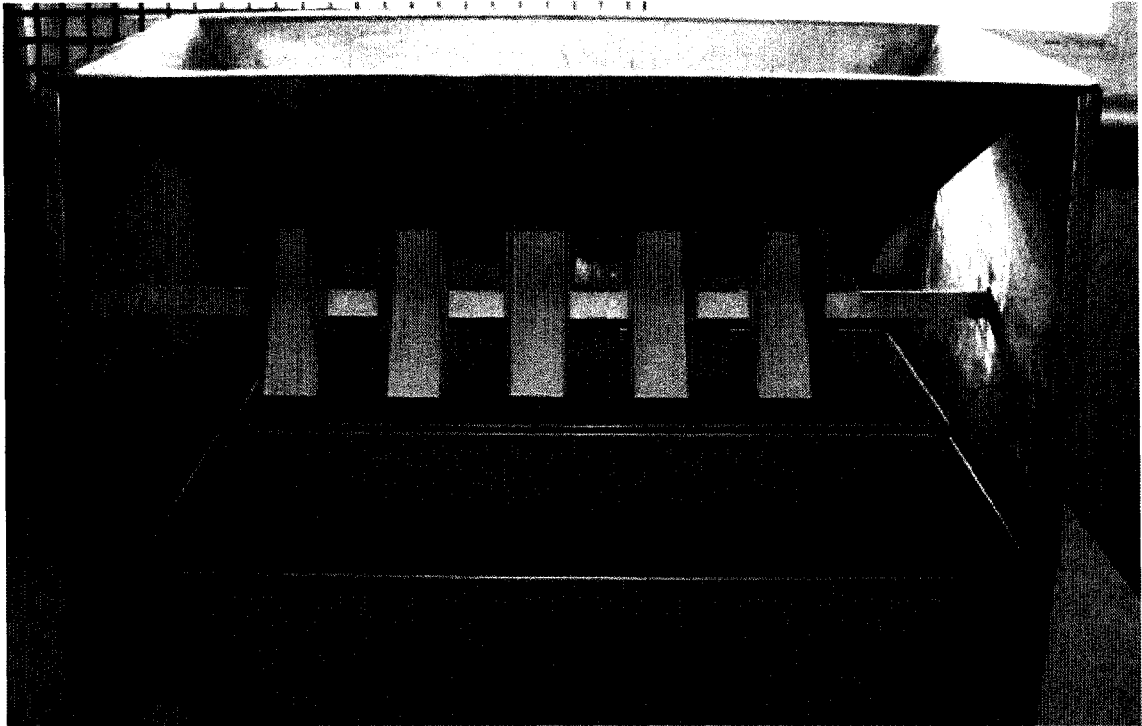


Figure 4.29 Splitter used to split the <5 mm sample

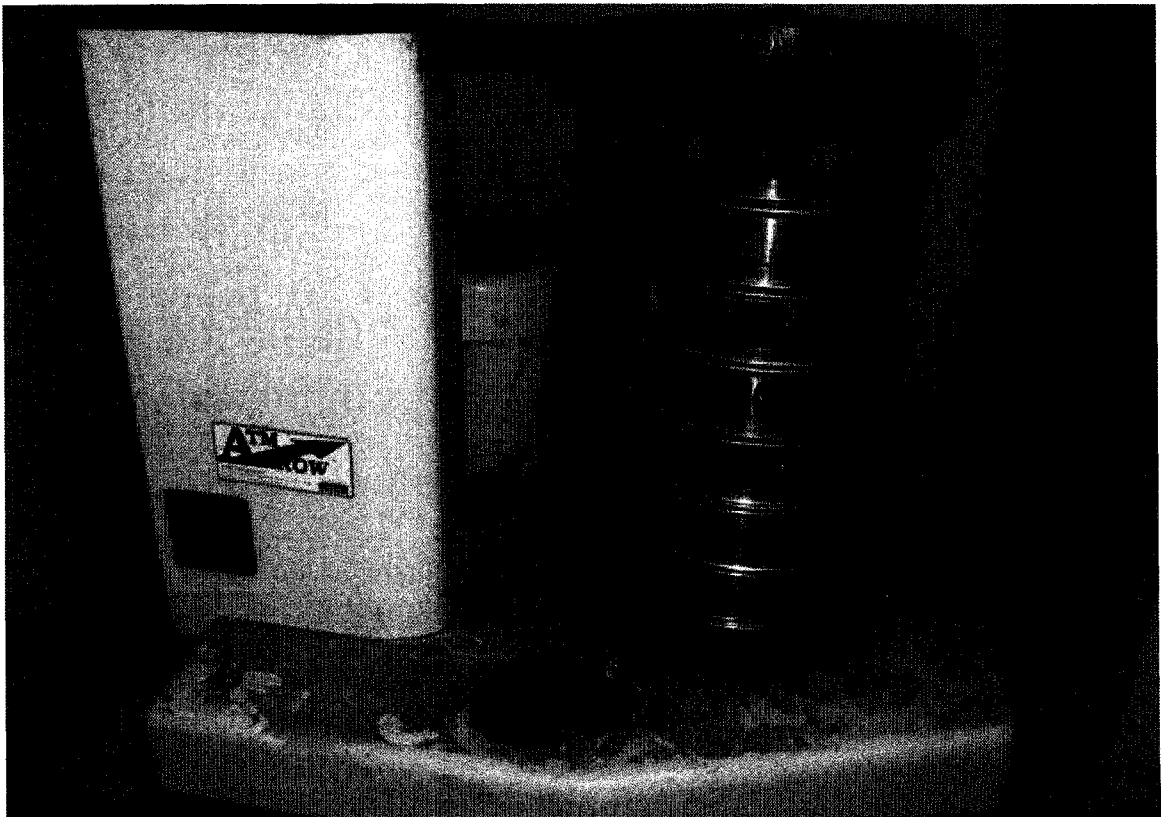


Figure 4.30 Arrow shaker for gradation of <5 mm fraction from CRF aggregate

### 4.5.3 Laboratory Moisture Content of CRF

A sample of the CRF being placed was collected in a plastic bucket at least twice per shift from the nearby nuclear test location and transported to the laboratory to determine the MC and to cast cylinders for the UCS test.

The CRF samples were collected in the buckets from the nearby density test location to verify the in situ MC measurement made by using the TMD nuclear gauge and to prepare the CRF cylinders at the laboratory. The CRF samples were placed on a steel tray and mixed properly with a scoop after brought to the laboratory. About 1 kg of CRF samples were placed in a pan and oven-dried at  $110 \pm 5^\circ\text{C}$  until its constant weight was reached to determine the MC present in the sample based on the ASTM D 4959-00, and the MC was calculated by using the Equation 4.3 provided in section 4.5.2.

The laboratory-measured values of the MC were compared with its in situ measurement made by the TMD nuclear gauge. Based on the laboratory moisture content, in situ  $\gamma_w$  measured by using the TDM nuclear gauge was corrected. The laboratory moisture corrected in situ  $\gamma_d$  is calculated based on the following formula:

$$\gamma_d = \frac{\gamma_w}{1 + w} \quad 4.4$$

where

$\gamma_d$  = lab MC corrected in situ dry density of CRF ( $\text{kg/m}^3$ )

$\gamma_w$  = in situ wet density of CRF measured by using the TDM nuclear gauge ( $\text{kg/m}^3$ )

$w$  = laboratory moisture content of CRF (%).

The laboratory MC corrected in situ  $\gamma_d$  was compared with the in situ  $\gamma_d$  measured by the TDM nuclear gauge. The in situ  $\gamma_d$  was calculated automatically and displayed by using the values of in situ  $\gamma_w$  and in situ MC measured by using the TDM nuclear gauge.

### 4.5.4 Test Cylinder Preparation and UCS Test

The CRF samples were collected in a bucket from the nearby in situ density and MC test location to prepare the cylinders for the UCS test. After being brought to the laboratory, the samples were placed in a squared steel pan of about 750 mm by 750 mm, and thoroughly mixed by using a scoop.

The diameters of the cast cylinders were either 100 mm or 150 mm with respective lengths of 200 mm or 300 mm, maintaining a length to diameter ratio of 2:1. The oversized aggregate was screened off and discarded by using a 25 mm screen, and only the <25 mm sized CRF samples were used for casting 100 mm diameter cylinders. A sample was placed into a 5 mm thick steel or 6 mm thick plastic mould, shown in Figure 4.31, in 3 layers. A standard proctor hammer was used to pound each layer 20 times. The whole CRF sample without screening was used to cast cylinders of 150 mm diameter into a steel mould in five layers, with each layer being pounded 20 times.

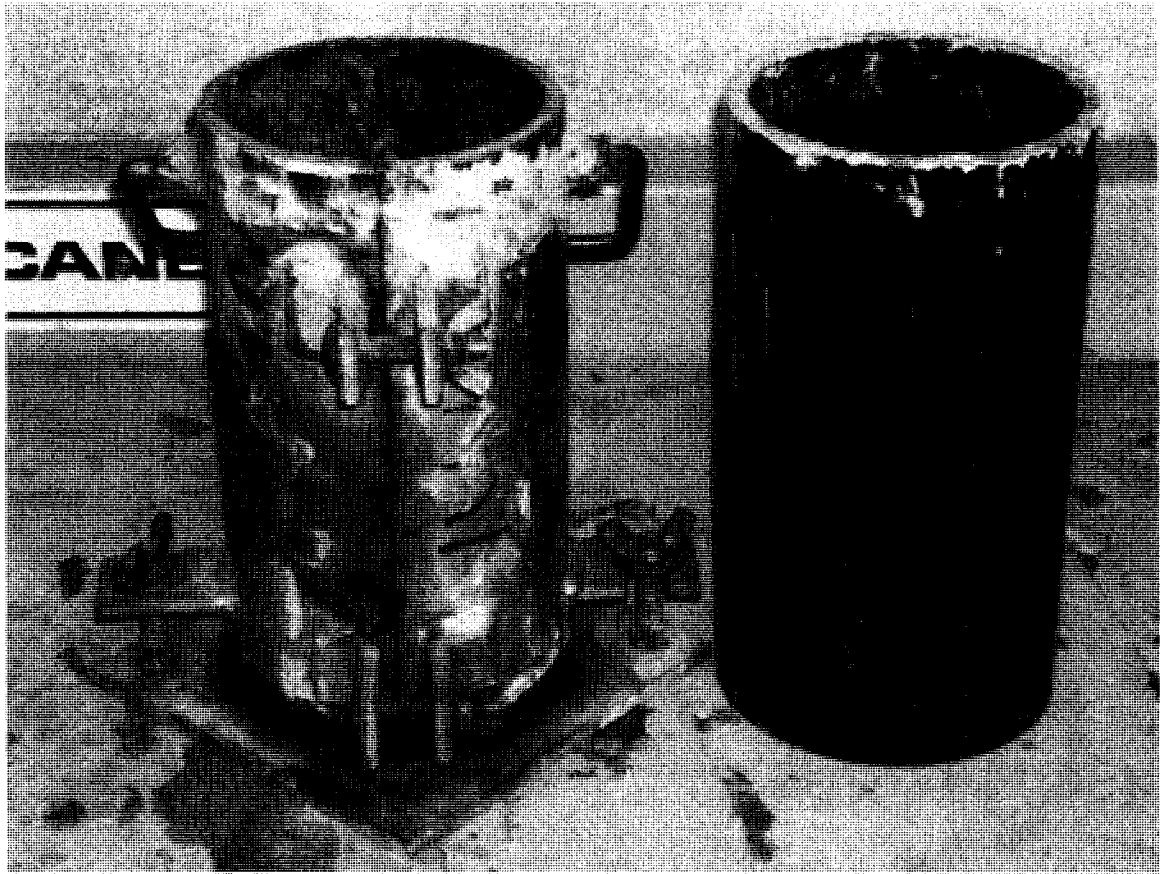


Figure 4.31 Steel and plastic moulds used to cast 100mm diameter cylinders.

The  $\gamma_d$  of the cylinder prepared at the laboratory for the UCS test was calculated based on the volume of the mould, the weight of the cylinders, and the amount of MC present in the CRF sample. The screened sample, passing through a 25 mm screen size, was used for MC calculation for preparing the 100 mm diameter cylinders, and the whole sample was used for preparing the 150 mm diameter cylinders. About 1 kg of each sample was oven-dried at  $110 \pm 5^\circ\text{C}$  to calculate the MC in the samples based on the ASTM D 4959-00, and the MC was calculated by using the Equation 4.3 provided in section 4.5.2.

The number of blows from proctor hammer per layer was estimated through a trial and error to obtain a  $\gamma_d$  of the cast cylinders close to or slightly higher than the required in situ density of  $2150 \text{ kg/m}^3$ .

The cylinders from the moulds were extracted after roughly 24 hours of their casting time by using compressed air for the 100 mm plastic mould and by just opening the steel mould for the 100 mm and 150 mm diameter cylinders. Each cylinder was named based on the number, which was printed on its side along with its UCS test date, as shown in Figure 4.32.

The DDM site had a curing-bath facility with that provided temperature adjustment for ordinary concrete cylinders. However, the CRF cylinders were weak and could not be cured in the same manner. The site had no moist room, so the CRF cylinders were cured

at a room temperature of about  $23 \pm 3^\circ\text{C}$ . The CRF cylinders were properly wrapped inside a moist jute cover, which was periodically moistened in order to prevent the cylinders from drying.

The capping-sulphur compound, CA-0100, from the Test Mark Industries was normally melted at  $260^\circ\text{F}$  inside a sulphur pot from the Ritehete Corporation. Both sides of the cylinders were capped by pouring the melted sulphur inside the groove at the base of the steel mould and vertically pressing the sides of the CRF cylinders inside the melted sulphur for about a minute. The capping process and the sulphur pot are shown in Figure 4.32. The cylinders were capped before the UCS test in order to obtain good contact between the cylinders' surface and the loading plates of the UCS test machine.

The UCS test of the cylinders was carried out 3, 7 and 28 days after their casting by maintaining a log of the cylinder-breaking day or the UCS test date. The vertical deformation of some of the test cylinders was measured by using a Mitutoyo dial gauge, as shown in Figure 4.33, with a precision of 0.01 mm and a maximum range of 20 mm. A magnet was attached to the side frame of the UCS test machine, and the dial gauge was set up on top of the bottom plate, which moved upward during the UCS test. The stress-strain curve was obtained by directly reading the applied stress in MPa from the machine's display unit, and the corresponding displacement value was obtained from the dial gauge at the same time. The stress rate was increased at 0.05 MPa/sec as there was no option for adjusting its displacement rate during the test.



Figure 4.32 Some of the cylinders after completion of their capping

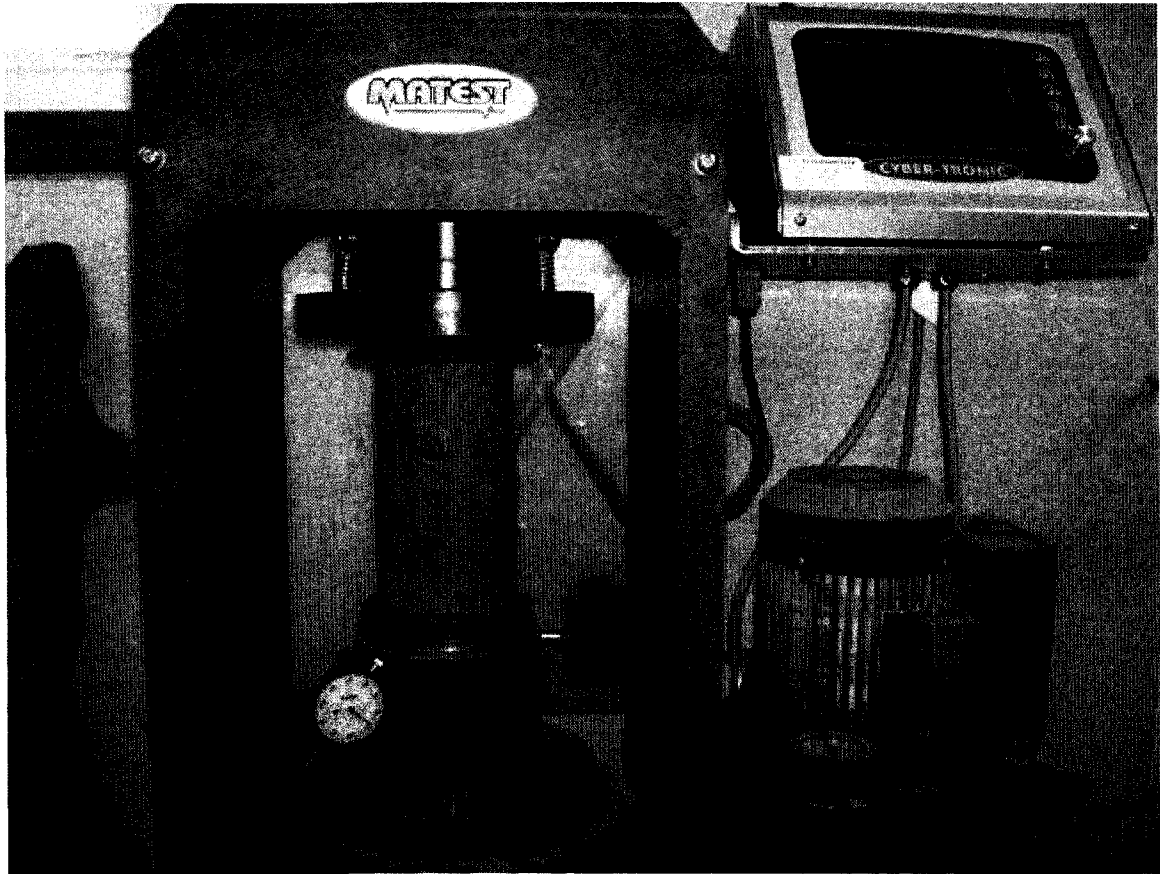


Figure 4.33 Matest compression test machine with dial gauge set up

The Matest UCS test machine, Model C064, with a capacity of 2000 kN load, suitable to test cubes up to 150 mm long on each side and cylinders up to a diameter of 160 mm with a length of 320 mm and a maximum vertical displacement of approximately 55 mm, was used to measure the UCS of the CRF cylinders, as shown in Figure 4.33.

The machine consists of a hydraulic jack, which allows the load to be applied to the specimen through an oil pressure circuit. Two hardened plates transmit the strength of the hydraulic jack to the specimen. A set of distant pieces can be installed on top of the lower plate to reduce the distance between the compression plates and to adapt it as per the dimensions of specimen. The machine's lower plate moves upward, and the upper plate remains fixed, compressing the specimen.

The machine has a display unit in the top right corner, as shown in Figure 4.33, which shows load and stress values during the testing. The machine allows the user to set up three sides of cubical or the diameter and length of a cylindrical test specimen. It automatically calculates the loading surface or contact area of the specimen during the testing and utilizes the result to calculate the stress value for the given load. The machine automatically stops once the value of the stress reaches its maximum, and it is usually hard to see the cracks or breaking pattern in the tested specimen. Therefore, the residual stress-strain behaviours could not be measured by this machine beyond its peak.

#### 4.5.5 Observations during Quality Control and Testing

The practice of carrying out the grain-size analysis of the CRF aggregate and its MC measurement as QC measures had been already adopted in the DDM site. A representative sample of aggregate from the stockpile was collected based on a visual basis and might have differed slightly according to the judgement of whoever happened to be collecting it. A standard for collecting the sample might help to minimize the personal variation and to obtain the best representative sample.

The practice of measuring the  $G_s$  of the cement slurry can provide useful information about the quality of the mixing of the cement with the water. However, the measurement would be more meaningful by establishing the accepted ranges of the  $G_s$  values for a given recipe based on mixing with same representative recipe and testing at the laboratory.

The practice of sampling, preparing and testing the CRF cylinders to measure the possible variability in the strength property within the CRF mass was already in place at the DDM site. Obviously, proper mixing of the collected sample or screened sample has to be carried out before selecting the samples for MC determination or preparing the CRF cylinders. However, the CRF sample obtained from the field to prepare the UCS cylinders may not represent the same sample as that used for the in situ measurement. Furthermore, considerable time elapses between the field sampling and the preparation of the cylinders. Using a representative sample from the mixing bay to prepare the cylinders and the in situ testing of the same CRF load after its compaction may possibly provide a better comparison among the test results.

The comparative strength and MC tests from the cylinders of 150 mm and 100 mm diameter would possibly give better results if both were prepared from the same batch of CRF. The prediction of the in situ strength from the 100 mm diameter cylinder becomes difficult due to screening off the >25 mm sample and increasing the cement and MCs in the CRF sample compared to the in situ condition. Carrying out more comparative tests between the 150 mm and 100 mm diameter samples may help to provide valuable conclusions so that the in situ strength can possibly be predicted from the tested 100 mm diameter sample. Cored samples, if they can be obtained, with a known period of curing time of possibly 28 days, may also be used for the comparison test.

Maintaining a uniform curing condition for the CRF cylinders, possibly in temperature-controlled moist chambers, obviously provides better strength results compared to the curing provided simply by covering the cylinders with a wet jute mate. The CRF cylinders are weak, and proper care has to be taken while stripping them out from their moulds and during their capping. It was observed that edges of the CRF cylinder were sometimes damaged while being stripped out from the moulds mainly because of the lack of proper cleaning and lubrication of the moulds. The proper capping of a cylinder with the damaged edges becomes slightly difficult compared to the capping of a normal CRF cylinder without the damaged edges and the cylinders with the damaged edges generally provided less strength during the UCS test.

The practice of selecting a single cylinder from each shift after 28 days and two cylinders after each 3 and 7 days of curing for the UCS test as per the specification may provide less number of UCS test data after 28 days. The selecting a single cylinder from each shift after 3 and 7 days, and 3 cylinders after 28 days of curing for the UCS test would provide more numbers of UCS test data after 28 days, as 28-day-strength is used to predict the in situ condition.

The UCS test machine stops automatically once no further increment of applied load is achieved. The complete breakage of the CRF cylinder is not possible, and sometimes even visual cracks are difficult to obtain when using this UCS testing machine. The breaking of a tested CRF cylinder clearly shows that failure occurs though the cemented zone, but failure through crushing of the aggregate is impossible.

## 5 Results and Discussion

The in situ and laboratory test results are presented and discussed in this chapter. The test results include the in situ densities and MC measured by using a TMD nuclear gauge; the  $G_s$  of the cement slurry; the aggregate grain-size distribution and MC measured in the laboratory; the MC of the CRF samples; the densities and MC of the UCS test specimens; and the measurements of their deformation. The test results from the trial mixes and actual placement are discussed separately in this chapter. Based on the field and laboratory test results from the DDM site and the values reported in the literature, the in situ parameters for this study site are predicted in this chapter.

### 5.1 Aggregate

The literature reviews in this thesis indicated that the aggregate strength, gradation, and MC should be the relevant aggregate properties when designing CRF. The aggregate produced from crushing and screening granite is sound and strong. In UCS tests carried out in 1998, Nishi - Khon/SNC – Lavalin (2004) reported that the average UCS for granite was 98.2 MPa with a minimum value of 72.6 MPa. The specified grain-size distribution follows the Talbot and Richard (1923) curve, with  $N$  ranging from 0.44 to 0.55, as shown in Figure 5.1.

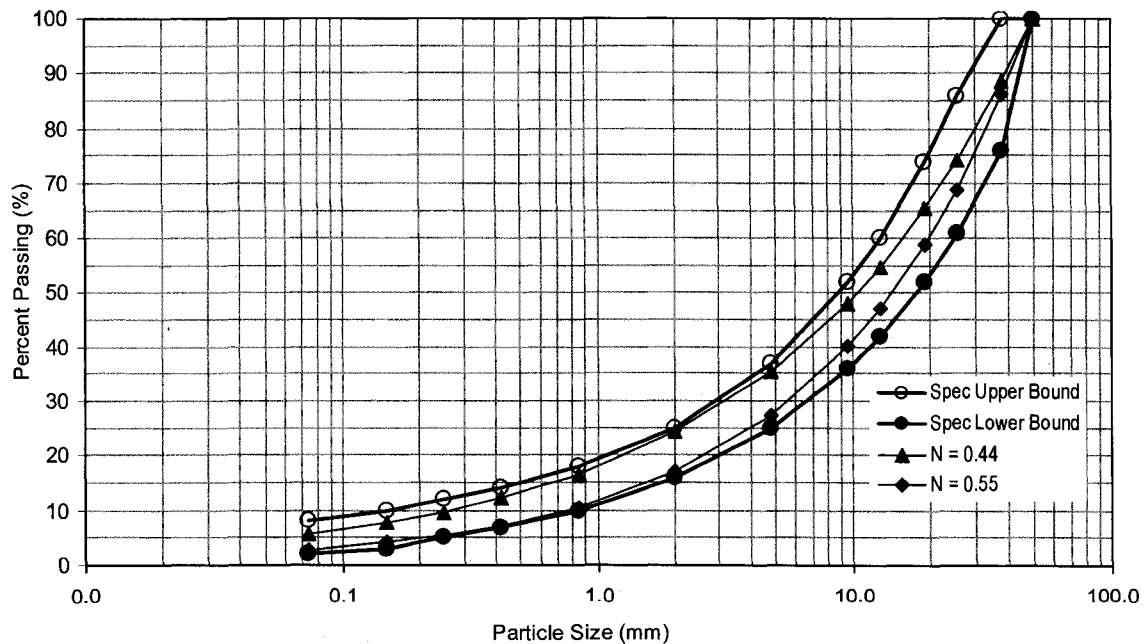


Figure 5.1 Specified grain-size distribution with Talbot and Richard (1923) curves

The 71 numbers of grain-size distributions of the aggregate measured during its production in 2006 and 30 numbers during preparation of the CRF in 2007 are presented in the Appendix, and the grain-size distribution curves are shown in Figure 5.2 and

Figure 5.3, respectively. Not all the grain-size curves fall within the specified limits; however, on average, the grain-size distribution for the aggregate lies within the specification, as shown in Figure 5.4.

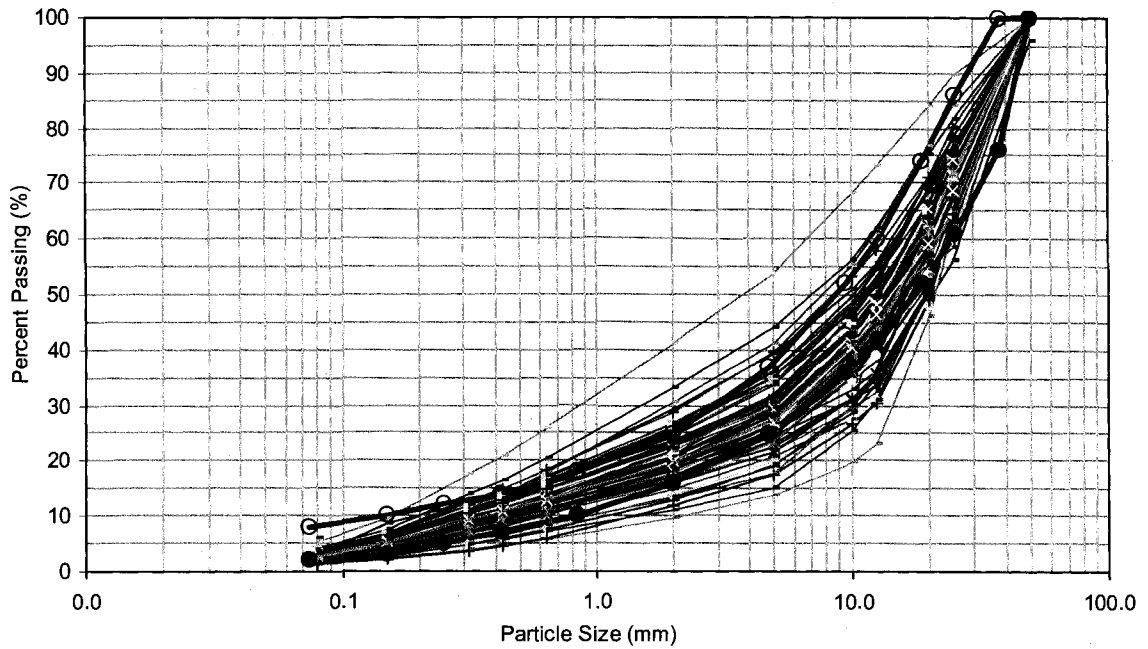


Figure 5.2 Grain-size analysis of CRF aggregate during production in 2006

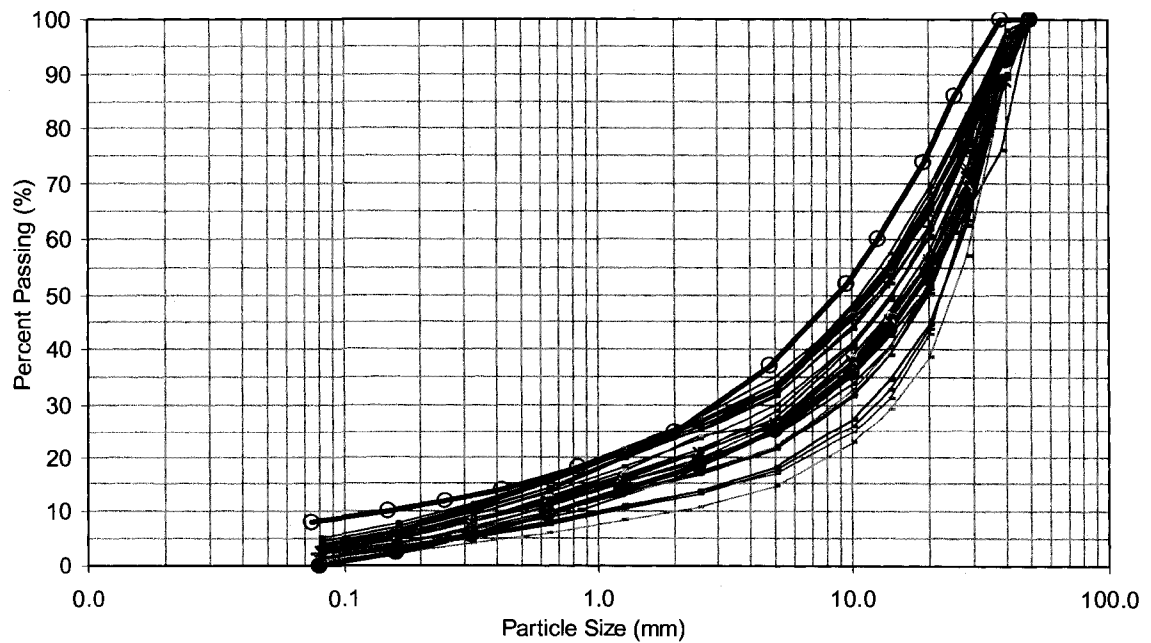


Figure 5.3 Grain-size analysis of CRF aggregate in 2007

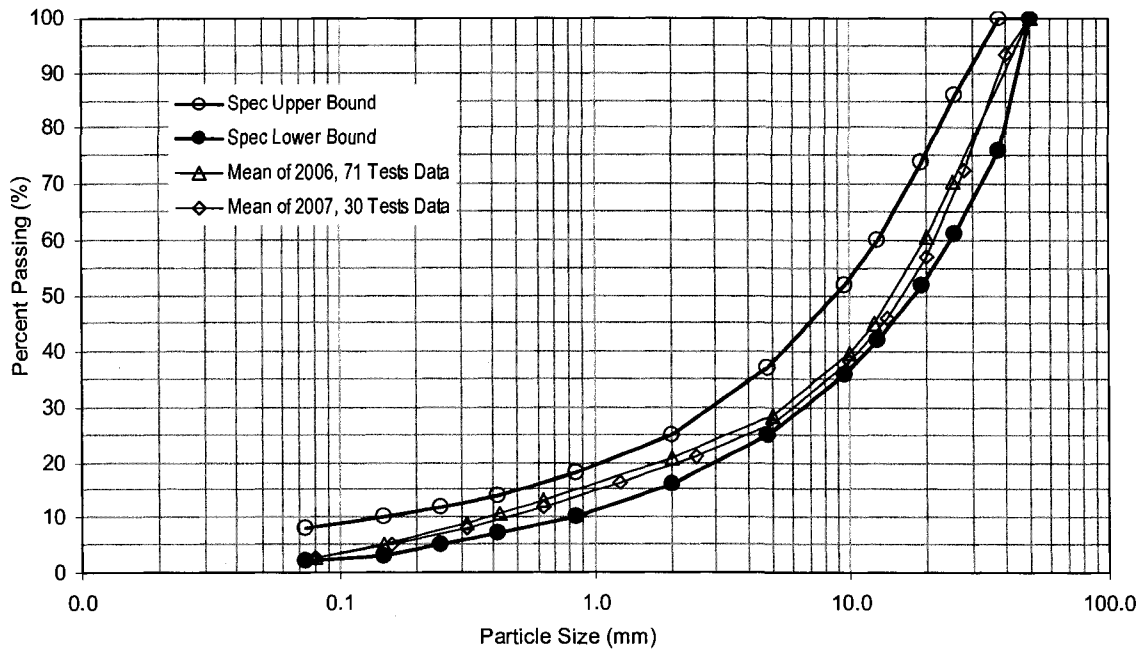


Figure 5.4 Mean gradation of CRF aggregate in 2006 and 2007 compared to its specification

The average coarse aggregate (>10 mm) is slightly more than 60%, and the fine aggregate is slightly less than 40%. The proportion of coarse and fine aggregate is close to the value specified by Brechtel et al. (1989) to obtain the optimum CRF strength.

The average  $C_u$  values are 3.64 and 3.33, respectively, during aggregate production (2006) and CRF preparation (2007). These values are well within the specified limits (1.44 to 6.54) as suggested by Annor (1999). However, the average values of  $C_c$  are 5.04 and 5.14, respectively, and are 50% lower than the lower limits (9.15 to 59.7) specified by Annor (1999).

The aggregate MC during the production of the aggregate in 2006 ranges from 0 to 6.4% with an average of 1.85% from 71 tests, and 0.5 to 2.1% with an average of 1.1% from 30 tests made during the preparation of the CRF in 2007. The average MC of the aggregate is very close to 2 to 3%, as reported by Stone (2007) for dry aggregate in general.

Since the CRF was transported by a haul truck, the aggregate segregation was expected to be less compared to that resulting from transportation on a conveyor as reported by Berry (1980), Yu and Counter (1983) and Yu (1989). Furthermore, limiting the aggregate top-size of <76 mm helped to minimize segregation (Stone, 2007). However, aggregate size segregation was observed to some extent during loading, dumping and placement, as the coarser aggregate tended to move towards the outer periphery of the loaded or dumped CRF mass during handling.

## 5.2 Trial Mix Results

Three trial mixes were prepared, placed, and tested at the mine site to provide some guidelines for CRF preparation and placement and to assess the CRF properties prior to the CRF actual placement within the pit. The trial mixes' recipes consist of batched cement slurry of 6 m<sup>3</sup> prepared by using 4504 kg of water and 4558 to 4562 kg of cement, and 42 m<sup>3</sup> of aggregate. The test results for the trial mixes are given in the Appendix, and a summary is presented in Table 5.1.

Table 5.1 In situ and laboratory densities and moisture content from trial mixes

Mix No.	Water to Cement Ratio	In Situ Dry Density (kg/m <sup>3</sup> )			In Situ Moisture Content, MC (%)			Lab MC (CRF)				Lab MC Corrected in Situ Dry Density (kg/m <sup>3</sup> )				Lab MC (Aggregates)				
		Nos. of Test	Min	Max	Ave	Min	Max	Ave	Nos. of Test	Min	Max	Ave	Nos. of Test	Min	Max	Ave	Nos. of Test	Min	Max	Ave
1		3	2089	2205	2157	3.8	7.7	5.2	9	4.6	6.9	5.6	3	2079	2196	2154	2	1.4	4.0	2.7
2	0.987	8	1911	2211	2029	4.0	7.5	5.4	6	2.6	6.0	3.7	2	1911	2080	1995	2	0.6	1.6	1.1
3	0.988	3	2108	2152	2133	7.3	8.2	7.6	4	6.3	7.8	7.1	3	2116	2166	2147	1	3.2	3.2	3.2
Average	0.988	14	1911	2211	2078	3.8	8.2	5.9	19	2.6	7.8	5.3	8	1911	2196	2112	5	0.6	4.0	2.2

The in situ  $\gamma_d$  of the CRF from 14 tests using a TMD nuclear gauge ranges from 1911 to 2211 kg/m<sup>3</sup> with an average of 2078 kg/m<sup>3</sup>, and the in situ MC ranges from 3.8 to 8.2% with an average of 5.9%. The laboratory (lab) MC of the CRF measured from 19 tests ranges from 2.6 to 7.8% with an average of 5.3%.

This corrected in situ  $\gamma_d$  of the CRF obtained by using the laboratory MC from eight tests ranges from 1911 to 2196 kg/m<sup>3</sup> with an average of 2112 kg/m<sup>3</sup>.

The measured values of the CRF-MC taken in the laboratory were compared with in situ measurements made by using a TMD nuclear gauge. The in situ  $\gamma_d$  was corrected based on the in situ  $\gamma_w$  and laboratory MC by using the Equation 4.4 provided in section 4.5.3. These methods provided reasonably close results, which are shown in Figure 5.5 and Figure 5.6, respectively.

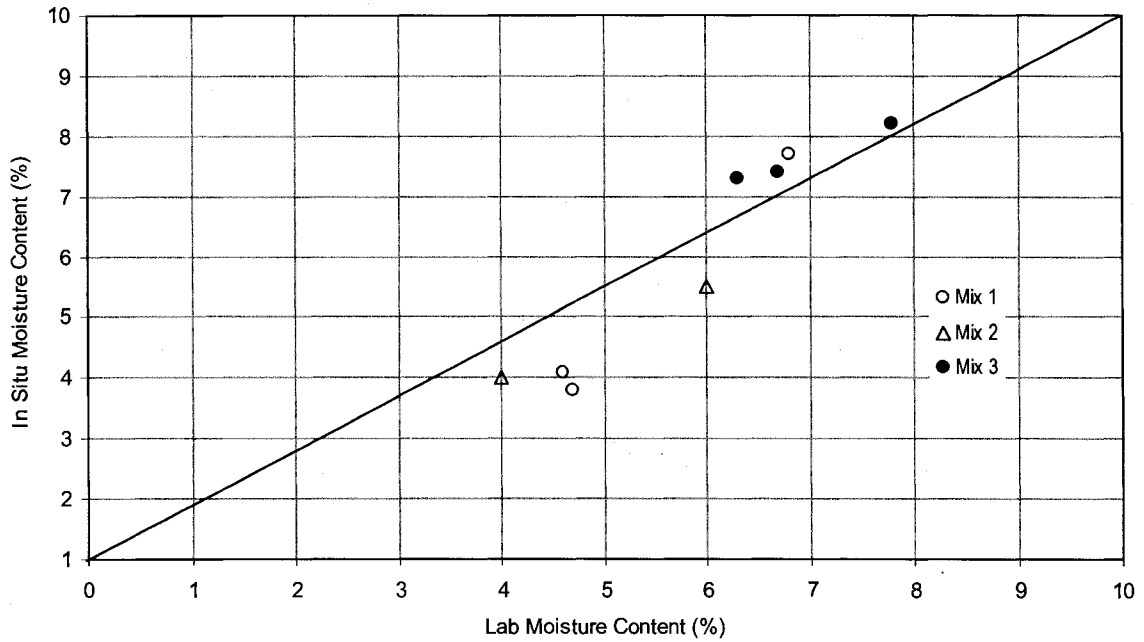


Figure 5.5 In situ versus laboratory moisture content for trial mixes

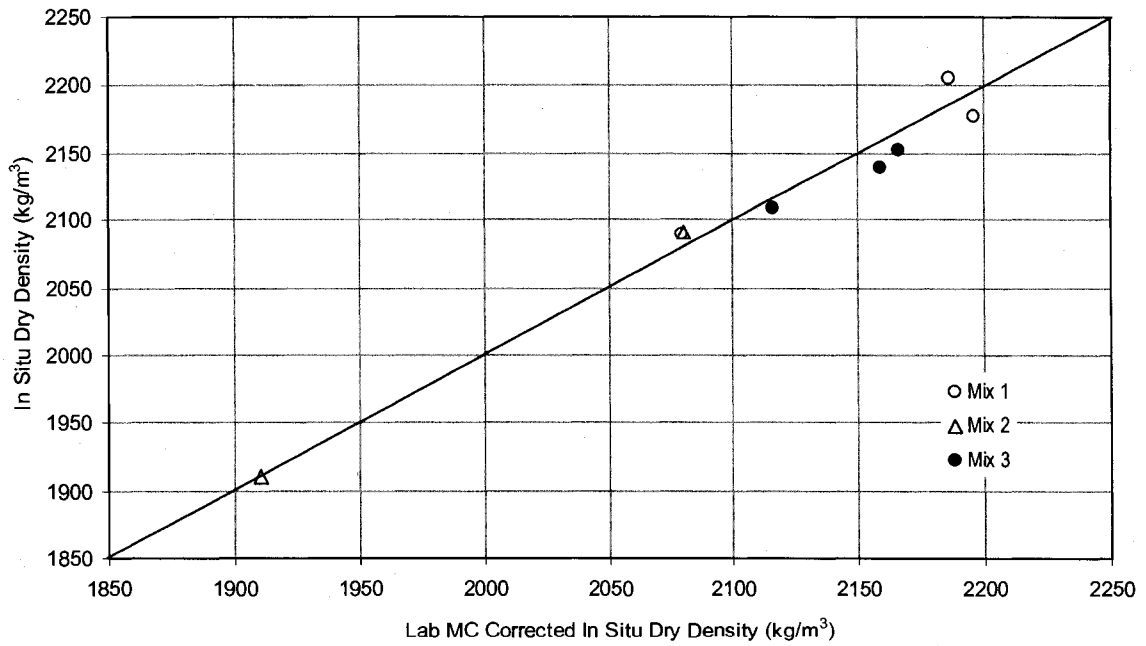


Figure 5.6 In situ versus laboratory moisture corrected in situ dry density

Based on the weight of the cement mixed and the given weight of the CRF aggregate, the percentage of the cement content in the CRF sample can be calculated. However, the calculated amount of cement will not always be present in a particular collected CRF sample. The actual amount depends on not only the actual mass of the cement and

aggregate used to prepare the CRF, but also on the uniformity of the cement slurry and its proper mixing with the aggregate. The  $G_s$  of the cement slurry can provide a rough indication of the uniformity of a slurry mix. However, measuring the quality of the mixing used to prepare the CRF and the cement content present in the CRF is difficult.

The cement content in a CRF sample is roughly estimated by using sieving and MC methods. For the first trial mix, a sieve analysis of the aggregate collected from the loader bucket (sample number S-109) and a CRF sample taken from the test pad (S-110) showed that the fines passing the 0.08 mm sieve were 3% and 8%, respectively providing a rough indication that the CRF samples had about 5% cement content.

For the second trial mix, the sieve analysis of the aggregate collected from the loader bucket (CRF-7), and a CRF sample taken from the test pad (CRF-4 and CFF-5) showed that the fines passing the 0.08 mm sieve were 2% and 4 to 5%, respectively, providing a rough indication that about 3% or even slightly less cement content was present in the CRF samples. All the test results are presented in the Appendix. This method may have been able to provide a rough estimation of the cement content present in the samples, but was not performed in the third trial mix due to the obvious variability in the fines content in the aggregate and the very tedious time-consuming process required in this situation.

The MC measured in the laboratory for the aggregate ranges from 1.4 to 4% for the first, 0.6 to 1.6% for the second, and 3.2% for the third trial mixes. From all the trial mixes, the MC of the aggregate from five tests had an average of 2.2%. The average MC of the aggregate was 1.8% during its production in 2006 and was assumed to be in the range of 1 to 2% in the stockpile.

The MC measured in the laboratory for the CRF samples ranges from 4.6 to 6.9% for the first, 2.6 to 6% for the second and 6.3 to 7.4% for the third trial mixes. The increments of the MC alone may not provide useful information about the cement content present in CRF due to the variability in the CRF aggregate's initial MC. However, these measurements indicate that variable cement content was present within the placed CRF. The third trial batch of CRF sample had a more consistent MC and measured in situ  $\gamma_d$ .

The CRF was compacted by a dozer as it spread the dumped CRF. The measured in situ  $\gamma_d$  is poorly correlated with the in situ MC. The maximum  $\gamma_d$  can be achieved at around 7 to 8% MC, as shown in Figure 5.7. Therefore, the recommended MC of the placed CRF should be 7 to 8% to obtain uniform properties within the placed CRF for the proposed mix proportions.

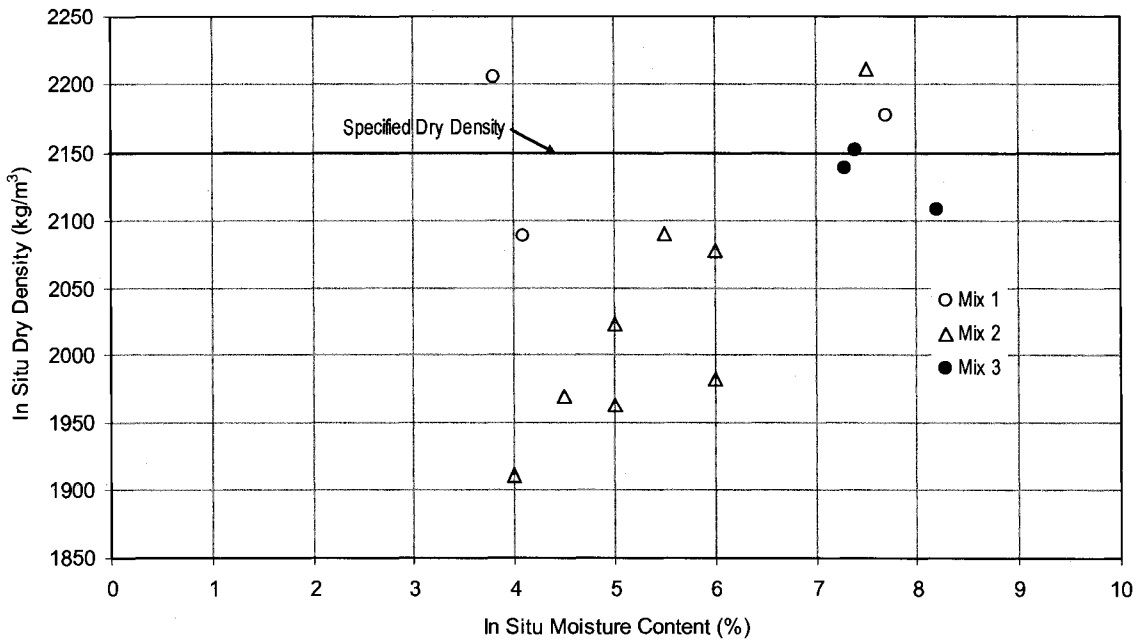


Figure 5.7 In situ dry density versus in situ moisture content for trial mixes

The 7-day UCS values for first and second trial mixes are 2.2 MPa and 4.2 MPa, respectively. The UCS values for 3, 7 and 28 days for the third trial mix are 3.7, 6.2 and 8.2 MPa, respectively, as shown in Figure 5.8. The  $\gamma_d$  of the cylinders from the third trial mix ranges from 2169 to 2178 kg/m<sup>3</sup>.

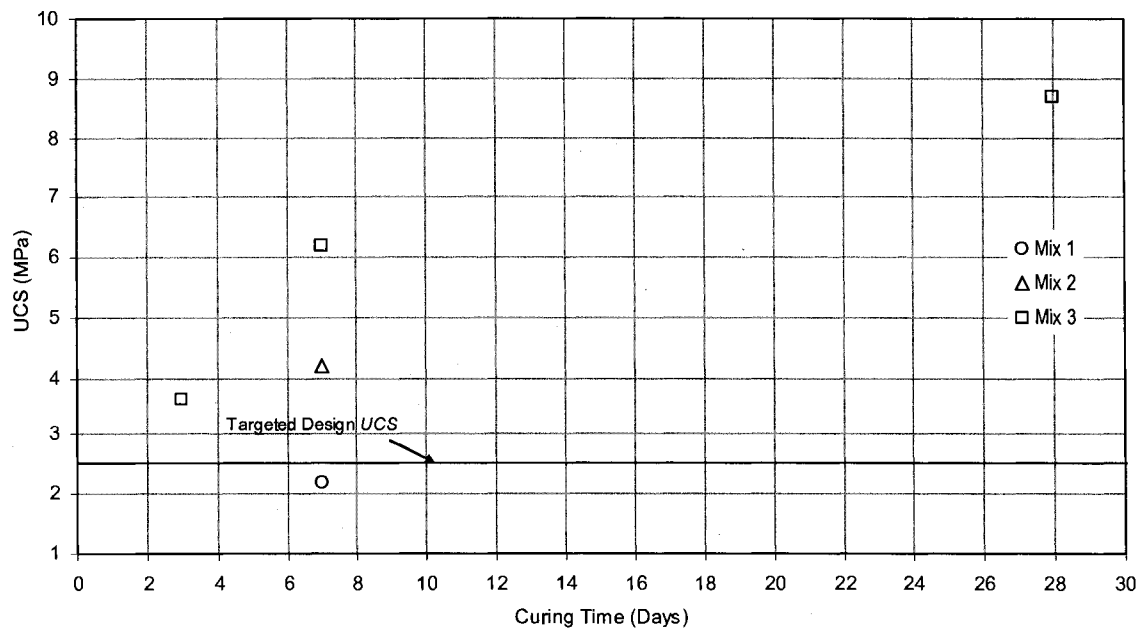


Figure 5.8 UCS versus age for trial mixes

### **5.3 Summary of Findings during Trial Mixes**

The testing of the trial mixes provided the values of the in situ density and the MC of the CRF. The mix and placement design for the CRF was expected to achieve an in situ  $\gamma_d$  of at least 2150 kg/m<sup>3</sup>. The testing showed that the achieved  $\gamma_d$  was often below this design specification. No special efforts were made to increase the in situ density beyond the values that were achieved. Essentially, the design specification for the  $\gamma_d$  was relaxed somewhat for the subsequent use of the CRF above the A154 N kimberlite pipe.

The comparison between the laboratory MC and in situ MC measured by using the TMD nuclear gauge shows that both methods provided similar results. This finding helped to validate the use of the TMD nuclear gauge for measuring the MC and  $\gamma_w$  and, thus, for determining the in situ  $\gamma_d$ .

Estimates of the cement content in the CRF indicated that it was quite variable (ranging from 2% to 5%) and substantially deviated from the design mixture at 6% cement content. This variability was likely due to inconsistent mixing and imprecise quantities of aggregate mixed in each batch. Hence, some variability in the CRF properties was expected.

A method for preparing CRF test cylinders to achieve at a  $\gamma_d$  close to the in situ density was found through a trial-and-error compaction process. The cylinders were tested to measure the UCS. The results showed that the achieved 28-day strength was well in excess of the design specification of 2.5 MPa (Dimitroff, 2007). This finding indicated that the 6% cement content and aggregate size distribution were more than acceptable.

The logistics and techniques used to prepare and place the CRF were qualitatively evaluated. The use of the mixing bay to mix batches of CRF was found to be adequate, and using a dozer to spread the CRF dumped from a haul truck worked well. It is predicted that the MC of the placed CRF should be around 7 to 8% to obtain the optimum  $\gamma_d$  by dozer compaction.

Based on trial mix results, it was decided for the subsequent use of the CRF to place it in one-metre lifts. It was expected that if a dozer were used to spread and level the CRF, it would have an in situ  $\gamma_d$  of nearly 2150 kg/m<sup>3</sup> and would have a 28-day UCS exceeding 4 MPa.

### **5.4 Cement Slurry and Mixing with Aggregate**

The w:c ratio for the cement slurry was maintained almost constant from the batch plant. For each batch of slurry, the quantity of water was constantly maintained at 4504 kg, whereas the cement content ranged from 4092 to 4575 kg with an average of 4557 kg. The w:c ratio typically fell within a range of 0.98 to 1.10.

The ratios of water and cement for preparing each batch of cement slurry are given in the Appendix. The quality of the water obtained from the lake and used to prepare the slurry

is close to that of distilled water, and, hence, the water quality at this site should not be a problem.

The design cement content for the CRF changed from a 6% ratio to 5.5% after September 8, 2007 (Table 5.2). The cement content ranged from 5.97 to 6.05% with an average of 6% cement content by weight of the aggregate from the 542 batch tickets obtained up to Sept. 8, 2007. The average cement content was 5.45% from eight random slurry truck tickets from Sept. 9 to 15, 2007. The average cement content varied from 5.5% to 6% by weight of aggregate, which is within the 5 to 7% range of values reported in the literature.

Table 5.2 Cement slurry recipes (water, cement contents and their ratio)

CRF cement (%)	Items	Minimum	Maximum	Average	Number of batches	Remarks
6% by weight of aggregate	Water (kg)	4504	4504	4504	542	Data from 11 Aug to 8 Sept 2007 with cement content 5.97 to 6.05% by weight of aggregate
	Cement (kg)	4504	4575	4557		
	w:c ratio	0.984	1.000	0.988		
5.5% by weight of aggregate	Water (kg)	4504	4504	4504	8	Data from 9 to 15 Sept. 2007 with cement content 5.5% by weight of aggregate
	Cement (kg)	4092	4096	4094		
	w:c ratio	1.100	1.100	1.100		

Generally, the  $G_s$  of the cement slurry was measured twice per shift to assess the slurry quality. The w:c ratio was also recorded at the same time from the tickets of the slurry delivery truck. The  $G_s$  from the 54 tests is given in the Appendix. The slurry  $G_s$  ranged from 1.47 to 1.54 with an average of 1.51, as summarized in Table 5.3. The variation of the  $G_s$  with the w:c ratio is presented in Figure 5.9. No reported values of the  $G_s$  of binder slurry are available in the literature, even though it emphasizes the need to measure the quality of the binder slurry.

The average  $G_s$  of cement slurry can be calculated based on the average w:c ratio and the  $G_s$  of the cement. The theoretical  $G_s$  of cement slurry for a given w:c ratio is calculated based on the following formula:

$$G_s (\text{cement slurry}) = \frac{G_s (\text{cement}) + (w:c) \cdot G_s (\text{cement})}{1 + (w:c) \cdot G_s (\text{cement})} \quad 5.1$$

Portland cement (Type 10) typically has a  $G_s$  of 3.15 (Lehigh, 2002). The calculated theoretical value of the  $G_s$  for 6% and 5.5% cement slurry is 1.52 and 1.48, respectively, which matches with the corresponding measured average value (Figure 5.9).

The key to producing effective CRF is to coat all of the aggregate with binder slurry (Yu, 1989; Farsangi, 1996). Therefore, the cement slurry quality and its proper mixing with the aggregate play a vital role in creating the CRF strength.

Table 5.3 Measured specific gravity of cement slurry with its water to cement ratio

CRF cement (%)	Items	Minimum	Maximum	Average	Number of tests	Remarks
6% by weight of aggregate	Water (kg)	4504	4504	4504	46	Data from 11 Aug to 8 Sept 2007 with cement content 5.97 to 6.05% by weight of aggregate
	Cement (kg)	4550	4570	4556		
	w:c ratio	0.986	0.990	0.989		
	Specific gravity	1.47	1.54	1.52		
5.5% by weight of aggregate	Water (kg)	4504	4504	4504	8	Data from 9 to 15 Sept. 2007 with cement content 5.5% by weight of aggregate
	Cement (kg)	4092	4096	4094		
	w:c ratio	1.100	1.101	1.100		
	Specific gravity	1.47	1.50	1.48		

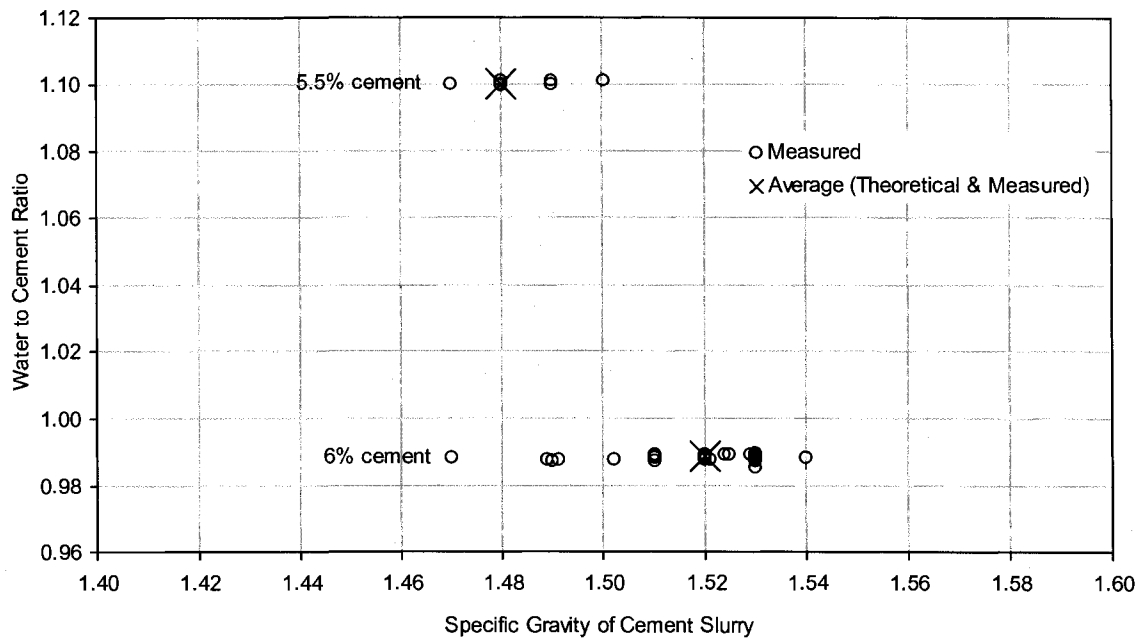


Figure 5.9 Water to cement ratio versus specific gravity of cement slurry

During preparation of the CRF, the weight of the aggregate placed in the mixing bay for preparing each batch of CRF is estimated by simply counting the number of loader buckets dumped into the mixing bay. A fully loaded bucket on a Caterpillar 988 G loader is assumed to carry 10140 kg of aggregate determined by weighing the aggregate loaded into the haul truck (seven loader buckets to prepare a batch of CRF). Using this technique, some variation in the aggregate quantity is obvious and expected. The cement content varies accordingly. Furthermore, no method is available for assessing quantitatively the quality of the process of mixing the cement slurry with the aggregate. The mixing is done solely based on visual observations and operator experience. The

presence of different cement and MC at different locations of the CRF during the trial mixes clearly indicated that some variability occurred in the mixing process. This variability was expected because the CRF was not prepared like concrete from a batch plant, which uses thorough mixing. However, the coating of the aggregate with cement slurry was ensured through visual inspection for each batch of CRF prepared in the mixing bay.

The quality of the mixing process was better than it would have been by simply spraying the binder slurry onto the aggregate while placed on a haul truck or while leaving a conveyor belt. Tesarik et al. (2003) and Young et al. (2007) reported a procedure for mixing and placing CRF at the Buick Mine that is similar to that used at DDM site. The in situ deformation modulus values reported by Tesarik et al. (2003) are more than double than those for methods where the slurry is simply poured over the aggregate in a truck box and then driven and dumped into a stope.

### 5.5 Nuclear Gauge and Laboratory Densities and Moisture Contents

All the measured TMD nuclear gauge and laboratory densities and MC are presented in the Appendix and are summarized in Table 5.4. The measured TMD nuclear gauge in situ  $\gamma_d$  of the CRF from 95 tests ranges from 1924 to 2253 kg/m<sup>3</sup> with an average of 2117 kg/m<sup>3</sup>. The in situ MC measured by using the TMD nuclear gauge ranges from 3.4 to 12.4% with an average of 7.2%.

The variation of the  $\gamma_d$  with the MC for a given compaction effort of the dozer, as shown in Figure 5.10, indicates that a MC between 5 to 8% gives a higher density, and that a MC of around 7% provides optimum compaction. These results are consistent with those found from the trial mixes.

Table 5.4 TMD nuclear gauge and laboratory data of densities and moisture contents

Measurement	Number of tests	Particulars	Minimum	Maximum	Average	Standard Deviation
In situ	95	Wet Density (kg/m <sup>3</sup> )	2072	2407	2270	79
		Dry Density (kg/m <sup>3</sup> )	1924	2253	2117	66
		MC (%)	3.4	12.4	7.2	1.7
		Calculated Void Ratio, $e$	0.20	0.40	0.28	0.04
		Porosity, $\eta$ (%)	17	29	22	2
Laboratory	86	Laboratory MC (%)	4.5	9.2	6.8	0.9
		Corrected Dry Density (kg/m <sup>3</sup> )	1916	2253	2125	75
Laboratory Cylinder	123	Wet Density (kg/m <sup>3</sup> )	2140	2407	2344	40
		Dry Density (kg/m <sup>3</sup> )	1953	2241	2148	51
		MC (%)	5.0	12.5	9.2	1.4

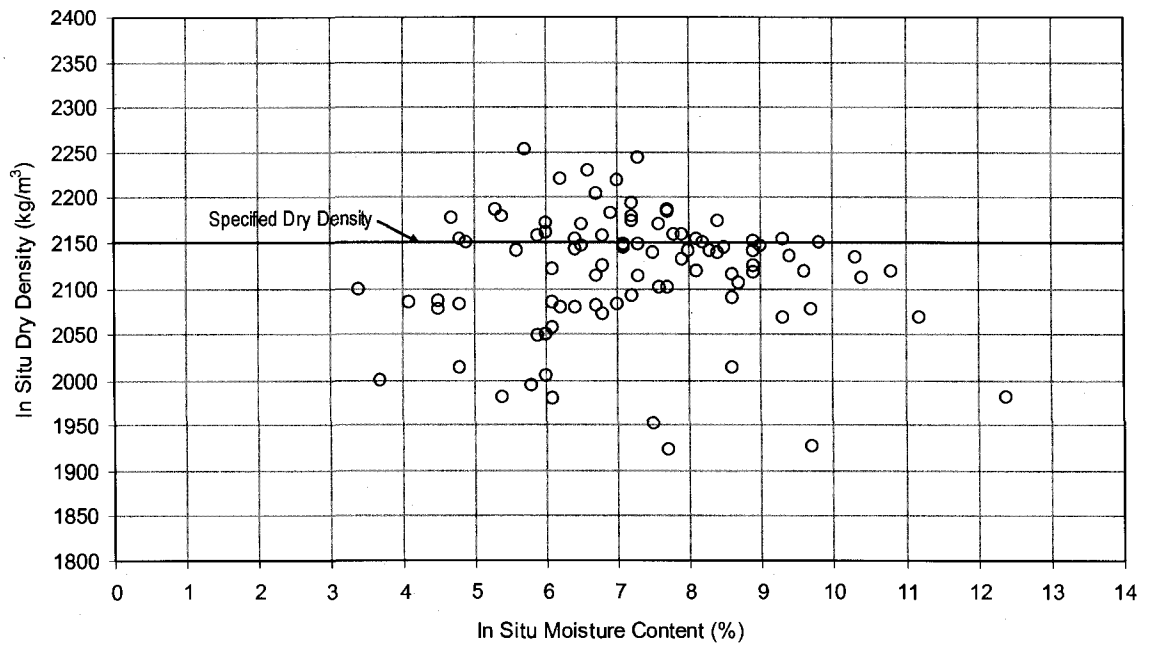


Figure 5.10 In situ dry density versus in situ moisture content

The 86 samples of the CRF collected near the TMD nuclear gauge test locations were tested in the laboratory. These samples had a MC ranging from 4.5 to 9.2% with an average of 6.8%. The corrected in situ  $\gamma_d$  based on the laboratory MC ranges from 1916 to 2253 kg/m<sup>3</sup> with an average of 2125 kg/m<sup>3</sup>. The laboratory versus in situ MC and dry densities are presented in Figure 5.11 and Figure 5.12, respectively.

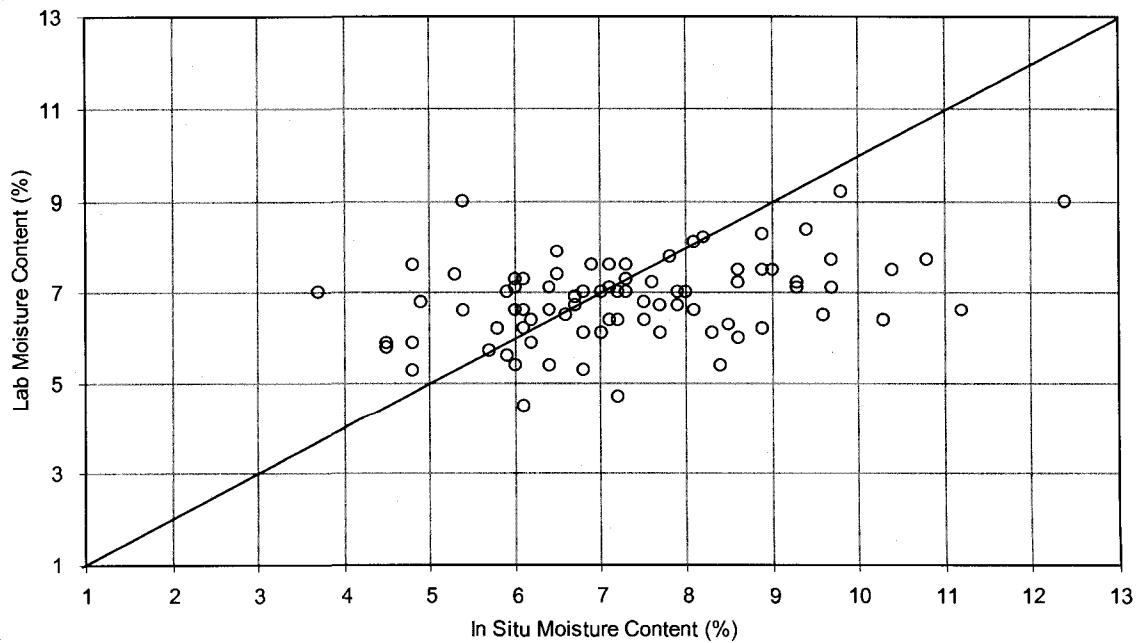


Figure 5.11 Laboratory versus in situ moisture content of CRF

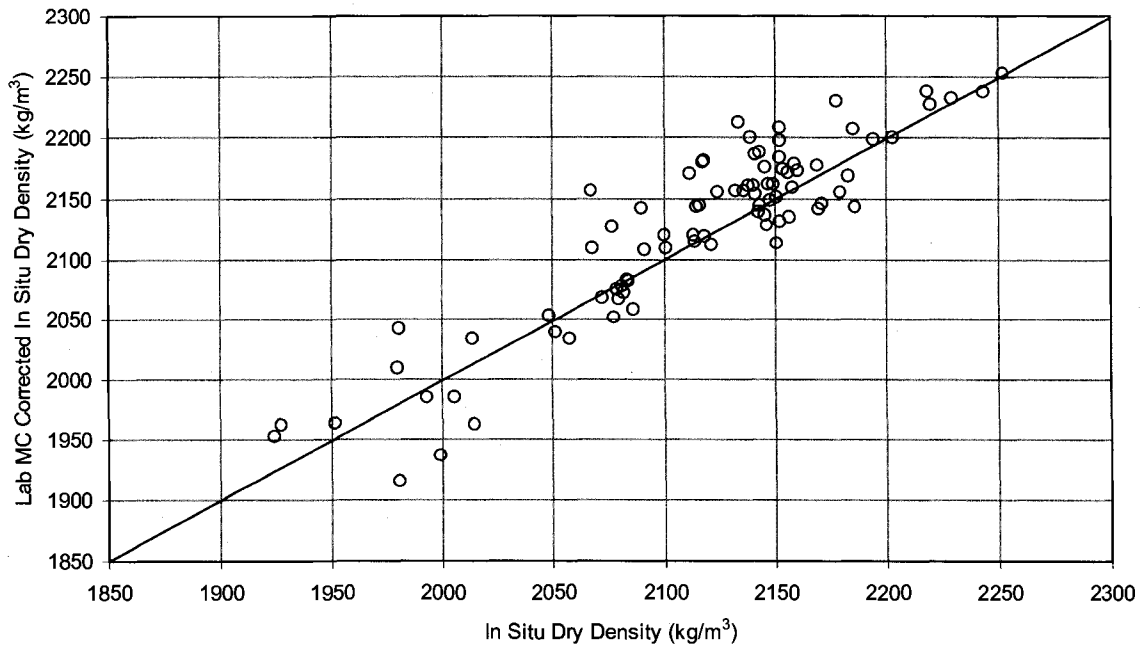


Figure 5.12 Laboratory-moisture corrected versus in situ dry density of CRF

Figure 5.12 shows that the in situ  $\gamma_d$  measured by using a TMD nuclear gauge is essentially the same as the corresponding laboratory corrected values. This result supports the use of the TMD nuclear gauge for measuring the in situ  $\gamma_d$ .

The in situ  $\gamma_t$  of the cored CRF samples studied by Hedley (1995) lies within the range of 1835 to 2161  $\text{kg/m}^3$  with an average of 2000  $\text{kg/m}^3$ . Therefore, this present study's measured densities are higher than but still close to Hedley's (1995) values. The higher density was achieved by using a loader and dozer for compaction. Tesarik et al. (2003) used a value of 2146  $\text{kg/m}^3$  in their numerical modeling of the Turquoise Ridge Mine, although they calculated this value from laboratory samples.

At the DDM site, the calculated  $e$  varies from 0.20 to 0.40 with an average of 0.28, and the  $\eta$  ranges from 17 to 29% with an average of 22%. The  $e$  is lower than the value of 0.51 reported by Yu (1990) and Farsangi (1996), and 0.37 reported by Nokken et al. (2007). The  $\eta$  is lower than the values of 33% to 45% reported by Hassani and Archibald (1998) and 0.27% reported by Nokken et al. (2007). The low  $e$  and  $\eta$  of the CRF at the DDM site were likely caused by the dozer's compaction during the CRF placement.

A total of 178 cylinders were prepared in the laboratory. The measured densities and MC from 177 cylinders (excluding one tested at 4 days) are summarized based on the curing time, cylinder diameter and cement content, and presented in Table 5.5. The overall  $\gamma_w$  of the tested cylinders varies from 2197 to 2477  $\text{kg/m}^3$  with an average of 2343  $\text{kg/m}^3$ , the  $\gamma_d$  from 1953 to 2316  $\text{kg/m}^3$  with an average of 2154  $\text{kg/m}^3$ , and the MC ranges from 4.9 to 12.5% with an average of 8.9%. The literature does not report the MC of prepared CRF cylinders. Annor (1999) and Kockler (2007) reported bulk densities of the CRF cylinders ranging from 1790 to 2430  $\text{kg/m}^3$  and from 2114 to 2163  $\text{kg/m}^3$ , respectively.

Table 5.5 Laboratory test results of densities and moisture content with curing time

Testing Parameters	Curing Time (Days)	Cement Content (%)	Cylinder Diameter (mm)	Number of tests	Minimum	Maximum	Average	Standard Deviation
Weight Density (kg/m <sup>3</sup> )	3	6.0	100	55	2197	2407	2342	41
		5.5	100	13	2264	2435	2331	40
		5.5	150	2	2473	2477	2475	3
		Total Test Data			70	2197	2477	2343
	7	6.0	100	52	2140	2480	2347	47
		5.5	100	13	2251	2433	2335	47
		5.5	150	4	2218	2460	2376	109
		Total Test Data			69	2140	2480	2347
	28	6.0	100	27	2275	2395	2350	27
		5.5	100	7	2272	2379	2330	41
		5.5	150	4	2242	2465	2352	104
		Total Test Data			38	2242	2465	2346
	Overall Test Data				177	2197	2477	2343
Dry Density (kg/m <sup>3</sup> )	3	6.0	100	55	1953	2236	2150	50
		5.5	100	13	2057	2278	2132	52
		5.5	150	2	2307	2313	2310	4
		Total Test Data			70	1953	2313	2151
	7	6.0	100	52	1962	2316	2150	61
		5.5	100	13	2078	2302	2139	55
		5.5	150	4	2112	2272	2222	75
		Total Test Data			69	1962	2316	2152
	28	6.0	100	27	2045	2241	2164	43
		5.5	100	7	2097	2179	2134	29
		5.5	150	4	2131	2304	2214	74
		Total Test Data			38	2045	2304	2164
	Overall Test Data				177	1953	2316	2154
MC (%)	3	6.0	100	55	5.6	12.5	8.9	1.4
		5.5	100	13	6.9	12.1	9.4	1.8
		5.5	150	2	7.1	7.2	7.2	0.1
		Total Test Data			70	5.6	12.5	9.0
	7	6.0	100	52	5.6	12.5	9.2	1.5
		5.5	100	13	5.7	12.1	9.2	1.9
		5.5	150	4	5.0	8.4	6.9	1.4
		Total Test Data			69	5.0	12.5	9.1
	28	6.0	100	27	5.0	12.5	8.6	1.5
		5.5	100	7	7.5	11.6	9.2	1.6
		5.5	150	4	4.9	7.7	6.2	1.4
		Total Test Data			38	4.9	12.5	9.1
	Overall Test Data				177	4.9	12.5	8.9

Figure 5.13 shows the in situ versus the corresponding laboratory MC of 100 mm diameter cylinders. The MC of the cylinders is typically higher than the in situ values because the preparation of the CRF cylinders involves screening off the >25 mm aggregate from the CRF samples. The remaining CRF will have higher MC and slurry content.

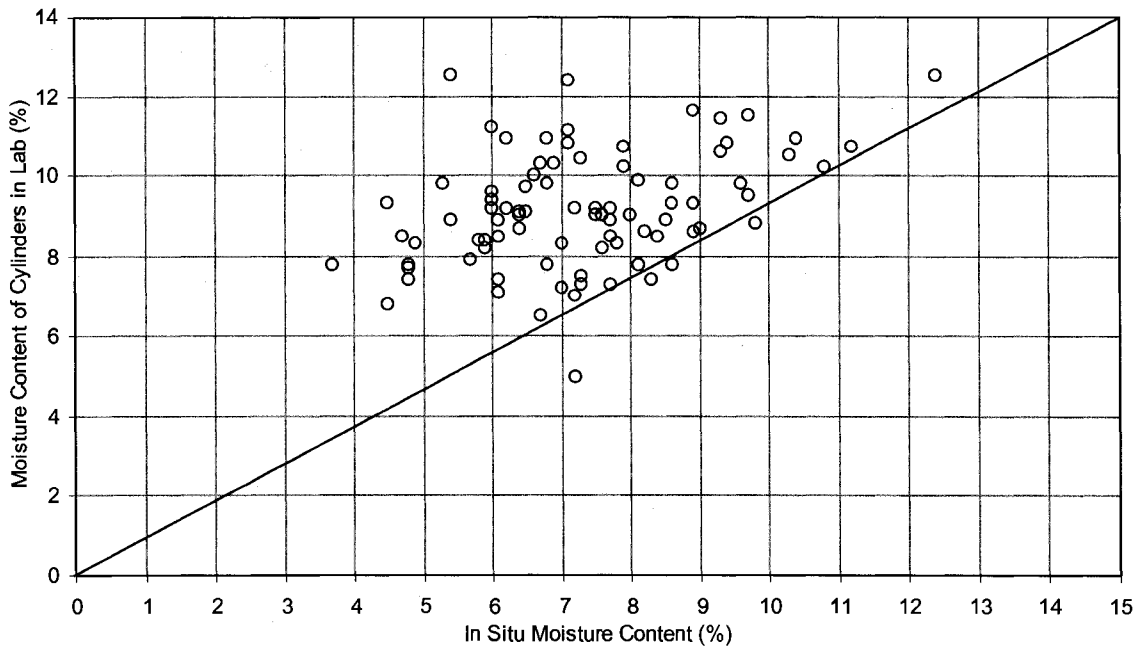


Figure 5.13 CRF-cylinder moisture content versus in situ moisture content

Figure 5.14 and Figure 5.15 show that the densities of the laboratory-prepared cylinders are higher than the in situ values because of the higher compaction effort in the laboratory while preparing the CRF cylinders compared to the in situ compaction provided by the dozer.

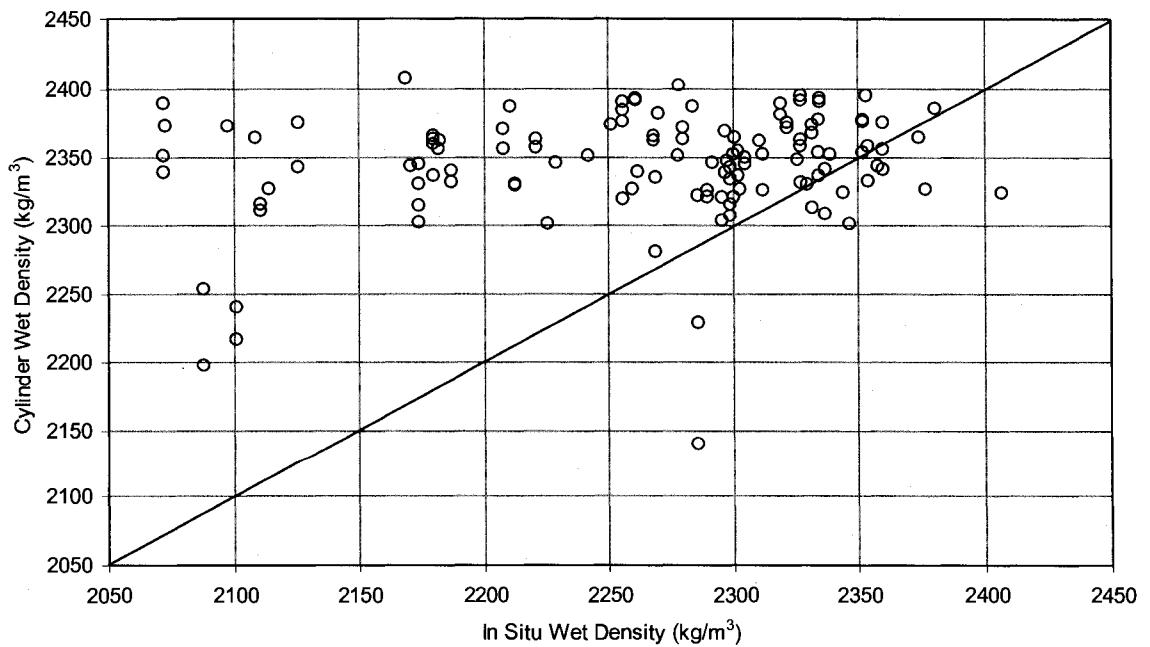


Figure 5.14 CRF-cylinder wet-density versus in situ wet density

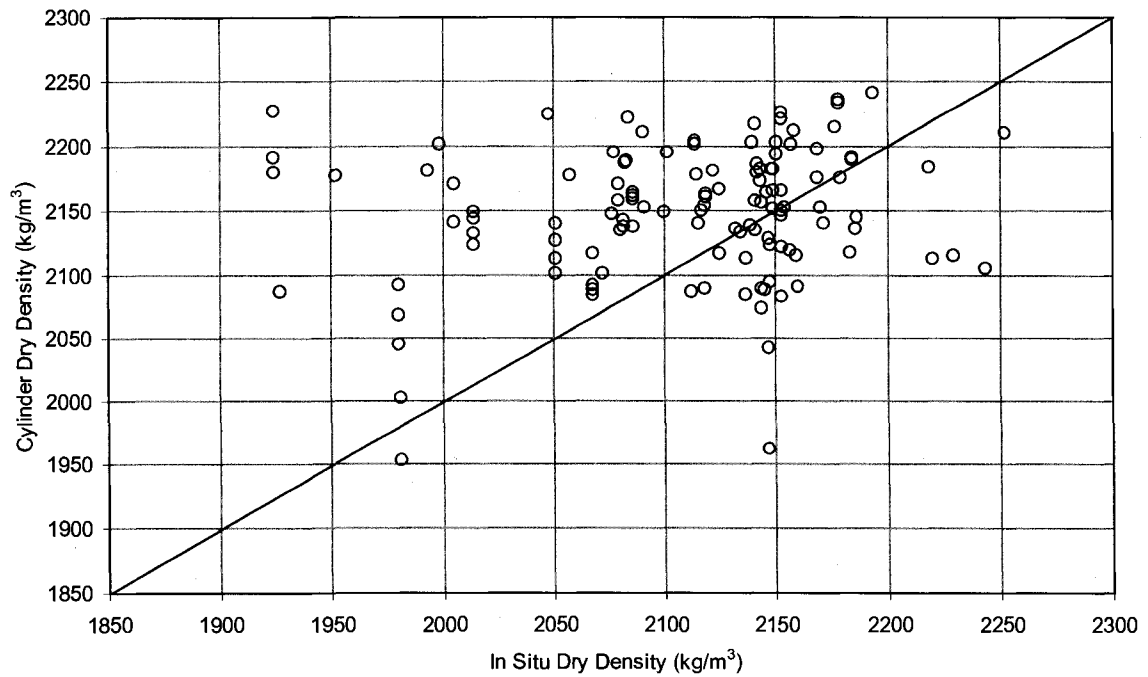


Figure 5.15 CRF-cylinder dry density versus in situ density

## 5.6 Unconfined Compressive Strength

The test results for the UCS values from 177 cylinders are presented in the Appendix. The UCS test results are summarized based on the curing time, cylinder diameter and cement content, and are presented in Table 5.6 and shown in Figure 5.16 with the curing time. The targeted 28-day-design UCS was 2.5 MPa (Dimitroff, 2007). The UCS increased with the curing time, as was expected and as reported in the literature.

Table 5.6 UCS (MPa) of CRF cylinders at different curing times

Curing Time (Days)	Cement Content (%)	Cylinder Diameter (mm)	Number of tests	Minimum	Maximum	Average	Standard Deviation
3	6.0	100	55	2.7	6.3	4.52	0.80
	5.5	100	13	2.4	6.0	3.83	0.93
	5.5	150	2	3.7	4.2	3.95	0.35
	Total Test Data		70	2.4	6.3	4.38	0.85
7	6.0	100	52	3.5	9.7	7.20	1.30
	5.5	100	13	4.8	8.3	6.16	0.99
	5.5	150	4	3.2	9.1	5.00	2.75
	Total Test Data		69	3.2	9.7	6.88	1.47
28	6.0	100	26	4.5	15.8	11.28	2.44
	5.5	100	7	6.1	11.6	7.91	1.95
	5.5	150	4	4.4	8.4	6.80	1.75
	Total Data (100 mm)		33	4.5	15.8	10.56	2.70
	Overall Test Data		37	4.4	15.8	10.16	2.86

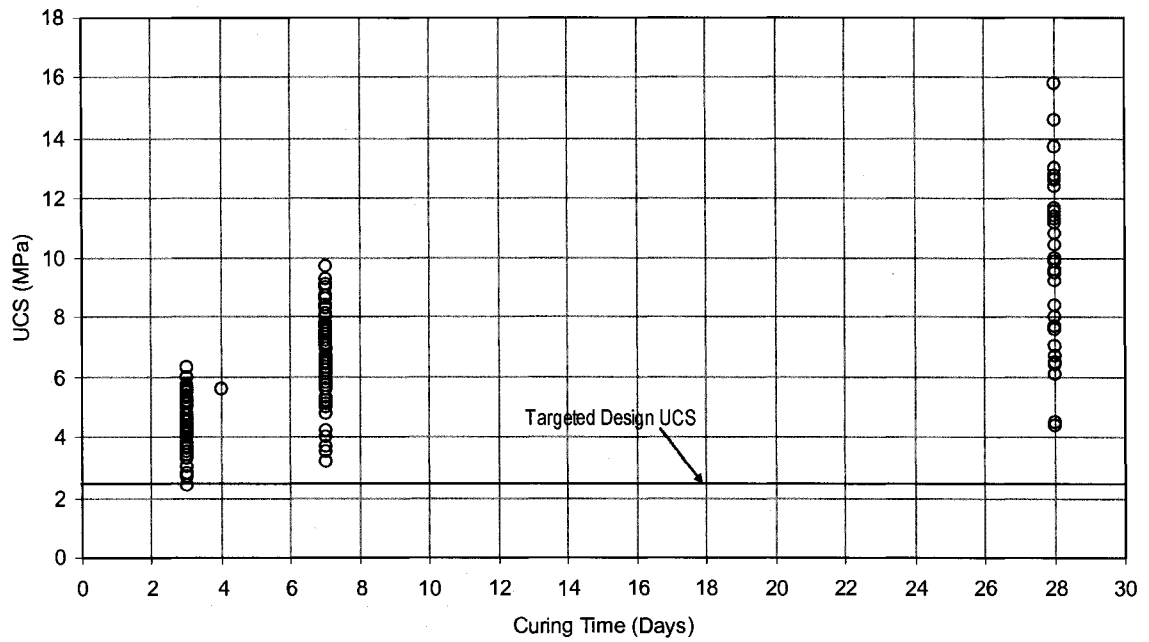


Figure 5.16 Unconfined compressive strength versus curing time

The UCS values are poorly correlated with the MC of the cylinders alone, as shown in Figure 5.17. This figure also indicates that the cylinders with a MC higher than 11% provided a lower UCS than the other cylinders.

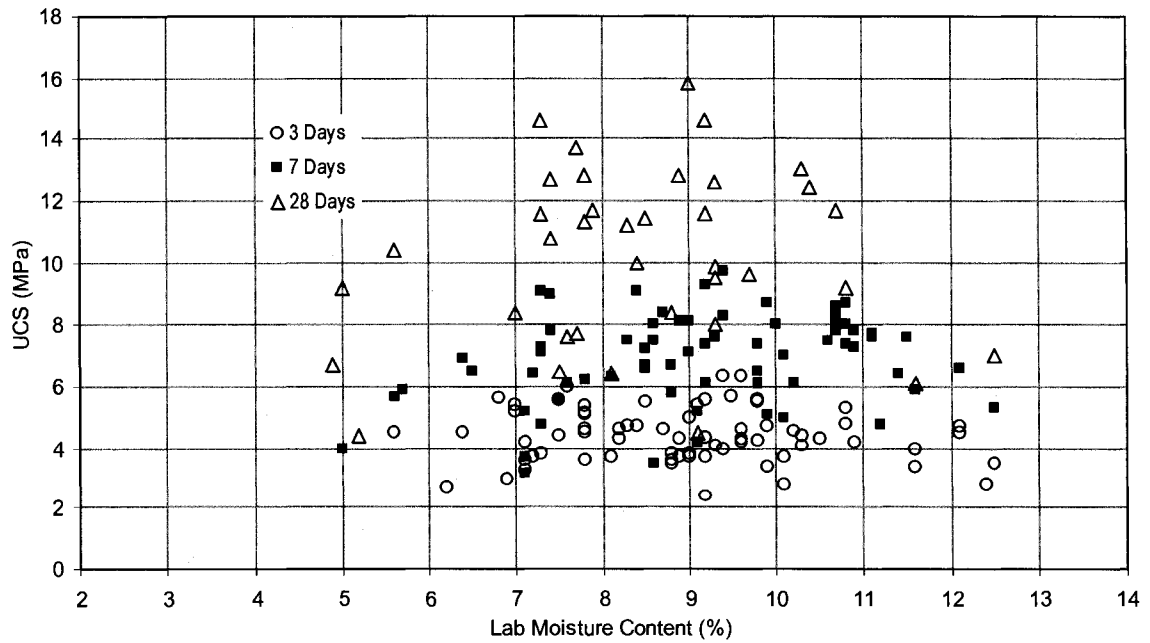


Figure 5.17 UCS versus moisture content of CRF cylinders

The UCS has a slight trend of increasing with the density with the poor correlation, possibly because of the variability in the cement content of the collected CRF samples used to prepare the cylinders, in the mixing, screening, and cylinder preparation as seen in Figure 5.18 and Figure 5.19.

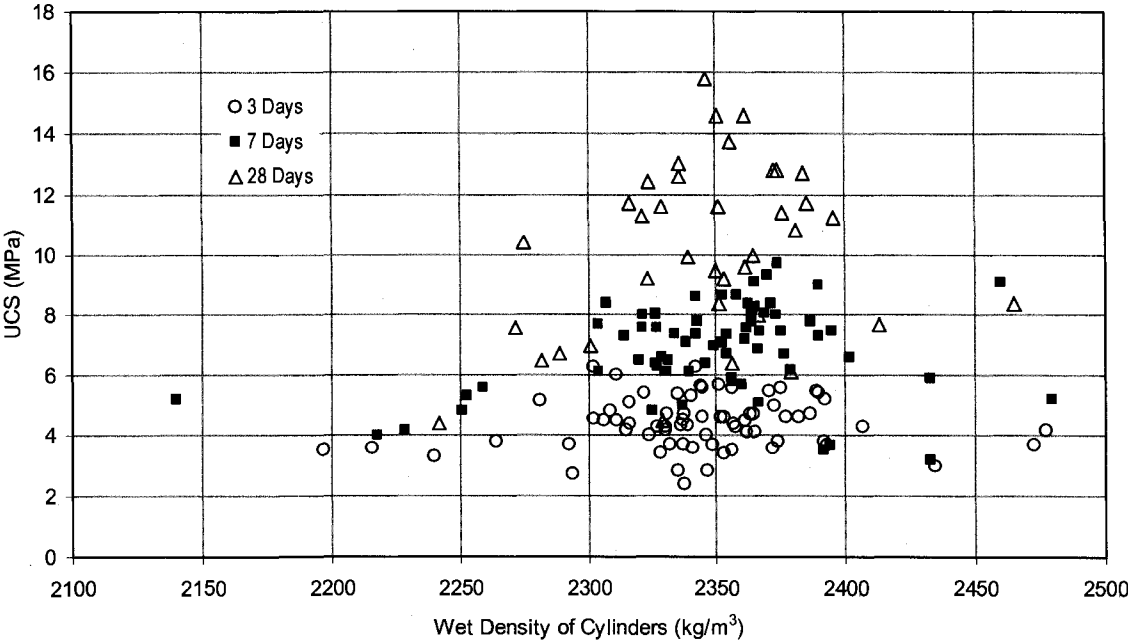


Figure 5.18 UCS versus wet density of CRF cylinders

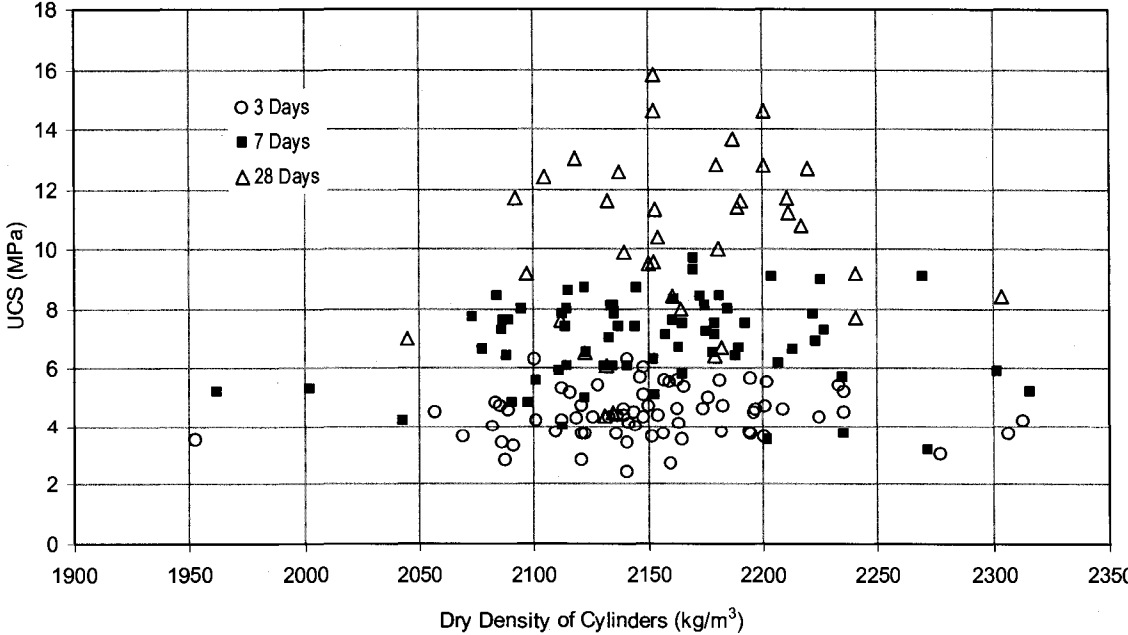


Figure 5.19 UCS versus dry density of cylinders

The increments in the 3- and 7-day strengths are around 1.2 times higher, whereas the 28-day strength is 1.4 times higher with increasing a cement content from 5.5% to 6% (Figure 5.20). However, the average values were obtained from a limited numbers of tests for 5.5% cement content, and the actual cement content in the samples may vary. The effect of the sample size on the UCS value is presented in Figure 5.21.

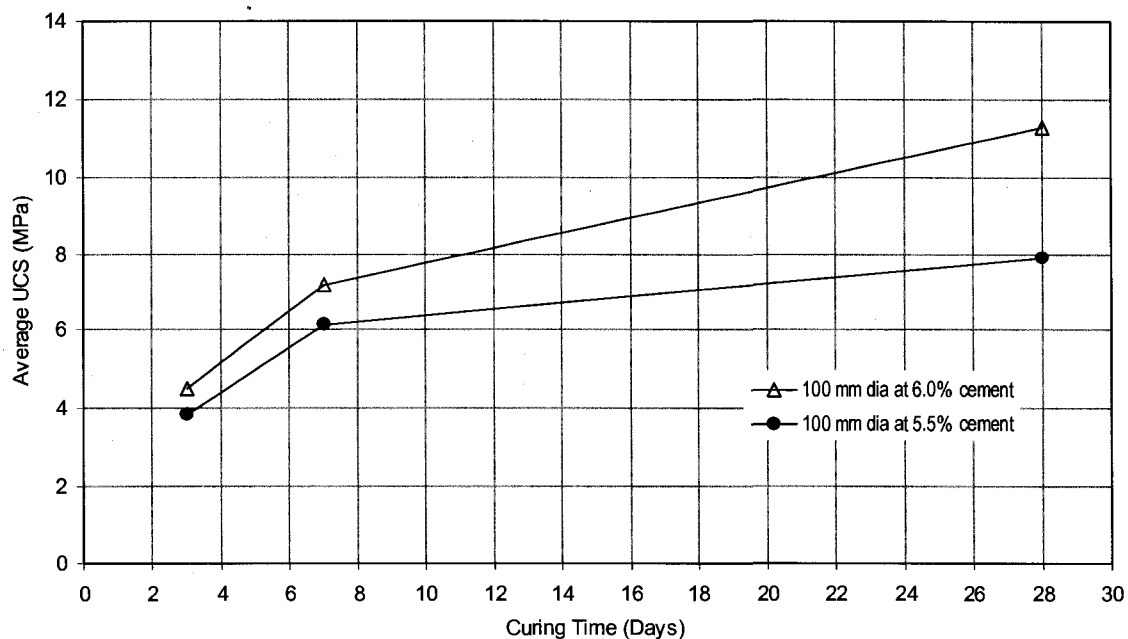


Figure 5.20 UCS at different cement contents versus curing time

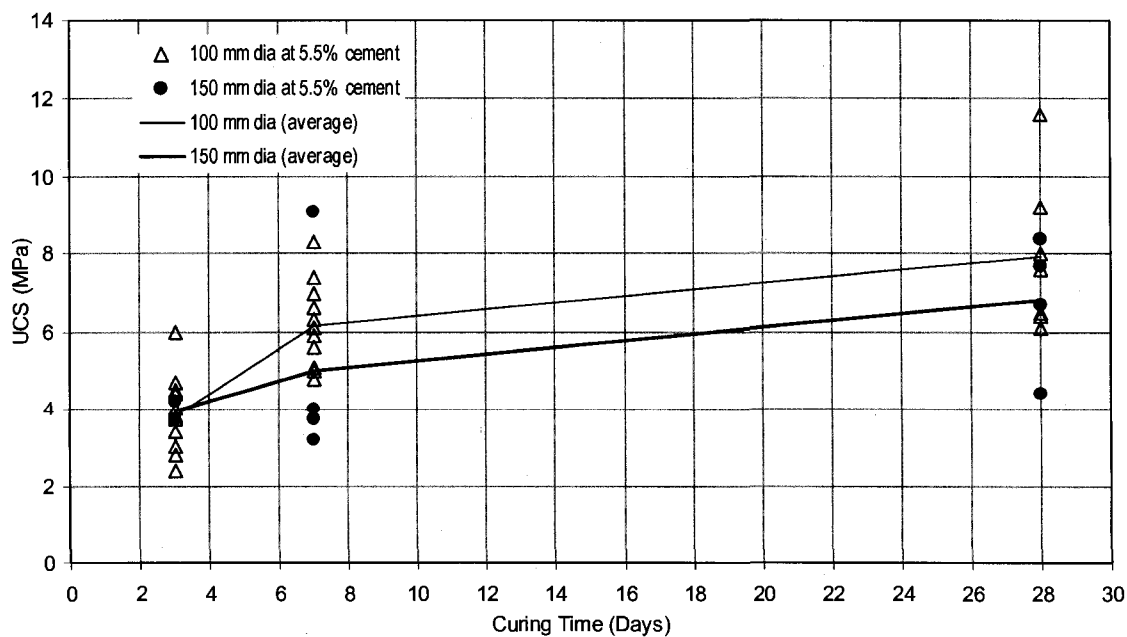


Figure 5.21 UCS of different CRF-cylinder sizes versus curing time

The 28-day UCS from the 150 mm cylinders is about 86% of the strength of the 100 mm diameter cylinders. These results were obtained from a limited number of 150 mm cylinder samples, and both the 100 mm and 150 mm diameter samples were prepared using the same cement slurry used to prepare the CRF samples.

Figure 5.22 compares the UCS of the CRF obtained at the DDM site with the various published results for the kind of CRF often used underground (4 to 7.8% cement and a w:c ratio ranging from 0.42 to 1).

The measured UCS is typically higher than the published values. However, directly comparing the results is difficult due to the variability in the mix design, sample size, preparation method, and curing time and condition.

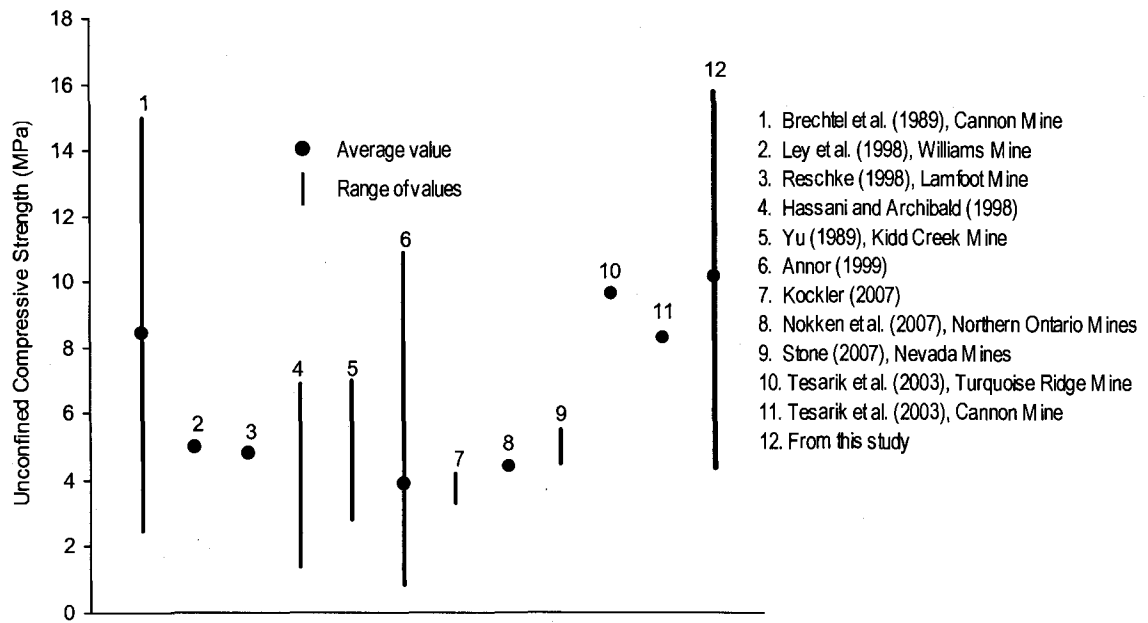


Figure 5.22 Laboratory UCS of CRF from this study compared with reported values

### 5.6.1 Relationship between Strength and Modulus

For some of the UCS tests, the overall axial deformation (strain) was recorded as the load was applied to the specimens. The vertical deformation was measured manually by using a dial gauge, and the corresponding stress value was obtained directly from the display unit of the UCS testing machine at a typical interval of 5 seconds during each UCS test.

The typical stress versus strain curves obtained after 7 days of curing for the 100 mm diameter CRF cylinders are shown in Figure 5.23. All 26 stress-strain curves obtained from the tests conducted on the 100 mm diameter cylinders with a curing time from 3, 7 and 28 days are presented in the Appendix. The tangential  $E$  calculated at 50% of the UCS and a summary of the test results are presented in Figure 5.23.

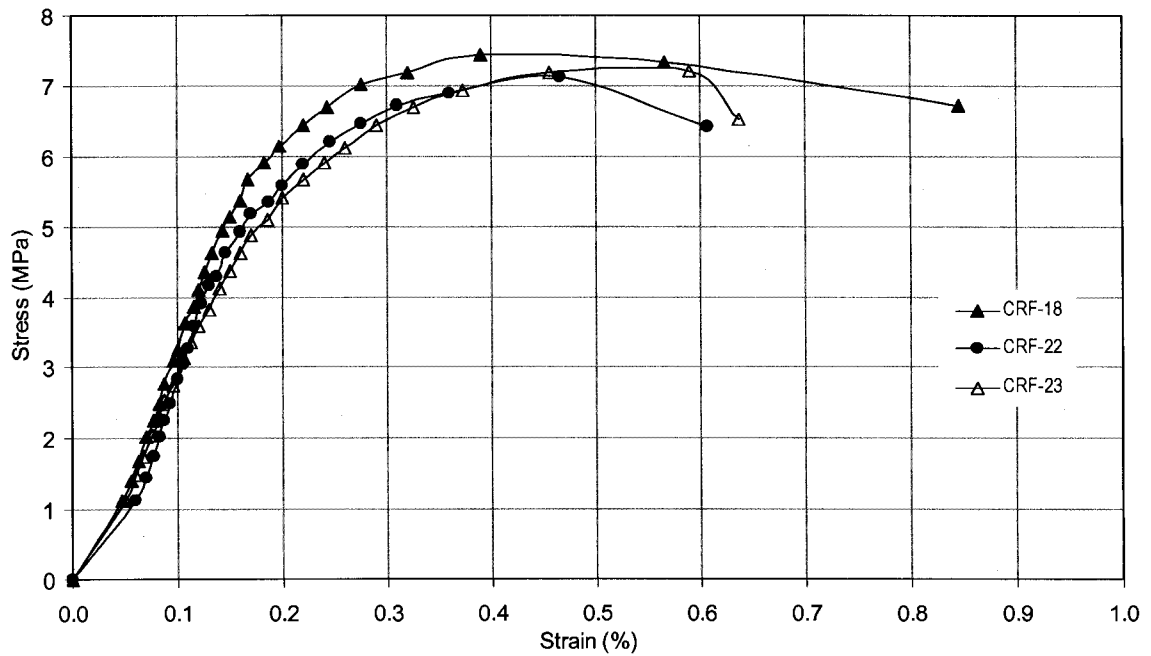


Figure 5.23 Stress-strain curves for 100 mm cylinders after 7 days of curing

Table 5.7 UCS and tangential Young's modulus (100 mm diameter specimens)

Number of tests	Curing Time (Days)	Cylinder No.	UCS (MPa)	Tangential Young Modulus, $E$ (GPa)
6	3	CRF-30	3.99	1.663
		CRF-31	4.24	1.570
		CFR-35	2.68	1.117
		CRF-36	3.64	1.517
		CFR-40	4.70	2.938
		CRF-41	5.45	2.477
17	7	CRF-3	5.77	3.304
		CRF-4	6.60	2.775
		CRF-8	3.50	2.500
		CRF-9	7.39	3.889
		CRF-13	7.68	3.339
		CRF-14	7.79	4.582
		CRF-18	7.45	4.139
		CRF-22	7.13	3.961
		CRF-23	7.22	3.610
		CRF-27	7.31	4.061
		CRF-28	6.05	3.025
		CRF-32	6.05	2.881
		CRF-33	6.52	3.622
		CRF-37	8.06	4.242
		CRF-38	6.37	3.747
3	28	CRF-5	11.32	5.666
		CRF-10	11.20	5.333
		CRF-15	9.10	3.500

A plot of the UCS versus corresponding  $E$  is shown in Figure 5.24. This figure provides a useful linear relationship:

$$E = 0.5012 \cdot UCS \quad 5.2$$

where

$E$  = tangential Young's modulus (GPa).

This relationship is similar to that of  $E = 0.5682 \cdot UCS$  provided by Gonano and Kirkby (1977) for cemented hydraulic fill and CRF and shown in Figure 5.24.

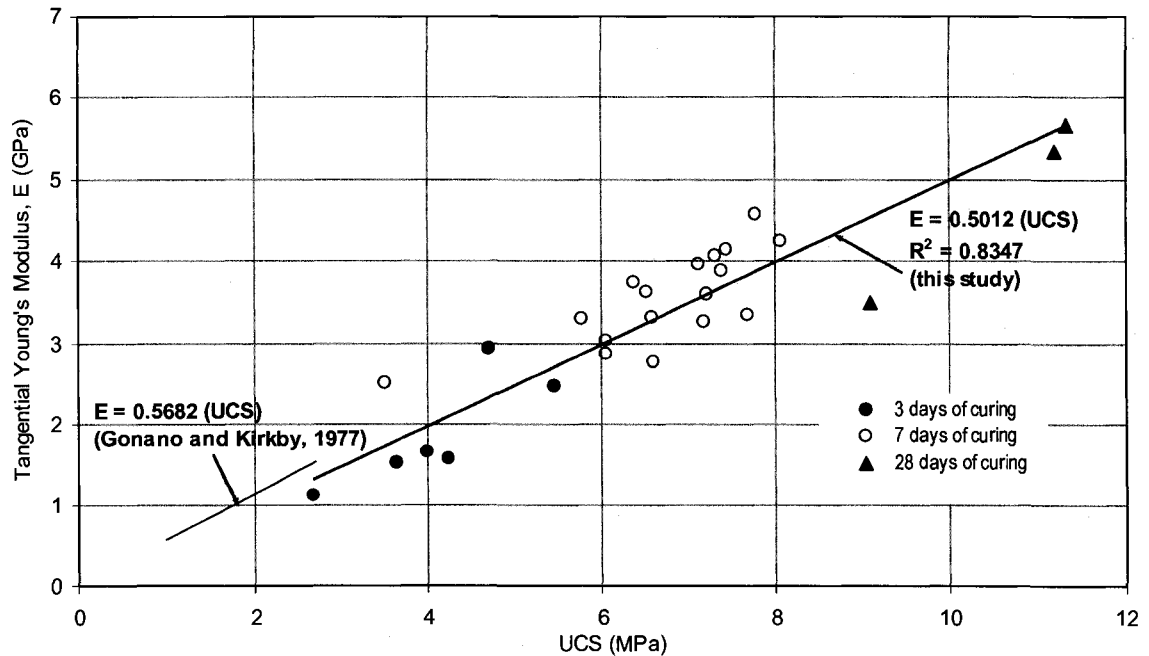


Figure 5.24 Linear relationship between UCS and  $E$  for CRF cylinders

When both  $E$  and the UCS values are expressed in MPa, then the  $UCS = 0.001995 \cdot E$  (in this present study), which is slightly lower than the UCS of  $0.00176 \cdot E$  provided by Gonano and Kirkby (1977). However, their proposed relationship was obtained at a low UCS (<3 MPa) and using the values of 6 test samples. The tested specimen size and curing age were not provided. Their CRF recipe consisted of siltstone aggregate with <25 to <300 mm and binder slurry, termed cemented hydraulic fill (CHF), and produced by mixing 3% Portland cement, 6% copper furnace slag and 91% tailings. The aggregate to CHF in the ratio of 1:1 to 3:1 by weight was mixed to produce CRF sample.

From the test results obtained at the DDM site, the UCS of the CRF can be estimated approximately by using 0.2% of its  $E$ , or the  $E$  can be predicted approximately by using 501 times the corresponding UCS value. However, the specimen size effect has to be considered while estimating the in situ value.

The plot of the UCS versus the  $E$ , as shown in Figure 5.25, provides a good correlation:

$$E = 0.4615 \cdot (UCS)^{1.0408} \quad 5.3$$

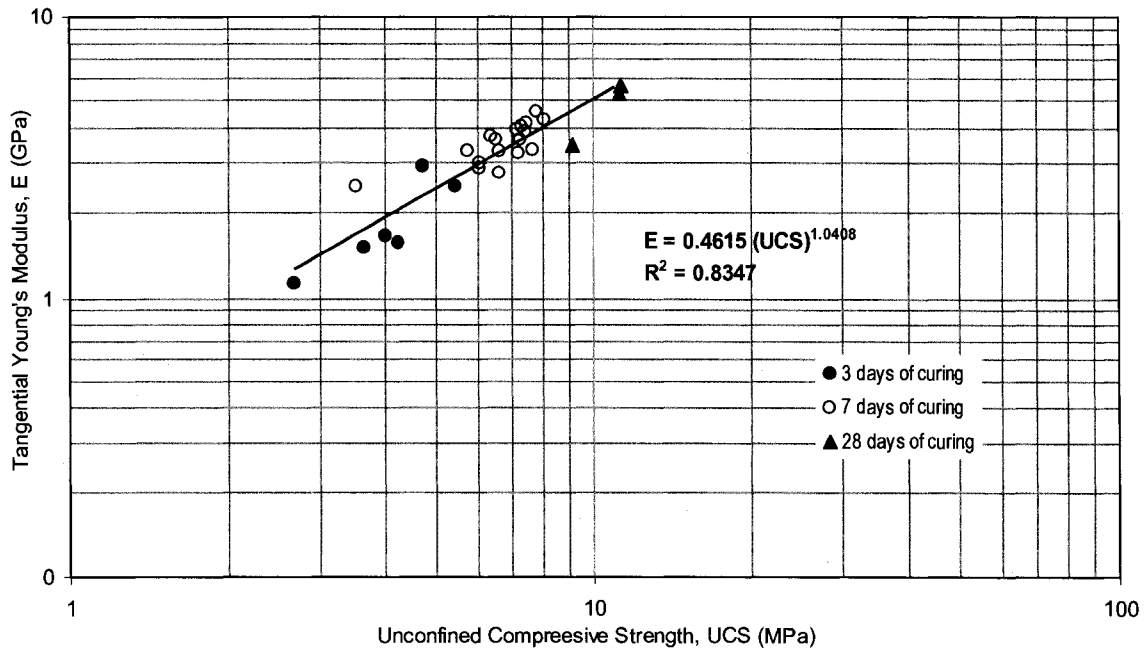


Figure 5.25 UCS versus Young's modulus of CRF cylinders

Figure 5.26 presents a comparison between the relationship established in this study and those reported by Swan (1985), Annor (1999) and Kockler (2007).

The relationship reported by Swan (1985) was obtained from selected mines using mainly CRF as mine backfill with a maximum UCS value of around 10 MPa and concrete samples with higher UCS values. The sample size, curing time and grain-size distribution of the CRF aggregate were not specified. The binder content provided for some of the mines ranged from 1.2 to 10.4%.

The relationship reported by Annor (1999) was based on 101 laboratory CRF cylindrical samples with 152 and 457 mm diameter prepared by using a cement content of 5 and 7% at a w:c ratio of around 0.8, and tested after curing times of 14, 28 and 56 days. The grain-size distribution of the aggregate for preparing the CRF sample was not specified. However, the coarse (<10 mm size) to fine fractions in the aggregate ranged between 64 to 78% and 22 to 36%, respectively. The maximum UCS value in Annor's (1999) proposed relationship was close to 10 MPa.

Kockler (2007) reported a modulus between 30% and 70% of the peak axial stress for nine 200 mm by 400 mm cylindrical CRF specimens cured for 7, 14 and 28 days. The CRF cylinders were prepared at 2.5% MC by using a <50 mm aggregate with the grain size close to the Talbot and Richard curve (1923) with  $N = 0.5$ . The CRF mixture was prepared by using 5.7% cement at a w:c ratio of 1. The maximum UCS in Kockler's (2007) proposed relationship was around 4.5 MPa.

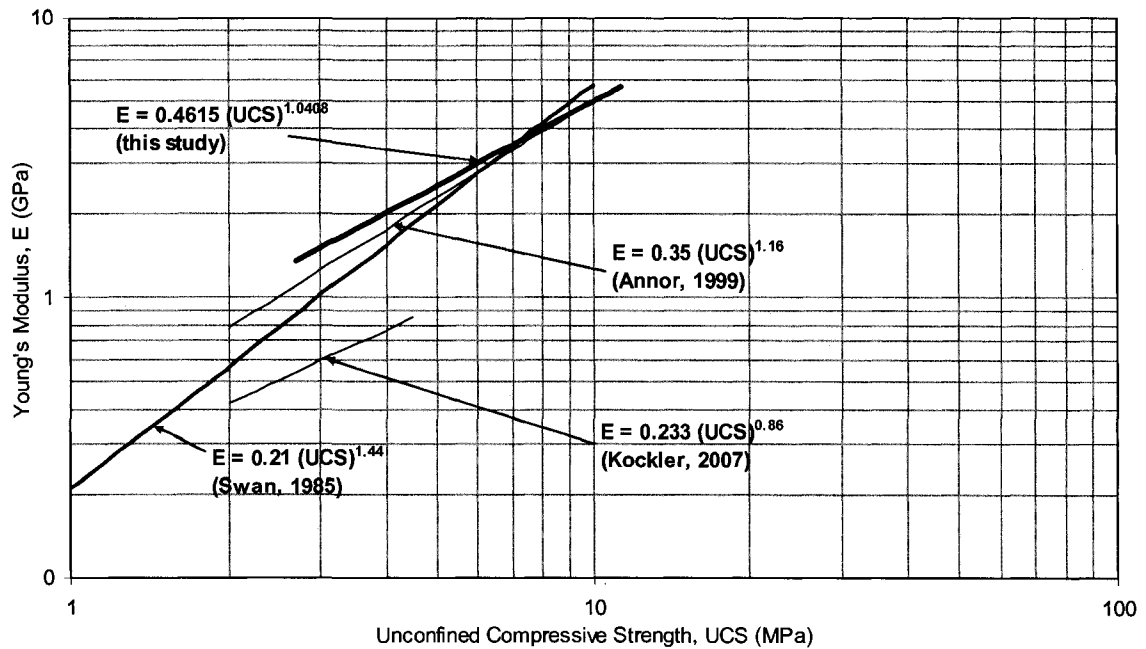


Figure 5.26 UCS versus Young's modulus of CRF from this study compared to Swan (1985), Annor (1999) and Kockler (2007)

The established relationship between the  $E$  and the UCS at the DDM site is higher than others reported up to a UCS of around 7 MPa, but it is close to the relationship reported by Annor (1999) for a UCS between 7 and 10 MPa. However, the established relationship is always higher than that reported by Kockler (2007). The established relationship at the DDM site may be compared with that of Kockler (2007) due to the nearly similar conditions except for the difference in the tested sample size. Kockler's (2007) results from testing the larger sizes indicate that increasing the sample size provides a lower UCS and, hence, lower modulus values. This observation is supported by the findings reported in the literature.

The  $E$  varies with the  $\gamma_d$  and MC of the CRF cylinders. Figure 5.27 shows an increasing trend of the  $E$  with  $\gamma_d$  and a decreasing trend with the MC of the cylinder. However, a poor correlation exists between these parameters in this study due to the likely variations in the cement content present in the CRF samples collected for preparing the cylinders, combined with the narrow range of their density and MC.

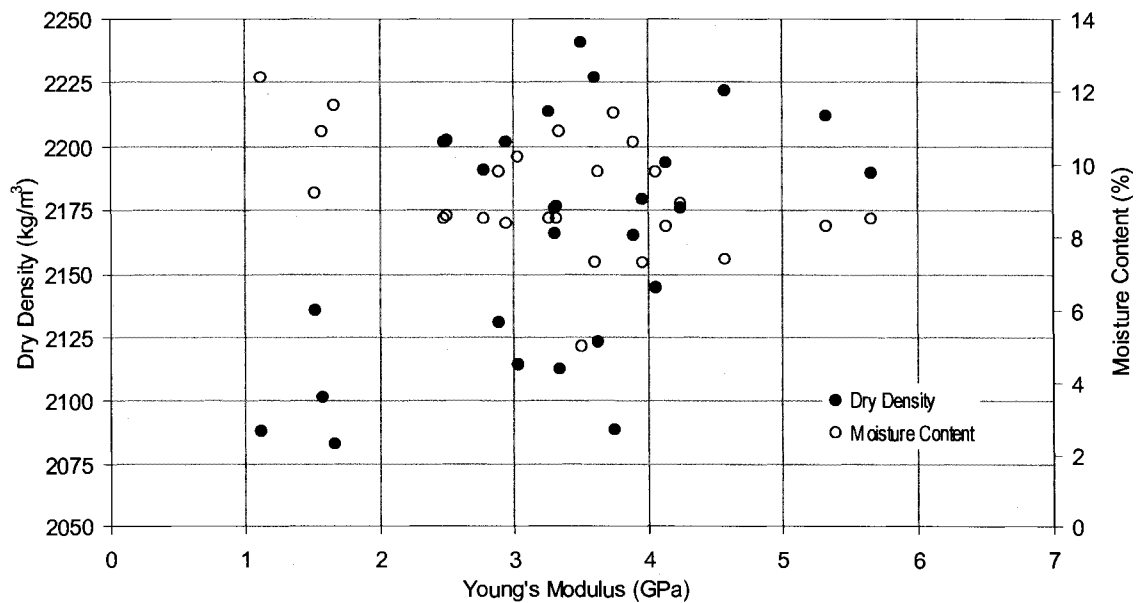


Figure 5.27 Dry density or moisture content versus Young's modulus for the CRF cylinders

## 5.7 Prediction of In Situ CRF Properties

### 5.7.1 Strength

The 28-day UCS of the 100 mm diameter cylinders from the DDM site varies from 4.5 to 15.8 MPa with an average of 10.6 MPa, and ranges from 4.4 to 8.4 MPa with an average of 6.9 MPa for the 150 mm diameter cylinders. The laboratory UCS of CRF reported in the literature usually ranges from slightly more than 1 MPa to nearly 7 MPa. Thus, the strength of the CRF tested at the DDM site tends to exceed many of the values reported elsewhere, as Figure 5.22 has already shown.

The UCS is typically assumed to be size-dependent, with a larger specimen size having a lower strength. This phenomenon extends to the prediction of the in situ UCS for CRF (Yu and Counter, 1983; Reschke, 1993). These researchers assumed that the in situ UCS would be about 2/3 of the strength measured from the 150 mm diameter specimens.

Based on the present study at the DDM site, UCS from 150 mm diameter cylinder is about 86% of the strength of the 100 mm diameter one. Based on the literature, in situ value is expected to be around 66% of UCS obtained from 150 mm diameter cylinder. Therefore, in situ UCS is predicted to be about 60% of the strength measured from the 100 mm diameter cylinders. The lower bound of the in situ UCS of the CRF at the DDM site is predicted to be about 4 MPa. None of the test results measured a strength lower than 4 MPa. The upper bound of the in situ UCS is conservatively predicted to be around 7 MPa, which is less than the average measured strength from the 150 and 100 mm diameter samples.

The UCS of the CRF at the DDM site was designed to be 2.5 MPa after 28 days (Dimitroff, 2007) which was easily achieved at the DDM site, even when using the lower bound on the in situ strength. The estimated in situ UCS of the RCC (indicated by 8 in Figure 5.28) is higher than CRF, probably because of higher compaction, longer curing (28 to 365 days) and higher cement content. Other than the RCC, the predicted UCS at the DDM site is slightly higher than most reported in situ values.

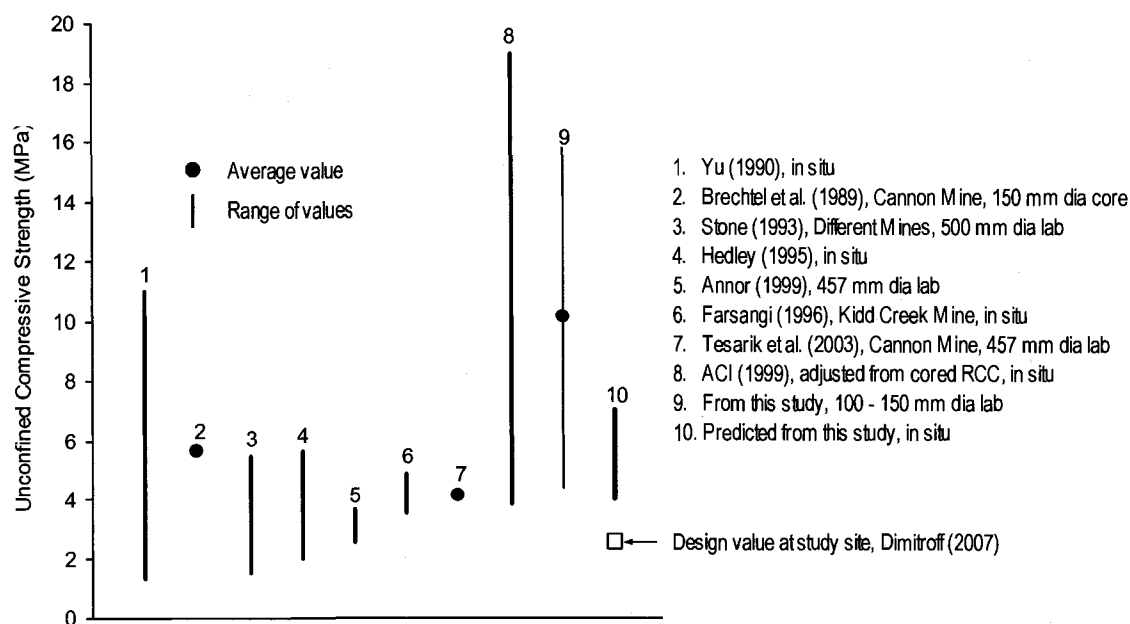


Figure 5.28 Predicted in situ UCS from this study compared with reported large-scale laboratory, in situ cored sample and estimated in situ values

The  $\phi$  of the CRF is predicted to range from 35 to 40° at the DDM site. These values are not based on test results, but inferred from the published values (Yu, 1989; Farsangi, 1996; Tesarik et al., 2003; Kockler, 2007). These same studies, and Brady and Brown (1993) provide guidance for estimating the cohesive component of the strength. The cohesion at the DDM site is predicted to range from 1 to 1.7 MPa, or roughly 25% of the UCS.

### 5.7.2 Elastic Properties

The  $E$  of the CRF was measured at the DDM site during UCS tests on 26 CRF-100 mm cylinder specimens. These data were used to establish a linear empirical relationship between the UCS and the  $E$ . The  $E$  of the CRF was found to be approximately 501 times the UCS. The assumption that this same relationship applies to the estimated in situ strength of the CRF yields a modulus range from 2 to 3.5 GPa at the DDM site.

In Figure 5.29, the predicted in situ modulus at the DDM site is compared with the reported values from a large-scale laboratory and in situ cored samples. This figure also presents the reported design values. The predicted in situ modulus of the CRF at DDM

site is slightly higher than most estimated and design values published elsewhere. However, the modulus lies within the measured in situ-modulus range obtained at the Buick Mine (indicated by 10 in Figure 5.29). The Buick Mine used similar placement and compaction practices to those used at the DDM site.

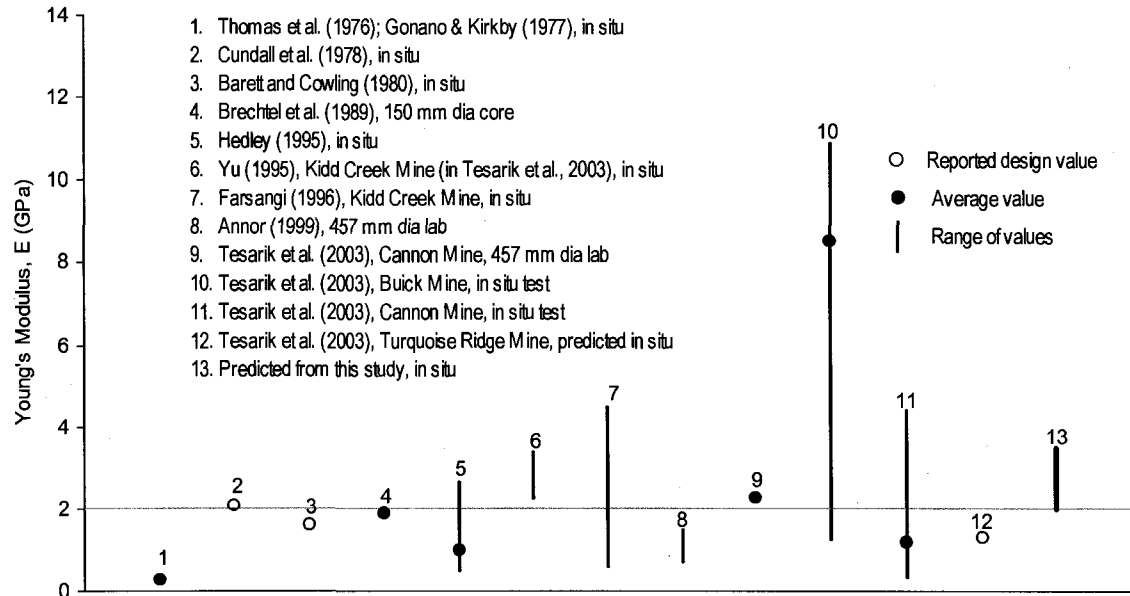


Figure 5.29 Predicted in situ modulus value compared with reported large-scale laboratory and in situ cored samples

The  $\nu$  for the CRF at the DDM site is estimated to range between 0.2 and 0.3, based on the values reported in the literature (Farsangi, 1996; Tesarik et al., 2003).

### 5.7.3 Density and Void Ratio

The average laboratory value of the  $\gamma_d$  from 177 cylinder samples is 2154 kg/m<sup>3</sup> compared to 2117 kg/m<sup>3</sup> from 95 in situ measurements at the DDM site. The measured in situ  $\gamma_d$  of the CRF at the DDM site typically lies between 2000 and 2200 kg/m<sup>3</sup>. These densities are similar to those reported by Tesarik et al. (2003) and Kockler (2007).

The  $e$  and  $\eta$  of the CRF at the DDM site can be estimated based on the measured in situ  $\gamma_d$  and the assumed  $G_s$  of the solids of 2.7. The calculated  $e$  varies from 0.20 to 0.40 with an average of 0.28, and the  $\eta$  ranges from 17 to 29% with an average of 22%. In the literature, the reported  $e$  ranges from 0.37 to 0.51, and the reported  $\eta$  varies from 27 to 33%. Thus, the  $e$  and  $\eta$  for the CRF placed at the DDM site are lower than the reported values. This difference is most likely due to the better spreading and compaction effort by the dozer at the DDM site.

The predicted in situ CRF properties at the DDM site are summarized in Table 5.8. These values provide a useful starting point for conducting strength or deformation

analysis of the CRF as the underground mining proceeds and undercuts the cap or crown pillar of the CRF.

Table 5.8 Predicted in situ parameters of the CRF at the Diavik Mine

Parameters	Ranges		Remarks
UCS, $\sigma_c$ (MPa)	4.0	7.0	Predicted from the measured values
Young's Modulus, $E$ (GPa)	2.0	3.5	
Dry Density, $\gamma_d$ (kg/m <sup>3</sup> )	2070	2140	
Friction Angle, $\phi$	35°	40°	Estimated based on the measured values and a literature review
Cohesion, $c$ (MPa)	0.8	1.7	
Poisson Ratio, $\nu$	0.2	0.3	
Void Ratio, $e$	0.2	0.4	Calculated
Porosity, $\eta$ (%)	17	29	

## 6 Conclusions and Recommendations

Based on the field observations, in situ and laboratory test results, and review of literature, the following conclusions and recommendations are made regarding the preparation, placement, sampling and testing of cemented rockfill. Some suggestions for the future research are also included.

### 6.1 CRF Preparation

- The quantity of the aggregate used to prepare each batch of the CRF was not accurately known because it was simply based on the counting the number of buckets dumped into the mixing bay. A more accurate system that involves weighing the aggregate would avoid a known variability in the test results.
- The grain size distribution of the aggregate used to make CRF at DDM is close to the recommended distributions found in literature but has a tendency to be slightly coarser than optimum. The aggregate may be improved by adding up to 5% sand. Rather than adding the sand directly to the aggregate, the best option to ensure thorough mixing is to add the sand to the cement when the cement slurry is prepared.
- The moisture content of the aggregate was within a narrow range of 1 to 2%. Therefore, the preparation of the cement slurry by adding a constant amount of water provides a consistent w:c ratio for the CRF and continuation of this practice is recommended. The mixed CRF had a moisture content of approximately 7%.
- The specify gravity of the cement slurry provides an indirect measure of the degree of mixing of the cement with the water. Measuring the specify gravity of the cement slurry is a good QC/QA practice and should be continued. For a 6% cement content in the CRF, the specify gravity of the cement slurry should be 1.52. For a 5.5% content in the CRF, the specify gravity of the cement slurry should be 1.48. These values should be explicitly included in the design specifications.
- Dumping the aggregate into the mixing bay while simultaneously pouring and mixing the cement slurry into the aggregate worked well for preparing the CRF in a timely manner. If delays are expected in the mixing process, the aggregate should be added to the mixing bay before the cement slurry is added.
- A mixing bay constructed with provision of a load-out opening may reduce the loading time and may make it easier to clean out the mixing bay after preparing each batch of CRF. When the site condition permits, it is desirable to locate the mixing bay close to the placement area to the transportation time.
- Coordination of the cement slurry preparation and CRF mixing is needed to avoid delays in having the cement slurry mixed into the aggregate.
- The main objective of mixing the aggregate and cement slurry in the mixing bay is to coat the aggregate thoroughly with the cement as per the design recipe. Field observations indicate that proper mixing requires about 10 to 15 minutes. The mixing time should be used as another QA/QA measure.

## **6.2 CRF Placement**

- The placement of the CRF recognized that the periphery and contacts between different lifts were potential zones of weakness. Special care and placement procedures were adopted in these areas to minimize the effect of cold joints and CRF segregation. The CRF placed at the highwall slope side was compacted by using an excavator bucket. All these good practices are recommended to continue in future.
- Plots of in situ density versus moisture content suggest that the maximum dry density is achieved at moisture contents close to 7%. This moisture content matches the CRF mix design.
- The specified target in situ dry density of the CRF was 2150 kg/m<sup>3</sup>. This density typically could not be achieved at DDM by using a dozer and excavator to spread and compact the CRF in lifts that were one metre thick. The average in situ dry density was 2117 kg/m<sup>3</sup>. This suggests that the design specification was too high and should be reduced slightly for a given compaction effort.

## **6.3 CRF Testing and Quality Control**

- The practise of conducting grain-size analysis and measuring the moisture content of the aggregate are good QC measures for the aggregate and should be continued.
- The measured in situ and laboratory moisture contents for the CRF are similar. Thus, the measured in situ dry density of the CRF is almost same as the laboratory moisture content corrected in situ dry density.
- Measuring the in situ moisture content and density of the CRF with a Troxler nuclear gauge should be continued in the future as an important QC/QA practise. From a practical perspective, the tests are easy and quick to perform and the results are available in real time thus providing an opportunity to rectify anomalous conditions should they occur.
- In order to obtain more representative laboratory specimens of the CRF, the CRF samples should be taken from the mixing bay as the CRF is being loaded into the haul truck. This would substantially reduce the time elapsed between CRF preparation and casting of laboratory cylinders. Obtaining samples of CRF from the compacted lifts in the field is not recommended.
- The practise of conducting 3- and 7-day unconfined compression tests only provides early indicative strength of CRF. Instead, the testing program should focus on 28-day test if the testing objective is to assess or determine the compressive strength of the CRF.
- The observed variability in the measured CRF strength may be caused by different curing temperatures and humidity. A proper curing chamber or a moist room at a constant temperature is recommended.
- The QC/QA process could benefit from establishing acceptable ranges in measurable parameters such as the specific gravity of the cement slurry, in situ density and moisture content of the CRF, required number of passes of the dozer to achieve an optimum compaction with a given lift thickness, and moisture content and density of prepared laboratory test specimens.
- The 100 mm diameter CRF cylinders prepared using the <25 mm screened CRF samples had 2% higher average moisture content compared to in situ CRF. This

indicates that there is probably higher cement content in the test specimens compared to in situ conditions.

- Laboratory specimens for conducting USC tests should have the same density as the in situ CRF.
- The 28-day UCS of the CRF at DDM was found to typically fall between 6 and 12 MPa. These values tend to be higher, with a lower void ratio and porosity, than the published values associated with CRF being used to fill stopes. This is possibly achieved because of the better mixing by the excavator, compaction effort by the dozer, and implementation of good QC/QA practices at DDM.
- An empirical relationship between the Young's modulus and unconfined compressive strength of the CRF at DDM was established:  $E = 501 \cdot UCS$ . This relationship is similar to other published relationship for CRF.
- Size effects on the CRF strength were observed for the 100 mm and 150 mm diameter cylinders. Lower strengths were measured with larger test specimens. This suggests that the in situ strength may be lower than the laboratory strength.
- Based on the test data obtained at DDM, the in situ CRF strength is estimated to be about 60% of the laboratory strength of 100 mm diameter test specimens.
- The predicted in situ strength of the CRF is approximately 4 to 7 MPa. This shows that the targeted 28-day design UCS of 2.5 MPa was easily achieved.

#### **6.4 Future Research**

- The optimum lift thickness and compaction effort along with the required number of passes by the dozer, have yet to be established. Further research to optimize the lift thickness and compaction effort may yield a stronger CRF with the same cement content.
- Future research could examine the replacement of some of the cement with flyash as a means for reducing the CRF costs.
- It is recommended that further research be carried out to assess the effect of the test-specimen size on strength in order to provide more confidence in extrapolating laboratory strengths to in situ CRF strength.
- Tensile strength test is recommended to establish correlation with the UCS of CRF cylinder.
- In situ coring of the cured CRF at various locations is recommended because this would provide test specimens that could be tested to verify if the measured in situ density by a nuclear gauge and predicted in situ strength are valid.
- The predicted strength and stiffness of the CRF should be useful input parameters for any future stability analyses of the CRF crown pillar.

## References

American Concrete Institute (2000), State-of-the-art report on roller-compacted concrete pavements, ACI Manual of Concrete Practice, ACI 325.10R-95, 32 p.

American Concrete Institute (1990), Roller compacted mass concrete, Committee 207.

American Concrete Institute (1998), Use of flyash in concrete, ACI 226.3R-87.

American Concrete Institute (1988), Roller-compacted mass concrete, ACI 207.5R-89.

American Society of Testing and Materials (1987), Standard Practice for Correction of Unit Weight and Water Content for Soils Containing Oversize Particles, ASTM Designation: D 4718-87.

American Society of Testing and Materials (2000), Standard Terminology Relating to Concrete and Concrete Aggregates, ASTM Designation: C 125-00.

American Society of Testing and Materials (2000), Standard Test Method for Water (Moisture) Content of Soil by Direct Heating, ASTM Designation: D 4959-00.

American Society of Testing and Materials (2005), Standard Test Method for Sieve Analysis for Fine and Coarse Aggregates, ASTM Designation: C 136-05.

American Society of Testing and Materials (1996), Standard Test Method for Density of Soil and Soil Aggregate in Place by Nuclear Methods (Shallow Depth), ASTM Designation: D 2922-91.

American Society of Testing and Materials (1996), Standard Test Method for Water Content of Soil and Rock in Place by Nuclear Methods (Shallow Depth), ASTM Designation: D 3017-88.

American Society of Testing and Materials (2005), Standard Test Method for Density of Bituminous Concrete in Place by Nuclear Methods, ASTM Designation: D 2950-05.

American Society of Testing and Materials (2005), Standard Test Methods for Laboratory Determination of Water (Moisture) Content of Soil and Rock by Mass, ASTM Designation: D 2216-05.

American Society of Testing and Materials (1995), Standard Test Methods for in Place Density of Unhardened and Hardened Concrete, Including Roller Compacted Concrete by Nuclear Methods, ASTM Designation: C 1040-93.

Annor, A. B. (1999), A Study of the Characteristics and Behaviour of Composite Backfill Material, PhD Thesis, Department of Mining and Metallurgical Engineering, McGill University.

Annor, A. B., Tarr, K. and Fynn, D. (2003), Mechanical properties of a composite backfill material, Presented at the 105th Annual Conference of CIM, Montreal (Quebec), May, Division Report CANMET-MMSL 03-023 (OPJ), Mining and Mineral Science Laboratories, Natural Resources Canada, Sudbury, 14 p.

Archibald, J. F., Lausch, P. and He, Z. X. (1993), Quality control problems associated with backfill use in mines, *CIM Bulletin*, vol. 86, no. 972, pp 53-57.

Arioglu, E. (1983), Engineering properties of cemented aggregate fill mixes for Uludand Tungsten Mine of Turkey, *Mining with Backfill: Proceedings of the International Symposium - Lulea*, S. Granholm ed., A. A. Balkema, pp 3-9.

Barrett, J. R. (1973), Structural aspects of cemented fill behaviour, *Proceedings of Jubilee Symposium on Mine Filling*, Mount Isa, Australia, August 19-22, AIMM, North West Queensland Branch, Victoria, pp 97-104.

Berry, P. (1980), Geomechanical investigations for the design of cemented fill, *Proceedings of Application of Rock Mechanics to Cut and fill Mining*, Lulea, Sweden, June 1-3, Institute of Mining and Metallurgy, London, pp 79-92.

Bloss, M. L., and Greenwood, A. G. (1998), Cemented rockfill research at Mount Isa Mines Limited, 1992-1997, *Minefill'98: Proceedings of the 6th International Symposium on Mining with Backfill*, M. Bose ed., Australian Institute of Mining and Metallurgy (AIMM), Brisbane, Queensland, pp 207-215.

Brady, B. H. G. and Brown, E. T. (1993), *Rock Mechanics for Underground Mining*, 2nd Edition, Chapman and Hall, pp 219-233.

Brauns, J. and Kast, K. (1990), Laboratory testing and quality control of rockfill-German practice, *Advances in Rockfill Structures*, Kluwer Academic Publishers, London, NATO Advance Science Institutes Series E, Applied Sciences, vol. 200, E. Maranha das Neves ed., June, pp 195-219.

Brechtel, C. E., Hardy, M. P., Bas-Dresh, J. and Knowlson, J. S. (1989), Application of high strength at the Cannon Mine, *Innovations in Mining Backfill Technology: Proceedings of the 4th International Symposium on Mining with Backfill*, F. P. Hassani, M. J. Scoble, and T. R. Yu eds., A. A. Balkema, pp 105-117.

Brotman, I., Crist, M. and Gaul, J. (2007), Roller compacted concrete pavement: Properties, design, and construction, *Geotechnical Special Publication*, no. 169.

Bryan, D. and Bonner, R. (2003), The Diavik Diamond Mine, Lac De Gras, Northwest Territories, Canada, *8th International Kimberlite Conference, Slave Province and Northern Alberta Field Trip Guidebook*, B. A. Kjarsgaard ed., pp 61-65.

Choi, Y-K. and Groon, J. L. (2001), RCC mix design - Soils approach, *Journal of Materials in Civil Engineering*, vol. 13, no. 1, April, pp 71-76.

Choi, Y-K. and Hansen, K. D. (2005), RCC/soil-cement: What's the difference?, *Journal of Materials in Civil Engineering*, vol. 17, no. 4, pp 371-378.

Dan, O. T (2004), The Basics of mine backfill, A review of some critical factors for cement aggregate fill, *Engineering and Mining Journal*, vol. 205, no. 12, pp 27-29.

Quebec Pavement (2005), Design and Construction of Roller Compacted Concrete Pavements in Quebec, P. Gauthier and J. Marchand eds., Nov., 111p.

Diavik Diamond Mines Inc. (2006), Sustainable Development of Diavik Diamond Mines Inc., <http://www.diavik.ca/PDF/2006%20Diavik%20Sustainable%20Development%20Report.pdf>, 21 January 2008, 56p.

Diavik Diamond Mines Inc. (2005a), Diavik Diamond Mines Inc., Photos, <http://www.diavik.ca/Photos/2005/1082.html>, 28 January 2008.

Diavik Diamond Mines Inc. (2005b), Diavik Diamond Mines Inc., Phase 2, <http://www.diavik.ca/Phase2.htm>, 28 January 2008.

Diavik Diamond Mines Inc. (2007a), A154 Extraction Plan – Note for the Record -Draft, Memorandum prepared by Sarah Greer and Marisol Valerio, June 15.

Diavik Diamond Mines Inc. (2007b), A154N Kimberlite Recovery Project – Weekly Progress Power Point Presentation A154N\_Schedule\_May07.ppt.

Diavik Diamond Mines Inc. (2007c), Diavik Diamond Mines Inc., Dialogue, 3rd Quarter, vol. 10, <http://www.diavik.ca/dialogue/dialogue%20Volume%2010%20Q3%202007.pdf>, 28 January 2008.

Dickhout, M. H. (1973), The role and behaviour of fill in mining, *Proceedings of Jubilee Symposium on Mine Filling*, Mount Isa, Australia, August 19-22, AIMM, North West Queensland Branch, Victoria, pp 2-11.

Dimitroff, S. (2007), EBA Engineering Consultants Ltd., Personal Communication.

Dismuke, S. and Diment, T. (1996), The testing, design, construction, and implementation of cemented rockfill (CRF) at Polaris, *CIM Bulletin*, vol. 89, no. 1005, pp 91-97.

Donovan, J., Dawson, J. and Bawden, W. F. (2007), David Bell Mine underhand cut and fill sill mat test, *Minefill 2007: 9th International symposium on Mining with Backfill, Innovations and Experience in Minefill Design*, Montreal, CD version, paper no. 2467.

EBA Engineering Consultants Ltd. (2007a), Technical Memo on Slope Stabilization for A154NE Wall Kimberlite Recovery Program at the DDMI, NWT, Letter to Diavik Diamond Mine, NWT, June 14.

EBA Engineering Consultants Ltd. (2007b), Work Plan for A154NE Wall Rock Slope Stabilization, Letter to Diavik Diamond Mine, NWT, May 23.

Evans, R., Ran, J. and Allan, R. (2007), Application of mine fill at Barrick Gold, Minefill 2007: 9th International symposium on Mining with Backfill, Innovations and Experience in Minefill Design, Montreal, CD version, paper no. 2499.

Farsangi, P. N. (1996), Improving Cemented Rockfill Design in Open Stopping, PhD Thesis, Department of Mining and Metallurgical Engineering, McGill University.

Farsangi, P. N. and Hara, A. (1993), Consolidated rockfill design and quality-control at Kidd Creek Mines, CIM Bulletin, vol. 86, no. 972, pp 68-74.

Farsangi, P. N., Hayward, A. G. and Hassani, F. P. (1996), Consolidated rockfill optimization at Kidd Creek Mines, CIM Bulletin, vol. 89, , no. 1001, June, pp 129-134.

Farzam, H., Rispin, M. and Karlson, R. (1998), The use of unique admixture technologies in mine backfill-technology description and case histories, Minefill'98: Proceedings of the 6th International Symposium on Mining with Backfill, M. Bose ed., Australian Institute of Mining and Metallurgy (AIMM), Brisbane, Queensland, pp 71-75.

Gao, P. W., Wu, S. X., Lin, P. H., Wu, Z. R. and Tang, M. S. (2006), Effect of flyash on deformation of roller-compacted concrete ACI Materials Journal, vol. 103, no. 5, pp 336-339.

Golder Associates (2007a), Diavik Diamond Mines Inc. Cemented Rockfill Materials for A154N Slope Cover, Technical Specification 1000-01, July 12, 5 p.

Golder Associates (2007b), Diavik Diamond Mines Inc. Cemented Rockfill Mixing and Placement for A154N Slope Cover, Technical Specification 1000-02, July 12, 5 p.

Gonano, L. P. and Kirkby R. W. (1977), In situ investigation of cemented rockfill in the 1100 orebody, Mount Isa Mine, Australian Commonwealth Scientific and Industrial Research Organization, Queensland Technical Report no. 47.

Hassani, F. and Archibald, J. (1998), Mine Backfill 1998, F. Hassani and Archibald eds., The Canadian Institute of Mining, Metallurgy and Petroleum, 308 p.

Hedley, D. G. F. (1995), Final report on the stiff backfill, Project for Mining Research Directorate, Canadian Rockburst Program, Ontario.

Helms, W. (1998), Preparation and transportation systems for cemented backfill, Mining Science and Technology 7 (1998), Elsevier Science Publishers, pp 183-193.

Henderson, A. M. and Lilley, C. R. (2001), Backfill selection and experience at the Kanowna Belle Gold Mine, Western Australia, Minefill 2001: 7th International Symposium on Mining with Backfill, D. Stone ed., SME, Littleton, Colorado, pp 379-387.

Hisham, Y. Q, Ibrahim, M. A. and Al-Abdul Wahhab, H.I.(2005), Proportioning RCCP mixes under hot weather conditions for a specified tensile strength, Cement and Concrete Research, vol. 35, no.2, pp 267–276.

Houlsby, A. C. (1990), Construction and design of cement grouting – A guide to grouting in rock foundations, John Wiley & Sons, pp 10-28.

Knissel, W. and Helms, W. (1983), Strength of cemented rockfill from washery refuse, Results from laboratory investigations, Mining with Backfill: Proceedings of the International Symposium, S. Granholm ed., A. A. Balkema, pp 31-37.

Kockler, M. (2007), Design of Cemented Rockfill Spans for Longhole Stopping at the Rain Mine, Carlin, Nevada, PhD Thesis, Mining Engineering-Metallurgy, University of Idaho.

Kokubu, K., Cabrerab, J. G. and Uenoa, A. (1996), Compaction properties of roller compacted concrete, Cement and Concrete Composites, vol. 18, no. 2, pp 109-117.

Kosmatka, S. H and Panarese, W. C. (1988), Design and control of concrete mixture, 13th Edition, Portland Cement Association, Illinois.

Lamos, A. W. (1993), An Assessment of the effects of ultrafine aggregate components on the properties of mine backfills, Minefill 93: Proceedings of 5th International Symposium on Mining with Backfill, M. Bose ed., H. W. Glen ed., SAIMM, Johannesburg, pp. 173-179.

Lamos, A. W. and Clark, I. H (1989), The Influence of material composition and sample geometry on the strength of cemented backfill, Innovations in Mining Backfill Technology: Proceedings of the 4th International Symposium on Mining with Backfill, F. P. Hassani, M. J. Scoble, and T. R. Yu eds., A. A. Balkema, Rotterdam, pp 89-94.

Landriault, D. (1992), Inco's backfill experience, Canadian Mining Journal, October, pp 39-48.

Landriault, D. and Goard, B. (1987), Research into high density backfill placement methods by the Ontario Division of Inco Limited, CIM Bulletin, vol. 80, no. 897, pp 46-50.

Lehigh Heidelberg Cement Group (2002), Lehigh Technical Services, <http://www.lehighnw.com/canada/pdf/DataSheets/DataTypeGU.pdf>, 26 February 2008.

Ley, G. M. M., Steed, C. M., Bronkhorst, D. and Gustas, R. (1998), Mining under backfill, CIM Bulletin, vol. 91, no. 1020, pp 65-71.

McKay, D. L. and Duke, J. D. (1983), Mining with backfill at Kidd Creek No. 2 Mine, Mining with Backfill: Proceedings of the International Symposium – Lulea, S. Granholm ed., A. A. Balkema, pp 161-172.

McKinstry, J. D. and Laukkannen, P. M. (1989), Fill operating practices at Isa Mine-1983-1988, Innovations in Mining Backfill Technology: Proceedings of the 4th International Symposium on Mining with Backfill, F. P. Hassani, M. J. Scoble, and T. R. Yu eds., A. A. Balkema, pp 361-368.

Nanni, A. (1988), Limestone crusher-run and tailings in compaction concrete for pavement applications, ACI Materials Journal, May-June, pp 158-163.

Nantel, J.H. (1998), Recent Developments and Trends in Backfill Practices in Canada, Minefill'98: Proceedings of the 6th International Symposium on Mining with Backfill, M. Bose ed., Australian Institute of Mining and Metallurgy (AIMM), Brisbane, Queensland, pp 11-14.

Nanthanathan, N. (2006), Backfill Optimization using Mine Tailings for Improved Ground Stability in Underground Mines, MASc Thesis, Mining Engineering, Dalhousie University, Nova Scotia, Halifax.

Neindorf, L. B. (1983), Fill operating practices at Mount Isa Mines, Mining with Backfill: Proceedings of the International Symposium – Lulea, S. Granholm ed., A. A. Balkema, pp 179-187.

Neville, A.M. (1987) Properties of concrete, Longman Scientific and Technical-Longman, Singapore.

Nishi - Khon/SNC - Lavalin (2004), Diavik Diamond Mines Inc. Detailed Design of Dike A418, Final Design Report, Volume I, November.

Nokken, M. R., Hassani, F. P. and Annor, A. B. (2007), An investigation into composite minefill characteristics, Minefill 2007: 9th International symposium on Mining with Backfill, Innovations and Experience in Minefill Design, Montreal, CD version, paper no. 2723.

Peterson, S. M. (1996), Cemented Rockfill Optimization in Vertical Block Mining, MSc Thesis, Department of Mining, Metallurgical and Petroleum Engineering, University of Alberta, Edmonton.

Peterson, S., Szymanski, J. and Planeta, S. (1998), A statistical model for strength estimation of cemented rockfill in vertical block mining, Minefill'98: Proceedings of the 6th International Symposium on Mining with Backfill, M. Bose ed., Australian Institute of Mining and Metallurgy (AIMM), Brisbane, Queensland, pp 173-177.

Pittman, D. and Ragan, S. (1986), A guide for design and construction of roller-compacted concrete Pavements, Final Report for US Army Corps of Engineers, Washington D. C., November.

Portland Cement Association (1987), Structural design of roller compacted concrete for industrial pavements, Concrete Information, pp 1-8.

Portland Cement Association (2004), Guide Specification for Construction of Roller-Compacted Concrete Pavements, Pavements, June, pp 1-7.

Quesnel, W. J. F, deRuiter, H. and Pervik, A. (1989), The assessment of cemented rockfill for regional and local support in rockburst environment, LAC Minerals Limited, Macassa Division, Innovations in Mining Backfill Technology: Proceedings of the 4th International Symposium on Mining with Backfill, F. P. Hassani, M. J. Scoble, and T. R. Yu eds., A. A. Balkema, pp 217-224.

Reschke, A. E. (1993), The Use of cemented rockfill at Namew Lake Mine, Manitoba, Canada, Minefill 93: Proceedings of 5th International Symposium on Mining with Backfill, M. Bose ed., H. W. Glen ed. SAIMM, Johannesburg, pp 101-108.

Reschke, A. E. (1998), The development of colloidal mixer based CRF systems, Minefill'98: Proceedings of the 6th International Symposium on Mining with Backfill, M. Bose ed., Australian Institute of Mining and Metallurgy (AIMM), Brisbane, Queensland, pp 65-70.

Reschke, A. E. (2007), Innovative CRF batch plant design at the Leeville Mine, Nevada, Minefill 2007: 9th International symposium on Mining with Backfill, Innovations and Experience in Minefill Design, Montreal, CD version, paper no. 2564.

Ribeiro, A. C. B. and de Almeida, I. R. (2000), Study on high performance roller compacted concrete, Materials and Structures, vol. 33, July, pp 398-402.

Rodrigues, J. D. (1990), Physical characterization and assessment of rock durability through index properties, Advances in Rockfill Structures, Kluwer Academic Publishers, NATO Advance Science Institutes Series E, Applied Sciences, vol. 200, E. Maranha das Neves ed., pp 7-34.

Roscoe Postle Associates Inc. (2005), Diavik Diamond Mine Mineral Reserve and Mineral Resource Audit Prepared for Aber Diamond Corporation, April, Report N143-101.

Sacrison, R. and Roberts, L. (2001), Meikle Mine backfill system – Case history, Minefill 2001: 7th International Symposium on Mining with Backfill, D. Stone ed., SME, Littleton, Colorado, pp 389-402.

SNC - Lavalin Engineers and Constructors (2000), Feasibility Study for Diavik Diamond Projects, Volume VII, Executive Summary Prepared for Aber Resources Ltd, April.

Stone, D. M. R. (1993), The Optimization of mix designs for cemented rockfill, Minefill 93: Proceedings of 5th International Symposium on Mining with Backfill, M. Bose ed., H. W. Glen ed. SAIMM, Johannesburg, pp 249-253.

Stone, D. M. R. (2007), Factors that affect cemented rockfill quality in Nevada mines, Minefill 2007: 9th International symposium on Mining with Backfill, Innovations and Experience in Minefill Design, Montreal, QC, Canada, CD version, paper no. 2539.

Swan, G. (1985), A new approach to cemented backfill design, CIM Bulletin, vol. 78, no. 884, pp 53-58.

Talbot A. N. and Richard, F. E. (1923), The Strength of concrete, its relation to the cement aggregates, and water, Engineering Experimental Station, University of Illinois, October, Bulletin no. 137.

Tangtermsirikul, S., Kaewkhluab, T. and Jitvutikrai, P. (2004), A compressive strength model for roller compacted concrete with flyash, Magazine of Concrete Research, vol. 56, no. 1, Feb., pp 35-44.

Tesarik, D. R., Seymour, J. B. and Jones, F. M. (2003), Determination of in situ deformation modulus for cemented rockfill, ISRM 2003-Technology Roadmap for Rock Mechanics, South African Institute of Mining and Metallurgy, pp 1209-1220.

Thomas, E. G., Natel, J. H. and Notley, K. R. (1979), Fill technology in underground metalliferous mines, International Academic Services Limited, Kingston, Ontario, pp 6-16.

Troxler Electronic Laboratories Inc. (2006), Manual of Operation and Instruction, Model 3430, Surface Moisture-Density Gauge, Edition 8.1.

Udd, J. E and Annor, A. B. (1993), Backfill research in Canada, Minefill 93: The South African Institute of Mining and Metallurgy, Symposium Series S13, Johannesburg, pp 361-368.

U. S. Army Corps of Engineers, Engineer Technical Letter (1993), Structural design using the roller-compacted concrete (RCC) construction process, Department of the Army, ELT 1110-2-343, May, pp 22p.

U. S. Army Corps of Engineers, Engineer Technical Letter (1995), Earth fill and rockfill construction, ELT 1110-2-1911, Section-5, Sept, 25p.

Wang, C. and Villaescusa, E. (2001), Factors influencing the strength of cemented aggregate fill. Minefill 2001, Proceedings of 7th International Symposium on Mining with Backfill, Seattle, D. Stone ed., Society for Mining, Metallurgy and Exploration (SME), pp. 81-87.

Wang, C., Tannant, D. D., Padrutt, A. and Millette, D. (2002), Influence of admixtures on cemented backfill strength, Mineral Resources Engineering, vol. 11, no. 3, pp 261-270.

Young, L. R. McIntire, H.E. and Yanske, T.R. (2007), CRF backfill at the Doe Run Company 1991-2006, Minefill 2007: 9th International Symposium on Mining with Backfill, Innovations and Experience in Minefill Design, Montreal, CD version, paper no. 2520.

Yu, T. R (1989), Some factors relating to the stability of consolidated rockfill at Kidd Creek, Innovations in Mining Backfill Technology: Proceedings of the 4th International

Symposium on Mining with Backfill, F. P. Hassani, M. J. Scoble, and T. R. Yu eds., A. A. Balkema, pp 279-286.

Yu, T R. (1990), Backfill alternatives in Ontario Mines, Canada, Ontario Mineral Development Agreement DSS File No. 09SQ.23440-6-9011; CANMET Project no. 142501-1987, Energy, Mines and Resources Canada, Ottawa.

Yu, T. R. and Counter, D. B (1983), Backfill practice and technology at Kidd Creek Mines, CIM Bulletin, vol. 91, no. 1020, pp 56-65.

Yu, T. R and Counter, D. B (1988), Use of flyash in backfill at Kidd Creek Mines, CIM Bulletin, vol. 81, no. 909, pp 45-50.

Zhu, Z. (2002), Analysis of Mine Backfill Behaviour and Stability, PhD Thesis, Department of Mining, Metals and Material Engineering, McGill University, Montreal.

Table A.1 In situ and laboratory densities, moisture contents and UCS values of three trial mixes in 2007

Mix No.	Date	Water to Cement Ratio	Troxler's Test Information					Laboratory Test					Location/Remarks	UCS (MPa)			Cyl. Dry Den. (kg/m <sup>3</sup> )		
			Test No.	Location	Elev. (m)	Wet Den. (kg/m <sup>3</sup> )	Dry Den. (kg/m <sup>3</sup> )	MC (%)	Sample No.	MC (%)	Dry Den. (kg/m <sup>3</sup> )	3 days		7 days	28 days	3 days	7 days	28 days	
1	16-Jun-07		1	Centre of Test Pad	0.50	2345	2177	7.7	T-1	6.8	2196	From Test Location		2.2					
			2	Centre of Test Pad	0.75	2175	2089	4.1	T-2	4.6	2079	From Test Location							
			3	Centre of Test Pad	1.00	2289	2205	3.8	T-3	4.7	2186	From Test Location							
									R-1	5.1		Random at Test Ramp							
									R-2	6.3		Random at Test Ramp							
									R-3	5		Random at Test Ramp							
									R-4	5.7		Random at Test Ramp							
									S-110	6.9		Uncompacted Mix for Seive							
									S-111	5		Uncompacted Mix near Test 3 for Seive							
									S-109	4		Aggregates from Loader Bucket for Seive							
2	10-Jul-07	0.987 (4504 kg water and 4562 kg cement)							S-112	1.4		Aggregates from 3 areas of Stockpile							
									CRF-01	2.6		SE of Test Pad							
										CRF-02	3.2		SW of Test Pad						
										CRF-03	2.8		Centre of Pad for Seive						
			D-01	Random at Test Pad	1.00	2203	2078	6.0											
			D-02	Random at Test Pad	1.00	2101	1982	6.0						4.2					
			D-03	Random at Test Pad	1.00	2125	2024	5.0											
			D-04	Random at Test Pad	1.00	2061	1963	5.0											
			CRF-04	Random at Test Pad	1.00	1987	1911	4.0	CRF-4	4.0	1911	From Test Location for Seive							
			D-06	Random at Test Pad	0.50	2377	2211	7.5											
D-07	Random at Test Pad	0.50	2058	1969	4.5														
2	20-Jul-07								CRF-5	6.0	2080	From Test Location for Seive							
									CRF-6	3.6		East Edge of Test Pad for Seive							
3	1-Aug-07	0.988 (4504 kg water and 4558 kg cement)							CRF-7	0.6		Aggregates from Loader Bucket for Seive							
										CRF-8	1.6		Aggregates from Stockpile for Seive						
									CRF-10	3.2		Aggregate from Stockpile							
			D-01	Eastside of Test Pad	1.00	2311	2152	7.4	CRF-11	6.7	2166	From Test Location	3.65	6.2	8.7	2172	2178	2169	
			D-02	Westside of Test Pad	1.00	2295	2139	7.3	CRF-12	6.3	2159	From Test Location							
			D-03	Centre of Test Pad	0.50	2281	2108	8.2	CRF-13	7.8	2116	From Test Location							
									CRF-14	7.4		Centre of Pad for Seive							

Table A.2 Grain size analysis and moisture content results of aggregate and CRF during trial mixes in 2007

Mix No.	Date	Seive Material	Sample No.	Sieve Size (mm)														Moisture (%)
				75	50	40	28	20	14	10	5	2.5	1.25	0.63	0.315	0.16	0.08	
1	16-Jun-07	Aggregate	S-109	100.0	100.0	94.2	78.4	60.3	50.4	41.3	28.1	20.6	15.9	11.7	8.3	5.6	3.5	2.4
2	10-Jul-07		CRF-7	100.0	100.0	78.6	47.9	28.9	19.5	14.7	9.6	7.7	6.4	5.2	4.0	2.9	1.9	0.6
			CRF-8	100.0	100.0	95.4	72.7	62.9	52.6	45.0	33.2	25.6	20.4	15.4	11.1	7.3	4.6	1.6
1	16-Jun-07	CRF	S-110	100.0	100.0	97.9	86.0	69.3	59.2	51.3	37.4	29.0	23.7	18.6	14.5	11.0	8.3	4.9
			S-111	100.0	100.0	99.5	97.7	91.2	81.7	74.6	60.6	51.0	43.3	36.2	30.8	26.1	22.5	4.8
2	10-Jul-07		CRF-4	100.0	100.0	94.7	47.2	34.7	25.2	19.9	14.2	11.7	10.1	8.6	7.2	5.9	4.8	4.0
			CRF-5	100.0	100.0	90.5	44.0	30.5	21.6	18.2	14.2	12.1	10.6	8.8	7.2	5.6	4.3	6.0
3	1-Aug-07		CRF-6	100.0	100.0	85.3	56.6	44.5	34.2	27.0	19.8	16.7	14.9	13.2	11.5	9.9	8.5	3.6
			CRF-22	100.0	97.7	94.5	79.7	66.5	55.7	48.4	37.8	31.7	27.7	23.5	19.5	15.8	12.6	7.4

Table A.3 Grain size analysis and moisture content during production of CRF aggregate in 2006

Date	Shift	Sample	Sieve Size (mm)																Moisture (%)
			50	25	20	14	12.5	10	5	2.5	2	1.25	0.63	0.5	0.425	0.315	0.15	0.08	
16-Aug-06	N	CRF #1	95.9	56.2	49.2	38.5		31.4	22.9	17.6		13.9		10.4				5.8	1.54
16-Aug-06	N	CRF #2	100.0	78.3	69.1		52.2	45.9	31.5		20.9		11.4		9.3	7.6	3.8	2.0	2.59
17-Aug-06	N	CRF #3	100.0	81.6	75.1		61.8	56.2	44.0		33.0		20.5		16.4	13.8	7.3	4.0	2.08
17-Aug-06	N	CRF #4	100.0	89.7	84.1		73.0	68.0	53.8		41.1		25.8		20.8	17.6	9.4	5.2	2.14
17-Aug-06	N	CRF #5	100.0	62.9	50.6		33.6	31.0	24.5		18.5		11.7		9.4	8.0	4.4	2.5	1.87
17-Aug-06	N	CRF #6	100.0	74.7	68.4		54.4	48.6	36.1		26.5		16.8		13.7	11.6	5.8	3.1	1.62
17-Aug-06	N	CRF #7	100.0	70.4	59.3		44.3	39.6	28.9		20.5		12.2		9.7	8.1	4.3	2.4	2.08
18-Aug-06	N	CRF #8	100.0	70.3	60.6		44.2	39.6	30.4		22.6		14.4		11.7	9.9	5.3	3.0	1.60
18-Aug-06	N	CRF #9	100.0	70.7	60.2		40.8	37.1	29.1		22.3		15.5		11.8	10.0	5.3	2.8	2.49
19-Aug-06	N	CRF #10	100.0	60.3	47.9		31.0	27.2	19.8		13.6		7.8		6.0	5.0	2.6	1.5	0.92
19-Aug-06	N	CRF #11	100.0	75.0	64.8		49.0	44.6	34.5		26.4		16.6		13.4	11.4	6.3	3.7	1.45
19-Aug-06	N	CRF #12	100.0	69.5	56.0		36.5	32.8	25.5		19.7		13.2		10.8	9.2	4.8	2.5	2.65
20-Aug-06	N	CRF #13	100.0	72.7	62.3		48.3	40.8	31.0		23.1		14.5		11.7	9.9	5.2	2.7	2.43
21-Aug-06	N	CRF #14	100.0	84.1	76.9		61.2	55.3	41.3		30.4		17.7		13.7	11.2	5.6	3.0	0.50
22-Aug-06	N	CRF #15	100.0	62.2	46.1		22.9	19.6	13.5		9.5		5.7		4.6	3.9	2.2	1.3	0.53
22-Aug-06	N	CRF #16	100.0	70.3	60.1		43.3	38.6	29.9		22.8		15.0		12.3	10.5	5.8	3.4	1.87
22-Aug-06	N	CRF #17	100.0	62.8	52.0		38.8	35.4	28.5		23.2		15.2		12.2	10.2	5.4	3.0	1.03
22-Aug-06	N	CRF #18	100.0	61.9	51.2		35.2	31.0	22.6		17.0		10.5		8.4	7.1	3.9	2.2	1.21
23-Aug-06	N	CRF #19	100.0	72.6	61.7		43.6	39.4	29.4		22.2		14.2		11.5	9.7	5.2	3.0	1.38
23-Aug-06	N	CRF #20	100.0	74.6	62.5		45.1	40.5	30.6		23.2		14.7		12.0	10.2	5.7	3.2	1.92
24-Aug-06	N	CRF #21	100.0	62.4	50.7		32.7	29.3	21.5		16.4		10.3		8.3	7.1	3.9	2.2	2.06
24-Aug-06	N	CRF #22	100.0	72.0	61.5		45.1	40.7	31.2		23.3		14.9		12.2	10.3	5.6	3.0	2.79
24-Aug-06	N	CRF #23	100.0	58.7	55.3		49.9	27.6	20.6		14.7		8.9		7.2	6.1	3.3	1.8	1.68
24-Aug-06	N	CRF #24	100.0	77.0	69.2		53.2	48.3	36.3		26.8		16.4		13.2	11.2	6.1	3.4	1.98
25-Aug-06	N	CRF #25	100.0	64.1	49.0		30.4	26.5	17.3		11.8		5.8		4.4	3.6	2.1	1.1	6.36
25-Aug-06	N	CRF #26	100.0	65.3	53.7		38.2	34.5	25.0		18.3		10.9		8.6	7.1	3.7	1.9	3.13
25-Aug-06	N	CRF #27	100.0	64.2	53.3		40.3	37.1	28.9		22.1		13.3		10.4	8.6	4.2	2.1	3.26
26-Aug-06	N	CRF #28	100.0	78.5	70.3		55.7	50.8	39.3		29.3		18.4		14.9	12.6	6.9	3.8	1.72
26-Aug-06	N	CRF #29	100.0	62.3	51.1		33.9	28.7	19.3		12.6		7.3		5.8	4.9	2.6	1.5	1.17
26-Aug-06	N	CRF #30	100.0	63.4	50.4		35.3	30.0	19.1		13.3		8.2		6.6	5.6	3.0	1.6	2.18
26-Aug-06	N	CRF #31	100.0	67.0	57.1		40.4	35.1	23.4		16.7		10.4		8.4	7.1	3.9	2.2	1.73
27-Aug-06	N	CRF #32	100.0	63.7	51.1		35.9	31.3	21.7		16.0		10.4		8.5	7.3	4.2	2.4	1.39
27-Aug-06	N	CRF #33	100.0	64.2	53.7		38.9	34.6	25.9		21.1		15.3		12.7	10.8	5.5	2.5	3.97
27-Aug-06	D	CRF #34	100.0	75.9	64.1		45.7	39.3	25.1		17.3		10.6		8.5	7.2	4.0	2.3	0.95
28-Aug-06	N	CRF #35	100.0	80.0	70.6		53.0	47.9	35.1		26.1		16.3		13.1	11.1	6.1	3.4	1.96
28-Aug-06	D	CRF #36	100.0	75.6	63.8		46.4	41.5	29.4		21.9		13.3		10.7	9.1	5.1	3.0	1.04
29-Aug-06	N	CRF #37	100.0	75.0	65.1		50.4	45.2	33.9		26.6		17.0		13.8	11.7	6.4	3.7	1.84
29-Aug-06	D	CRF #38	100.0	72.4	59.1		41.1	35.3	23.6		17.2		10.2		8.0	6.7	3.4	1.7	0.12
30-Aug-06	N	CRF #39	100.0	73.3	62.7		47.8	42.8	31.2		22.8		14.0		11.2	9.4	4.8	2.3	0.00
30-Aug-06	N	CRF #40	100.0	74.4	62.5		45.8	40.5	26.6		17.8		10.5		8.4	7.1	4.0	2.3	1.30
31-Aug-06	N	CRF #41	100.0	74.6	65.5		48.9	43.3	30.5		22.5		14.1		11.4	9.6	5.2	3.0	1.45
31-Aug-06	N	CRF #42	100.0	71.6	59.4		43.5	38.7	26.5		19.1		12.8		10.6	9.2	5.4	2.8	1.78
1-Sep-06	N	CRF #43	100.0	80.3	71.1		58.0	53.2	39.5		28.7		18.2		14.8	12.5	6.5	3.4	2.75
1-Sep-06	D	CRF #44	100.0	63.1	52.8		41.2	36.5	26.1		19.0		12.6		10.4	9.0	5.0	2.8	3.05
1-Sep-06	N	CRF #45	100.0	68.5	59.3		42.1	37.3	25.5		17.9		10.9		8.8	7.5	4.2	2.4	1.71
2-Sep-06	N	CRF #46	100.0	67.6	57.5		36.7	29.8	17.9		13.0		8.7		7.2	6.2	3.6	2.1	2.12
2-Sep-06	D	CRF #47	100.0	74.6	64.2		51.9	47.6	34.2		24.4		15.5		12.6	10.8	6.0	3.5	1.66
5-Sep-06	D	CRF #53	100.0	62.5	53.7		42.4	38.3	26.4		17.8		11.1		9.1	7.8	4.5	2.6	1.16
6-Sep-06	N	CRF #54	100.0	69.8	62.5		51.4	47.0	35.1		25.1		15.9		13.0	11.1	6.4	3.7	1.58
6-Sep-06	N	CRF #55	100.0	71.4	62.7		48.4	43.0	29.4		22.1		14.3		11.6	9.8	5.5	3.2	1.46
7-Sep-06	N	CRF #56	100.0	76.1	68.6		54.9	49.7	36.0		25.7		15.7		12.7	10.7	6.0	3.6	1.33
7-Sep-06	N	CRF #57	100.0	73.8	63.7		48.3	43.1	31.2		22.6		14.7		12.1	10.3	5.9	3.4	1.60
7-Sep-06	N	CRF #58	100.0	71.4	62.2		48.7	43.6	31.0		21.5		12.9		10.3	8.8	5.0	2.9	1.54
8-Sep-06	N	CRF #59	100.0	75.8	66.4		49.8	42.4	28.2		19.8		12.4		10.1	8.6	5.0	3.0	1.43
8-Sep-06	N	CRF #60	100.0	73.7	62.7		49.4	44.2	29.5		20.8		12.8		10.4	8.8	5.0	2.9	1.74
9-Sep-06	N	CRF #61	100.0	73.3	65.4		49.8	44.1	31.6		23.7		16.3		14.0	12.5	8.7	2.9	1.66
9-Sep-06	N	CRF #62	100.0	68.4	60.0		45.2	39.8	28.2		20.7		13.7		11.2	9.7	5.6	3.2	1.92
9-Sep-06	N	CRF #63	100.0	74.2	65.3		48.3	41.3	26.1		18.2		11.7		9.7	8.3	4.9	2.9	1.70
10-Sep-06	N	CRF #64	100.0	67.7	57.8		44.3	39.8	28.2		19.9		12.6		10.3	8.7	4.8	2.7	1.76
10-Sep-06	N	CRF #65	100.0	72.2	61.1		46.2	41.5	28.4		20.0		12.6		10.3	8.8	5.0	2.8	2.04
11-Sep-06	N	CRF #66	100.0	64.5	57.0		42.8	37.7	25.1		17.0		10.6		8.6	7.3	4.2	2.5	1.29
11-Sep-06	N	CRF #67	100.0	69.0	59.5		43.8	37.9	25.9		18.4		11.8		9.7	8.3	4.8	2.6	1.83
12-Sep-06	D	CRF #68	100.0	75.7	64.2		46.6	40.2	26.9		19.1		12.3		10.1	8.7	5.0	2.8	2.33
12-Sep-06	N	CRF #69	100.0	74.9	66.3		52.9	47.4	33.6		24.4		15.2		12.4	10.5	5.9	3.2	2.23
13-Sep-06	N	CRF #70	100.0	63.9	51.9		31.1	25.4	15.1		10.9		7.0		5.7	4.8	2.7	1.5	1.85
13-Sep-06	N	CRF #71	100.0	66.9	57.3		42.1	36.5	24.5		17.3		11.2		9.2	7.9	4.6	2.6	2.00
14-Sep-06	N	CRF #72	100.0	68.7	59.0		46.5	40.4	26.9		19.7		12.9		10.6	9.2	5.2	3.0	2.09
14-Sep-06	N	CRF #73	100.0	71.9	61.3		43.1	36.1	23.4		16.1		10.5		8.7	7.5	4.4	2.6	1.41
14-Sep-06	N	CRF #74	100.0	64.7	57.9		44.2	39.1	27.1		19.6		13.0		10.7	9.2	5.0	2.7	2.33
15-Sep-06	N	CRF #75	100.0	64.8	56.5		45.4	40.7	27.6		19.5		12.8		10.6	9.1	5.2	3.0	1.78
16-Sep-06	N	CRF #76	100.0	76.5	69.0		53.0	46.0	32.1		23.0		14.8		12.2	10.4	5.9	3.3	2.27

Table A.4 Grain size analysis and moisture content of CRF aggregate during preparation of CRF in 2007

Date	Sample	Shift	Sieve Size (mm)													Moisture (%)
			50	40	28	20	14	10	5	2.5	1.25	0.63	0.315	0.16	0.08	
11-Aug-07	CRF-15	D	100.0	91.4	67.6	51.4	40.5	33.8	24.3	19.1	15.3	11.6	8.5	5.8	3.8	1.6
12-Aug-07	CRF-16	D	100.0	96.5	79.5	65.6	53.6	46.0	33.9	26.3	21.0	15.8	11.4	7.7	5.0	1.7
12-Aug-07	CRF-17	N	100.0	95.4	81.7	68.3	55.9	47.4	33.1	26.7	21.1	15.6	11.0	7.2	4.5	1.6
13-Aug-07	CRF-18	D	100.0	92.0	67.4	50.1	38.8	31.5	21.4	16.7	13.2	9.7	6.6	4.0	2.1	1.2
14-Aug-07	CRF-19	D	100.0	89.4	64.9	42.7	31.2	24.6	16.9	13.5	10.9	8.2	5.7	3.6	2.1	0.7
14-Aug-07	CRF-20	N	100.0	92.8	67.6	51.1	38.9	31.6	21.6	17.2	13.5	9.8	6.7	4.0	2.1	0.9
15-Aug-07	CRF-21	D	100.0	96.6	72.7	57.9	46.7	38.0	26.7	20.8	16.4	12.1	8.4	5.3	2.9	0.9
15-Aug-07	CRF-22	N	100.0	88.9	65.5	51.6	42.3	35.4	24.4	19.6	15.4	11.3	7.9	5.0	2.9	1.1
16-Aug-07	CRF-23	D	100.0	89.9	56.9	38.7	29.0	22.5	14.4	10.8	8.3	6.1	4.1	2.3	1.0	0.5
16-Aug-07	CRF-24	D	100.0	95.0	79.8	66.7	55.5	46.7	33.9	27.1	21.1	15.3	10.5	6.6	3.7	1.1
24-Aug-07	CRF-25	N	100.0	91.2	70.0	56.0	46.0	38.2	26.2	20.8	16.2	11.8	8.2	5.2	3.0	0.5
24-Aug-07	CRF-26	D	100.0	96.7	82.5	69.5	57.1	48.1	32.8	25.8	19.8	14.4	10.0	6.5	3.9	2.1
25-Aug-07	CRF-27	N	100.0	88.7	69.7	55.7	45.4	38.1	26.9	20.7	16.1	11.7	8.1	4.9	2.6	0.9
25-Aug-07	CRF-28	D	100.0	96.4	78.2	66.1	54.8	46.5	32.7	25.3	19.4	13.8	9.1	5.2	2.3	1.2
26-Aug-07	CRF-29	N	100.0	91.1	68.5	56.1	46.2	38.9	26.8	23.7	17.3	12.5	8.0	6.1	2.8	1.1
26-Aug-07	CRF-30	D	100.0	92.6	67.3	54.0	43.6	35.9	24.9	18.4	13.8	9.4	5.6	2.4	0.0	1.1
27-Aug-07	CRF-31	N	100.0	94.0	77.9	61.7	49.1	40.3	27.6	21.2	16.6	12.0	8.1	4.8	2.3	1.1
27-Aug-07	CRF-32	D	100.0	92.7	63.2	43.5	32.8	25.9	17.4	13.2	10.3	7.5	5.0	2.9	1.3	0.9
28-Aug-07	CRF-33	N	100.0	96.1	77.4	64.0	53.9	46.4	35.1	27.6	21.5	15.6	10.7	6.7	3.7	1.4
28-Aug-07	CRF-34	D	100.0	95.1	73.0	55.4	45.2	37.5	26.0	19.6	15.0	10.6	7.0	3.8	1.4	1.1
29-Aug-07	CRF-35	D	100.0	93.5	72.2	56.3	45.2	37.5	26.0	19.6	15.1	10.7	7.0	3.9	1.5	1.0
2-Sep-07	CRF-36	N	100.0	94.4	70.0	52.3	40.0	32.6	21.9	16.8	13.1	9.6	6.6	4.1	2.2	0.9
2-Sep-07	CRF-37	D	100.0	95.1	76.1	62.2	52.3	45.5	32.5	25.9	20.6	15.2	10.6	6.6	3.7	1.1
3-Sep-07	CRF-38	N	100.0	95.6	75.8	60.5	49.6	41.0	28.8	20.7	15.8	11.0	6.9	4.3	2.3	1.1
3-Sep-07	CRF-39	D	100.0	90.0	62.4	44.6	34.5	27.4	18.2	13.6	10.6	7.8	5.4	3.2	1.4	0.8
4-Sep-07	CRF-40	N	100.0	92.2	69.9	56.0	46.0	38.1	26.4	20.7	16.2	11.8	8.1	4.9	2.6	1.0
8-Sep-07	CRF-41	N	100.0	97.6	80.1	65.3	54.6	46.1	32.6	25.3	19.8	14.4	9.8	6.1	3.3	1.3
9-Sep-07	CRF-42	N	100.0	97.9	81.0	65.0	52.7	44.3	31.3	25.0	19.6	14.4	9.9	6.1	3.3	1.2
11-Sep-07	CRF-43	N	100.0	94.7	77.6	60.3	49.1	41.3	29.9	23.2	18.2	13.3	9.1	5.5	2.8	1.1
12-Sep-07	CRF-44	N	100.0	93.2	76.7	62.4	51.8	43.7	31.7	25.3	19.7	14.3	9.8	6.1	3.4	1.1

Table A.5 Batch plant records of preparing cement slurry

Date	Time	Ticket No.	Water (kg)	Cement (kg)	w:c ratio
10-Jul-07	11:49 AM	17658	4,504	4,562	0.987
1-Aug-07	8:37 AM	17932	4,504	4,558	0.988
11-Aug-07	9:40 AM	18039	4,504	4,564	0.987
11-Aug-07	9:56 AM	18040	4,504	4,556	0.989
11-Aug-07	10:29 AM	18041	4,504	4,558	0.988
11-Aug-07	10:51 AM	18042	4,504	4,564	0.987
11-Aug-07	12:23 PM	18044	4,504	4,556	0.989
11-Aug-07	12:40 PM	18045	4,504	4,558	0.988
11-Aug-07	1:24 PM	18047	4,504	4,574	0.985
11-Aug-07	1:42 PM	18048	4,504	4,558	0.988
11-Aug-07	2:06 PM	18049	4,504	4,552	0.989
11-Aug-07	2:21 PM	18050	4,504	4,558	0.988
11-Aug-07	2:36 PM	18051	4,504	4,556	0.989
11-Aug-07	2:50 PM	18052	4,504	4,560	0.988
11-Aug-07	3:26 PM	18053	4,504	4,556	0.989
11-Aug-07	3:40 PM	18054	4,504	4,564	0.987
11-Aug-07	3:56 PM	18055	4,504	4,562	0.987
11-Aug-07	4:13 PM	18056	4,504	4,558	0.988
11-Aug-07	4:29 PM	18057	4,504	4,558	0.988
11-Aug-07	4:55 PM	18058	4,504	4,558	0.988
12-Aug-07	8:12 AM	18059	4,504	4,558	0.988
12-Aug-07	8:26 AM	18060	4,504	4,558	0.988
12-Aug-07	8:43 AM	18061	4,504	4,556	0.989
12-Aug-07	8:58 AM	18062	4,504	4,558	0.988
12-Aug-07	9:12 AM	18063	4,504	4,556	0.989
12-Aug-07	9:26 AM	18064	4,504	4,556	0.989
12-Aug-07	9:41 AM	18065	4,504	4,568	0.986
12-Aug-07	9:55 AM	18066	4,504	4,556	0.989
12-Aug-07	10:09 AM	18067	4,504	4,558	0.988
12-Aug-07	10:25 AM	18068	4,504	4,562	0.987
12-Aug-07	10:43 AM	18069	4,504	4,558	0.988
12-Aug-07	11:32 AM	18070	4,504	4,558	0.988
12-Aug-07	11:46 AM	18071	4,504	4,556	0.989
12-Aug-07	12:01 PM	18072	4,504	4,556	0.989
12-Aug-07	12:16 PM	18073	4,504	4,560	0.988
12-Aug-07	12:30 PM	18074	4,504	4,564	0.987
12-Aug-07	12:43 PM	18075	4,504	4,562	0.987
12-Aug-07	12:55 PM	18076	4,504	4,556	0.989
12-Aug-07	1:07 PM	18077	4,504	4,558	0.988
12-Aug-07	1:20 PM	18078	4,504	4,558	0.988
12-Aug-07	1:32 PM	18079	4,504	4,558	0.988
12-Aug-07	1:48 PM	18080	4,504	4,558	0.988
12-Aug-07	2:01 PM	18081	4,504	4,558	0.988
12-Aug-07	2:14 PM	18082	4,504	4,558	0.988
12-Aug-07	2:30 PM	18083	4,504	4,572	0.985
12-Aug-07	2:45 PM	18084	4,504	4,556	0.989
12-Aug-07	3:25 PM	18085	4,504	4,556	0.989
12-Aug-07	3:37 PM	18086	4,504	4,552	0.989
12-Aug-07	3:49 PM	18087	4,504	4,552	0.989
12-Aug-07	4:02 PM	18088	4,504	4,556	0.989
12-Aug-07	4:15 PM	18089	4,504	4,556	0.989
12-Aug-07	4:34 PM	18090	4,504	4,560	0.988
12-Aug-07	4:51 PM	18091	4,504	4,558	0.988
12-Aug-07	5:06 PM	18092	4,504	4,560	0.988
12-Aug-07	5:21 PM	18093	4,504	4,556	0.989
12-Aug-07	5:53 PM	18094	4,504	4,552	0.989

Table A.5 (Contd.) Batch plant records of preparing cement slurry

Date	Time	Ticket No.	Water (kg)	Cement (kg)	w:c ratio
12-Aug-07	6:07 PM	18095	4,504	4,556	0.989
12-Aug-07	6:29 PM	18096	4,504	4,556	0.989
12-Aug-07	6:46 PM	18097	4,504	4,554	0.989
12-Aug-07	7:04 PM	18098	4,504	4,560	0.988
12-Aug-07	7:22 PM	18099	4,504	4,560	0.988
12-Aug-07	7:44 PM	18100	4,504	4,564	0.987
12-Aug-07	8:02 PM	18101	4,504	4,558	0.988
12-Aug-07	8:42 PM	18102	4,504	4,552	0.989
12-Aug-07	9:04 PM	18103	4,504	4,554	0.989
12-Aug-07	9:24 PM	18104	4,504	4,554	0.989
12-Aug-07	9:46 PM	18105	4,504	4,550	0.990
12-Aug-07	10:51 PM	18106	4,504	4,560	0.988
13-Aug-07	12:11 AM	18107	4,504	4,560	0.988
13-Aug-07	12:26 AM	18108	4,504	4,562	0.987
13-Aug-07	12:48 AM	18109	4,504	4,560	0.988
13-Aug-07	1:11 AM	18110	4,504	4,558	0.988
13-Aug-07	1:31 AM	18111	4,504	4,558	0.988
13-Aug-07	1:52 AM	18112	4,504	4,558	0.988
13-Aug-07	2:13 AM	18113	4,504	4,560	0.988
13-Aug-07	2:29 AM	18114	4,504	4,558	0.988
13-Aug-07	3:17 AM	18115	4,504	4,558	0.988
13-Aug-07	4:11 AM	18116	4,504	4,552	0.989
13-Aug-07	4:38 AM	18117	4,504	4,558	0.988
13-Aug-07	4:54 AM	18118	4,504	4,554	0.989
13-Aug-07	5:15 AM	18119	4,504	4,558	0.988
13-Aug-07	5:32 AM	18120	4,504	4,556	0.989
13-Aug-07	5:57 AM	18121	4,504	4,560	0.988
13-Aug-07	6:16 AM	18122	4,504	4,560	0.988
13-Aug-07	6:48 AM	18123	4,504	4,558	0.988
13-Aug-07	7:04 AM	18124	4,504	4,558	0.988
13-Aug-07	7:32 AM	18125	4,504	4,558	0.988
13-Aug-07	7:44 AM	18126	4,504	4,562	0.987
13-Aug-07	8:08 AM	18127	4,504	4,558	0.988
13-Aug-07	8:20 AM	18128	4,504	4,562	0.987
13-Aug-07	8:34 AM	18129	4,504	4,554	0.989
13-Aug-07	8:48 AM	18130	4,504	4,560	0.988
13-Aug-07	9:01 AM	18131	4,504	4,558	0.988
13-Aug-07	9:14 AM	18132	4,504	4,562	0.987
13-Aug-07	9:26 AM	18133	4,504	4,554	0.989
13-Aug-07	9:39 AM	18134	4,504	4,564	0.987
13-Aug-07	9:53 AM	18135	4,504	4,552	0.989
13-Aug-07	10:05 AM	18136	4,504	4,556	0.989
13-Aug-07	10:18 AM	18137	4,504	4,558	0.988
13-Aug-07	10:31 AM	18138	4,504	4,560	0.988
13-Aug-07	11:24 AM	18139	4,504	4,556	0.989
13-Aug-07	11:36 AM	18140	4,504	4,552	0.989
13-Aug-07	11:48 AM	18141	4,504	4,562	0.987
13-Aug-07	12:01 PM	18142	4,504	4,560	0.988
13-Aug-07	12:13 PM	18143	4,504	4,552	0.989
13-Aug-07	12:25 PM	18144	4,504	4,558	0.988
13-Aug-07	12:37 PM	18145	4,504	4,560	0.988
13-Aug-07	12:49 PM	18146	4,504	4,566	0.986
13-Aug-07	1:01 PM	18147	4,504	4,560	0.988
13-Aug-07	1:13 PM	18148	4,504	4,564	0.987
13-Aug-07	1:26 PM	18149	4,504	4,558	0.988
13-Aug-07	1:38 PM	18150	4,504	4,556	0.989

Table A.5 (Contd.) Batch plant records of preparing cement slurry

Date	Time	Ticket No.	Water (w), kg	Cement (c), kg	w:c ratio
13-Aug-07	1:51 PM	18151	4,504	4,552	0.989
13-Aug-07	2:04 PM	18152	4,504	4,536	0.993
13-Aug-07	2:34 PM	18153	4,504	4,554	0.989
13-Aug-07	3:06 PM	18154	4,504	4,560	0.988
14-Aug-07	1:50 PM	18155	4,504	4,558	0.988
14-Aug-07	2:03 PM	18156	4,504	4,552	0.989
14-Aug-07	2:16 PM	18157	4,504	4,556	0.989
14-Aug-07	2:29 PM	18158	4,504	4,556	0.989
14-Aug-07	2:41 PM	18159	4,504	4,560	0.988
14-Aug-07	2:53 PM	18160	4,504	4,554	0.989
14-Aug-07	3:06 PM	18161	4,504	4,556	0.989
14-Aug-07	3:17 PM	18162	4,504	4,558	0.988
14-Aug-07	3:29 PM	18163	4,504	4,560	0.988
14-Aug-07	3:41 PM	18164	4,504	4,562	0.987
14-Aug-07	3:53 PM	18165	4,504	4,556	0.989
14-Aug-07	4:05 PM	18166	4,504	4,554	0.989
14-Aug-07	4:17 PM	18167	4,504	4,556	0.989
14-Aug-07	4:29 PM	18168	4,504	4,562	0.987
14-Aug-07	4:45 PM	18169	4,504	4,554	0.989
14-Aug-07	4:57 PM	18170	4,504	4,556	0.989
14-Aug-07	5:21 PM	18171	4,504	4,554	0.989
14-Aug-07	5:34 PM	18172	4,504	4,560	0.988
14-Aug-07	5:49 PM	18173	4,504	4,556	0.989
14-Aug-07	6:03 PM	18174	4,504	4,558	0.988
14-Aug-07	6:20 PM	18175	4,504	4,560	0.988
14-Aug-07	6:34 PM	18176	4,504	4,556	0.989
14-Aug-07	6:50 PM	18177	4,504	4,560	0.988
14-Aug-07	7:07 PM	18178	4,504	4,562	0.987
14-Aug-07	7:24 PM	18179	4,504	4,556	0.989
14-Aug-07	7:44 PM	18180	4,504	4,558	0.988
14-Aug-07	8:04 PM	18181	4,504	4,558	0.988
14-Aug-07	8:18 PM	18182	4,504	4,558	0.988
14-Aug-07	8:36 PM	18183	4,504	4,558	0.988
14-Aug-07	8:56 PM	18184	4,504	4,558	0.988
14-Aug-07	9:16 PM	18185	4,504	4,560	0.988
14-Aug-07	9:37 PM	18186	4,504	4,560	0.988
14-Aug-07	10:03 PM	18187	4,504	4,554	0.989
14-Aug-07	10:23 PM	18188	4,504	4,560	0.988
14-Aug-07	11:30 PM	18189	4,504	4,556	0.989
14-Aug-07	11:50 PM	18190	4,504	4,552	0.989
15-Aug-07	12:04 AM	18191	4,504	4,558	0.988
15-Aug-07	12:28 AM	18192	4,504	4,554	0.989
15-Aug-07	12:56 AM	18193	4,504	4,556	0.989
15-Aug-07	1:18 AM	18194	4,504	4,560	0.988
15-Aug-07	1:35 AM	18195	4,504	4,562	0.987
15-Aug-07	2:00 AM	18196	4,504	4,558	0.988
15-Aug-07	2:16 AM	18197	4,504	4,554	0.989
15-Aug-07	2:39 AM	18198	4,504	4,556	0.989
15-Aug-07	3:31 AM	18199	4,504	4,560	0.988
15-Aug-07	9:24 AM	18201	4,504	4,550	0.990
15-Aug-07	9:24 AM	18200	4,504	4,558	0.988
15-Aug-07	10:01 AM	18202	4,504	4,562	0.987
15-Aug-07	10:14 AM	18203	4,504	4,560	0.988
15-Aug-07	10:38 AM	18204	4,504	4,556	0.989
15-Aug-07	10:49 AM	18205	4,504	4,560	0.988
15-Aug-07	11:32 AM	18206	4,504	4,560	0.988

Table A.5 (Contd.) Batch plant records of preparing cement slurry

Date	Time	Ticket No.	Water (kg)	Cement (kg)	w:c ratio
15-Aug-07	11:47 AM	18207	4,504	4,554	0.989
15-Aug-07	12:02 PM	18208	4,504	4,554	0.989
15-Aug-07	12:16 PM	18209	4,504	4,552	0.989
15-Aug-07	12:34 PM	18210	4,504	4,558	0.988
15-Aug-07	12:46 PM	18211	4,504	4,562	0.987
15-Aug-07	1:05 PM	18212	4,504	4,556	0.989
15-Aug-07	1:16 PM	18213	4,504	4,560	0.988
15-Aug-07	1:44 PM	18214	4,504	4,556	0.989
15-Aug-07	1:57 PM	18215	4,504	4,560	0.988
15-Aug-07	2:19 PM	18216	4,504	4,558	0.988
15-Aug-07	2:35 PM	18217	4,504	4,558	0.988
15-Aug-07	3:20 PM	18218	4,504	4,554	0.989
15-Aug-07	3:35 PM	18219	4,504	4,556	0.989
15-Aug-07	3:50 PM	18220	4,504	4,554	0.989
15-Aug-07	4:03 PM	18221	4,504	4,556	0.989
15-Aug-07	4:22 PM	18222	4,504	4,558	0.988
15-Aug-07	4:33 PM	18223	4,504	4,552	0.989
15-Aug-07	8:22 PM	18224	4,504	4,556	0.989
15-Aug-07	8:52 PM	18225	4,504	4,554	0.989
15-Aug-07	9:09 PM	18226	4,504	4,556	0.989
15-Aug-07	9:30 PM	18227	4,504	4,558	0.988
15-Aug-07	10:09 PM	18228	4,504	4,562	0.987
16-Aug-07	12:16 AM	18229	4,504	4,558	0.988
16-Aug-07	12:56 AM	18230	4,504	4,554	0.989
16-Aug-07	1:31 AM	18231	4,504	4,560	0.988
16-Aug-07	2:06 AM	18232	4,504	4,560	0.988
16-Aug-07	2:42 AM	18233	4,504	4,552	0.989
16-Aug-07	3:51 AM	18234	4,504	4,556	0.989
16-Aug-07	4:33 AM	18235	4,504	4,562	0.987
16-Aug-07	5:06 AM	18236	4,504	4,556	0.989
16-Aug-07	5:45 AM	18237	4,504	4,556	0.989
16-Aug-07	6:23 AM	18238	4,504	4,554	0.989
16-Aug-07	6:58 AM	18239	4,504	4,556	0.989
16-Aug-07	7:42 AM	18240	4,504	4,554	0.989
16-Aug-07	8:22 AM	18241	4,504	4,556	0.989
16-Aug-07	9:05 AM	18242	4,504	4,554	0.989
16-Aug-07	9:47 AM	18243	4,504	4,560	0.988
16-Aug-07	11:43 AM	18244	4,504	4,556	0.989
16-Aug-07	12:35 PM	18245	4,504	4,554	0.989
16-Aug-07	1:15 PM	18246	4,504	4,556	0.989
16-Aug-07	1:32 PM	18247	4,504	4,556	0.989
16-Aug-07	1:53 PM	18248	4,504	4,560	0.988
16-Aug-07	2:09 PM	18249	4,504	4,558	0.988
16-Aug-07	2:28 PM	18250	4,504	4,504	1.000
16-Aug-07	3:21 PM	18252	4,504	4,554	0.989
16-Aug-07	3:36 PM	18253	4,504	4,556	0.989
16-Aug-07	4:00 PM	18254	4,504	4,554	0.989
16-Aug-07	4:31 PM	18256	4,504	4,558	0.988
16-Aug-07	4:46 PM	18257	4,504	4,504	1.000
16-Aug-07	5:20 PM	18259	4,504	4,558	0.988
16-Aug-07	5:37 PM	18260	4,504	4,558	0.988
16-Aug-07	6:01 PM	18261	4,504	4,556	0.989
24-Aug-07	8:16 AM	18345	4,504	4,558	0.988
24-Aug-07	8:51 AM	18347	4,504	4,564	0.987
24-Aug-07	9:06 AM	18348	4,504	4,558	0.988
24-Aug-07	9:32 AM	18349	4,504	4,556	0.989

Table A.5 (Contd.) Batch plant records of preparing cement slurry

Date	Time	Ticket No.	Water (kg)	Cement (kg)	w:c ratio
24-Aug-07	9:48 AM	18350	4,504	4,564	0.987
24-Aug-07	10:23 AM	18352	4,504	4,562	0.987
24-Aug-07	10:38 AM	18353	4,504	4,562	0.987
24-Aug-07	11:43 AM	18355	4,504	4,554	0.989
24-Aug-07	12:13 PM	18357	4,504	4,554	0.989
24-Aug-07	12:28 PM	18358	4,504	4,554	0.989
24-Aug-07	1:02 PM	18360	4,504	4,564	0.987
24-Aug-07	1:19 PM	18361	4,504	4,554	0.989
24-Aug-07	1:48 PM	18363	4,504	4,554	0.989
24-Aug-07	2:05 PM	18364	4,504	4,556	0.989
24-Aug-07	2:30 PM	18365	4,504	4,558	0.988
24-Aug-07	3:27 PM	18367	4,504	4,558	0.988
24-Aug-07	3:53 PM	18369	4,504	4,560	0.988
24-Aug-07	4:13 PM	18370	4504	4560	0.988
24-Aug-07	4:42 PM	18372	4,504	4,558	0.988
24-Aug-07	4:58 PM	18373	4,504	4,558	0.988
24-Aug-07	5:25 PM	18375	4,504	4,558	0.988
24-Aug-07	5:43 PM	18376	4,504	4,560	0.988
24-Aug-07	6:06 PM	18377	4,504	4,575	0.984
24-Aug-07	10:11 PM	18388	4,504	4,558	0.988
24-Aug-07	10:30 PM	18389	4,504	4,554	0.989
24-Aug-07	10:48 PM	18390	4,504	4,558	0.988
24-Aug-07	11:41 PM	18391	4,504	4,558	0.988
24-Aug-07	6:40 PM	18378	4,504	4,558	0.988
24-Aug-07	6:59 PM	18379	4,504	4,558	0.988
24-Aug-07	7:25 PM	18380	4,504	4,556	0.989
24-Aug-07	7:46 PM	18381	4,504	4,556	0.989
24-Aug-07	8:05 PM	18382	4,504	4,558	0.988
24-Aug-07	8:28 PM	18383	4,504	4,556	0.989
24-Aug-07	8:48 PM	18384	4,504	4,562	0.987
24-Aug-07	9:05 PM	18385	4,504	4,558	0.988
24-Aug-07	9:36 PM	18386	4,504	4,554	0.989
24-Aug-07	9:51 PM	18387	4,504	4,556	0.989
25-Aug-07	6:25 AM	18408	4,504	4,554	0.989
25-Aug-07	7:13 AM	18410	4,504	4,554	0.989
25-Aug-07	7:41 AM	18411	4,504	4,558	0.988
25-Aug-07	8:06 AM	18412	4,504	4,556	0.989
25-Aug-07	8:26 AM	18413	4,504	4,552	0.989
25-Aug-07	8:49 AM	18414	4,504	4,558	0.988
25-Aug-07	9:08 AM	18415	4,504	4,558	0.988
25-Aug-07	9:34 AM	18416	4,504	4,552	0.989
25-Aug-07	9:50 AM	18417	4,504	4,560	0.988
25-Aug-07	10:13 AM	18418	4,504	4,558	0.988
25-Aug-07	10:34 AM	18419	4,504	4,558	0.988
25-Aug-07	12:22 PM	18420	4,504	4,552	0.989
25-Aug-07	12:39 PM	18421	4,504	4,556	0.989
25-Aug-07	1:05 PM	18422	4,504	4,558	0.988
25-Aug-07	1:27 PM	18423	4,504	4,556	0.989
25-Aug-07	1:46 PM	18424	4,504	4,556	0.989
25-Aug-07	2:13 PM	18425	4,504	4,558	0.988
25-Aug-07	3:39 PM	18426	4,504	4,554	0.989
25-Aug-07	3:55 PM	18427	4,504	4,556	0.989
25-Aug-07	4:23 PM	18428	4,504	4,554	0.989
25-Aug-07	4:40 PM	18429	4,504	4,560	0.988
25-Aug-07	5:02 PM	18430	4,504	4,562	0.987
25-Aug-07	5:28 PM	18431	4,504	4,560	0.988

Table A.5 (Contd.) Batch plant records of preparing cement slurry

Date	Time	Ticket No.	Water (w), kg	Cement (c), kg	w:c ratio
25-Aug-07	5:46 PM	18432	4,504	4,558	0.988
25-Aug-07	6:17 PM	18433	4,504	4,560	0.988
25-Aug-07	6:33 PM	18434	4,504	4,556	0.989
25-Aug-07	1:11AM	18395	4,504	4,556	0.989
25-Aug-07	1:28 AM	18396	4,504	4,554	0.989
25-Aug-07	1:47 AM	18397	4,504	4,556	0.989
25-Aug-07	10:36 PM	18444	4,504	4,556	0.989
25-Aug-07	11:41 PM	18445	4,504	4,550	0.990
25-Aug-07	11:57 PM	18446	4,504	4,558	0.988
25-Aug-07	12:11AM	18392	4,504	4,554	0.989
25-Aug-07	12:28 AM	18393	4,504	4,556	0.989
25-Aug-07	12:47 AM	18394	4,504	4,558	0.988
25-Aug-07	2:04 AM	18398	4,504	4,560	0.988
25-Aug-07	2:23 AM	18399	4,504	4,550	0.990
25-Aug-07	2:41 AM	18400	4,504	4,554	0.989
25-Aug-07	3:57 AM	18401	4,504	4,558	0.988
25-Aug-07	4:22 AM	18402	4,504	4,556	0.989
25-Aug-07	4:38 AM	18403	4,504	4,558	0.988
25-Aug-07	4:57 AM	18404	4,504	4,554	0.989
25-Aug-07	5:16 AM	18405	4,504	4,558	0.988
25-Aug-07	5:35 AM	18406	4,504	4,556	0.989
25-Aug-07	6:01 AM	18407	4,504	4,556	0.989
25-Aug-07	6:55 AM	18409	4,504	4,558	0.988
25-Aug-07	6:58 PM	18435	4,504	4,560	0.988
25-Aug-07	7:22 PM	18436	4,504	4,554	0.989
25-Aug-07	7:47 PM	18437	4,504	4,570	0.986
25-Aug-07	8:08 PM	18438	4,504	4,560	0.988
25-Aug-07	8:27 PM	18439	4,504	4,554	0.989
25-Aug-07	8:54 PM	18440	4,504	4,560	0.988
25-Aug-07	9:38 PM	18442	4,504	4,558	0.988
25-Aug-07	9:55 PM	18443	4,504	4,556	0.989
26-Aug-07	6:54 AM	18461	4,504	4,556	0.989
26-Aug-07	7:27 AM	18462	4,504	4,556	0.989
26-Aug-07	8:07 AM	18498	4,504	4,552	0.989
26-Aug-07	8:11 AM	18464	4,504	4,554	0.989
26-Aug-07	8:28 AM	18465	4,504	4,558	0.988
26-Aug-07	9:00 AM	18466	4,504	4,556	0.989
26-Aug-07	9:17 AM	18467	4,504	4,556	0.989
26-Aug-07	9:48 AM	18468	4,504	4,554	0.989
26-Aug-07	10:26 AM	18470	4,504	4,554	0.989
26-Aug-07	10:43 AM	18471	4,504	4,560	0.988
26-Aug-07	11:40 AM	18473	4,504	4,548	0.990
26-Aug-07	12:20 PM	18476	4,504	4,548	0.990
26-Aug-07	12:54 PM	18478	4,504	4,560	0.988
26-Aug-07	1:10 PM	18479	4,504	4,558	0.988
26-Aug-07	1:53 PM	18482	4,504	4,560	0.988
26-Aug-07	2:33 PM	18484	4,504	4,554	0.989
26-Aug-07	3:44 PM	18487	4,504	4,552	0.989
26-Aug-07	4:11 PM	18489	4,504	4,554	0.989
26-Aug-07	4:29 PM	18490	4,504	4,558	0.988
26-Aug-07	5:21 PM	18493	4,504	4,554	0.989
26-Aug-07	1:18 AM	18449	4,504	4,552	0.989
26-Aug-07	1:37 AM	18450	4,504	4,556	0.989
26-Aug-07	10:01 PM	18502	4,504	4,556	0.989
26-Aug-07	10:35 PM	18503	4,504	4,558	0.988
26-Aug-07	11:50 PM	18504	4,504	4,556	0.989

Table A.5 (Contd.) Batch plant records of preparing cement slurry

Date	Time	Ticket No.	Water (kg)	Cement (kg)	w:c ratio
26-Aug-07	12:32 AM	18447	4,504	4,556	0.989
26-Aug-07	12:48 AM	18448	4,504	4,558	0.988
26-Aug-07	2:11 AM	18451	4,504	4,554	0.989
26-Aug-07	2:29 AM	18452	4,504	4,560	0.988
26-Aug-07	3:40 AM	18453	4,504	4,550	0.990
26-Aug-07	4:00 AM	18454	4,504	4,556	0.989
26-Aug-07	4:33 PM	18456	4,504	4,556	0.989
26-Aug-07	4:50 AM	18457	4,504	4,560	0.988
26-Aug-07	5:27 AM	18458	4,504	4,558	0.988
26-Aug-07	5:56 AM	18459	4,504	4,558	0.988
26-Aug-07	6:31 AM	18460	4,504	4,558	0.988
26-Aug-07	7:08 PM	18495	4,504	4,548	0.990
26-Aug-07	7:49 PM	18497	4,504	4,556	0.989
26-Aug-07	8:43 PM	18499	4,504	4,556	0.989
26-Aug-07	9:12 PM	18500	4,504	4,564	0.987
26-Aug-07	9:40 PM	18501	4,504	4,558	0.988
27-Aug-07	7:19 AM	18520	4,504	4,556	0.989
27-Aug-07	7:37 AM	18521	4,504	4,560	0.988
27-Aug-07	8:10 AM	18522	4,504	4,560	0.988
27-Aug-07	8:27 AM	18523	4,504	4,552	0.989
27-Aug-07	9:07 AM	18525	4,504	4,556	0.989
27-Aug-07	9:39 AM	18526	4,504	4,556	0.989
27-Aug-07	10:16 AM	18527	4504	4558	0.988
27-Aug-07	11:50 AM	18529	4,504	4,550	0.990
27-Aug-07	12:08 PM	18530	4,504	4,562	0.987
27-Aug-07	12:25 PM	18531	4,504	4,554	0.989
27-Aug-07	12:45 PM	18532	4,504	4,564	0.987
27-Aug-07	1:10 PM	18533	4,504	4,558	0.988
27-Aug-07	1:29 PM	18534	4,504	4,554	0.989
27-Aug-07	1:46 PM	18535	4,504	4,556	0.989
27-Aug-07	2:05 PM	18536	4,504	4,556	0.989
27-Aug-07	2:34 PM	18538	4,504	4,554	0.989
27-Aug-07	3:28 PM	18539	4,504	4,556	0.989
27-Aug-07	4:24 PM	18541	4,504	4,558	0.988
27-Aug-07	5:14 PM	18542	4,504	4,558	0.988
27-Aug-07	1:16 AM	18508	4,504	4,552	0.989
27-Aug-07	10:11 PM	18549	4,504	4,556	0.989
27-Aug-07	10:41 PM	18550	4,504	4,554	0.989
27-Aug-07	11:46 PM	18551	4,504	4,558	0.988
27-Aug-07	12:05 AM	18505	4,504	4,554	0.989
27-Aug-07	12:33 AM	18506	4,504	4,554	0.989
27-Aug-07	12:53 AM	18507	4,504	4,560	0.988
27-Aug-07	2:27 AM	18509	4,504	4,554	0.989
27-Aug-07	2:43 AM	18510	4,504	4,558	0.988
27-Aug-07	3:32 AM	18511	4,504	4,556	0.989
27-Aug-07	3:48 AM	18512	4,504	4,552	0.989
27-Aug-07	4:24 AM	18513	4,504	4,556	0.989
27-Aug-07	4:40 AM	18514	4,504	4,560	0.988
27-Aug-07	5:08 AM	18515	4,504	4,556	0.989
27-Aug-07	5:24 AM	18516	4,504	4,560	0.988
27-Aug-07	5:47 AM	18517	4,504	4,556	0.989
27-Aug-07	6:24 AM	18518	4,504	4,558	0.988
27-Aug-07	6:44 AM	18519	4,504	4,558	0.988
27-Aug-07	8:08 PM	18544	4,504	4,556	0.989
27-Aug-07	8:23 PM	18545	4,504	4,554	0.989
27-Aug-07	8:56 PM	18546	4,504	4,554	0.989

Table A.5 (Contd.) Batch plant records of preparing cement slurry

Date	Time	Ticket No.	Water (w), kg	Cement (c), kg	w:c ratio
27-Aug-07	9:14 PM	18547	4,504	4,538	0.993
27-Aug-07	9:54 PM	18548	4,504	4,554	0.989
28-Aug-07	6:59 AM	18566	4,504	4,552	0.989
28-Aug-07	7:37 AM	18567	4,504	4,556	0.989
28-Aug-07	7:56 AM	18568	4,504	4,554	0.989
28-Aug-07	8:45 AM	18570	4,504	4,552	0.989
28-Aug-07	9:11 AM	18571	4,504	4,558	0.988
28-Aug-07	9:35 AM	18572	4,504	4,558	0.988
28-Aug-07	9:56 AM	18573	4,504	4,554	0.989
28-Aug-07	10:20 AM	18574	4,504	4,558	0.988
28-Aug-07	10:53 AM	18576	4,504	4,556	0.989
28-Aug-07	12:00 PM	18577	4,504	4,556	0.989
28-Aug-07	1:12 PM	18580	4,504	4,558	0.988
28-Aug-07	1:52 PM	18581	4,504	4,554	0.989
28-Aug-07	2:39 PM	18582	4,504	4,556	0.989
28-Aug-07	3:17 PM	18584	4,504	4,556	0.989
28-Aug-07	4:07 PM	18586	4,504	4,562	0.987
28-Aug-07	4:25 PM	18587	4,504	4,558	0.988
28-Aug-07	5:09 PM	18589	4,504	4,554	0.989
28-Aug-07	5:25 PM	18590	4,504	4,556	0.989
28-Aug-07	5:56 PM	18591	4,504	4,556	0.989
28-Aug-07	6:12 PM	18592	4,504	4,558	0.988
28-Aug-07	1:07AM	18555	4,504	4,560	0.988
28-Aug-07	1:38 AM	18556	4,504	4,558	0.988
28-Aug-07	1:53 AM	18557	4,504	4,560	0.988
28-Aug-07	10:23 PM	18603	4,504	4,556	0.989
28-Aug-07	11:51 PM	18604	4,504	4,558	0.988
28-Aug-07	12:01 AM	18552	4,504	4,554	0.989
28-Aug-07	12:24 AM	18553	4,504	4,558	0.988
28-Aug-07	12:52 AM	18554	4,504	4,556	0.989
28-Aug-07	2:14 AM	18558	4,504	4,554	0.989
28-Aug-07	2:31AM	18559	4,504	4,558	0.988
28-Aug-07	3:34 AM	18560	4,504	4,560	0.988
28-Aug-07	3:52 AM	18561	4,504	4,558	0.988
28-Aug-07	4:24 AM	18562	4,504	4,560	0.988
28-Aug-07	4:40 AM	18563	4,504	4,556	0.989
28-Aug-07	5:11AM	18564	4,504	4,556	0.989
28-Aug-07	5:29 AM	18565	4,504	4,558	0.988
28-Aug-07	7:02 PM	18593	4,504	4,556	0.989
28-Aug-07	7:17 PM	18594	4,504	4,556	0.989
28-Aug-07	7:56 PM	18595	4,504	4,552	0.989
28-Aug-07	8:25 PM	18597	4,504	4,550	0.990
28-Aug-07	8:44 PM	18598	4,504	4,554	0.989
28-Aug-07	9:10 PM	18599	4,504	4,556	0.989
28-Aug-07	9:38 PM	18601	4,504	4,560	0.988
28-Aug-07	9:53 PM	18602	4,504	4,554	0.989
29-Aug-07	7:51 AM	18613	4,504	4,558	0.988
29-Aug-07	8:38 AM	18615	4,504	4,550	0.990
29-Aug-07	9:30 AM	18617	4,504	4,556	0.989
29-Aug-07	10:16 AM	18619	4,504	4,556	0.989
29-Aug-07	11:11 AM	18621	4,504	4,560	0.988
29-Aug-07	12:13 PM	18623	4,504	4,556	0.989
29-Aug-07	1:13 PM	18626	4,504	4,558	0.988
29-Aug-07	1:17AM	18608	4,504	4,552	0.989
29-Aug-07	1:44 AM	18609	4,504	4,558	0.988
29-Aug-07	12:16 AM	18605	4,504	4,554	0.989

Table A.5 (Contd.) Batch plant records of preparing cement slurry

Date	Time	Ticket No.	Water (kg)	Cement (kg)	w:c ratio
29-Aug-07	12:38 AM	18606	4,504	4,556	0.989
29-Aug-07	12:59 AM	18607	4,504	4,562	0.987
29-Aug-07	2:13 AM	18610	4,504	4,554	0.989
29-Aug-07	2:39 AM	18611	4,504	4,560	0.988
29-Aug-07	4:01 AM	18612	4,504	4,550	0.990
2-Sep-07	8:27 AM	18643	4,504	4,558	0.988
2-Sep-07	9:26 AM	18646	4,504	4,560	0.988
2-Sep-07	10:16 AM	18649	4,504	4,560	0.988
2-Sep-07	11:06 AM	18652	4,504	4,556	0.989
2-Sep-07	12:07 PM	18654	4,504	4,556	0.989
2-Sep-07	1:07 PM	18657	4,504	4,552	0.989
2-Sep-07	2:05 PM	18661	4,504	4,554	0.989
2-Sep-07	2:55 PM	18664	4,504	4,560	0.988
2-Sep-07	4:01 PM	18667	4,504	4,560	0.988
2-Sep-07	5:05 PM	18670	4,504	4,554	0.989
2-Sep-07	10:21 PM	18680	4,504	4,562	0.987
2-Sep-07	11:42 PM	18681	4,504	4,550	0.990
2-Sep-07	11:59 PM	18682	4,504	4,558	0.988
2-Sep-07	7:37 PM	18673	4,504	4,558	0.988
2-Sep-07	8:21PM	18674	4,504	4,550	0.990
2-Sep-07	8:37PM	18675	4,504	4,558	0.988
2-Sep-07	9:04 PM	18676	4,504	4,554	0.989
2-Sep-07	9:21 PM	18677	4,504	4,558	0.988
2-Sep-07	9:41 PM	18678	4,504	4,556	0.989
2-Sep-07	9:58 PM	18679	4,504	4,558	0.988
3-Sep-07	7:36 AM	18694	4,504	4,562	0.987
3-Sep-07	8:23 AM	18697	4,504	4,558	0.988
3-Sep-07	9:14 AM	18699	4,504	4,554	0.989
3-Sep-07	9:59 AM	18701	4,504	4,556	0.989
3-Sep-07	10:49 AM	18703	4,504	4,558	0.988
3-Sep-07	11:32 AM	18704	4,504	4,562	0.987
3-Sep-07	12:22 PM	18706	4,504	4,552	0.989
3-Sep-07	12:44 PM	18707	4,504	4,560	0.988
3-Sep-07	1:12 PM	18709	4,504	4,564	0.987
3-Sep-07	1:39 PM	18711	4,504	4,556	0.989
3-Sep-07	2:06 PM	18713	4,504	4,558	0.988
3-Sep-07	3:48 PM	18716	4,504	4,556	0.989
3-Sep-07	4:18 PM	18718	4,504	4,558	0.988
3-Sep-07	4:43 PM	18720	4,504	4,556	0.989
3-Sep-07	4:59 PM	18721	4,528	4,560	0.993
3-Sep-07	1:19 AM	18686	4,504	4,560	0.988
3-Sep-07	1:36 AM	18687	4,504	4,556	0.989
3-Sep-07	1:54 AM	18688	4,504	4,558	0.988
3-Sep-07	10:18 PM	18730	4,504	4,558	0.988
3-Sep-07	11:51 PM	18731	4,504	4,552	0.989
3-Sep-07	12:59 AM	18685	4,504	4,562	0.987
3-Sep-07	12:19 AM	18683	4,504	4,552	0.989
3-Sep-07	12:42 AM	18684	4,504	4,554	0.989
3-Sep-07	2:14 AM	18689	4,504	4,564	0.987
3-Sep-07	2:31 AM	18690	4,504	4,560	0.988
3-Sep-07	3:40 AM	18691	4,504	4,552	0.989
3-Sep-07	4:18 AM	18692	4,504	4,558	0.988
3-Sep-07	5:04 AM	18693	4,504	4,554	0.989
3-Sep-07	8:24 PM	18724	4,504	4,560	0.988
3-Sep-07	8:39 PM	18725	4,504	4,560	0.988
3-Sep-07	8:58 PM	18726	4,504	4,552	0.989

Table A.5 (Contd.) Batch plant records of preparing cement slurry

Date	Time	Ticket No.	Water (kg)	Cement (kg)	w:c ratio
3-Sep-07	9:20 PM	18727	4,504	4,556	0.989
3-Sep-07	9:51 PM	18729	4,504	4,560	0.988
4-Sep-07	7:18 AM	18743	4,504	4,558	0.988
4-Sep-07	7:34 AM	18744	4,504	4,560	0.988
4-Sep-07	8:06 AM	18745	4,504	4,550	0.990
4-Sep-07	8:23 AM	18746	4,504	4,556	0.989
4-Sep-07	8:50 AM	18747	4,504	4,560	0.988
4-Sep-07	9:05 AM	18748	4,504	4,554	0.989
4-Sep-07	9:31 AM	18749	4,504	4,558	0.988
4-Sep-07	9:49 AM	18750	4,504	4,558	0.988
4-Sep-07	10:15 AM	18751	4,504	4,558	0.988
4-Sep-07	10:28 AM	18752	4,504	4,560	0.988
4-Sep-07	10:58 AM	18753	4,504	4,560	0.988
4-Sep-07	11:11 AM	18754	4,504	4,556	0.989
4-Sep-07	11:39 AM	18755	4,504	4,560	0.988
4-Sep-07	12:01 PM	18756	4,504	4,552	0.989
4-Sep-07	12:22 PM	18757	4,504	4,554	0.989
4-Sep-07	12:39 PM	18758	4,504	4,558	0.988
4-Sep-07	1:17 PM	18760	4,504	4,554	0.989
4-Sep-07	1:31 PM	18761	4,504	4,558	0.988
4-Sep-07	1:59 PM	18763	4,504	4,550	0.990
4-Sep-07	2:27 PM	18765	4,504	4,560	0.988
4-Sep-07	2:54 PM	18767	4,504	4,556	0.989
4-Sep-07	3:06 PM	18768	4,504	4,554	0.989
4-Sep-07	3:38 PM	18770	4,504	4,558	0.988
4-Sep-07	4:09 PM	18771	4,504	4,556	0.989
4-Sep-07	4:28 PM	18772	4,504	4,556	0.989
4-Sep-07	4:44 PM	18773	4,504	4,558	0.988
4-Sep-07	1:23 AM	18735	4,504	4,562	0.987
4-Sep-07	1:52 AM	18736	4,504	4,552	0.989
4-Sep-07	12:07 AM	18732	4,504	4,554	0.989
4-Sep-07	12:26 AM	18733	4,504	4,558	0.988
4-Sep-07	12:55 AM	18734	4,504	4,572	0.985
4-Sep-07	2:19 AM	18737	4,504	4,556	0.989
4-Sep-07	3:35 AM	18738	4,504	4,550	0.990
4-Sep-07	3:51 AM	18739	4,504	4,556	0.989
4-Sep-07	4:27 AM	18740	4,504	4,562	0.987
4-Sep-07	4:42 AM	18741	4,504	4,554	0.989
4-Sep-07	5:12 AM	18742	4,504	4,556	0.989
8-Sep-07		18854	4504	4556	0.989
9-Sep-07		18876	4,504	4096	1.100
11-Sep-07		18955	4,504	4094	1.100
11-Sep-07		18936	4,504	4094	1.100
12-Sep-07		18979	4,504	4092	1.101
13-Sep-07		19001	4,504	4094	1.100
13-Sep-07		18997	4,504	4092	1.101
15-Sep-07		19057	4,504	4092	1.101
15-Sep-07		19049	4,504	4094	1.100

Table A.6 Test results of specific gravity of cement slurry

Date	Shift	Ticket No.	Water (kg)	Cement (kg)	w:c ratio	Specific Gravity
12-Aug-07	D	18087	4504	4552	0.989	1.525
12-Aug-07	D	18097	4504	4552	0.989	1.520
12-Aug-07	N	18108	4504	4562	0.987	1.490
12-Aug-07	N	18115	4504	4553	0.989	1.510
13-Aug-07	D	18138	4504	4560	0.988	1.520
14-Aug-07	D	18159	4504	4560	0.988	1.521
14-Aug-07	D	18168	4504	4562	0.987	1.530
14-Aug-07	N	18186	4504	4560	0.988	1.530
14-Aug-07	N	18196	4504	4558	0.988	1.470
15-Aug-07	D	18209	4504	4552	0.989	1.529
15-Aug-07	D	18223	4504	4552	0.989	1.524
15-Aug-07	N	18231	4504	4560	0.988	1.489
15-Aug-07	N	18235	4504	4560	0.988	1.491
16-Aug-07	D	18243	4504	4560	0.988	1.502
16-Aug-07	D	18254	4504	4554	0.989	1.520
24-Aug-07	D	18355	4504	4554	0.989	1.520
24-Aug-07	D	18372	4504	4556	0.988	1.530
24-Aug-07	N	18382	4504	4558	0.988	1.510
24-Aug-07	N	18398	4504	4558	0.988	1.520
25-Aug-07	D	18417	4504	4560	0.988	1.530
25-Aug-07	D	18429	4504	4560	0.988	1.520
25-Aug-07	N	18437	4504	4570	0.986	1.530
25-Aug-07	N	18450	4504	4556	0.989	1.540
26-Aug-07	D	18464	4504	4552	0.989	1.520
26-Aug-07	D	18493	4504	4554	0.989	1.510
26-Aug-07	N	18498	4504	4552	0.989	1.510
26-Aug-07	N	18512	4504	4552	0.989	1.520
27-Aug-07	D	18523	4504	4552	0.989	1.530
27-Aug-07	D	18542	4504	4558	0.988	1.530
27-Aug-07	N	18554	4504	4556	0.989	1.510
27-Aug-07	N	18561	4504	4558	0.988	1.520
28-Aug-07	D	18571	4504	4558	0.988	1.530
28-Aug-07	D	18586	4504	4562	0.987	1.510
28-Aug-07	N	18595	4504	4552	0.989	1.530
28-Aug-07	N	18608	4504	4552	0.989	1.530
29-Aug-07	D	18619	4504	4556	0.989	1.510
2-Sep-07	D	18619	4504	4552	0.989	1.520
2-Sep-07	D	18670	4504	4554	0.989	1.530
2-Sep-07	N	18676	4504	4554	0.989	1.530
2-Sep-07	N	18692	4504	4558	0.988	1.520
3-Sep-07	D	18716	4504	4556	0.989	1.530
3-Sep-07	N	18733	4504	4552	0.989	1.520
3-Sep-07	N	18738	4504	4550	0.990	1.530
4-Sep-07	D	18754	4504	4556	0.989	1.520
4-Sep-07	D	18767	4504	4556	0.989	1.530
8-Sep-07	N	18854	4504	4556	0.989	1.520
9-Sep-07	N	18876	4504	4096	1.100	1.480
11-Sep-07	N	18936	4504	4094	1.100	1.480
11-Sep-07	N	18955	4504	4094	1.100	1.480
12-Sep-07	N	18979	4504	4092	1.101	1.500
13-Sep-07	N	18997	4504	4092	1.101	1.490
13-Sep-07	N	19001	4504	4094	1.100	1.470
15-Sep-07	N	19049	4504	4094	1.100	1.490
15-Sep-07	N	19057	4504	4092	1.101	1.480

Table A.7 In situ and laboratory results of CRF with aggregate sieve sample number during placement of CRF

Placement Date	Shift	Aggregate Sieve Sample No.	In-situ Results from Troxler						Laboratory			CRF Cylinders						
			Density Test No.	Wet Density (kg/m <sup>3</sup> )	Dry Density (kg/m <sup>3</sup> )	Moisture Content MC (%)	Calculated Void Ratio	Porosity (%)	MC of CRF (%)	In-situ Dry Density (Lab MC Corrected) (kg/m <sup>3</sup> )	MC of CRF (%) (minus 25 mm)	Cylinder No.	Wet Density (kg/m <sup>3</sup> )	Dry Density (kg/m <sup>3</sup> )	Curing Time (Days)	UCS Test Date	UCS (MPa)	Dia (mm)
11-Aug-07	D	CRF-15	D-01	2360	2149	9.8	0.256	20.4	9.2	2161	8.8	CRF-01	2374	2182	3	14-Aug-07	3.80	100
			CRF-02	2341	2151	3	14-Aug-07	3.60										
			CRF-03	2356	2165	7	18-Aug-07	5.80										
			D-02	2289	2106	8.7	0.282	22.0										
			D-03	2351	2203	6.7	0.225	18.4	6.9	2199								
			D-04	2352	2184	7.7	0.236	19.1										
12-Aug-07	D	CRF-16	D-05	2352	2184	7.7	0.236	19.1			8.5	CRF-04	2376	2190	7	18-Aug-07	6.70	
			CRF-05	2375	2189	28	8-Sep-07	11.40										
			D-01	2354	2134	10.3	0.265	21.0	6.4	2212	10.5	CRF-06	2357	2133	3	15-Aug-07	4.30	
			D-02	2098	1952	7.5	0.383	27.7	6.8	1964	9.0	CRF-07	2372	2177	3	15-Aug-07	5.00	
			D-03	2327	2151	8.2	0.255	20.3	8.2	2151	8.6	CRF-08	2391	2202	7	19-Aug-07	3.50	
			D-04	2353	2153	9.3	0.254	20.3	7.1	2197	10.6	CRF-09	2395	2165	7	19-Aug-07	7.50	
	N	CRF-17	D-05	2327	2159	7.8	0.251	20.1	7.8	2159	8.3	CRF-10	2395	2212	28	9-Sep-07	11.20	
			D-06	2339	2146	9	0.258	20.5	7.5	2176	8.7	CRF-11	2351	2163	3	15-Aug-07	4.60	
			D-07	2374	2219	7	0.217	17.8	6.1	2238	8.3	CRF-12	2364	2183	3	15-Aug-07	4.70	
			D-08	2358	2220	6.2	0.216	17.8	5.9	2227	10.9	CRF-13	2343	2113	7	19-Aug-07	7.80	
13-Aug-07	D	CRF-18	D-09	2211	2084	6.1	0.296	22.8	6.2	2082	7.4	CRF-14	2386	2222	7	19-Aug-07	7.80	
			D-10	2352	2194	7.2	0.231	18.7	7.0	2198	5.0	CRF-15	2353	2241	28	9-Sep-07	9.20	
			D-01	2270	2090	8.6	0.292	22.6	6.0	2142	7.8	CRF-16	2382	2210	3	16-Aug-07	4.60	
			D-02	2326	2144	8.5	0.259	20.6	6.3	2188	8.9	CRF-17	2348	2156	3	16-Aug-07	3.70	
14-Aug-07	D	CRF-19	D-03	2256	2151	4.9	0.255	20.3	6.8	2112	8.3	CRF-18	2375	2193	7	20-Aug-07	7.50	
			D-04	2109	1993	5.8	0.354	26.2	6.2	1986	8.4	CRF-19	2364	2181	28	10-Sep-07	10.00	
			D-01	2261	2101	7.6	0.285	22.2	7.2	2109	9.0	CRF-20	2392	2194	3	17-Aug-07	3.80	
			CRF-21	2393	2195	3	17-Aug-07	3.70										
	N	CRF-20	D-02	2072	1924	7.7	0.403	28.7	6.1	1953	7.3	CRF-22	2338	2179	7	21-Aug-07	7.10	
			CRF-23	2389	2227	7	21-Aug-07	7.30										
			CRF-24	2351	2191	28	11-Sep-07	11.60										
			D-03	2171	2078	4.5	0.300	23.1	5.8	2052	6.8	CRF-25	2344	2195	3	17-Aug-07	5.63	
			D-04	2302	2172	6	0.243	19.6	7.3	2145	9.2	CRF-26	2336	2139	3	17-Aug-07	4.36	
			D-05	2302	2186	5.3	0.235	19.0	7.4	2143	9.8	CRF-27	2354	2144	7	21-Aug-07	7.40	
15-Aug-07	D	CRF-21	D-06	2330	2159	7.9	0.250	20.0	7.0	2178	10.2	CRF-28	2330	2114	7	21-Aug-07	6.10	
			D-07	2334	2183	6.9	0.237	19.1	7.6	2169	10.3	CRF-29	2336	2118	28	11-Sep-07	13.00	
			D-01	2344	2152	8.9	0.254	20.3	6.2	2207	11.6	CRF-30	2324	2082	3	18-Aug-07	4.00	
			D-02	2356	2173	8.4	0.242	19.5										
D-03	2213	2072	6.8	0.303	23.3	7.0	2068	10.9	CRF-31	2330	2101	3	18-Aug-07	4.20				
D-04	2330	2174	7.2	0.242	19.5													

Table A.7 (Contd) In situ & laboratory results of CRF with aggregate sieve sample number during placement of CRF

Placement Date	Shift	Aggregate Sieve Sample No.	In-situ Results from Troxler					Laboratory				CRF Cylinders							
			Density Test No.	Wet Density (kg/m <sup>3</sup> )	Dry Density (kg/m <sup>3</sup> )	Moisture Content MC (%)	Calculated Void Ratio	Porosity (%)	MC of CRF (%)	In-situ Dry Density (Lab MC Corrected) (kg/m <sup>3</sup> )	MC of CRF (%) (minus 25 mm)	Cylinder No.	Wet Density (kg/m <sup>3</sup> )	Dry Density (kg/m <sup>3</sup> )	Curing Time (Days)	UCS Test Date	UCS (MPa)	Dia (mm)	
15-Aug-07	D	CRF-21	D-05	2187	2014	8.6	0.341	25.4	7.5	2034	9.8	CRF-32	2340	2131	7	22-Aug-07	6.10	100	
			D-06	2073	1999	3.7	0.351	26.0	7	1937	7.8	CRF-33	2331	2123	7	22-Aug-07	6.50		
			D-07	2313	2124	8.9	0.271	21.3					CRF-34	2372	2201	28	12-Sep-07		12.80
	N	CRF-22	D-01	2298	2146	7.1	0.258	20.5	7.6	2136	12.4	CRF-35	2347	2088	3	18-Aug-07	2.80		
			D-02	2354	2186	7.7	0.235	19.0	6.7	2206	9.2	CRF-36	2332	2136	3	18-Aug-07	3.70		
			D-03	2297	2179	5.4	0.239	19.3	6.6	2155	8.9	CRF-37	2369	2175	7	22-Aug-07	8.10		
			D-04	2260	2068	9.3	0.306	23.4	7.2	2108	11.4	CRF-38	2326	2088	7	22-Aug-07	6.40		
			D-05	2242	2091	7.2	0.291	22.5	6.4	2107	9.2	CRF-39	2351	2153	28	12-Sep-07	14.60		
			D-01	2284	2157	5.9	0.252	20.1	7.0	2135	8.4	CRF-40	2387	2202	3	19-Aug-07	4.70		
16-Aug-07	D	CRF-23, 24	D-02	2319	2139	8.4	0.262	20.8	5.4	2200	8.5	CRF-41	2389	2202	3	19-Aug-07	5.50		
			D-03	2279	2177	4.7	0.240	19.4				CRF-42	2402	2213	7	23-Aug-07	6.60		
			D-04	2183	2057	6.1	0.312	23.8	7.3	2034		CRF-43	2361	2176	7	23-Aug-07	7.20		
			D-05	2319	2141	8.3	0.261	20.7	6.1	2186		7.4	CRF-44	2381	2217	28	13-Sep-07		10.80
			D-01	2171	2100	3.4	0.286	22.2											
24-Aug-07	D	CRF-25	D-02	2101	1980	6.1	0.363	26.7	4.5	2011	7.1	CRF-45	2240	2092	3	27-Aug-07	3.30		
												CRF-46	2216	2069	3	27-Aug-07	3.60		
			D-03	2301	2133	7.9	0.266	21.0	6.7	2157	10.7	CRF-47	2364	2136	7	31-Aug-07	7.80		
			D-04	2213	2080	6.4	0.298	23.0	7.1	2066	9.1	CRF-48	2364	2136	7	31-Aug-07	8.10		
	N	CRF-26	D-01	2334	2169	7.6	0.245	19.7	7.2	2177	8.2	CRF-49	2329	2135	28	21-Sep-07	4.50		
												CRF-50	2353	2175	3	27-Aug-07	4.60		
			D-02	2332	2141	8.9	0.261	20.7	8.3	2153	8.6	CRF-51	2377	2197	3	27-Aug-07	4.60		
				2332	2141	8.9	0.261	20.7	8.3	2153		CRF-52	2373	2185	7	31-Aug-07	8.00		
				2332	2141	8.9	0.261	20.7	8.3	2153		CRF-53	2367	2180	7	31-Aug-07	7.50		
			D-03	2311	2170	6.5	0.244	19.6	7.9	2142		9.7	CRF-54	2361	2152	28	21-Sep-07	9.60	
25-Aug-07	D	CRF-27	D-01	2174	2051	6	0.316	24.0	6.6	2039	9.6	CRF-55	2330	2126	3	28-Aug-07	4.30		
				2174	2051	6	0.316	24.0	6.6	2039		CRF-56	2345	2139	3	28-Aug-07	4.60		
				2174	2051	6	0.316	24.0	6.6	2039		CRF-65	2315	2112	3	28-Aug-07	4.20		
				2174	2051	6	0.316	24.0	6.6	2039		CRF-66	2302	2101	3	28-Aug-07	6.30		
			D-02	2114	1927	9.7	0.401	28.6	7.7	1963	11.5	CRF-57	2327	2087	7	1-Sep-07	7.60		
			D-03	2377	2230	6.6	0.211	17.4	6.5	2232	10.0	CRF-58	2326	2115	7	1-Sep-07	8.00		
	D-04	2251	2122	6.1	0.273	21.4	6.6	2112	8.9	CRF-59	2374	2180	28	22-Sep-07	12.80				
	N	CRF-28	D-01	2322	2119	9.6	0.274	21.5	6.5	2180	9.8	CRF-60	2371	2159	3	28-Aug-07	5.50		
				2322	2119	9.6	0.274	21.5	6.5	2180		CRF-61	2375	2163	3	28-Aug-07	5.60		
			D-02	2208	2079	6.2	0.299	23.0	6.4	2075	9.2	CRF-62	2356	2157	4	29-Aug-07	5.60		
			2208	2079	6.2	0.299	23.0	6.4	2075	CRF-63		2370	2170	7	1-Sep-07	9.30			
D-03	2182	2082	4.8	0.297	22.9	5.3	2072	7.7	CRF-64	2355	2187	28	22-Sep-07	13.70					

Table A.7 (Contd) In situ & laboratory results of CRF with aggregate sieve sample number during placement of CRF

Placement Date	Shift	Aggregate Sieve Sample No.	In-situ Results from Troxler						Laboratory			CRF Cylinders						
			Density Test No.	Wet Density (kg/m <sup>3</sup> )	Dry Density (kg/m <sup>3</sup> )	Moisture Content MC (%)	Calculated Void Ratio	Porosity (%)	MC of CRF (%)	In-situ Dry Density (Lab MC Corrected) (kg/m <sup>3</sup> )	MC of CRF (%) (minus 25 mm)	Cylinder No.	Wet Density (kg/m <sup>3</sup> )	Dry Density (kg/m <sup>3</sup> )	Curing Time (Days)	UCS Test Date	UCS (MPa)	Dia (mm)
26-Aug-07	D	CRF-29	D-01	2286	2146	6.5	0.258	20.5	7.4	2128	9.1	CRF-67	2322	2128	3	29-Aug-07	5.40	100
				2286	2146	6.5	0.258	20.5	7.4	2128		CRF-68	2229	2043	7	2-Sep-07	4.20	
				2286	2146	6.5	0.258	20.5	7.4	2128		CRF-69	2140	1962	7	2-Sep-07	5.20	
			D-02	2303	2156	6.8	0.252	20.1	6.1	2171	9.8	CRF-70	2327	2119	3	29-Aug-07	4.26	
			D-03	2290	2160	6	0.250	20.0	5.4	2173	11.2	CRF-71	2325	2091	7	2-Sep-07	4.80	
			D-04	2332	2112	10.4	0.278	21.8	7.5	2169	10.9	CRF-72	2314	2087	7	2-Sep-07	7.30	
	D-05	2407	2243	7.3	0.204	16.9	7.6	2237	10.4	CRF-73	2324	2105	28	23-Sep-07	12.40			
	N	CRF-30	D-01	2337	2136	9.4	0.264	20.9	8.4	2156	10.8	CRF-74	2340	2112	3	29-Aug-07	5.30	
				2337	2136	9.4	0.264	20.9	8.4	2156		CRF-75	2309	2084	3	29-Aug-07	4.80	
				2280	2143	6.4	0.260	20.6	6.6	2139		8.7	CRF-76	2371	2182	7	2-Sep-07	
			2280	2143	6.4	0.260	20.6	6.6	2139	CRF-77	2362		2173	7	2-Sep-07	8.40		
			D-03	2297	2115	8.6	0.277	21.7	7.2	2143	9.3		CRF-78	2339	2140	28	23-Sep-07	
D-01			2278	2077	9.7	0.300	23.1	7.1	2127	9.5	CRF-79	2351	2147	3	30-Aug-07	5.69		
27-Aug-07	D	CRF-31	D-02	2305	2148	7.3	0.257	20.4	7.3	2148	7.5	CRF-80	2345	2181	3	30-Aug-07	5.57	
			D-03	2256	2114	6.7	0.277	21.7	6.7	2114	6.5	CRF-81	2320	2178	7	3-Sep-07	6.50	
			D-04	2229	2083	7	0.296	22.8	7	2083	7.2	CRF-82	2346	2188	7	3-Sep-07	6.40	
			D-05	2290	2118	8.1	0.275	21.5	8.1	2118	7.8	CRF-83	2321	2153	28	24-Sep-07	11.30	
			D-01	2269	2125	6.8	0.271	21.3	5.3	2155		CRF-84	2335	2166	3	30-Aug-07	5.37	
	N	CRF-32	D-01	6.8	0.271	21.3	5.3	2155	10.8	CRF-85	2281	2116	3	30-Aug-07	5.16			
				2300	2148	7.1	0.257	20.5		6.4	2162	CRF-86	2321	2095	7	3-Sep-07	8.00	
				2300	2148	7.1	0.257	20.5		6.4	2162	CRF-87	2352	2123	7	3-Sep-07	8.70	
			D-03	2305	2117	8.9	0.276	21.6	7.5	2144	9.3	CRF-88	2350	2150	28	24-Sep-07	9.50	
			D-01	2262	2100	7.7	0.286	22.2	6.7	2120	8.9	CRF-89	2339	2148	3	31-Aug-07	4.33	
			D-02	2347	2118	10.8	0.275	21.5	7.7	2179	10.2	CRF-90	2302	2089	3	31-Aug-07	4.54	
			D-03	2299	2139	7.5	0.263	20.8	6.4	2161	9.2	CRF-91	2334	2137	7	4-Sep-07	7.40	
28-Aug-07	D	CRF-33	D-04	2268	2114	7.3	0.277	21.7	7.0	2120	7.3	CRF-92	2365	2204	7	4-Sep-07	9.10	
			2268	2114	7.3	0.277	21.7	7.0	2120	CRF-93		2361	2200	28	25-Sep-07	14.60		
			D-01	2169	2048	5.9	0.318	24.1	5.6	2054	9.3	CRF-94	2407	2225	3	31-Aug-07	4.30	
			2180	2086	4.5	0.294	22.7	5.9	2059	CRF-95		2365	2164	3	31-Aug-07	4.10		
	2180	2086	4.5	0.294	22.7	5.9	2059	CRF-96	2362	2161		7	4-Sep-07	7.60				
	2180	2086	4.5	0.294	22.7	5.9	2059	CRF-97	2359	2158		28	25-Sep-07					
	2180	2086	4.5	0.294	22.7	5.9	2059	CRF-98	2336	2137		28	25-Sep-07	12.60				
	D-01	2126	2006	6	0.346	25.7	7.1	1985	9.4	CRF-99		2342	2141	3	1-Sep-07	6.30		
	2126	2006	6	0.346	25.7	7.1	1985	CRF-100		2374	2170	7	5-Sep-07	9.70				
	D-02	2088	1981	5.4	0.363	26.6	9.0	1916		CRF-101	2197	1953	3	1-Sep-07	3.50			
29-Aug-07	D	CRF-35	D-03	2088	1981	5.4	0.363	26.6	9.0	1916	12.5	CRF-102	2253	2003	7	5-Sep-07	5.30	
				2226	1980	12.4	0.363	26.7	9.0	2042		CRF-103	2301	2045	28	26-Sep-07	7.00	

Table A.7 (Contd) In situ & laboratory results of CRF with aggregate sieve sample number during placement of CRF

Placement Date	Shift	Aggregate Sample No.	Density Test No.	In-situ Results from Toxler										Laboratory		CRF Cylinders			
				Wet Density (kg/m <sup>3</sup> )	Dry Density (kg/m <sup>3</sup> )	Moisture Content MC (%)	Calculated Void Ratio	Porosity (%)	MC of CRF (Lab MC Corrected) (%)	In-situ Dry Density (kg/m <sup>3</sup> )	MC of CRF (%)	Density (minus 25 mm)	Cylinder No.	Wet Density (kg/m <sup>3</sup> )	Dry Density (kg/m <sup>3</sup> )	Curing Time (Days)	UCS Test Date	UCS (MPa)	Dia (mm)
2-Sep-07	D	CRF-36	D-01	2221	2082	6.7	0.297	22.9	6.9	2078	10.3	CRF-104	2362	2141	3	5-Sep-07	4.10	100	
			D-02	2296	2144	7.1	0.289	20.6	7.1	2144	11.1	CRF-106	2321	2089	7	9-Sep-07	7.60		
			D-03	2292	2154	6.4	0.283	20.2	5.4	2175	9.0	CRF-108	2346	2152	28	30-Sep-07	15.80		
		N	CRF-37	D-01	2335	2178	7.2	0.240	19.3	4.7	2230	7.0	CRF-109	2392	2236	3	5-Sep-07		5.20
				D-02	2312	2141	8	0.261	20.7	7.0	2161	9.0	CRF-111	2326	2134	7	9-Sep-07		8.10
				D-03	2381	2253	5.7	0.199	16.6	5.7	2253	7.9	CRF-113	2385	2210	28	30-Sep-07		11.70
	D	CRF-38	D-01	2111	2014	4.8	0.340	25.4	7.6	1962	7.8	CRF-114	2311	2144	3	6-Sep-07	4.50		
			D-02	2299	2067	11.2	0.306	23.4	6.6	2157	10.7	CRF-116	2342	2116	7	10-Sep-07	8.60		
			D-03	2299	2067	11.2	0.306	23.4	6.6	2157	10.7	CRF-117	2307	2084	7	10-Sep-07	8.40		
		N	CRF-39	D-01	2250	2140	5.6	0.262	20.7	6.6	2183	9.9	CRF-119	2331	2121	3	6-Sep-07		4.70
				D-02	2327	2153	8.1	0.254	20.3	6.6	2183	9.9	CRF-120	2363	2150	3	6-Sep-07		4.70
				D-03	2327	2153	8.1	0.254	20.3	6.6	2183	9.9	CRF-121	2358	2146	7	10-Sep-07		8.70
3-Sep-07	D	CRF-39	D-04	2256	2153	4.8	0.254	20.3	5.9	2130	7.4	CRF-122	2390	2225	7	10-Sep-07	9.00		
			D-05	2256	2153	4.8	0.254	20.3	5.9	2130	7.4	CRF-123	2384	2220	28	1-Oct-07	12.70		
			D-06	2256	2153	4.8	0.254	20.3	5.9	2130	7.4	CRF-124	2361	2236	3	7-Sep-07	4.50		
		N	CRF-39	D-07	2256	2153	4.8	0.254	20.3	5.9	2130	7.4	CRF-125	2360	2235	7	11-Sep-07	5.70	
				D-08	2256	2153	4.8	0.254	20.3	5.9	2130	7.4	CRF-126	2337	2196	3	7-Sep-07	4.50	
				D-09	2256	2153	4.8	0.254	20.3	5.9	2130	7.4	CRF-127	2366	2224	7	11-Sep-07	6.90	
	D	CRF-40	D-10	2256	2153	4.8	0.254	20.3	5.9	2130	7.4	CRF-128	2275	2154	28	2-Oct-07	10.40		
			D-11	2256	2153	4.8	0.254	20.3	5.9	2130	7.4	CRF-129	2372	2200	3	11-Sep-07	3.60		
			D-12	2256	2153	4.8	0.254	20.3	5.9	2130	7.4	CRF-130	2379	2207	7	15-Sep-07	6.20		
		N	CRF-41	D-13	2256	2153	4.8	0.254	20.3	5.9	2130	7.4	CRF-131	2356	2165	3	11-Sep-07	3.50	
				D-14	2256	2153	4.8	0.254	20.3	5.9	2130	7.4	CRF-132	2354	2164	7	15-Sep-07	6.70	
				D-15	2256	2153	4.8	0.254	20.3	5.9	2130	7.4	CRF-133	2351	2161	28	6-Oct-07	8.40	
8-Sep-07	N	CRF-41	D-16	2256	2153	4.8	0.254	20.3	5.9	2130	7.4	CRF-134	2294	2160	3	11-Sep-07	2.70		
			D-17	2256	2153	4.8	0.254	20.3	5.9	2130	7.4	CRF-135	2480	2316	7	15-Sep-07	5.20		
			D-18	2256	2153	4.8	0.254	20.3	5.9	2130	7.4	CRF-136	2337	2123	3	12-Sep-07	3.70		
	D	CRF-42	D-19	2256	2153	4.8	0.254	20.3	5.9	2130	7.4	CRF-137	2349	2134	7	16-Sep-07	7.00		
			D-20	2256	2153	4.8	0.254	20.3	5.9	2130	7.4	CRF-138	2346	2144	3	12-Sep-07	4.00		
			D-21	2256	2153	4.8	0.254	20.3	5.9	2130	7.4	CRF-139	2337	2123	3	12-Sep-07	3.70		

Table A.7 (Contd) In situ & laboratory results of CRF with aggregate sieve sample number during placement of CRF

Placement Date	Shift	Aggregate Sieve Sample No.	In-situ Results from Troxler					Laboratory		CRF Cylinders									
			Density Test No.	Wet Density (kg/m <sup>3</sup> )	Dry Density (kg/m <sup>3</sup> )	Moisture Content MC (%)	Calculated Void Ratio	Porosity (%)	MC of CRF (%)	In-situ Dry Density (Lab MC Corrected) (kg/m <sup>3</sup> )	MC of CRF (%) (minus 25 mm)	Cylinder No.	Wet Density (kg/m <sup>3</sup> )	Dry Density (kg/m <sup>3</sup> )	Curing Time (Days)	UCS Test Date	UCS (MPa)	Dia (mm)	
9-Sep-07	N	CRF-42									9.4	CRF-139	2365	2162	7	16-Sep-07	8.30	100	
											9.3	CRF-140	2366	2165	28	7-Oct-07	8.00		
												7.2	CRF-141	2473	2307	3	12-Sep-07	3.70	150
									8.4	CRF-142	2460	2269	7	16-Sep-07	9.10				
11-Sep-07	N	CRF-43									12.1	CRF-143	2306	2057	3	14-Sep-07	4.50	100	
												CRF-144	2329	2078	7	18-Sep-07	6.60		
													CRF-145	2338	2086	3	14-Sep-07	4.70	
												10.8	CRF-146	2342	2114	7	18-Sep-07	7.40	150
													CRF-147	2323	2097	28	9-Oct-07	9.20	
												7.1	CRF-148	2477	2313	3	14-Sep-07	4.20	
										CRF-149	2394	2235	7	18-Sep-07	3.70				
12-Sep-07	N	CRF-44									8.1	CRF-150	2293	2121	3	15-Sep-07	3.70	100	
												CRF-151	2327	2153	7	19-Sep-07	6.30		
													CRF-152	2356	2179	28	10-Oct-07	6.40	
												10.1	CRF-153	2335	2121	3	15-Sep-07	2.80	150
													CRF-154	2337	2123	7	19-Sep-07	5.00	
												6.9	CRF-155	2435	2278	3	15-Sep-07	3.00	
										CRF-156	2433	2302	7	19-Sep-07	5.90				
13-Sep-07	N										11.6	CRF-157	2328	2086	3	16-Sep-07	3.40	100	
												CRF-158	2356	2111	7	20-Sep-07	5.90		
													CRF-159	2379	2132	28	11-Oct-07	6.10	
												9.9	CRF-160	2353	2141	3	16-Sep-07	3.40	150
													CRF-161	2366	2153	7	20-Sep-07	5.10	
												7.1	CRF-162	2433	2272	7	20-Sep-07	3.20	
										CRF-163	2413	2240	28	11-Oct-07	7.70				
14-Sep-07	N										7.6	CRF-164	2311	2148	3	17-Sep-07	6.00	100	
												CRF-165	2304	2141	7	21-Sep-07	6.10		
													CRF-166	2272	2112	28	12-Oct-07	7.60	
15-Sep-07	N										4.9	CRF-167	2289	2182	28	12-Oct-07	6.70	150	
												CRF-168	2316	2154	3	18-Sep-07	4.40		
												7.5	CRF-169	2259	2101	7	22-Sep-07	5.60	100
													CRF-170	2282	2123	28	13-Oct-07	6.50	
												7.3	CRF-171	2264	2110	3	18-Sep-07	3.80	150
													CRF-172	2251	2098	7	22-Sep-07	4.80	
16-Sep-07	N										5.0	CRF-173	2218	2112	7	22-Sep-07	4.00	100	
												CRF-174	2242	2131	28	13-Oct-07	4.40		
												9.2	CRF-175	2338	2141	3	19-Sep-07	2.40	150
													CRF-176	2331	2135	7	23-Sep-07	6.10	
										CRF-177	2329	2133	28	14-Oct-07	11.60				
										7.0	CRF-178	2465	2304	28	14-Oct-07	8.40	150		

Note: CRF prepared with 6% cement until Sept. 8; after Sept. 8 CRF prepared with 5.5% cement

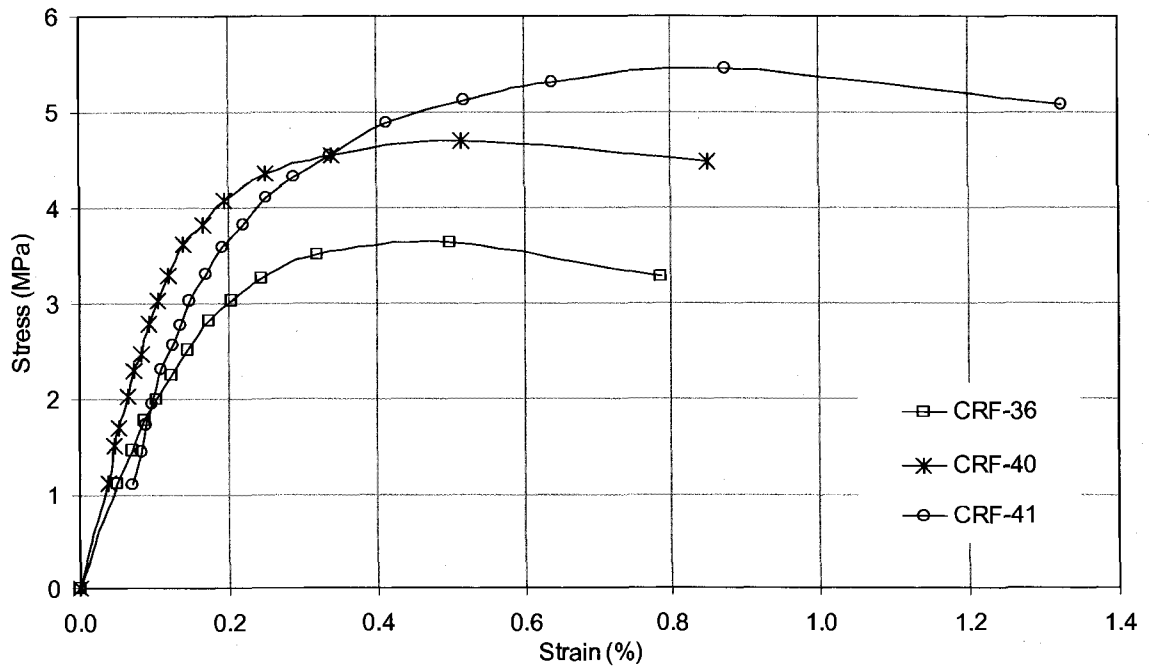
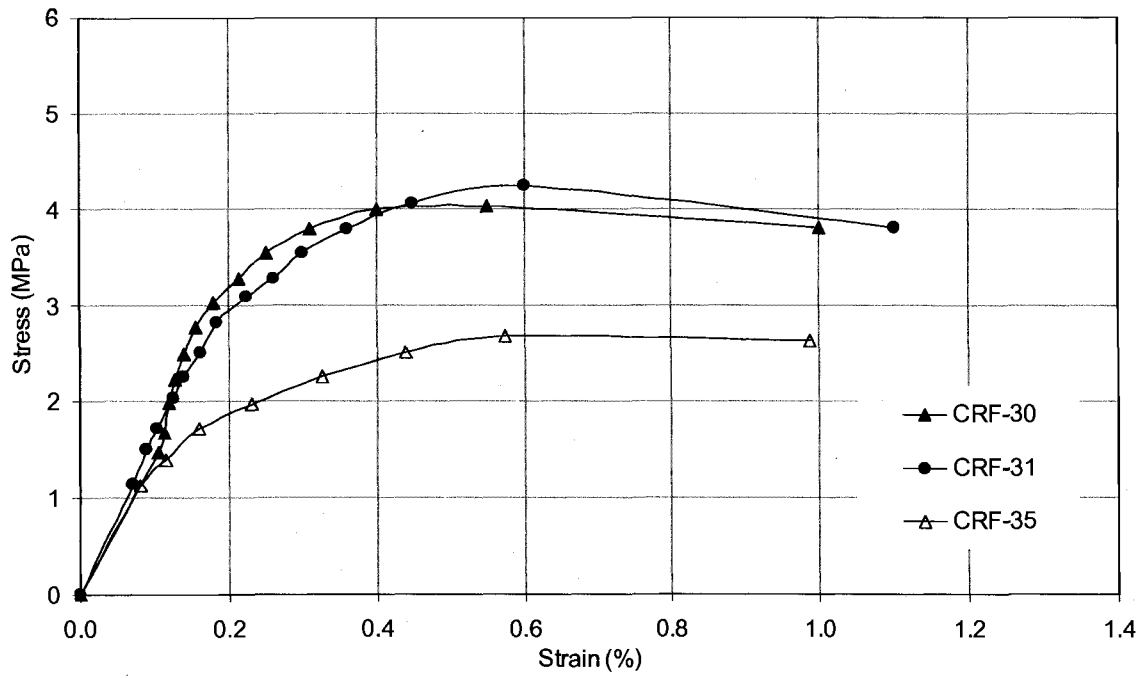


Figure A.1 Stress-strain curves for 100 mm cylinders after 3 days of curing

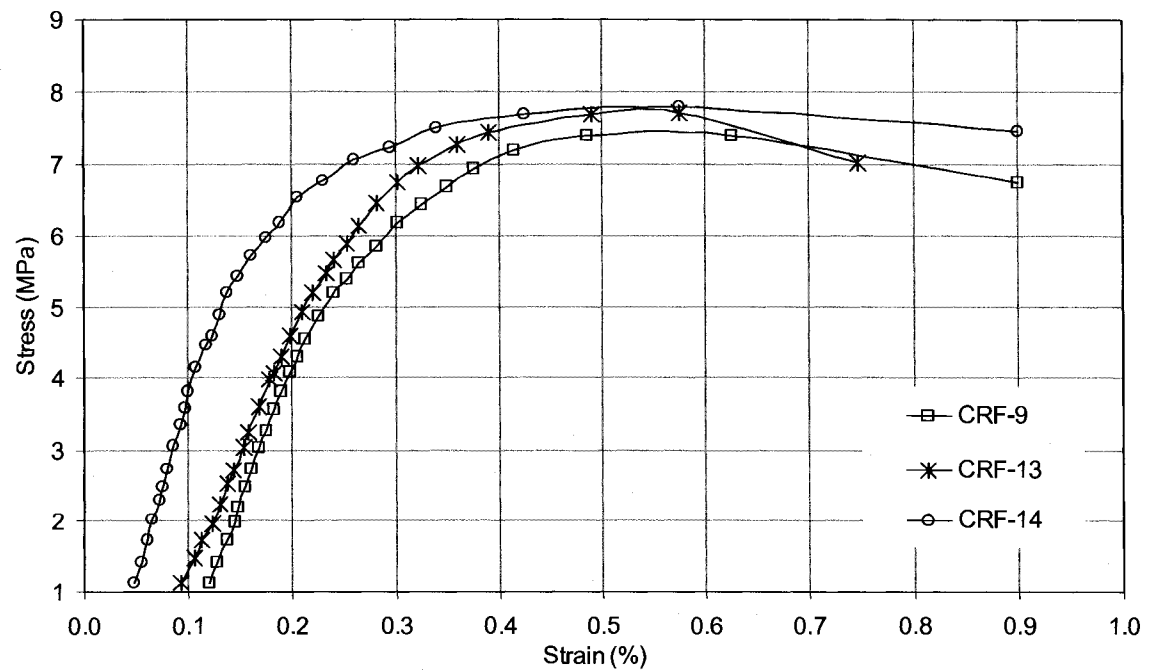
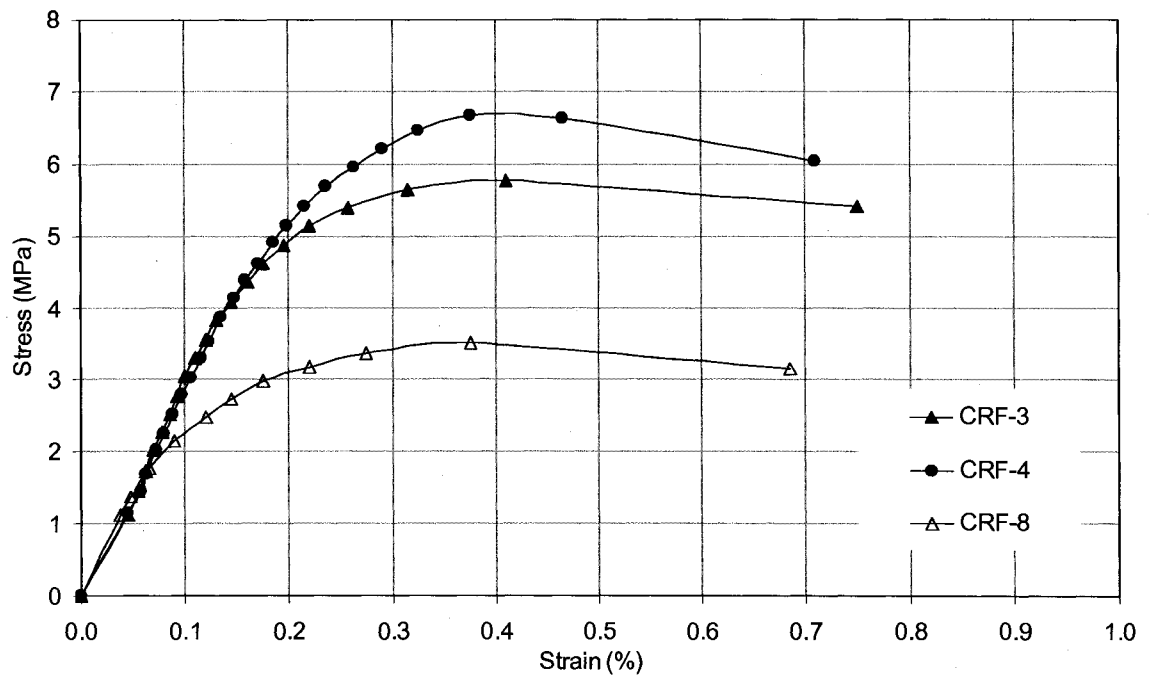


Figure A.2 Stress-strain curves for 100 mm cylinders after 7 days of curing

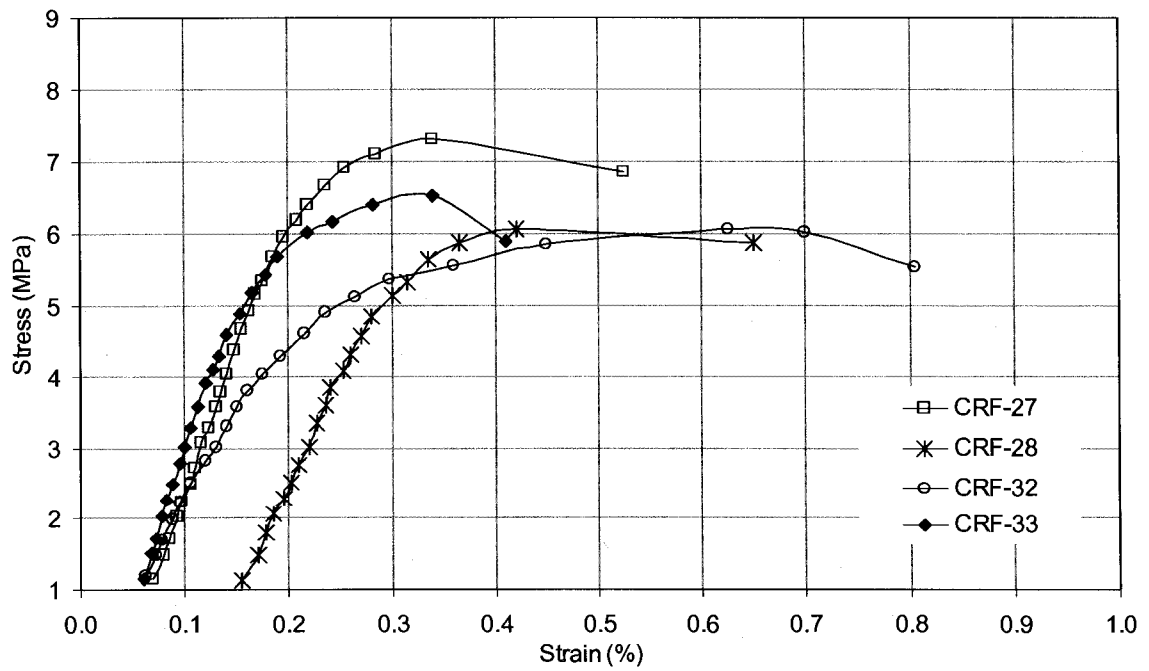
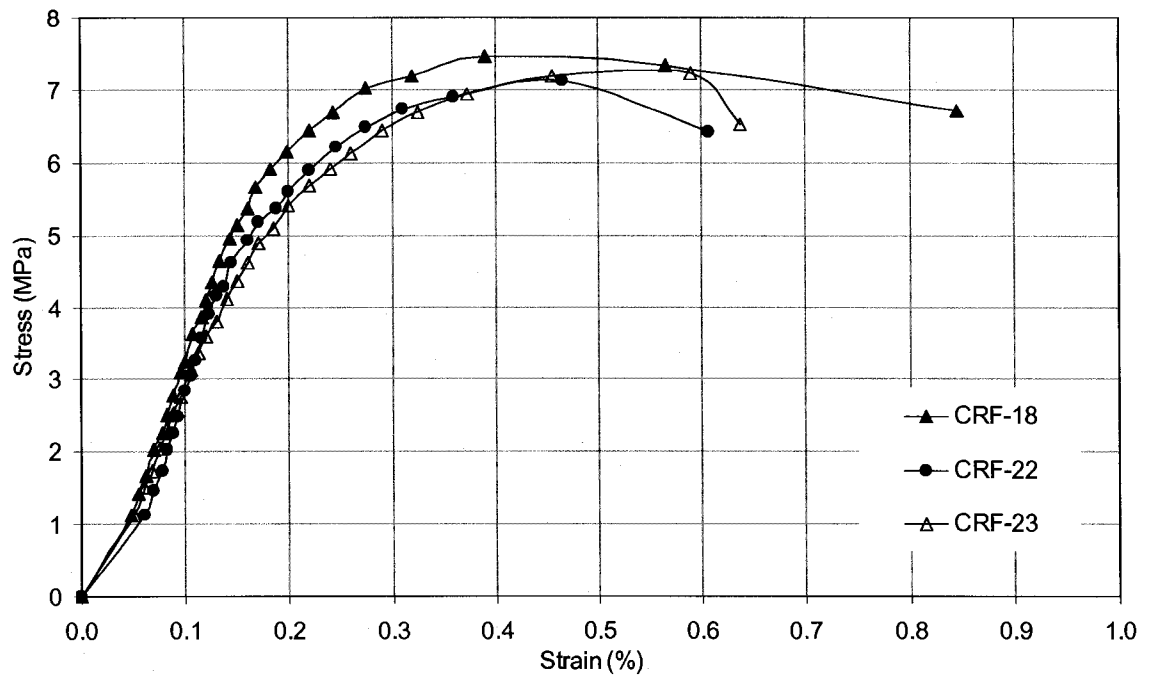


Figure A.3 Stress-strain curves for 100 mm cylinders after 7 days of curing

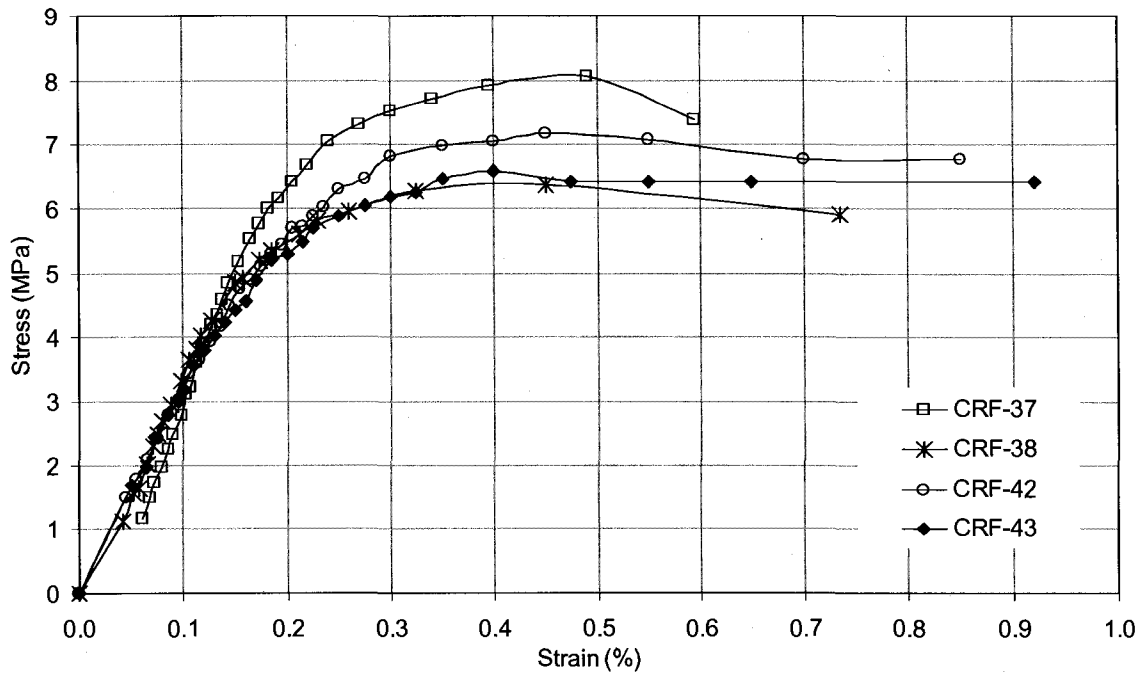


Figure A.4 Stress-strain curves for 100 mm cylinders after 7 days of curing

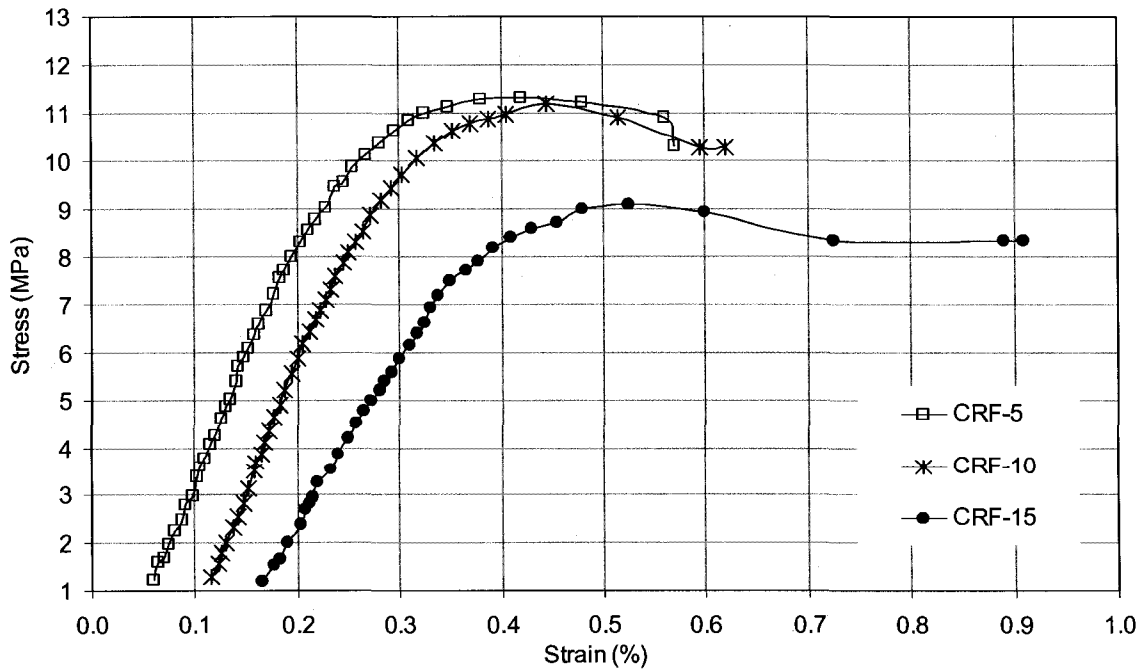


Figure A.5 Stress-strain curves for 100 mm cylinders after 28 days of curing